# Transcriptome wide characterization of target sites and alternative splicing regulation mediated by RBM10

Dissertation zur Erlangung des akademischen Grades
Doktor der Naturwissenschaften
(Dr. rer. nat.)

eingereicht am Fachbereich Biologie-Chemie-Pharmazie
der Freien Universität Berlin

vorgelegt von
**Yongbo WANG**
王勇波
aus Hubei, China

Berlin
2012

Die vorliegende Arbeit wurde von September 2008 bis September 2012 am

**Max-Delbrück-Centrum für Molekulare Medizin**

unter der Anleitung von

**Dr. Wei Chen**

angefertigt.

1. Gutachter: Prof. Dr. Constance Scharff

2. Gutachter: Prof. Dr. Markus Wahl

Disputation am.....Dec. 20th, 2012.....

# DEDICATION

**I hereby faithfully dedicate this dissertation to my beloved wife, Yali Gong (龚雅丽), who has always been making great efforts to improve and supprot me from every aspect of my life and patiently waiting for me in Shanghai, China.**

**August, 2012**
**Berlin**
**Yongbo Wang**

# TABLE OF CONTENTS

# ACKNOLEDGEMENTS

Four year's PhD study and life in Berlin is an invaluable experience to me, during which I have learned a lot of things that will be lifetime benefits for me. I am very grateful to all the people who have enlightened and helped me.

First of all, I would like to express my deep gratitude to my supervisor Dr. Wei Chen for providing me a great opportunity to work in his lab, bringing me into the field of "novel sequencing technology, medical and functional genomics" and "splicing regulation and genetic diseases". I am greatly appreciated for his brilliant supervisions and suggestions, enthusiastic encouragement and helpful critiques in my PhD projects as well as efficient and critical revisions of my thesis. I strongly believe that the ideas and experience I obtained in his lab will be priceless in my future career.

I am grateful to Prof. Dr. Constance Scharff for kindly being my external supervisor in Free University of Berlin, critically reviewing my thesis and always being so nice to me. Prof. Dr. Markus Wahl for generously reviewing my thesis and his suggestions. Prof. Dr. Norbert Huebner and Dr. Markus Landthaler for kindly being my PhD committee members and their evaluations and advices on my PhD projects.

For the project "Transcriptome wide characterization of target sites and alternative splicing regulation mediated by RBM10", I would like to thank Dr. Andreas Gogol-Doering for his excellent work in RNA-Seq and PAR-CLIP data analysis, many insightful discussions and his help with "ZUSAMMENFASSUNG". Dr. Sebastian Froehler for PAR-CLIP data analysis. Dr. Yuhui Hu for her helpful suggestions in perturbation experiments and discussions. Marvin Jens for sharing the PAR-CLIP data analysis pipeline and his suggestions. Jonas Maaskola for the RBM10 sequence motif analysis. Claudia Quedenau for assisting validation experiments: qPCR and EMSA. Anna-Maria Stroehl for helping with siRNA knockdown experiments. Mirjam Feldkamp and Claudia Langnick for performing sequencing. Yasuhiro Murakawa from Dr. Markus Landthaler's lab for sharing the PAR-CLIP technique.

# ACKNOLEDGEMENTS

For the project "*De novo* assembly and validation of Planaria transcriptome by massive parallel sequencing and shotgun proteomics", I greatly appreciate the directions from Prof. Dr. Nikolaus Rajewsky particularly in doing science out of interests and intuition, precisely defining scientific questions and strict scientific way of thinking and writing. Thank Catherine Adamidi for her instructions on experimental techniques at the beginning of my PhD work, which was a very good start for me. Xintian You and Dr. Dominic Gruen for their intensive data analysis. Dr. Guido Mastrobuoni for proteomics study and all other members contributed to this project.

I also would like to thank all the other members from Chen lab, including Dr. Na Li, Dr. Wei Sun, Wei Sun (Sunny), Gangcai Xie, Ana Babic, Martina Weigt, Madlen Sohn, Qingsong Gao, Tao Chen and Hang Du, for their help, discussions and the wonderful time we had together. Thank Jennifer Stewart and Sabrina Deter for their kind help with the registration in Free University of Berlin and dealing with my working contact in MDC. Thank all the other members of BIMSB for creating the open and cooperative working atmosphere. I would like to extend my thanks to the Chinese Community in MDC, which is an active, diligent and cooperative group. Together with them, I not only learned a lot in our scientific seminars but also had a lot of fun during leisure time.

Moreover, I would like to gratefully acknowledge the China Scholarship Council (CSC) for supporting me with four years' scholarship.

Lastly but very importantly, I would like to express my special thanks and faithful gratitude to my parents and elder brother. They have all the time been doing their best to endorse me making my own decisions and pursuing my interests. I can not make it here without them.

# SUMMARY

Defects in *RBM10* have been identified as the cause of TARP syndrome and other less severe developmental disorders. Although the RNA-binding protein encoded by *RBM10* has been identified as a component of spliceosome, very little is known so far about the target genes as well as the molecular mechanism underlying the regulation mediated by RBM10. Here, we used photoactivatable-ribonucleoside-enhanced crosslinking and immunoprecipitation to identify 89,247 RBM10 binding sites in 6,396 target genes. Those binding sites are enriched in the vicinity of both 5' and 3' splice sites in introns and in exons, which implicated the potential role of RBM10 in splicing regulation. In consistent with this, we also found that RBM10 binds specifically to U2 snRNA. Based on RNA sequencing, we determined 281 and 356 alternative splicing events following RBM10 depletion or overexpression respectively. Notably, the splicing changes upon RBM10 knockdown and overexpression are largely anti-correlated, indicating these alternative splicing were sensitive to cellular RBM10 abundance and were probably under its direct regulation. Finally, we showed that an in-frame deletion of RBM10 identified in the patient changed its normal nuclear localization and thereby disrupted its function in splicing regulation. Taken together, our extensive genome-wide datasets demonstrate that RBM10 functions as a novel splicing regulator via its direct binding to pre-mRNA substrates and potentially coordinates interplays between core splicing machinery and other splicing regulators.

# 1 INTRODUCTION

## 1.1 Pre-mRNA splicing and its regulation

### 1.1.1 Pre-mRNA splicing

In human and other complex metazoans, most protein-coding genes are expressed as pre-messenger RNAs (pre-mRNAs) from which introns are removed and the flanking sequences (exons) are joined to produce mature, functional mRNAs, which is called 'pre-mRNA splicing' (Green 1986). Pre-mRNA splicing is accomplished by spliceosome, a multi-component ribonucleoprotein (RNP) complex comprised of five small nuclear ribonucleoprotein particles (snRNPs: U1, U2, U4, U6 for major-class spliceosome, U11, U12, U4ata, U6atac for minor-class spliceosome, and U5 is shared by both) and numerous auxiliary proteins (Patel and Steitz 2003; Wahl et al. 2009; Will and Lührmann 2010). Two sequential transesterification reactions take place in the splicing process: (1) the 2′ OH group of the branch adenosine exerts a nucleophilic attack on the 5′ splice site (ss), resulting in cleavage at this site and ligation of the 5′ end of the intron to the branch adenosine, forming a lariat structure; (2) 3′ OH group of the 5′ exon attacks the 3′ ss, giving rise to the ligation of the 5′ and 3′ exons (generating the mRNA), and release of the intron (Figure. 1.1) (Green 1991). During the splicing process, spliceosome undergoes extraordinary compositional and structural alterations, mediated by highly coordinated and dynamic RNA-RNA, RNA-protein and protein-protein interactions. Most of the binary interactions involved in splicing are usually weak and strengthened by multiple interactions, providing the splicing machinery with its accuracy and at the same time remarkable flexibility (Wahl et al. 2009). Importantly, both the core components and the exceptional dynamics of spliceosome are largely conserved between metazoans and yeast (Fabrizio et al. 2009; Stevens et al. 2002). It is generally regarded that intricate interplays between pre-mRNA substrates and splicing machinery determine the splicing outcomes. The regulatory elements in pre-mRNAs and the major spliceosome assembly process are described below.

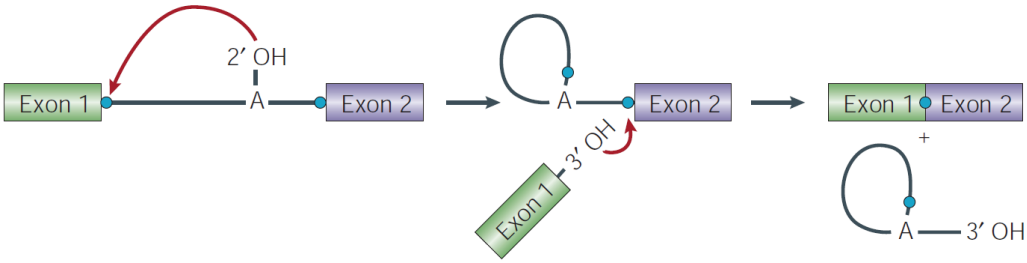


**Figure 1.1 Schematic illustration of the two-step transesterification reactions in pre-mRNA splicing.** Color boxes and solid line represent exons and intron, respectively. Nucleophilic attacks involved in the first and second steps of splicing launched by the 2′ hydroxyl of the branch-point adenosine (A) and by the 3′ hydroxyl of the upstream exon are marked with red arrows. Phosphodiester bonds are indicated with blue dots. The ligated exons and the lariat intron products are shown on the right. Adapted from (Patel and Steitz 2003).

### 1.1.2 *Cis*-regulatory elements in pre-mRNA splicing

Information in pre-mRNA substrate contributing to splice site recognition includes the short and consensus sequences at 5' splice site (ss), 3'ss and branch point site (BPS) which is typically located 30-50 nucleotides upstream of the 3'ss in human (Figure 1.2A). In metazoans but not in yeast, a polypyrimidine tract (PPT) is just downstream of the BPS (Figure 1.2A) (Burge et al. 1999; Will and Lührmann 2010). However, those short sequence are in general relatively degenerate, especially in complex metazoans, therefore are often not sufficient to specifically guide spliceosome assembly. Additional flanking *cis*-regulatory elements in pre-mRNA are required to facilitate splice site recognition and selection. Based on their position and function, these *cis*-elements are divided into four categories: exonic splicing enhancers (ESEs), exonic splicing silencers (ESSs), intronic splicing enhancers (ISEs), and intronic splicing silencers (ISSs) (Figure 1.2B). They serve as binding sites for *trans* regulatory factors, such as members of SR and hnRNP protein families, which in turn regulate splicing by either promoting or preventing the recruitment of basal splicing machinery (Figure 1.2B) (Blencowe 2000; Fairbrother et al. 2002; Wang and Burge 2008).

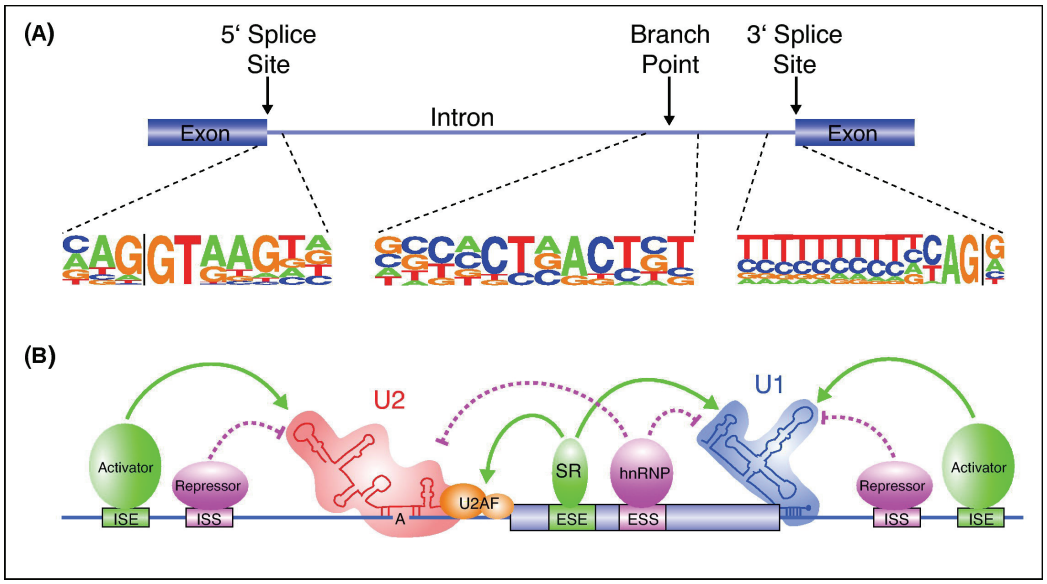


**Figure 1.2 *Cis*-regulatory elements in pre-mRNA substrate.** (A) Conserved sequence consensuses at the 5' splice site, branch point site and 3' splice site of human U2 type introns are shown. (B) Schematic illustration of four types of regulatory sequences: exonic splicing enhancers (ESEs), exonic splicing silencers (ESSs), intronic splicing enhancers (ISEs), and intronic splicing silencers (ISSs). They are bound by *trans* regulators, such as members of SR and hnRNP proteim family, to either enhance or repress splicing via interacting with basal splicing machinery. Adapted from (Mcmanus and Graveley 2011).

### 1.1.3 Spliceosome assembly pathways

Through extensive *in vitro* biochemical studies of the separated spliceosomal complexes under physiological conditions (Agafonov et al. 2011; Behzadnia et al. 2007; Bessonov et al. 2008; Deckert et al. 2006; Makarov et al. 2002), it is now clear that spliceosome assembles on pre-mRNA in a stepwise and ordered manner (Figure 1.3A). For short introns (<200-250 nt), spliceosome initially assembles across introns. It starts with ATP-independent binding of the U1 snRNP through base-pairing interactions of the 5' end of the U1 snRNA to the 5' splice site (ss) of the intron, the binding of the SF1/BBP protein to the BPS, the U2 auxiliary factor 65 kDa subunit (U2AF65) to the polypyrimidine tract, and U2AF35 to 3'ss, respectively. These molecular interactions, together with protein-protein interactions between SF1/BBP and U2AF65 as well as the tight interaction between U2AF65 and U2AF35 hetero-

dimmer, form spliceosomal E complex and play crucial roles in the initial recognition of the 5' ss and 3' ss of an intron. Subsequently, the U2 snRNA interacts with pre-mRNA's BPS via base pairing in an ATP-dependent manner with its adenosine bulged out. This base pairing interaction is stabilized by protein complexes of the U2 snRNP, resulting in the formation of the A complex (or prespliceosome complex). Association of U2 leads to the displacement of SF1/BBP from the BPS and the association of SF3b14a/p14 with the BPS adenosine. After the formation the A complex, the U4/U6-U5 pre-assembled tri-snRNPs are recruited, generating the B complex which contains all snRNPs whereas is still catalytically inactive. Major compositional and conformational rearrangements take place resulting in the releasing of U1 and U4 snRNPs and U5 snRNA binding to the exon sequences near splice site to juxtapose the neighboring exons. At this stage, 5' end of U6 snRNA, replacing U1 snRNA, base pairs with 5'ss by its conserved ACAGA box. In addition, extensive base paring and structural rearrangements happen between U6 and U2 for subsequent catalytic activation, generate the activated spliceosome (the B activated complex). The activated spliceosome then carries out the first catalytic step of splicing, yielding the C complex which undergoes further rearrangements and then catalyzes the second step of splicing. After the splicing reactions, the spliceosome are dissociated and the released snRNPs are recycled for new rounds of splicing.

In the case of long introns (>250 nt), spliceosomal components first assemble across an exon (Fox-Walsh et al. 2005), a process called exon definition (Berget 1995) (Figure 1.3B). In the exon definition process, the U1 snRNP binds to the 5′ ss downstream of an exon, components of U2 snRNP associate with the polypyrimidine tract/3′ ss and BPS upstream of the exon, respectively. Regulatory sequences within the exon recruit protein factors such as the SR protein family members, which bridge the cross exon interactions and stabilize the exon definition complex (Hoffman and Grabowski 1992; Reed 2000). Since catalytic steps of splicing take place across an intron, the cross exon complex must be switched to cross intron complex, a process that is currently not well characterized yet (Will and Lührmann 2010).

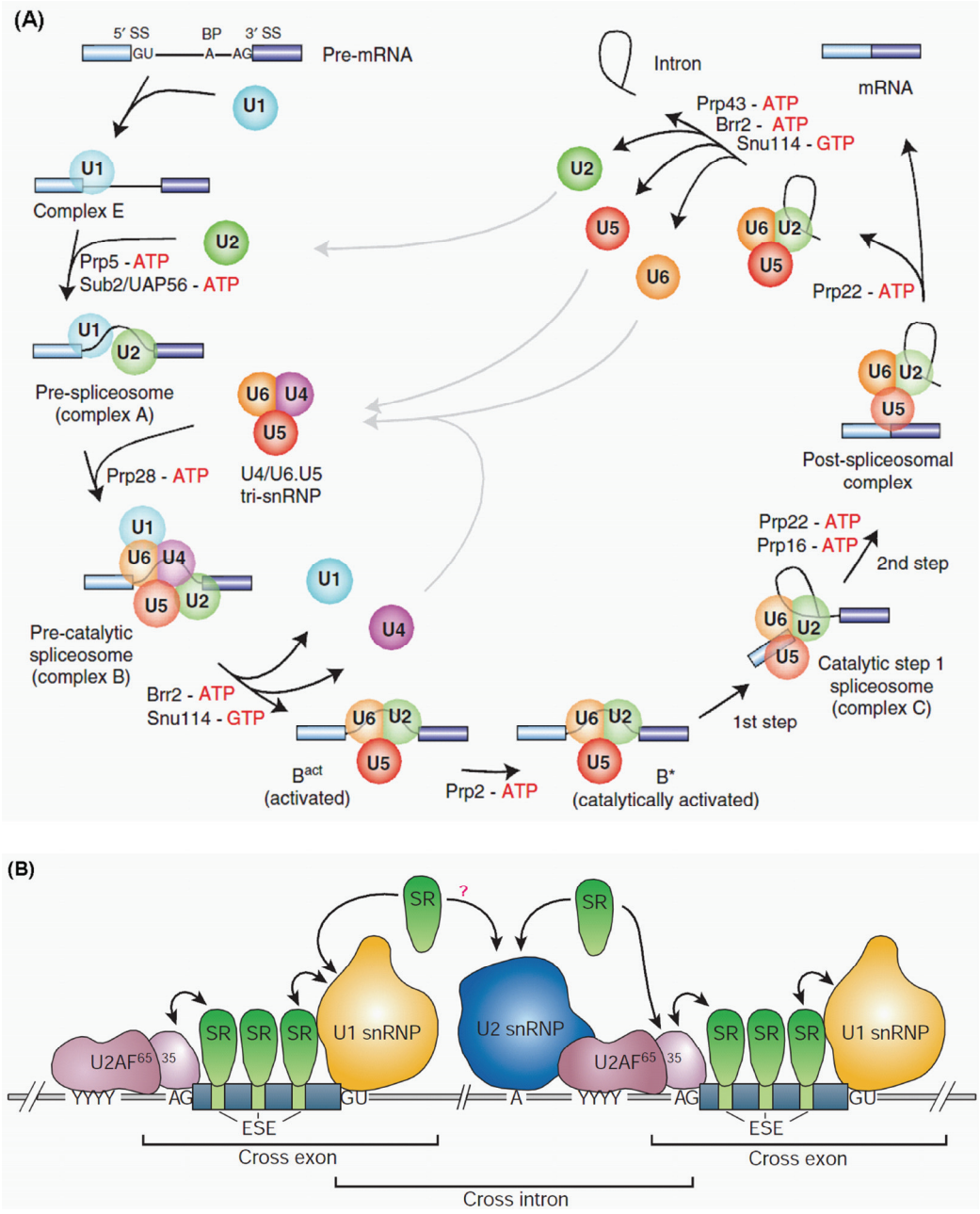


**Figure 1.3 Pre-mRNA splicing by major spliceosome**. (A) Canonical cross-intron assembly, catalysis and disassembly pathway of the major spliceosome. Exon and intron sequences in pre-mRNA are indicated by boxes and lines, respectively. The stepwise interactions of the snRNPs (colored circles), but not those of non-snRNP proteins, and the formation of various spliceosomal complexes that can be resolved biochemically are shown. The specific steps at which the evolutionarily conserved DExH/D-box RNA ATPases/helicases act to facilitate conformational changes are highlighted. Adapted from (Will and Lührmann 2010). (B) Model of cross-exon splicing complexes assembly for long introns. The cross exon interactions are

mediated by protein factors such as SR protein that bind to ESE. How the cross-exon complexes are switched to cross-intron complexes and enter the splicing pathway shown in (A) remains largely unclear to date. Adapted from (Maniatis and Tasic 2002).

## 1.2 Alternative splicing

### 1.2.1 Alternative splicing is an important layer of gene expression control

In multicellular eukaryotes, many exons are alternatively spliced, producing multiple mRNA species from a single pre-mRNA that encode proteins with different or even antagonistic functions, termed alternative splicing (AS) (Breitbart et al. 1987). AS is an important layer of gene expression regulation and greatly enhance the proteomic diversity (Blencowe 2006). Among other processes including alternative transcription start sites, alternative polyadenylation, RNA editing and posttranslational modifications, AS is considered as one of the major sources, and perhaps the most important one, that contribute to proteome expansion in metazoans (Maniatis and Tasic 2002; Nilsen and Graveley 2010). Recent studies show that more than 94% human genes undergo AS events (Pan et al. 2008; Wang et al. 2008). More importantly, AS regulations have been demonstrated to play pivotal roles in different cell types (Boutz et al. 2007; Makeyev et al. 2007), developmental stages (Gerstein et al. 2010; Graveley et al. 2011; Ramani et al. 2010), across tissues (Pan et al. 2008; Wang et al. 2008), sex determination (Baker 1989; Nagoshi and Baker 1990) and in response to external stimuli (Shin and Manley 2004; Xie and Black 2001).

### 1.2.2 Types of alternative splicing

The basic AS patterns can be classified into: cassette exon inclusion or skipping, alternative 5’ splice sites, alternative 3’ splice sites, intron retention, mutually exclusive alternative exons, alternative promoter and first exon, and alternative poly A site and last exon (Figure 1.4). Genes can adopt single or combinational patterns to generate functionally distinct isoforms. It has been estimated that 80% of the AS events affect ORFs (Modrek and Lee 2002), leading to amino acid deletion/insertion or frameshift. The remaining 20 % falls within the untranslated regions (UTR) and

influences *cis* regulatory elements that control mRNA stability, localization and translational efficiency (including miRNA binding sites) (Bassell and Kelic 2004; Keene 2007). Besides, a large proportion (estimated to be one third) of AS events introduce premature stop codons (PTC) which could potentially trigger mRNA degradation via nonsense mediated decay (NMD) pathway (Green et al. 2003; Lewis et al. 2003).

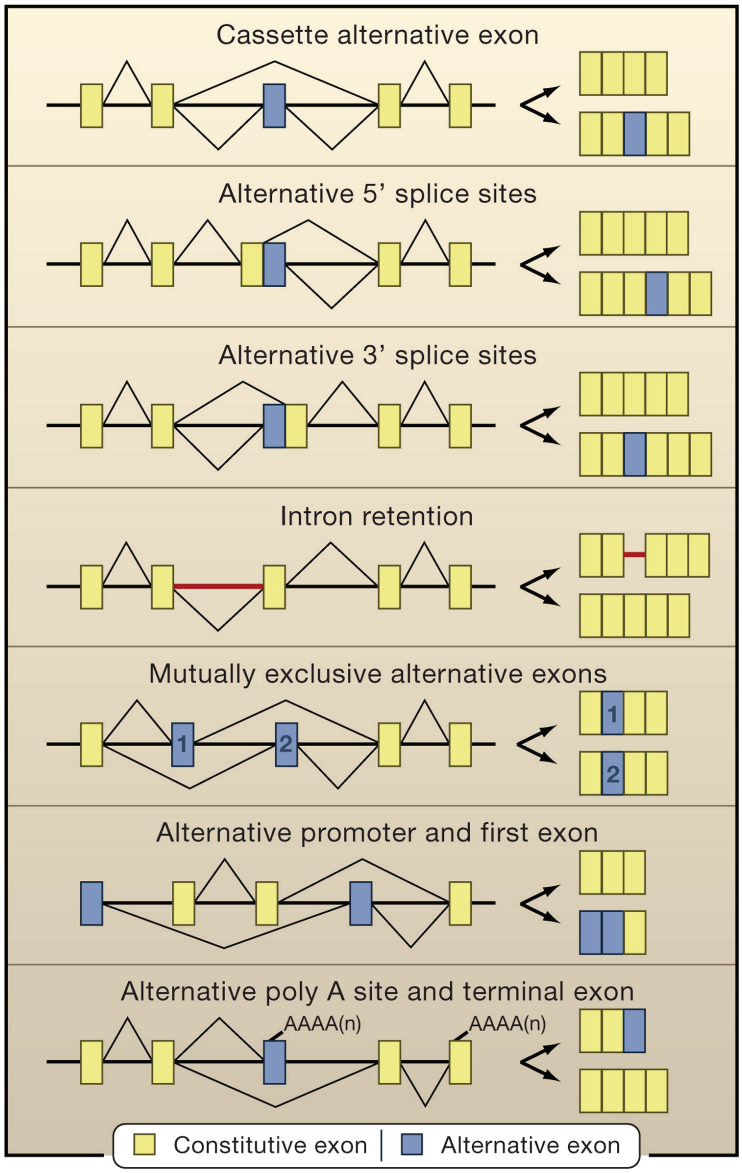


**Figure 1.4 Types of alternative splicing.** Yellow and blue boxes indicate constitutive and alternative exon, respectively. Black line represents intron that is spliced, while the red line represents intron that is retained to be an exon. Adapted from (Blencowe 2006).

### 1.2.3 General mechanisms of alternative splicing

Alternative splicing (AS) is generally thought to be controlled by cooperative interplays between RNA binding proteins (RBPs), regulatory elements in nascent transcripts and the basal splicing apparatus (Black 2003; Chen and Manley 2009; Witten and Ule 2011). More specifically, splicing regulating RBPs bind directly to splice sites, or interact with specific sequences in pre-mRNA to facilitate or block the recruitment of splicing machinery, which in turn stimulate or repress splice site usage (i.e. modulating alternative splicing). AS choices have been found to occur at different stages of the splicing process, encompassing: (1) the splice site recognition and early step of spliceosome assembly, which is the most frequent cases uncovered to date (Chen and Manley 2009) and exemplified by splicing regulation of survival of motor neuron (*SMN*) exon7 (Figure1.5A) (Cartegni et al. 2006; Cartegni and Krainer 2002; Kashima and Manley 2003); (2) splice site pairing, a typical example is the prevention of *Fas* (*CD95*) exon 6 inclusion by RNA binding motif protein 5 (RBM5) (Figure1.5B) (Bonnal et al. 2008); (3) either or combinational effects of (1) and (2) in distinct contexts, as illustrated by polypyrimidine tract-binding protein (PTB) and its neuronal counterpart nPTB (Figure1.5C); (4) even the conformational rearrangement before catalytic steps (Lallena et al. 2002; Sharma et al. 2008). Although the exact biochemical mechanisms remain not well understood, more and more studies and corresponding regulatory models are emerging and greatly deepen our apprehension of AS regulation (Nilsen and Graveley 2010).

Considering huge disparity between the number of splicing regulators and the AS events identified so far, it is not surprising to rationalize the findings that a single splicing regulator can often modulate a large number of AS events (Ule et al. 2005; Xue et al. 2009; Yeo et al. 2009; Zhang et al. 2010). Members of SR (Long and Caceres 2009; Shepard and Hertel 2009) and hnRNP protein families (Han et al. 2010) are so far the most studied ones among all the identified splicing regulators. SR proteins, named by containing arginine/serine-rich (RS) protein domain, usually bind to exonic splicing enhancers (ESEs) and are generally thought to activate splicing by promoting the enrollment of splicing machinery. By contrast, hnRNPs, which are also highly abundant RBPs but lack of an RS domain, often bind to exonic splicing silencers (ESSs) and/or intronic splicing silencers (ISSs), and are generally considered

to repress splicing by interfering with the engagement of core spliceosomal machinery. It should be noted that some proteins containing RS domain negatively regulate splicing (Cowper et al. 2001), while several hnRNPs have been found to function as splicing activators (Smith and Valcárcel 2000), or modulate splicing in a position dependent way, such as hnRNP C (Konig et al. 2010). The ultimate alternative splicing decisions are therefore made by combinational effects of the similar (synergic) or opposing (antagonistic) splicing regulatory signals (Black 2003; Smith and Valcárcel 2000).

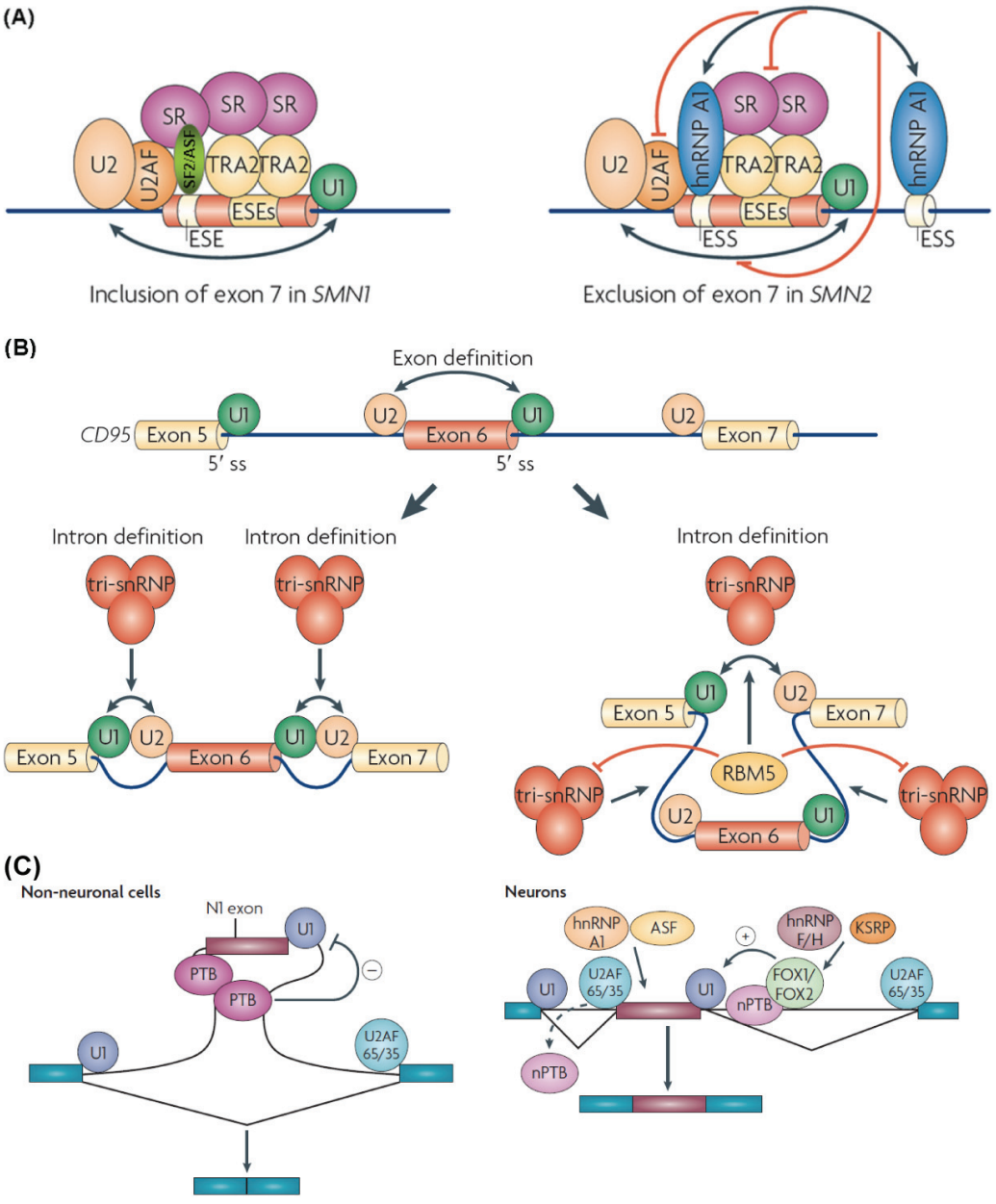

**Figure 1.5 General mechanisms of alternative splicing regulation.** (A) Alternative slicing regulation by splice site recognition and selection, as exemplified by splicing regulation of *SMN* exon7. A single nucleotide variation in exon 7 creates an ESS in *SMN2* that is bound by heterogeneous nuclear ribonucleoprotein particle A1 (hnRNP A1), thereby inhibiting the formation of stabilized U2 snRNP complex and compromising the enhancing activity of TRA2 which binds to ESE, resulting in exon 7 skipping. Instead, ESE in exon 7 of *SMN1* is bound by SF2/ASF, thereby promoting inclusion. Adapted from (Chen and Manley 2009). (B) Alternative slicing regulation by intervening with splice site pairing, as exemplified by RBM5 mediated splicing regulation of *CD95* exon6. RBM5 inhibits the exon 6 inclusion by blocking tri-snRNP recruitment between the neighboring exons and promoting cross-intron complex formation between exon 5 and exon 7, rather than block U1 and U2 snRNP to splice sites. Adapted from (Chen and Manley 2009). (C) Different modes of alternative slicing regulation under distinct contexts, as illustrated by PTB and its neuronal counterpart nPTB for regulating *SRC* N1 exon. In non-neuronal cells, PTB binds to elements in the N1 3′ splice site and in the downstream intron, thereby blocking the assembly of pre-spliceosomal E complex. In addition, multiple PTB binding has been shown to facilitate the splice site paring between distal exons by "looping out" exon N1. In neurons, neural PTB (nPTB) replaces PTB and enhances exon N1 inclusion through binding to the downstream regulatory element that act as an ISE, destabilizing the PTB binding to upstream silencer elements, and coordinative/competitive actions of other splicing RBPs, such as SF2/ASF, hnRNP H and KSRP. Adapted from (Li et al. 2007).

AS events exhibit dramatic difference between distinct tissues (Pan et al. 2008; Wang et al. 2008). However, only a few tissue-specific splicing regulators have been identified to present, such as NOVA1 and NOVA2 (Ule et al. 2006; Ule et al. 2005), nPTB (Boutz et al. 2007), FOX1 and FOX2 (Gehman et al. 2011; Yeo et al. 2009), RBM20 (Guo et al. 2012), RBM35 (Warzecha et al. 2009) and RBM11 (Pedrotti et al. 2011) and so on. Studies indicated that the ubiquitously expressed splicing regulators also participate in the tissue specific alternative splicing regulation through their fluctuated abundance in different tissues (Black 2003; Chen and Manley 2009; Zhang et al. 2008). It is now generally regarded that tissue specific alternative splicing is shaped by differentially expression of tissue specific splicing regulators and/or

variable concentrations and/or modifications of ubiquitously expressed splicing regulators (Black 2003; Chen and Manley 2009).

Remarkably, several lines of evidence demonstrate that transcription, including the transcription rate (Hicks et al. 2006), formation of local secondary structure of the nascent transcript (Vargas et al. 2011) and chromatin status (Kornblihtt et al. 2004), can affect the pattern of alternative splicing (Figure 1.6). This is plausible given that splicing in general takes place cotranscriptionally (Listerman et al. 2006; Luco et al. 2011). Several studies indicated that exon in nascent transcript is tethered to the transcription elongation factor after emerging from the RNA polymerase, allowing the engagement of the splicing machinery and inclusion of exon (Dye et al. 2006). Conversely, very fast transcription rate and/or inefficient tethering could cause exon skipping. In addition, another study showed the altered chromatin structure affected the transcription rate, thereby changed the decision of AS (Allo et al. 2009). Moreover, it has recently been shown that histone H3 trimethylated at lysine residue 36 (H3K36me3), a marker for active transcription, specifically marks exons and occurs more frequently on constitutive exons (those are always included in mRNA) compared with alternative exons (Kolasinska-Zwierz et al. 2009; Schwartz et al. 2009). These findings suggest a kinetic mechanism for transcription-coupled alternative splicing control.

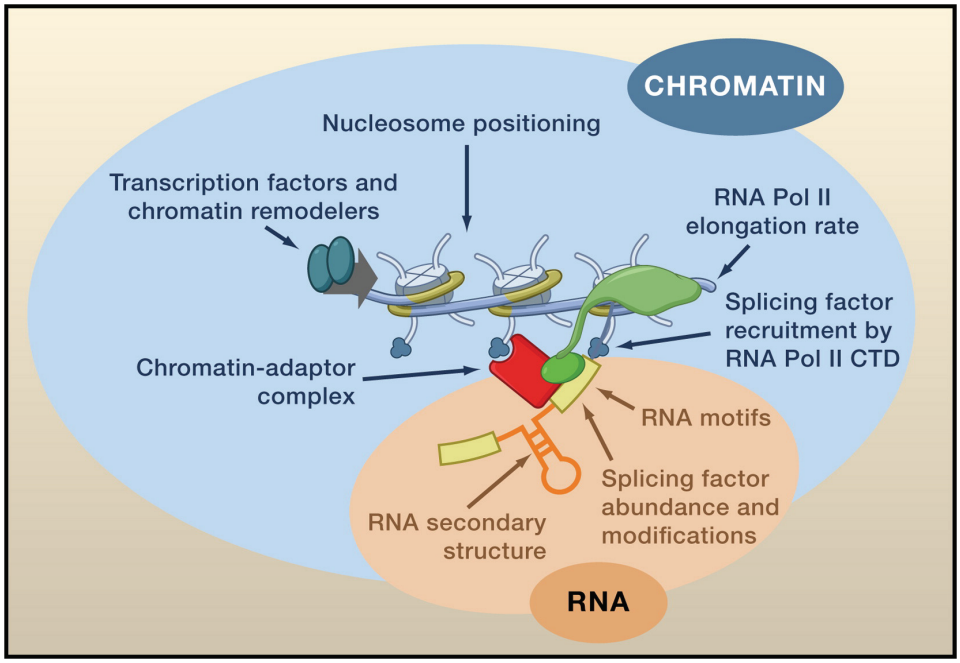

**Figure 1.6 An integrated model for transcription coupled alternative splicing regulation.** Transcription, controlled by transcription factors and chromatin status, affects the formation of local secondary structures (highlighted in orange) in nascent RNA and the concomitant recruitment of splicing regulators, thus modulates splicing outcomes. Adapted from (Luco et al. 2011).

## 1.3. Alternative splicing and human diseases

Alternative splicing (AS) provides the organism with tremendous plasticity and complexity, however on the other hand increases the susceptibility to diseases. Defects in splicing are regarded as a primary cause of diseases, and the mechanisms of which can be classified into two main groups: (1) disruption of *cis*-elements within the affected gene, including splice sites as well as the splicing cis-regulatory elements; (2) disruption of *trans*-acting factors that influence the basal splicing or splicing regulation, comprising of component of core splicing machinery and splicing regulators (Cooper et al. 2009; Faustino and Cooper 2003; Wang and Cooper 2007).

### 1.3.1 *Cis*-effects: disruption of splicing code

Mutations in splice site consensus and the splicing regulatory sequences contribute to perhaps as high as ~50% of known human inherited disorders (Cartegni et al. 2002; Cooper et al. 2009). These mutations could change the encoded protein, alter the ratio of natural protein isoforms, or introduce a premature termination codon (PTC) (Frischmeyer and Dietz 1999) that could potentially lead to mRNA degradation through NMD pathway, thereby cause diseases. One representative example of *cis*-effects is Duchenne muscular dystrophy (DMD) caused by mutation in the massive *dystrophin* gene. A large number of point mutations have been identified to cause aberrant splicing in this gene, which in turn led to the disease phenotype. For example, a T->A substitution in exon 31 simultaneously create a premature stop codon and an exonic splicing slilencer (ESS), leading to exon 31 skipping and a mild form of DMD (Disset et al. 2006). Another notable example is the Frontotemporal dementia and Parkinsonism linked to Chromosome 17 (FTDP17), which is an autosomal dominant disorder caused by mutations in the *MAPT* gene that encodes tau. Numerous point mutations within and around *MAPT* exon 10 could destruct the exonic or intronic

splicing elements and alter the normal 1:1 ratio of isoforms with or without exon 10. The disrupted splicing in turn destroys the balance between tau proteins containing either four or three microtubule-binding domains (R) and causes FTDP17 (Liu and Gong 2008).

### 1.3.2 *Tans*-effects: defects of splicing machinery or splicing regulators

In comparison to *cis* effects that affect particular genes, mutations in components of spliceosome or splicing regulators could potentially affect the splicing of a large number of genes, directly or through secondary effects. Therefore, mutations or stoichiometric changes in these regulators can extensively change the AS patterns of their targets.

Very few mutations in core spliceosomal components have been found by far, indicating that they are indispensible for essential cellular functions. One notable example is the autosomal dominant form of retinitis pigmentosa (adRP) that caused by mutations in five proteins belonging to U4/U6-U5 tri-snRNPs: *PPRF31, PPRF8, PPRF3, RP9*, and *SNRNP200* (Mordes et al. 2006). Another striking example is spinal muscle atrophy (SMA) that caused by mutations in *SMN* gene (Lefebvre et al. 1995; Lunn and Wang 2008). SMN complex plays essential roles in snRNA biogenesis. Surprisingly, it has been found that each snRNA is affected differently in distinct tissue of SMN-deficient mouse rather than a uniform decrease (Zhang et al. 2008). The third remarkable example is the finding that point mutations in *U4atac* snRNA, a core component of the minor spliceosome, were linked with microcephalic osteodysplastic primordial dwarfism type I (MOPD I, also known as Taybi–Linder Syndrome), an autosomal recessive genetic and severe developmental disorder characterized by extreme intrauterine growth retardation, neurological and skeleton muscle abnormalities (Edery et al. 2011; He et al. 2011). These three examples bring about two important but yet unanswered questions: (1) how mutations in those ubiquitously expressed, essential components cause tissue-specific pathologies; (2) which downstream target genes are the functionally important ones responsible for the specific phenotypes.

Unlike the scarcely observed mutations in spliceosomal core components, a diverse cohort of splicing regulators, such as TDP43, QKI, NOVA1, RBMYA1, RBM20, and A2BP1, have been found to cause or associate with diseases, particularly in neurological and psychiatric diseases (Gabut et al. 2008; Lukong et al. 2008; Ule 2008). Among these, TDP43 is a well-characterized example that belongs to hnRNP family and has similar protein structure with hnRNP A1 and A2 (Buratti and Baralle 2008; Buratti et al. 2005). It has been initially found to bind to the HIV *trans*-acting response elements (TAR), functioning as a transcriptional repressor of HIV, and subsequently been found to link with several different diseases. Firstly, mutations in *TARDBP*, the gene encodes TDP43, are found to associate with both sporadic and familial amyotrophic lateral sclerosis (ALS) (Daoud et al. 2009; Kabashi et al. 2008; Rutherford et al. 2008; Sreedharan et al. 2008). In addition, TDP43 has been shown to increase the binding to expanded polymorphic (UG)m repeats in intron 8 of *CFTR*, mutation of which causes cystic fibrosis, leading to the skipping of exon 9 and in turn increasing the disease severity (Ayala et al. 2006; Buratti et al. 2004; Buratti et al. 2001). Also, cytoplasmic aggregation of TDP43, which normally resides in nucleus, was found in affected regions of brains from individuals with frontotemporal dementia (FTD), Alzheimer disease and amyotrophic lateral sclerosis (ALS) (Barmada et al. 2010; Winton et al. 2008).

Moreover, splicing abnormalities, particularly owing to mutation or changed expression of splicing regulators, have been commonly linked with cancers (David and Manley 2010; Wang and Cooper 2007). An excellent example is an SR protein, SF2/ASF1 (i.e. SRSF1), which has been characterized as a proto-oncogene (Karni et al. 2007). Elevated expression of SF2/ASF1 has been detected in various cancers (David and Manley 2010). SF2/ASF1 overexpression was shown to induce an oncogenic isoform of ribosomal protein S6 kinase-β1 (S6K1) that stimulates transformation. This finding directly connects SF2/ASF1's oncogenic activity with its splicing regulation activity (Karni et al. 2007). Additionally, increased SF2/ASF1 was shown to promote splicing of *RON*, the tyrosine kinase receptor proto-oncogene, to a constitutively active form (Δ*RON* ) which increased migration and invasiveness, via direct binding to an ESE within the downstream exon (Ghigna et al. 2005). Another striking example is the recent discovery that somatic mutations in spliceosomal

proteins, including SF3B1, U2AF1, ZRSR2, SF1, PRPF40B, U2AF2, and SF3A1, are associated with myelodysplastic syndrome (MDS), which often progresses to acute myeloid leukemia (AML), chronic lymphocytic leukemia (CLL) and chronic myelomonocytic leukemia (CMML) (Abdel-Wahab and Levine 2011; Makishima et al. 2012; Papaemmanuil et al. 2011; Wang et al. 2011; Yoshida et al. 2011). Most of the detected mutations in these splicing factors are missense mutations and occurred in a mutually exclusive manner except ZRSR2, indicating that disease phenotypes are perhaps more likely caused by an alteration of the protein function and/or partial loss of function. Interestingly, all these proteins are involved in U2 dependent splice site recognition, suggesting a role of common dysregulated splicing patterns in the pathologies of those pre-leukemia and leukemia syndromes.

### 1.3.3 Splicing and disease diagnosis, prognosis and targeted therapies

Recent advances in high throughput technologies dramatically expedite the identification of disease associated/causing splicing defects, as well as the characterization of splicing molecular signatures resulting from defects of *trans*-acting factors. Those results not only improve our understanding of normal splicing regulatory mechanisms, but also provide us very useful targets for disease diagnosis, prognosis and importantly raise the possibilities for molecular therapies by specifically intervening with splicing (Cooper et al. 2009; Wang and Cooper 2007). The emerging therapeutic strategies include: (1) conventional small molecules targeting specific transcript or protein isoform (Figure 1.7A); (2) oligonucleotide mediated therapies targeting splicing regulatory signal or specific isoform (Figure 1.7B-D); (3) RNA based correction of the aberrant isoform (Figure 1.7E) (Garcia-Blanco et al. 2004; Wang and Cooper 2007). Although considerable progress has been achieved in the investigation of those therapeutic strategies, clinical applications await rigorous specificity and efficacy test as well as circumvention of general delivery issues.

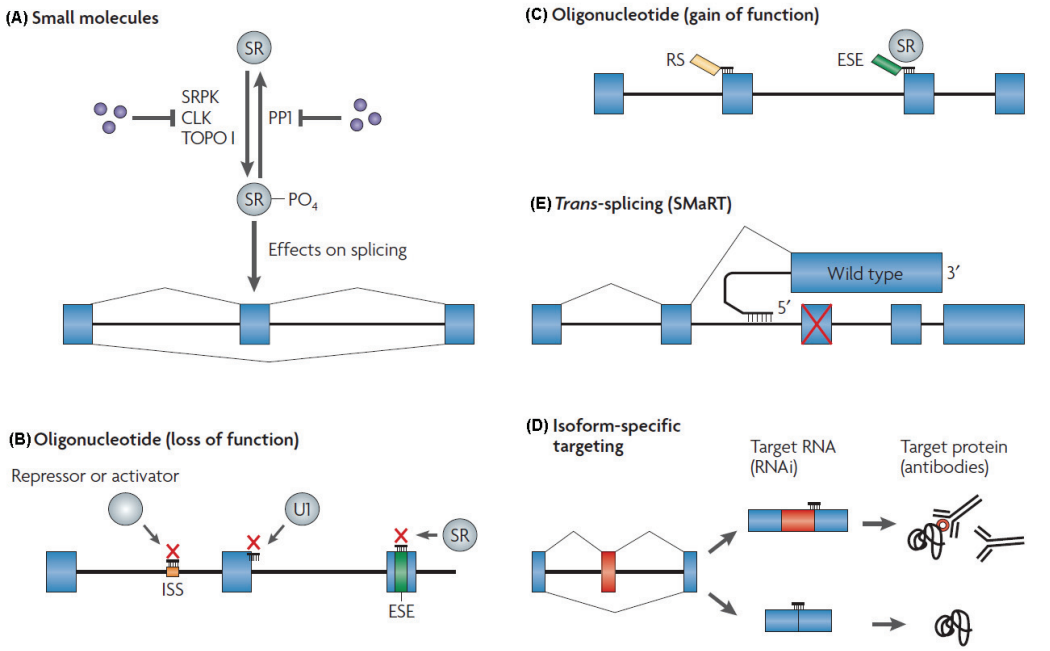


**Figure 1.7 Therapeutic strategies by manipulating splicing.** (A) Utility of small molecules to target kinases or phosphatases that modify splicing regulators. The advantage of this strategy is the relatively easy delivery and dosage control, whereas the shortcoming is the lack of specificity. (B,C) Application of modified antisense oligonucleotides with enhanced stability and resistance to RNase H mediated degradation. They can either be used to block splicing signals, such as splice site, ESE, ISS and so on, and act in a loss of function mode (B), or in conjugation with effecter peptide, such as RS domain, and act in a gain of function mode (C). (D) Isoform specific RNAi or antibody is used to degrade aberrant mRNA or block the abnormal protein, respectively. (E). *Trans* splicing is employed to correct the defective mRNA. Adapted from (Wang and Cooper 2007).

## 1.4 Technologies for global mapping of RBP-RNA interactions and analysis of alternative splicing

The long standing goals of splicing research are to: (1) decipher the general regulatory modes of all splicing regulators, including the discovery of novel *cis* elements, to enable predicting splicing outcomes under specific physiological or pathological contexts; (2) determine the functional consequences of alternative splicing events; (3) apply the defined splicing signatures in diagnosis, prognosis and manipulate splicing

events in therapies of human diseases. Achieving those goals necessitates robust systematic mapping of splicing RBP-RNA interactions and detection of alternative splicing events. The process has been dramatically accelerated by recent advancements in high throughput technologies, in particular crosslinking immunoprecipitation (CLIP) and RNA sequencing.

### 1.4.1. Technologies for global mapping of RBP-RNA interactions

Since splicing related RBPs often modulate hundreds even thousands of functional targets, elucidating the regulatory roles of those RBPs requires comprehensive identification of the RBP-RNA interactions and quantification of the splicing outcomes induced by such interactions (Polymenidou et al. 2011; Ule et al. 2006; Yeo et al. 2009; Zhang et al. 2010). The initial systematic method to identify *in vivo* targets of a given RBP was RIP-chip (Ribonucleoprotein ImmunoPrecipitation followed by microarray) (Keene et al. 2006), which has been successfully implemented to uncover a number of functional RNA targets and regulatory elements of RBPs (Hogan et al. 2008). The major shortcomings of this technique is perhaps that it can neither identify the precise location of binding sites nor detect potential binding to introns thus can hardly applicable to investigate splicing regulating RBPs with intronic binding sites (Lebedeva et al. 2011). Crosslinking immunoprecipitation (CLIP) overcomes these shortcomings by several modifications: (1) ultraviolet (UV) light irradiation to crosslink RBP with bound RNAs, generating a covalent bond; (2) purification under very stringent conditions to get rid of contaminations and increase specificity; (3) digestion of the bound RNA to small fragments, typically 20-100 nt, and coupled with sequencing to enhance the resolution in mapping binding sites. Recently developed CLIP based methods, including HIS-CLIP (Licatalosi et al. 2008; Zhang and Darnell 2011), iCLIP (Konig et al. 2010; Konig et al. 2011) and PAR-CLIP (Hafner et al. 2010), take advantage of specific mutations or termination introduced by reverse transcriptase in the crossling sites, thereby could identify the direct RBPs binding sites with nucleotide resolution. In PAR-CLIP (photoactivatable ribonucleoside enhanced crosslinking and immunoprecipitation) (Figure 1.8), photoactivatable nucleosides 4-thiouridine (4SU) that can strongly enhance the crosslinking efficacy are incorporated into nascent RNAs and crosslinked at low

energy pulse of UV (365 nm). 4SU labeled and crosslinked cells were lysed, immunoprecipitated with RBP specific antibody. The bound RNAs were partially digested by RNase T1 or RNase I and radioactively labeled. RBP-RNA complexes were then resolved on a denaturing gel and the band corresponds to RBP-RNA complexes were excised. The RNA was recovered, converted in to cDNA and sequenced. One notable feature of PAR-CLIP is that occurrence of T to C conversions in the crosslinked nucleosides is not only the diagnostic of genuine RBP-RNA interactions versus background or contaminated signals but also allowing identification of binding sites at nucleotide resolution (Hafner et al. 2010). Those remarkable merits distinguish PAR-CLIP from RIP and other CLIP based methods, nevertheless, it so far has mostly been applied in cell lines and recently in *C. elegans* (Jungkamp et al. 2011). It relies on efficient photoactivatable nucleotide analog labeling, impeding its applications in complex animal system and human tissues where the efficient labeling is not easily achievable or could hardly be done. In those cases, other CLIP based technologies, such as iCLIP (Konig et al. 2010) and HIST-CLIP (Licatalosi et al. 2008), can be effective alternatives.

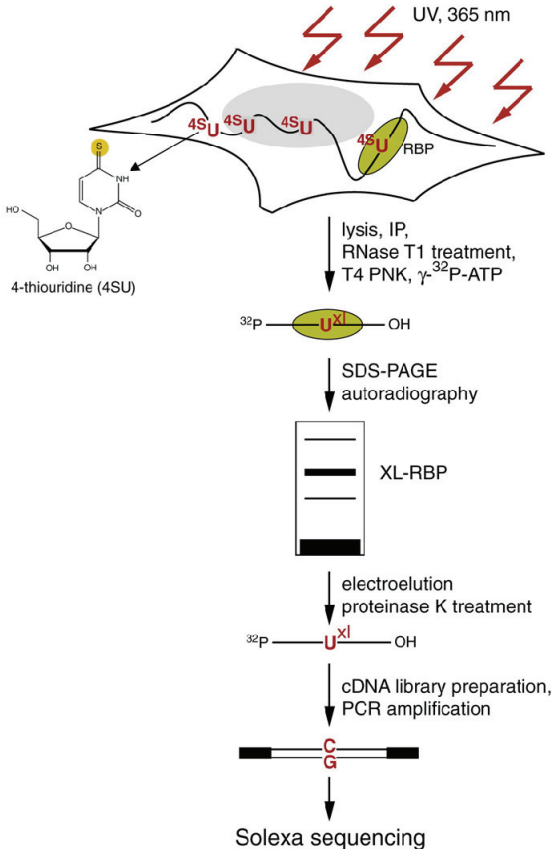

**Figure 1.8 Schematic illustration of PAR-CLIP workflow.** Photoactivatable nucleosides 4-thiouridine (4SU) are incorporated into nascent RNAs to enhance the crosslinking efficacy. RBP and its bound RNAs are crosslinked at low energy pulse of UV (365 nm). The crosslinked cells were then lysed, immunoprecipitated with RBP specific antibody. The bound RNAs were partially digested by RNase T1 or RNase I and radioactively labeled with $\gamma^{32}$P-ATP. The radioactively labeled RBP-RNA complexes were then resolved on a denaturing gel and the band corresponds to RBP-RNA complexes were excised. The RBP is digested and the bound RNA fragments were recovered, converted into cDNA and sequenced. Notably, T to C conversions in crosslinking sites occur during reverse transcription, which is not only a diagnostic of genuine RBP-RNA interactions but also permits identification of binding sites at nucleotide resolution.

### 1.4.2. Technologies for global analysis of alternative splicing

In order to understand how those RBP-RNA binding events shape specific outcomes, i.e. how they control splicing, it is crucial to systematically determine the alternative splicing events. Specific microarray, including splice junction array, exon array and genomic tiling array, and RNA sequencing technologies have been demonstrated to be powerful methodologies for global splicing analyses in a number of previous studies (Griffith et al. 2010; Moore and Silver 2008; Ozsolak and Milos 2011). Splice junction array uses junction specific probes to assess alternative splicing events and probes within constitutive exons to indicate the presence or absence of the transcripts (Johnson et al. 2003). It is a very convenient and relatively cheap method, however it is dependent on prior knowledge of splicing events thus can not used to detect novel splicing events. Moreover, the junction probes design is constrained to span junction locations, therefore is often optimal. Exon array uses probe sets based on annotated exons to quantify exon expressions within transcripts and identify differentially expressed exons (Kapur et al. 2007). It could detect novel exon variations generated by splicing, but often suffers with high false negative and false positive rates probably due to variable sensitivities and specificities of probes (Okoniewski and Miller 2008). Tiling arrays does not need the exon annotations and theoretically allows detection of additional splicing events, such as intron retention, or non-annotated exons, apart from

annotated exon usage (Juneau et al. 2007; Zhang et al. 2007). Nevertheless, the increase of expense and substantial computational challenges impedes its applications in global splicing analysis. RNA sequencing, especially with the recent prominent improvements of sequencing read length and throughput, as well as developments of computational analysis strategies (Garber et al. 2011), could in principle identify all splicing patterns at single nucleotide resolution independent of prior exon annotations. Sequencing reads are aligned to the genome and/or transcriptome, thereafter the junction spanning reads are utilized to define splicing events (Pan et al. 2008; Wang et al. 2008). It, together with appropriate analysis pipeline, for example Cufflinks (Trapnell et al. 2010), can also be applied to estimate expression level of the transcript isoform. Although the computational analysis for determining alternative splicing events based on RNA sequencing is still challenging, the rapid revolution of technology, such as sequencing technology with exceptional longer read length or even direct RNA sequencing, and advancement of analysis pipelines would eventually overcome all the difficulties.

## 1.5 RBM10 in human diseases

Recently, defects in a potential splicing regulator, RNA binding motif protein 10 (RBM10), have been identified to cause X-linked recessive disorders. In a genetic mutation screening study of TARP syndrome (MIM 311900), an X-linked pleiotropic developmental anomaly syndrome, a nonsense and a frameshift mutations in RBM10 were identified as causative mutations in two patients from two afflicted families respectively (Johnston et al. 2010). More recently, an in-frame deletion in RBM10 was found in two patients suffered with multi-organ malformations, including cleft palate, muscular dystrophy, severe mental retardation, hearing loss and ventricular septal defect etc. (manuscript in revision). These findings implicated that the previously functionally uncharacterized protein might play important roles in normal mammalian development and cognitive abilities. Furthermore, expression of *RBM10* was found to be positively correlated with the proapoptotic *Bax*, and *VEGF* gene (Martínez-Arribas et al. 2006), and the large isoform was shown to be positively correlated with wild type p53, RBM5 in human breast cancer (Rintala-Maki et al. 2007). Together with several other RNA binding motif (RBM) family proteins (RBMX, RBM3, RBM5, RBM6 etc.), RBM10 has been postulated as a putative apoptosis modulator that could

involve in modulating cancer proliferation and apoptosis (Rintala-Maki et al. 2007; Sutherland et al. 2005).

## 1.6 Previous studies on RBM10

RBM10 locates in the X chromosome (Xp11.23) and encodes a 930 amino acid protein with sequence motif found in variety of factors involved in pre-mRNA splicing and other aspects of RNA metabolism (Glisovic et al. 2008; Keene 2007). These domains include two RNA recognition motif (RRM) domains, two zinc fingers, and a G patch (Figure 1.9) (Sutherland et al. 2005). In addition, an OCRE domain (Callebaut and Mornon 2005), a novel domain made of imperfect, aromatic-rich octamer repeats, has been found in RBM10 and its prologues, RBM5 and RBM6, as well as angiogenic factor VG5Q. This domain might play a role for proper protein folding and mediating protein-protein interaction (Callebaut and Mornon 2005). RBM10 is conserved across many vertebrate species and broadly expressed across human tissues. It has been shown that RBM10 predominantly localized in the extranucleolar nucleoplasm and constitute hundreds of punctuate and irregular nuclear domains closely adjacent nuclear speckles, which change their structures in a reversible manner with alteration of RNA polymerase II transcription activity (Inoue et al. 2008). In addition, RBM10 has been identified as a spliceosome component (Rappsilber et al. 2002), more specifically a component of U2 snRNPs (Makarov et al. 2011), spliceosomal A (or prespliceosomal) (Agafonov et al. 2011; Behzadnia et al. 2007) and B complexes (Agafonov et al. 2011; Bessonov et al. 2008) and could physically interact with multiple spliceosomal components (Hegele et al. 2012), further suggesting its potential role in pre-mRNA splicing regulation in spice site recognition and/or splice site communication steps. Its closest paralogue RBM5 (sharing 48% identity with RBM10), a putative tumor suppressor of lung and other cancers (Sutherland et al. 2005), has been shown to regulate alternative splicing of apoptosis related genes, *Fas* receptor (*CD95*) and c-*FLIP*, resulting in isoforms with antagonistic functions in programmed cell death (Bonnal et al. 2008). Moreover, *in vitro* studies showed that RBM10 can bind single stranded RNA with a GGU motif via RanBP2 zinc finger domain (Nguyen et al. 2011) and its rat homolog can bind to RNA homopolymers,

with a preference for G and U polyribonucleotide (Inoue et al. 1996). These studies suggest that RBM10 is a putative splicing regulator with RNA binding capacities.


**Figure 1.9 Schematic representation of RBM10 protein domains.** RBM10 contains several domains, including two RNA recognition motif (RRM) domains, two zinc fingers, and a G patch, which are commonly found in other RNA processing regulators, as well as a less studied OCRE domain. The nuclear localization signal (NLS) and deletion identified in patient affected with X-linked multi-organ malformations are highlighted.

## 1.7 Objective of this project

Previous studies demonstrate that RBM10 is RNA binding protein and a potential splicing regulator that are associated with human diseases, however, the *in vivo* RNA binding sites and targets of RBM10 are almost completely unknown, and the potential regulatory mechanisms mediated by RBM10 remain largely unexplored. In this project, we would like to: (1) identify the transcriptome-wide binding sites of RBM10 by PAR-CLIP; (2) determine RBM10 dependent effects in gene expression and particularly alternative splicing by RNA sequencing; (3) integrate the RNA binding sites and functional consequences induced by RBM10 perturbations to unravel the regulatory roles of RBM10; (4) explore the possible mechanisms underlying disease phenotypes induced by RBM10 defects. The experimental design is depicted in Figure 1.10.

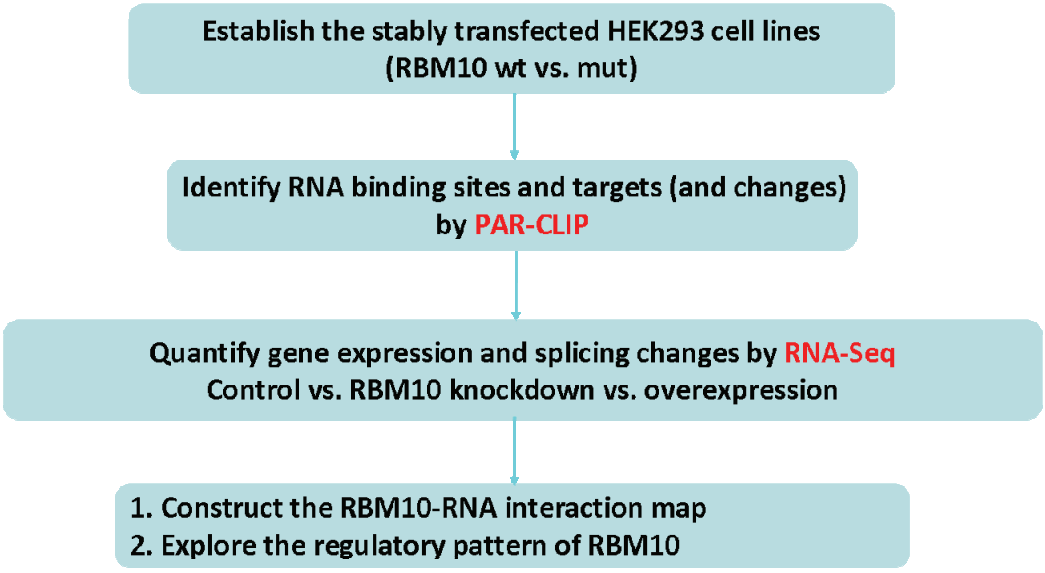


**Figure 1.10 Schematic representation of experimental design.** To explore the regulatory mechanisms of RBM10 and infer that underlie disease pathologies, we choose HEK293 cells as a model and will first establish stable cell lines inducibly expressing RBM10 wild type (wt) and mutant (mut) respectively. Then we will identify transcriptome wide RNA binding sites of both RBM10 wt and mut by PAR-CLIP and determine changes induced by RBM10 overexpression or knockdown with respect to gene expression and particularly alternative splicing by RNA sequencing. Finally, we will integrate the binding events with the detected changes to construct a regulatory map of RBM10 and speculate on the functional links between mutation and disease phenotypes.

# 2 MATERIALS AND METHODS

## 2.1 Materials

### 2.1.1 Cell lines

**(1) HEK 293 Flp-In T-REx Cell Line**: human embryonic kidney cell line that contains a single integrated FRT site and stably expresses high levels of the Tet repressor protein. The cell line is kindly provided by Landthaler Lab in Max Delbrück Center for Molecular Medicine (MDC) and commercially available at Invitrogen.

**(2) Stable HEK 293 Flp-In T-REx Cell Line inducibly expressing FLAG/HA tagged RBM10**: RBM10 wild type (WT) and mutant (MUT) were integrated into HEK 293 Flp-In T-REx Cell Line, respectively.

**(3) Lymphoblast cell lines**: derived from two normal controls and one patient carrying an in-frame deletion in RBM10. The cells were kindly provided by Kalscheuer Lab in Max Planck Institute for Molecular Genetics (MPIMG)**.**

### 2.1.2 Vectors

- pENTR/D-TOPO (Invitrogen)
- pOG44 (Part of the Flp-In Core System by Invitrogen, courtesy of Landthaler Lab)
- pFRT_TO_DESTFLAGHA (www.addgene.com, courtesy of Landthaler Lab)
- pFRT_DESTFLAGHA_eGFP (www.addgene.com, courtesy of Landthaler Lab)

### 2.1.3 Cell culture mediums

- **Maintenance medium for HEK 293 Flp-In T-REx cell line:**

High glucose DMEM (Gibco) supplemented with 10% final concentration FBS (heat inactivated, Gibco), 100 U/ml of penicillin and 100 µg/ml streptomycin (Gibco), 15 µg/ml blasticidin (InvivoGen) and 100 µg/ml zeocin (InvivoGen).

- **Antibiotic free medium for transfection:**

DMEM with 10% final concentration FBS.

- **Stable cell line selection medium:**

DMEM with 10% final concentration of FBS, 100 U/ml of penicillin and 100 µg/ml streptomycin, 100 µg/ml hygromycin and 15 µg/ml blasticidin.
(No blasticidin for the pFRT_DESTFLAGHA_eGFP cells.)

- **Freezing medium:**

90% FBS and 10% DMSO. Cool to 4°C before using.

### 2.1.4 Enzymes

- Calf intestinal alkaline phosphatase (CIP) (New England Biolabs)
- Gateway LR Clonase II enzyme mix (Invitrogen)
- GoTaq DNA Polymerase (Promega)
- Phusion High-Fidelity DNA polymerase (Finnzymes)
- Proteinase K (lyophilizate) (Roche Diagnostics)
- Restriction enzymes (New England Biolabs)
- RNase T1 (Fermentas)
- SuperScript II reverse transcriptase (Invitrogen)
- SuperScript III reverse transcriptase (Invitrogen)
- T4 Polynucleotide Kinase (Fermentas)
- T4 RNA ligase 1 (New England Biolabs)
- T4 RNA ligase2, truncated (New England Biolabs)

### 2.1.5 Kits

- Agencourt AMPure XP Kit (Beckman Coulter)
- Agilent RNA 6000 Nano and Pico Kit (Agilent Technologies)
- Agilent DNA 1000, 7500 Kit (Agilent Technologies)
- DNAfree Kit (Ambion)
- Dynabeads Protein G (Invitrogen)
- Dynabeads Oligo (dT) (Invitrogen)
- GeneJET Plasmid Miniprep Kit (Fermentas)
- Lipofectamine 2000 reagent (Invitrogen)
- Lipofectamine RNAiMAX reagent (Invitrogen)
- NEBNext DNA Library Prep. Kit (NEB)

- pENTR/D-TOPO Cloning Kit (Invitrogen)
- QIAquick PCR Purification and Gel Extraction Kit (Qiagen)
- Qubit dsDNA HS Assay (Invitrogen)
- SYBR Green PCR Master Mix (Applied Biosystems)
- SYBRGreen Masrermix I (Roche)
- Trueseq DNA Library Preparation Kit (Illumina)
- Illumina Sequencing Kit (Illumina)

### 2.1.6 Chemicals

Chemicals used in experiments were purchased from the following companies: Roth (Germany), Sigma (Germany), Roche (Germany), Invitrogen (Germany), InvivoGen (Germany) and Applied Biosystems.

### 2.1.7 Other reagents

Other regents not listed above are specified in the experimental methods, including siRNAs, antibodies, solutions and buffers, and primer sequences etc.

### 2.1.8 Major Equipments

- ABI PRISM 7500 Sequence Detection Systems (Applied Biosystems)
- Agarose gel electrophoresis equipment (Bio-Rad)
- Agilent 2100 Bioanalyzer (Agilent Technologies)
- Bio-Rad Tetrad 2 Peltier Thermo Cycler (Bio-Rad)
- Cell incubator (Hereaus Instruments)
- Centrifuges: 5417R, 5804R (Eppendorf)
- D-Tube Dialyzer Midi rack and tubes (EMD Biosciences)
- Exposure Screen and Cassette (Kodak)
- Fujifilm FAS 4000 (Fujifilm)
- Fujifilm FLA-7000 PhosphorImager (Fujifilm)
- Heraeus Multifuge 3SR Plus Centrifuge (Heraeus Centrifuge UK)
- Illumina Genome Analyzer IIx (Illumina)

- Illumina HiSeq 2000 (Illumina)
- MilliQBiocel water purification system (Millipore)
- NanoDrop ND-1000 (NanoDrop Technologies)
- *Owl P10DS* Dual Gel Vertical Electrophoresis System (Bio-Rad)
- PAGE electrophoreses equipment (Invitrogen)
- pH Meter 537 (WTW)
- Qubit Fluorometer (Invitrogen)
- Roche LightCycler 480 Real-Time PCR System (Roche)
- Sorvall RC-6 Plus Superspeed Centrifuge (Thermo Scientific)
- Thermomixer (Eppendorf)
- Trans-Blot SD Semi-Dry Transfer Cell (Bio-Rad)
- Ultrasonic homogenizer Sonopuls HD 2070 (BANDELIN)
- Vortex-Genie 2 (Scientific Industries)
- UV crosslinker Stratalinker 2400 (Stratagene)
- Western blotting equipment (BioRad)
- XCell SureLock Mini-Cell Electrophoresis System (Invitrogen)

## 2.2 EXPERIMENTAL METHODS

### 2.2.1 Cloning of RBM10 into Gateway expression vector

#### 2.2.1.1 Total RNA extraction

Total RNA from HEK 293 Flp-In T-REx cells and lymphoblast cells respectively were extracted by TRIzol following the manufacturer's protocol. Briefly, 1 ml of TRIzol reagent (Invitrogen) was added to cells from per well of 6-well plate (or up to 10 million cells). The cells in TRIzol were homogenized by passing through a 26 G needle 8-10 times and incubated at room temperature for 5 min. After homogenization, 0.2 ml of chloroform was added to per mL TRIZOL lysate and mixed by vigorous shaking for 15 sec. The mixture was incubated at room temperature for 3 min, transferred to a pre-spun 2ml Phase-Lock-Gel tube (5 Prime), and centrifuged at 18,000 x *g* for 15 min at 4°C to separate phase. The upper aqueous phase containing RNA was carefully aspirated to a fresh, nuclease-free tube. The RNA was then precipitated by adding one volume of isopropanol and 1/10 volume of 5 M NaCl, and centrifuged at 18,000 x *g* for 10 min at 4°C. Finally, the RNA pellet

was washed with 75% ethanol, air-dried and dissolved in nuclease-free water. The dissolved total RNA was quantified by NanoDrop (NanoDrop Technologies) and the quality was assessed by Agilent 2100 Bioanalyzer (Agilent Technologies) according to the manufacturer's instructions.

#### 2.2.1.2 Reverse transcription (RT) and PCR

TRIzol extracted total RNA was treated with TURBO DNase (Ambion) following the manufacturer's protocol. Reverse transcription was performed using 1 µg of DNase treated total RNA, oligo $(dT)_{20}$ and Superscript III reverse transcriptase (Invitrogen) as following. 1 µg of DNase treated total RNA, 1 µl oligo $(dT)_{20}$ primer (50 µM), 1 µl dNTPs (10 mM each, Fermentas) and $H_2O$ was mixed to 13 µL volume, incubated at 65 °C for 5 minutes and placed on ice immediately for at least 2 min. Then 7 µl RT mix containing: 4 µL First Strand (FS) buffer (Invitrogen), 1 µL DTT (0.1 M, Invitrogen), 1 µl RNaseOUT (40 U/µl, Invitrogen) and 1 µl Superscript III (200 U/ µl, Invitrogen), was added to the reaction and gently mixed. The reaction was incubated at in a PCR block using the program: 50 °C 50 min, 70 °C 15 min, 4°C hold. The RT product was put on ice for following experiments or stored at -20 °C for 2-3 weeks.

The RT product was used as template to amplify the full length coding sequence (CDS) of RBM10 by Phusion High-Fidelity DNA Polymerase (Finnzymes) in the following 50 µL reaction system: 34.5 µl $H_2O$, 10 µL 5 x Phusion HF buffer, 1 µl dNTPs (10 mM each), 1 µL forward primer (10 µM), 1 µl reverse primer (10 µM), 0.5 µL Phusion Polymerase (2 U/µl) with PCR program: 98 °C 30 sec, (98 °C 10 sec, 70 °C 20 sec, 72 °C 2 min) x 35 cycles, 72 °C 10 min, 4 °C hold. The PCR product was purified by QIAquick PCR Purification Kit (Qiagen) according to the manufacturer's protocol and quantified by Nanodrop.

**Sequences of PCR primers:**

RBM10_CDS_Forward

5'-CACCATGGAGTATGAAAGACGTGGTGGTCG-3'

(CACC is the protruding sequence in pENTR/D-TOPO vector which entails the directional insertion of PCR product into the vector.)

RBM10_CDS _Reverse

5'-TCACTGGGCCTCGTTGAAGCGGGTC-3'

### 2.2.1.3 Cloning of RBM10 into Gateway expression vector

The purified full-length CDS of RBM10 wildtype (WT) and mutant (MUT) were ligated into pENTR/D-TOPO vector respectively according to the manufacturer's protocol. The ligated product was transformed into One Shot TOP10 chemically competent E. coli (Invitrogen) following the manufacturer's protocol. Colonies were picked out, screened by colony PCR using Gotaq polymerase (Promega) together with M13_F and RBM10_Ctrl_Rev primers (Table 2.1), and expanded in LB medium supplemented with 50 μg/ml kanamycin (Sigma). The plasmids were extracted using GeneJET Plasmid Miniprep Kit (Fermentas), quantified by Nanodrop and verified by Sanger sequencing using vector and RBM10 specific primers as listed in Table 2.1 (LGC Genomics, Germany).

| | Name | Sequences |
|---|---|---|
| **Colony screening** | M13-F | 5´-GTAAAACGACGGCCAG-3´ |
| | RBM10_Ctrl_Rev | 5'-CCAGGATGTTGAGGGAGTGCTGA-3' |
| **Sanger sequencing** pENTR/D-TOPO_RBM10 | M13-F (LGC Genomics, Germany ) | 5'-CCAGGGTTTTCCCAGTCACG-3' |
| | RBM10_Seq_1 | 5'-GCTGATGCGGAACAAATCT-3' |
| | RBM10_Seq_2 | 5'-CCTTCATCCAGCTCTCCAC-3' |
| | RBM10_Seq_3 | 5'-GCATCTACCAACAATCAGC-3' |
| | RBM10_Seq_4 | 5'-GCTTCCAGCCTATCAGCTC-3' |
| | SeqL-E (LGC Genomics, Germany) | 5'-GTTGAATATGGCTCATAACAC-3' |
| **Sanger sequencing** pFRT_TO_DEST FLAGHA_RBM10 | pFRT_TO_DESTFLAGHA forward primer | 5' -CGCAAATGGGCGGTAGGCGTG-3' |
| | pFRT_TO_DESTFLAGH reverse primer | 5'- TAGAAGGCACAGTCGAGG-3' |

**Table 2.1 Sequences of primers for colony screening and Sanger Sequencing.** Note that RBM10_Seq_4 is within the deletion identified in patient, therefore not used for verifying RBM10 MUT.

RBM10 was then exchanged from pENTR/D-TOPO into pFRT_TO_DESTFLAGHA vector by LR reaction using Gateway LR Clonase II enzyme mix (Invitrogen) following the manufacturer's protocol. The LR reaction product was transformed into

One Shot TOP10 chemically competent E. coli (Invitrogen) following the manufacturer's protocol. Colonies were picked out, screened by colony PCR using RBM10 specific primers: RBM10_CDS_Forward and RBM10_CDS _Reverse, and expanded in LB medium supplemented with 100 µg/ml ampicillin (Sigma). The plasmids were extracted using GeneJET Plasmid Miniprep Kit (Fermentas), quantified by Nanodrop and confirmed by Sanger sequencing using vector primers (Table 2.1) (LGC Genomics, Germany), generating the expression vector: pFRT_TO_DESTFLAGHA_RBM10 (Figure 2.1).

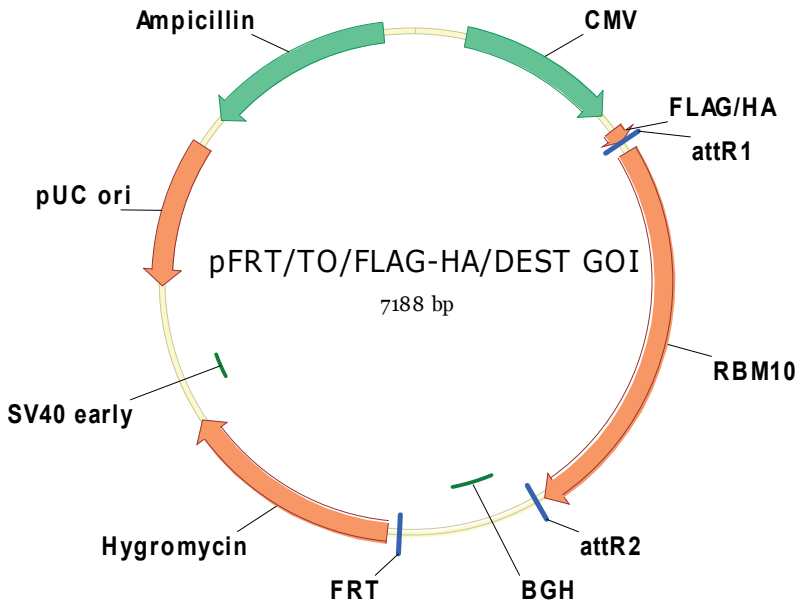


**Figure 2.1 Vector maps of pFRT_TO_DESTFLAGHA_RBM10.** Vector properties, including replication origins, antibiotic resistance and recombination sites, are shown.

### 2.2.2 Establishing stable cell lines

0.9 µg pOG44 and 0.1 µg pFRT_TO_DESTFLAGHA_RBM10 was mixed (maximum 3 µl) and transfected into one well of 12-well plate HEK 293 Flp-In T-REx cells using Lipofectamine 2000 following the manufacturer's recommendations. pOG44 only and pFRT_TO_DESTFLAGHA_ eGFP were transfected as negative and positive control respectively. Transfection efficiency was assessed by eGFP expression 24 hours after transfections. 48 hours after transfection, the cells were transferred to 10-cm cell culture plate and cultured with antibiotic-free medium (Materials 2.1.3) for 12 hours

until they attached to the bottom. Then selective medium (Materials 2.1.3) with appropriate antibiotics was added and changed every 2-3 days for a total 10-14 days until the distinct foci can be identified. 4-8 separate single colonies were carefully picked out by pipet tip, each of which was resuspended in 20 µl trypsin in one well of a conical bottom 96-well plate and incubated at room temperature for 5 min. 20 µl selective medium was added to each well and the cells were resuspended by pipetting up and down again. The resuspended cells were transferred into a flat bottom 96-well plate containing 80 µl/well of selection medium, cultured and expanded sequentially with selective medium to a 24-well plate, a 12-well plate, a 6-well plate and then a 10-cm plate, 15-cm plate respectively. The rest colonies were treated by typsin (Gibco), well resupended and directly cultured with selective medium in 6-well or 10-cm plate depending on the number of cells. During the cell expansion process, a small fraction of cells were prepared in one well of 6-well plate, induced with 1 mg/mL doxycycline for 16 hours and collected to assess the expression of target protein by western blot. A serial of doxycycline concentrations: 0, 10, 20, 50, 100, 200, 400, 1000 ng/mL respectively, were tested to obtain optimal protein expression levels for different experiments. Established stable cell lines were used for following experiments, or kept in freezing medium (Materials 2.1.3) and frozen in liquid nitrogen. All the cell culture was performed in a 37 °C incubator with 5 % $CO_2$.

### 2.2.3 PAR-CLIP

The PAR-CLIP method described here is modified from (Hafner et al. 2010; Lebedeva et al. 2011).

#### 2.2.3.1 4-thiouridine labeling, doxycycline induction and crosslinking

Stable HEK293 Flp-In T-REx cells inducibly expressing FLAG/HA-tagged RBM10 were grown in selective medium. Typically, ten 15-cm plates of 80 % confluent cells were used for one PAR-CLIP experiment. 4-thiouridine (4SU) and doxycycline (Dox) were diluted in selective medium together, added to the cells to the final concentration of 100 µM, 10 ng/mL respectively and incubated for 16 hours. After labeling and induction, the medium was aspirated from the plates and the cells were crosslinked on ice using Stratalinker (Stratagene) with 365nm UV-lamps (Energy setting: 1500 µJ x

100/cm$^2$). Cells were scraped off in cold PBS and pelleted by centrifugation at 1,000 x g for 5 min at 4°C.

#### 2.2.3.2 Cell lysis and immunoprecipitation (IP)

Crosslinked Cell pellet was lysed in 3 volumes of high salt lysis buffer (50 mM Tris-HCl pH 7.2, 500 mM NaCl, 1% NP40, 1 mM DTT, complete protease inhibitor (Roche)) and sonicated with ultrasonic homogenizer Sonopuls HD 2070 (BANDELIN) (settings: 45 SEC, CYCLE 2 x 10%, POWER 70 %). Cell lysate was cleared by centrifugation at 13,000 rpm for 15 min at 4ºC using Sorvall RC-6 Plus Superspeed Centrifuge (Thermo Scientific) and filtered through a 5 µm membrane syringe filter (Pall). The filtered lysate was partially digested with RNaseT1 (Fermentas) at a final concentration 1U/µl for 15 min in a room temperature water bath and subsequently cooled on ice for 5 min. RBM10-RNA complexes were immunoprecipitated from partially digested cell lysate using monoclonal anti-FLAG (Sigma, F1804) conjugated to magnetic Protein G Dynabeads (Invitrogen) and incubation for 1 hour at 4ºC on the rotation wheel. For 1 ml of cell lysate, 25 µl beads and 10 µg of antibody were used. Beads were washed three times with IP wash buffer (50 mM Tris-HCl pH 7.5, 300 mM KCl, 0.5% NP-40, 0.5 mM DTT, protease inhibitor cocktail) and resuspeneded in original bead volume of IP wash buffer, subsequently treated wtih RNase T1 at final concentration of 10 U/µl for 5 min in room temperature water bath. The RNase T1 treated beads were immediately washed three times with ice-cold high salt wash buffer (50 mM Tris-HCl pH 7.5, 500 mM KCl, 0.05% NP-40, 0.5 mM DTT, protease inhibitor cocktail), three times with 1x NEB buffer 3 and resuspended in one bead volume of NEB buffer 3 containing 0.5 U/µl Calf Intestinal Phosphatase (NEB). Dephosphorylation was performed at 37ºC in a thermomixer (Eppendorf) with shaking at 800 rpm for 30 min. Beads were then washed twice with phosphotase wash buffer (50 mM Tris-HCl pH 7.5, 20 mM EGTA, 0.5% NP-40), twice with PNK buffer without DTT (50 mM Tris-HCl pH 7.5, 50 mM NaCl, 10 mM $MgCl_2$) and then labeled with 5 µl $\gamma$-$^{32}$P-ATP (final concentration of 0.5µCi/µl) (Perkin-Elmer, NEG 502A) in PNK buffer with 5 mM DTT by T4 polynucleotide kinase (T4 PNK) (NEB). The labeling reaction was carried out at 37ºC with 800 rpm shaking for 30 min. ATP (Fermentas) was added to a final concentration of 100 µM and the reaction was further incubated for 5 min. After radioactive

labeling, the beads were washed five times with 800 µl PNK buffer without DTT and resuspended in 40 µl of 2x SDS-PAGE loading buffer (20% glycerol (v/v), 160 mM Tris-HCl pH 6.8, 4% SDS (w/v), 200 mM DTT, 0.2% bromophenol blue).

#### 2.2.3.3 SDS-PAGE and electroelution of RNA

Beads in SDS loading buffer were boiled at 95ºC for 5 min and placed on magnetic rank. The supernatant was loaded into two wells of an SDS gel (NuPAGE Novex 4-20% BT Gel, Invitrogen). The gel was run at 200 V for ~1 hour in 1 x MOPS SDS running buffer (Invitrogen), exposed for 10 min on a phosphorimaging screen and visualized on Fujifilm FLA-7000 PhosphorImager (Fujifilm). The radioactive band corresponding to RBM10-RNA complexes (~130 KDa) was cut out from the gel and placed into D-Tube Dyalyzer Kit MWCO 3.5kDa (Novagen). 800 µl 1 x MOPS SDS running buffer was filled into the tube and RBM10-RNA complexes were electroeluted from the gel for 1.5 h at 100V and 2 min by reversing the current in 1 x MOPS SDS running buffer. The elution containing RBM10-RNA complexes (~700 µl) was taken out into nuclease free low binding tubes (Eppendorf). Subsequently, RBM10 was digested by adding equal volume of 2 x proteinase K buffer (200 mM Tris-HCl pH 7.5, 150 mM NaCl, 12.5 mM EDTA, 2% SDS) with proteinase K (Roche) at final concentration of 2 mg/ml and incubation at 55ºC for 60 min. RNA was then recovered by phenol-chloroform extraction and ethanol precipitation with GlycoBlue (Ambion).

#### 2.2.3.4 RNA cloning and sequencing

Sequencing libraries were constructed using the small RNA cloning protocol (Hafner et al. 2008). The RNA pellet was resuspended in ligation mix containing: 2 µl of 10× RNA ligase buffer without ATP, 10 µl of PEG8000 (50%), 1 µl of 100 µM preadenylated 3'adapter, 6 µl H2O. The mixture was denatured at 95ºC for 30 sec and put on ice for 5 min. 1 µl T4 RNA Ligase K227Q (NEB, M0351S) was added and the reaction was incubated at 16 ºC for 16 hours. The radiolabeled 19 and 35 nt RNA markers were included as control. Ligation product was mixed with 20 µl 2 x formamide RNA loading dye (50 mM EDTA-NaOH pH 8.0, 0.05 % (w/v) Bromophenol blue in formamide), separated by 15% denatured PAGE (UreaGel -

SequaGel - System, National Diagnostics, EC-833) and exposed for at least 2 hours. The 3'adaptor ligated product and size markers were cut out from the gel and eluted by 0.4 M NaCl for 16 hours at 4ºC with 800 rpm shaking in thermomixer, respectively. The eluted RNA was precipitated by ethanol, using Glycoblue. The pellet was resuspended in 5'ligation mix containing: 2 µl of 10× T4 RNA Ligase buffer with ATP, 10 µl PEG8000 (50%), 5 µl $H_2O$ and 1 µl of 100 µM 5' ligation adapter and denatured at 95ºC for 30 sec. 2 µl T4 RNA Ligase 1 (NEB, M0204) was added and the reaction was incubated for 1.5 hours at 37ºC. The ligation product including size markers were separated by 12% denatured PAGE and exposed overnight. The 5'adaptor ligated product and size markers were cut out from the gel and eluted by 0.3 M NaCl for 16 hours at 4ºC with 800 rpm shaking in thermomixer. The eluted RNA was precipitated by ethanol with 1 µl of 100 µM reverse transcription (RT) primer, using Glycoblue. The RNA pellet was resuspended in 14.3 µl RT mix containing: 5.6 µl $H_2O$, 1.5 µl of 0.1 M DTT, 4.2 µl 10× dNTPs (2 mM each), 3 µl 5× First Strand buffer and denatured at 95ºC for 30 sec and put on ice. The mixture was incubated at 50ºC for 3 min, then 0.75 µl of Superscript III (invitrogen) was added and incubated at 42ºC for 30 min. After RT, 85 µl H2O was added to the reaction. The diluted reverse transcription (RT) product was amplified by Phusion polymerase in the following 50 µl reaction system: 27.75 µl H2O, 10 µl 5x Phusion HF buffer, 1.25 µl dNTPs (10 mM), 0.25 µl 5' PCR primer (100 µM), 0.25 µl 3' PCR primer (100 µM), 0.5 µl Phusion DNA Polymerase, 10 µl RT product. The optimal PCR cycle was determined by assessing aliquots of PCR products taken out from different cycles on 2.5% low melting agarose gel (Lonza). Three PCR reactions were setup with optimal cycle, precipitated by ethanol with glycoblue, re-dissolved in nuclease free $H_2O$, and separated by 2.5% low melting agarose gel (Lonza). The band within correct size range was cut out, extracted by Qiagen gel extraction kit and resuspended in 15 µl $H_2O$. The purified library was quantified by Qubit, the size range was assessed by Bioanalyzer DNA 1000 chip, sequenced on an Illumina HiSeq for 1 x 50 cycles following the manufacturer's protocol.

**Oligo sequences:**

3'adaptor (DNA except for the 5' riboadenylate (rApp) residue)

5' -rAppTCGTATGCCGTCTTCTGCTTGT-3'

(The barcoded 3' adaptors with 6 additional nucleotides at 5'end were used for multiplexing.)

5' adapter (RNA)

5'- GUUCAGAGUUCUACAGUCCGACGAUC-3'

RT primer (3' PCR primer) (DNA)

5' –CAAGCAGAAGACGGCATACGA-3'

5' PCR primer (DNA)

5' –AATGATACGGCGACCACCGACAGGTTCAGAGTTCTACAGTCCGA-3'

### 2.2.4 RBM10 knockdown

siRNA (Applied Biosystems, s15747 and 121554) against RBM10 was reverse transfected at a final concentration 20 nM with Lipofectamine RNAiMAX (Invitrogen) in HEK293 Flp-In T-REx cells following the manufacturer's protocol. Controls were treated with only transfection reagents. Cells were harvested 24, 48 and 72 hours after transfection respectively. Total RNA was extracted using Trizol (Invitrogen) and the quality was assessed by Agilent Bioanalyzer according to the manufacturer's instructions. The knockdown efficiency was assessed by qPCR and western blot.

**siRNA sequences:**

s15747_sense

5'-CCGCUGUGCUCAAAUCUGAtt-3'

s15747_antisene

5'-UCAGAUUUGAGCACAGCGGgt -3'

121554_sense

5'-GGUGUCGAUGCACUACAGUtt-3'

121554_antisense

5'-ACUGUAGUGCAUCGACACCtt-3'

### 2.2.5 RBM10 overexpression

Stable HEK293 Flp-In T-REx cells inducibly expressing FLAG-HA-tagged RBM10 was induced with 10 ng/mL doxycycline for 16 hours. Control was treated with equal

amount of medium. Total RNA was extracted using Trizol (Invitrogen) and the quality was assessed by Agilent Bioanalyzer according to the manufacturer's instructions. The overexpression efficiency was assessed by qPCR and western blot as described below.

### 2.2.6 mRNA sequencing

mRNA sequencing was performed using 1 μg total RNA following Illumina mRNA-Seq library preparation protocol (Illumina) as illustrated in Figure 2.2. Briefly, poly (A) RNA was isolated by two rounds of oligo $(dT)_{25}$ Dynabeads (Invitrogen) purification. Purified poly (A) RNA was fragmented at 94 ºC for 3.5 minutes using 5 x fragmentation buffer (200 mM Tris-Acetate, pH 8.1, 500 mM KOAc, 150 mM MgOA), as described in (Adamidi et al. 2011). The fragmented RNA were purified by Agencourt RNAClean XP SPRI beads (Agencourt, A63987) and converted to first strand cDNA using random hexmer primer (Invitrogen) and Supescript II (Invitrogen), followed by second strand cDNA synthesis with E.coli DNA pol I (Invitrogen) and RNAse H (Invitrogen) and Agencourt AMPure XP beads (Agencourt) purification. Then the paired-end sequencing library was prepared from purified double stranded (ds) cDNA either automatically using SPRI-TE Nucleic Acid Extractor (BECKMAN COULTER) following the manufacturer's instructions, or manually using NEBNext DNA Library Prep. Kit (NEB). In short, the ds cDNA was end repaired, A tailed and ligated with Illumina paired end sequencing adaptor (Illumina). Each step was purified by Agencourt AMPure XP SPRI beads (Agencourt). The purified ligated product was amplified by Phusion polymerase with the following PCR program: 98°C 30 sec, (98°C, 10 sec, 65°C 30 sec, 72°C 30 sec) x 15 cycles, 72°C 5 min, 4°C hold. The PCR product was then purified by Agencourt AMPure XP beads (Agencourt) as the sequencing library. The prepared library was quantified by Qubit using DNA HS kit (Invotrogen), quality assessed by Bioanalyzer, and sequenced on Illumina HiSeq for 2 x 100 cycles following the standard protocol.

**Oligos sequences used in solexa paired-end (PE) sequencing:**

PE Adapters

5'p-GATCGGAAGAGCGGTTCAGCAGGAATGCCGAG-3'

5' –ACACTCTTTCCCTACACGACGCTCTTCCGATCT-3'

PE PCR Primer 1.0

5'-AATGATACGGCGACCACCGAGATCTACACTCTTTCCCTACACGACGCTC TTCCGATCT-3'

PE PCR Primer 2.0

5'-CAAGCAGAAGACGGCATACGAGATCGGTCTCGGCATTCCTGCTGAACC GCTCTTCCGATCT-3'

PE Sequencing Primer

5' –ACACTCTTTCCCTACACGACGCTCTTCCGATCT-3'

5'- CGGTCTCGGCATTCCTGCTGAACCGCTCTTCCGATCT-3'

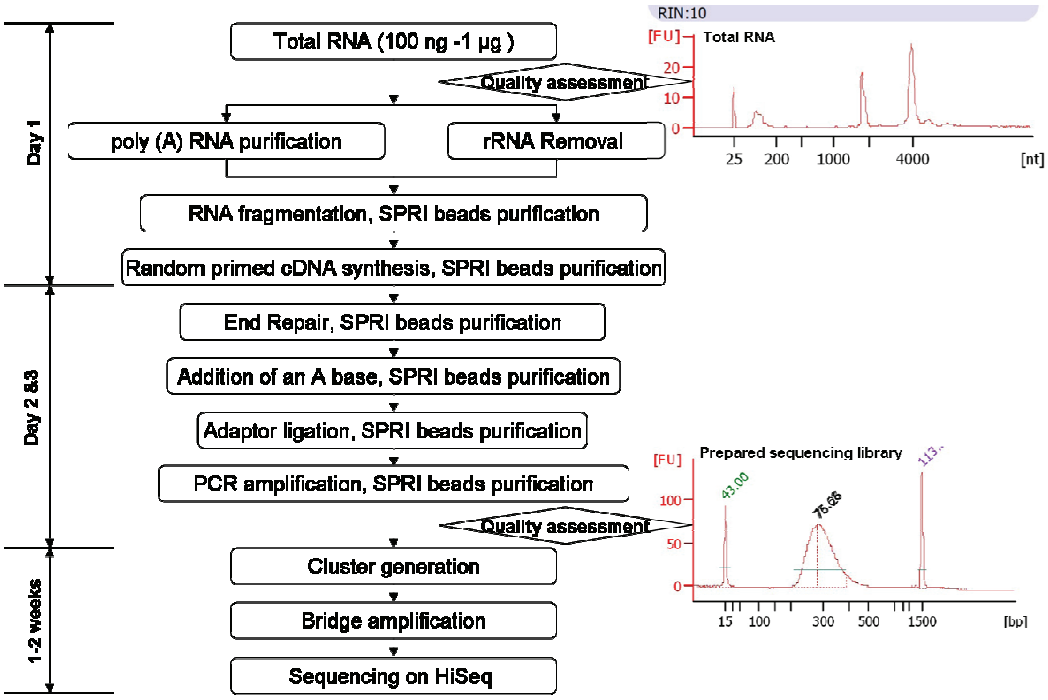


**Figure 2.2 Workflow of RNA_sequencing library preparation.** The quality of total RNA and prepared library were controlled by Bioanalyzer as exemplified on the right. SPRI: Solid Phase Reversible Immobilization (SPRI).

### 2.2.7 qRT-PCR

Trizol extracted total RNA was treated with TURBO DNase (Ambion) following the manufacturer's protocol. Reverse transcription was performed using 1 µg of DNase treated total RNA, random hexamer and Superscript III reverse transcriptase

(Invitrogen) according to manufacturer's protocol. qPCR was carried out using SYBRGreen Masrermix I (Roche) on LightCycler 480 (Roche) or using SYBRGreen Masrermix (Applied Biosystems) on ABI PRISM 7500 Sequence Detection Systems (Applied Biosystems) according to manufacturer's instructions. First stranded cDNA was diluted 1:20 and 2 µl was used as template in a 20 µl qPCR reaction system: 7 µl $H_2O$, 10 µl 2 x Master Mix, 0.5 µl Forward primer, 0.5 µl Reverse primer, 7 µl template. All assays were performed in triplicates. For expression quantification, the average fold change was calculated by normalization to *GAPDH*. For exon inclusion or exclusion quantification, the relative ratios were calculated by normalization to corresponding constitutive exons and compared between knockdown and control, overexpression and control, respectively. Sequences of all PCR primers are listed in Table 2.2.

| Targets | Forward | Reverse |
|---|---|---|
| **RBM10_5UTR** | 5'-CAGTCTCGGACTTGGTTGTTG-3' | 5'-CTTCCTGCAGGGACTCTTCTC-3' |
| **RBM10_CDS** | 5'-CTCTACTATGACCCCAACTCCCA-3' | 5'- GTCCGCCTCTCCCCATCCCA-3' |
| **RBM10_Pri** | 5'-GCAGGGAAGGACAGAGTGTT-3' | 5'- TGATTTGGTCAAGCCCTCTC-3' |
| **GAPDH** | 5'-TGCACCACCAACTGCTTAGC-3' | 5'-GGCATGGACTGTGGTCATGAG-3' |
| **PCBP2-C** | 5'-CGCCAAAATCAATGAGATCC-3' | 5'-CCAGTGATGGTAACCTGCCTA-3' |
| **PCBP2-I1** | 5'-TCAGTGGCATTGAATCCAGC-3' | 5'-TTATGCAGCCAATCAAATCG-3' |
| **PCBP2-I2** | 5'-ACACCGGATTCAGTGCAGGT-3' | 5'-CGATTATGCAGCCAATCAAAT-3' |
| **SAT1-C** | 5'-TGAGGAACCACCTCCTCCTA-3' | 5'-TTGATCAGCCGCAGTATGTC-3' |
| **SAT1-I1A** | 5'-CGGAAGGTTACAGTCTCTAGC-3' | 5'-GCAAAACCAACAATGCTGTG-3' |
| **SAT1-I1B** | 5'-CTGGACTCCGGAAGGTTACA-3' | 5'-TGCTGTGTCCTCATTTATCATG-3' |
| **SAT1-I2** | 5'-CACTGGACTCCGGAAGGACA-3' | 5'-GATCCTATGCCAAAGCCTCT-3' |
| **POLDIP3-C** | 5'-TCGAATCAAAGGGAAAGTGC-3' | 5'-AGGGGAACTCCTCTTCAAGC-3' |
| **POLDIP3-I1** | 5'-CCATCCAGGTTCCACAGCAG-3' | 5'-GTTTGGCCTGGTGGTTATTG-3' |
| **POLDIP3-I2** | 5'-CACCAAAACCATCCAGAATTTA-3' | 5'-CCTGAGGCTGCAAACTTCAT-3' |
| **PDHA1-C** | 5'-TGGCAGCTTTGTGGAAATTA-3' | 5'-CAGGAATGAAATCGCCTCTC-3' |
| **PDHA1-I1** | 5'-CATCGTGGGAGCGCAGGTG-3' | 5'-CGAATATCTGGCCCTGGTTA-3' |
| **PDHA1-I2** | 5'-ATCGTGGGAGCGCAGGGC-3' | 5'-TCAACAGACGTTCCCATTCC-3' |
| **CASP8-C** | 5'-TGGAGAAGAGGGTCATCCTG-3' | 5'-TCTTGTTGATTTGGGCACAGA-3' |
| **CASP8-I1** | 5'-CAGCAAAGAGAGAAGCAGCAG-3' | 5'-TGGAGAGTCCGAGATTGTCAT-3' |
| **CASP8-I2** | 5'-TGGAGAAGAGGGTCATCCTG-3' | 5'-CACACAACTCCTCCCCTTTG-3' |
| **NCOR2-C** | 5'-CGCTCAAGGCAGAGAAGAAG -3' | 5'-GGTAGCACTGGAGTCGCTGT -3' |
| **NCOR2-I2** | 5'- GTGGAGGATGAGGAGATGGA -3' | 5'- GTTGTTGACAGTGGCTTCAG -3' |
| **LEF1-C** | 5'-TGGCAGCCCTATTTCAGTTT-3' | 5'-TGCAAACCAGTCTGCTGAAC-3' |
| **LEF1-I1** | 5'-CAGGAATCTGCATCAGGTACA -3' | 5'-GGAATGAGCTTCGTTTTCCA-3' |
| **LEF1-I2** | 5'- CAGGAATCTGCATCAGGTGG -3' | 5'- ACAGTCTGGGTTTTCAACAAG -3' |

| | | |
|---|---|---|
| **CREBBP-C** | 5'-AACGTCCAGTTGCCACAAG-3' | 5'-ACTGAGCCCATGCTGTTCAT-3' |
| **CREBBP-I1** | 5'-CATGCAAGTTTCTCAAGGGAT-3' | 5'-TGGACAGAGTGGTTCATTGG-3' |
| **CREBBP-I2** | 5'-CCTGTGAGACCTCCAAGGAT-3' | 5'-AGCCCATGCTGTTCATCTG-3' |
| **RBM5-C** | 5'-TTGGTGATTCAAGGAAAGCAC-3' | 5'-CAAAGCCAATCTTCAAACTTAGG-3' |
| **RBM5-I1A** | 5'-GGATGGAAGCCAATCAGAAA-3' | 5'- CAAACTTAGGTCTGGGATTGC-3' |
| **RBM5-I1B** | 5'-CGCCTTCGTGGAGTTTTATC-3' | 5'- CCTTGAATCACCAACTTTTTCTG-3' |
| **RBM5-I2** | 5'-GCTGATGAAGAGGAAAACAGAAA-3' | 5'-CAAACTTAGGTCTGGGATTGC-3' |
| **CLK2-C** | 5'-CGGGGAGATGCCTACTATGA-3' | 5'-GCTGCGGTAACTGCTGTTC-3' |
| **CLK2-I1** | 5'-CCGCTCATCTTCGCACAG-3' | 5'-GTCCCCTCTCCTAAGGTGCT-3' |
| **CLK2-I2** | 5'-AATATCAGCGGGAGAACAGC-3' | 5'-GGTGCTAACGATTTCATCGAAG-3' |
| **ATG16L1-C** | 5'-CCCCAGGACAATGTGGATAC -3' | 5'-CACACAAGGCAGTAGCTGGT-3' |
| **ATG16L1-I1** | 5'-CAGAGCAGCCACTAAGCGAC-3' | 5'-GGGACTGGGAAGGAAGAGAC-3' |
| **ATG16L1-I2** | 5'-AGCAGAGCAGCCACGAGAC-3' | 5'-CACACAAGGCAGTAGCTGGT-3' |
| **HOTAIR-C** | 5'-CGCAGTGGAATGGAACGGA-3' | 5'-AACTCTGGGCTCCCTCTCTC-3' |
| **HOTAIR-I1** | 5'-TGCTCTCAATCAGAAAGGTCC -3' | 5'-AACTCTGGGCTCCCTCTCTC-3' |
| **HOTAIR-I2** | 5'-ACTGCTCCGTGGGGTCCT-3' | 5'-AACTCTGGGCTCCCTCTCTC-3' |
| **NPNT-C** | 5'-TGTCGTTATGGTGGGAGGAT-3' | 5'-TGACACTGTCCCCAAGACTG-3' |
| **NPNT-I1** | 5'-GGGACAGTGTCAGCCTTTCT-3' | 5'-GTGGTTGGCACACAGCTTTG-3' |
| **NPNT-I2** | 5'-TGGCCTATGTCGTTATGGTG-3' | 5'-TGGTTGGCACACAGGCTG-3' |
| **PHACTR2-C** | 5'-TGCCTCAGACACTCCAGTTG-3' | 5'-GTTCTGTTCGTCGGCTCTTC-3' |
| **PHACTR2-I2** | 5'-GGCAGAAGATAAGAAAGCTGG-3' | 5'-TGAGGTGGATGAAGTGGATG-3' |
| **BCOR-C** | 5'-GCCGACTGGGAAAGGTTGAA-3' | 5'-GTTCTGCAATGGCCTCCTCC-3' |
| **BCOR-I1** | 5'-CCGCTGCTTACTGTGAGCGT-3' | 5'-AGTCTTTGGTTGCTGGGTGG-3' |
| **BCOR-I2** | 5'-CAACGGGCATTGCAGCGT-3' | 5'-AGTCTTTGGTTGCTGGGTGG-3' |
| **SPTAN1_C** | 5'-GGAACTGGGTGAGAAGCGTA-3' | 5'-CTCCGACCTCCTCACTTGTC-3' |
| **SPTAN1_I1** | 5'-GGAGCAGATTGACAATCAGAC-3' | 5'-CCAACATGCCTTTACGCTTC-3' |
| **SPTAN1_I2** | 5'- AGGAGCAGATTGACAATCAATA -3' | 5'-TCGCTTCACGGAACAACATA-3' |
| **UBN1_C** | 5'-GGCTTCACCCTACAAATCCA-3' | 5'-TGGACAGGAATAGGGACAGG-3' |
| **UBN1_I1** | 5'- CCTGTCCATGTGCTCTCCTT-3' | 5'-AGTGCAAGCCAGCCAGAAG-3' |
| **UBN1_I2** | 5'-CCTGTCCATGTGCTCTCCTT-3' | 5'-GTGAAGCTGAGAAGCACTGT-3' |

**Table 2.2 Sequences of qPCR primers.** UTR: untranslated region; CDS, coding sequence; Pri, primary. I1 (A/B) represents PCR primer specifically amplifying the transcript isoform with the respective exon included; I2 represents PCR primer specifically amplifying the isoform with the respective exon excluded; C represents PCR primer amplifying the neighboring constitutive exon.

### 2.2.8 Western blot

Cells were lysed in RIPA lysis buffer (50 mM Tris pH 8.0, 150 mM NaCl, 1.0% NP-40, 0.5% sodium deoxycholate, 0.1% SDS, complete protease inhibitor (Roche)) and

sonicated by using Biorupter (UCD-300, Diagenode) with the setting: high energy mode, 10 cycles, 30 sec-on and 30 sec-off each. Additional cycles were performed if the cell lysate was viscous after sonication. The cell lysate was centrifuged at 18,000 x g for 10 min at 4°C. The supernatant in 1 x SDS-PAGE loading buffer was boiled at 95°C for 5 minutes, centrifuged at 18,000 x g for 2 min and resolved by 10% SDS-PAGE in 1 x SDS running buffer (25 mM Tris base,190 mM glycine, 0.1% SDS) at 160 V for ~1 hour until the dye runs to the bottom of the gel chamber. Proteins were transferred to PVDF membrane (GE healthcare) using semi-dry blotting apparatus (BioRad) at 20 V for ~1 hour for RBM10. The membrane was blocked in 5% non-fat milk, washed once with 1 x TBST (50 mM Tris.HCl, pH 7.4, 150 mM NaCl, 0.1% Tween 20) and incubated with primary antibody diluted in 1 x TBST for 1 hour at room temperature or 4°C overnight with gentle shaking. After primary antibody incubation, the membrane was washed three times with 1 x TBST, 5 min each, and incubated with HRP-conjugated secondary antibody at room temperature for 1 hour. The secondary antibody incubated membrane was washed three times with 1 x TBST, 5 min each, developed with SuperSignal Kit (Thermo) and detected by LAS-4000 imaging system (Fujifilm) following the manufacturer's instructions. The following antibodies were used: rabbit polyclonal anti-RBM10 (Abcam, ab26046, 1:2000), mouse monoclonal anti-HA (Covance, MMS-101P, 1:4000), monoclonal anti-FLAG (Sigma, F1804, 1:4000), and secondary HRP-conjugated goat anti-mouse or human IgG (Santa Cruz, 1:2000).

### 2.2.9 Immunofluorescence

The cells were induced with appropriate concentration of doxcycline for 16 hours when induction of the protein expression is needed. Cells grown on sterile cover slides were gently washed once with 1 x PBS, fixed with freshly prepared 3.7% paraformaldehyde (PFA) (Invitrogen) in 1 x PBS for 20 min at room temperature, and rinsed for 2 min in 1 x PBS. The fixed cells were permeabilized in 0.1% Triton X-100 in 1 x PBS for 15 min at room temperature, washed 3 times with 1 x PBS, and blocked by 5.0% BSA in PBS for 1 hour at room temperature. The blocked cells with the excess blocking solution drained away were transferred to humid chamber, incubated with 200 µl primary antibody freshly diluted at in antibody dilution solution

(0.5% BSA in PBS) for 2 hours at room temperature or 4 °C overnight. Subsequently, the cells were washed 3 times with 1 x PBS, 5 min each, and blocked for 20 min at room temperature. After draining away the blocking solution, the cells were incubated with 200 µl fluorochrome-conjugated secondary antibody freshly diluted in antibody dilution solution for 40 min at room temperature. After draining away the excess secondary antibody solution, the cells were stained with 1:5000 DAPI (Invitrogen) diluted in antibody dilution solution for 5 min at room temperature, washed 3 times with 1 x PBS, 5 min each, and air dried. The dried cells were then mounted on the microscopic glass slide with Prolong Gold Antifade Reagent (Invitrogen) and observed under Leica SP5 confocal microscope (Leica) following the manufacturer's manual. The following antibodies were used: rabbit polyclonal anti-RBM10 (Abcam, ab26046, 1:200), rabbit polyclonal anti-RBM10 (NB100-55265, 1:200), mouse monoclonal anti-HA (Covance, MMS-101P, 1:400), Alexa Fluor 488 goat anti-rabbit IgG (Invitrogen, A-11034, 1:400), and Alexa Fluor 568 goat anti-mouse IgG (A-11004, 1:600).

## 2.3 COMPUTATIONAL METHODS

### 2.3.1 PAR-CLIP analysis

The PAR-CLIP analysis is performed using a custom computational pipeline described in (Lebedeva et al. 2011) and briefly summarized below.

#### 2.3.1.1 Reads mapping and cluster identification

PAR-CLIP barcode-adapter sequences were removed from the read ends using FAR (http://sourceforge.net/projects/theflexibleadap/). After adaptor removal, reads were aligned to the human reference genome hg19 (Fujita et al. 2011) using BWA 0.5.9-r16 (Li and Durbin 2009) without seeding and allowing for one mismatch. Unique alignments on the reference genome hg19 were converted into BAM format using SAMtools 0.1.18 (Li et al. 2009a). Binding clusters were identified as continuously covered sequence regions comprising of overlapping reads and further filtered by two criteria: (a) the number of T to C conversions; (b) an entropy score reflecting the sequence variability of reads within the cluster, considering that redundant reads are likely to be PCR artifacts. The cutoffs for the number of T to C conversions and the

entropy score were chosen to obtain a false positive rate of less than 5% by treating antisense-clusters as false positives.

#### 2.3.1.2 Overlapped cluster definition

We first identified binding clusters for each biological replicate separately and then defined overlapped clusters to create a set of highly confident binding clusters, which were obtained requiring the preferred crosslinking sites, i.e. the position with highest number of T to C conversions within a cluster, to be within the binding regions identified in both replicates.

#### 2.3.1.3 Binding sites annotation and target transcript identification

Reproducible clusters were aligned to all UCSC RefSeq transcripts (Fujita et al. 2011). For each reproducible cluster, the genomic location of the binding site was determined by the position with the highest number of conversion events, as this position most likely represents the preferred position for crosslinking. Transcripts containing at least one reproducible binding cluster were identified as RBM10 targets. In addition, the distribution of PAR-CLIP reads along intron-exon and exon-intron junctions was computed to investigate the binding preference.

#### 2.3.1.4 Motif analysis

41nt windows centered on preferred crosslink sites of identified exonic and intronic binding clusters were compared with corresponding random background respectively. The resulting enriched 7 and/or 5-mers were aligned to generate a sequence consensus as the sequence motif.

#### 2.3.1.5 Analysis for snRNA binding analysis

Sequencing reads from the PAR-CLIP experiments for: RBM10, AGO2 and HuR were mapped to all snRNAs annotated in ENSEMBL (Hubbard et al. 2002) using BWA without seeding and allowing for two mismatches. The fraction of mappable reads to each type of snRNA is summarized in piecharts. To further study RBM10 binding on two specific snRNAs (U2 and U6), sequencing reads were mapped onto

the U2 and U6 consensus sequences as obtained from (Patel and Steitz 2003) using BWA with the same parameters as above.

### 2.3.2 RNA-sequencing analysis

#### 2.3.2.1 Quantification of gene expression

The gene expression levels were estimated by RPKM (reads per kilobase of exon per million mapped RNA-Seq reads, (Mortazavi et al. 2008)) using uniquely mappable reads. Differentially expressed genes were determined by a sliding window method motivated by Yang et. al. (Yang et al. 2002). A Z-value was defined as the gene expression change (i.e. the difference between the $\log_2$ RPKM values) divided by the standard deviation of the gene expression changes of the 1% genes having a similar expression level and was computed for each gene. Genes showing significant expression level changes were identified by combining the rankings of different biological replicates using the rank product method (Hong et al. 2006).

#### 2.3.2.2 Quantification of alternative splicing

RNA-Sequencing reads were mapped against a set of sequences containing all Refseq transcript exons (UCSC Genome Browser) as well as all possible exon-exon junctions between all ordered pairs of exons from the same gene. The number of spliced-in reads and spliced-out reads were counted for each exon. A spliced-in read for a given exon can be mapped only to this exon or to junctions with this exon, where the read and the exon must overlap by at least 6 bp. A spliced-out read for a given exon can either be mapped only to exon-exon junctions skipping the given exon (where the read overlaps with both exons of the junction by at least 6 bp), or it is a spliced-in read of an incompatible exon, which belongs to the same gene but cannot be spliced together because they overlap but have different 5' or 3' ends. The percentage spliced in (PSI) value of an exon is the number of spliced in reads divided by the sum of spliced in and spliced out reads. The Z-value of an exon splicing change is the PSI-value change between two conditions divided by the standard deviation of the PSI-value changes of the 1% exons with similar read count. Finally, the replicates were combined with the rank product method (Hong et al. 2006) applied to lists of exons ordered by their Z-values.

# 3 RESULTS

## 3.1 Identification of an in-frame deletion within RBM10 in patients afflicted with an X-linked recessive disorder

In a large scale X-chromosome mutation screening project, using exome sequencing, we and our collaborators at Max-Planck-Institute for Molecular Genetics, identified a deletion of 1292 nt (chrX:47,044,423-47,045,714, hg19) in *RBM10* as the causative mutation in patients from a family affected with an X-linked recessive disorder characterized by multi-organ malformations, including cleft palate, muscular dystrophy, severe mental retardation, hearing loss and ventricular septal defect etc (Figure 3.1A and 3.1B) (manuscript in revision). It removed six exons of *RBM10.* Based on the gene annotation, the deletion did not disrupt the open reading frame of RBM10, and instead removed, 239 amino acids from the encoded protein (651 to 889 at NP_005667), spanning the second zinc finger domain and partially G patch domain (Figure 1.9). We confirmed the expression of RBM10 mutant (MUT) and wild type (WT) by RT-PCR and western blot in patient and healthy control derived lymphoblast cells. Both mRNA and protein of RBM10 MUT expressed at similar levels in patient derived cells as WT in the control, but with a smaller size, as expected (Figure 3.1C and 3.1D).

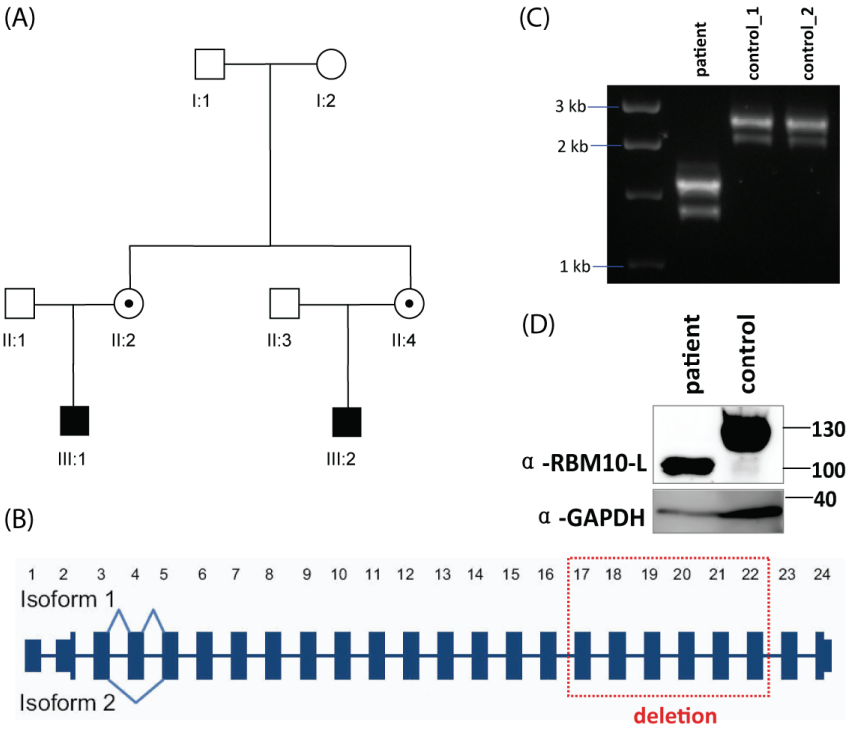


**Figure 3.1 Identification of an in-frame deletion within RBM10 in patients affected with an X-linked recessive disorder.** (A) The pedigree of the afflicted family. Two affected males are marked as black boxes, and two female carries are indicated as cycles with a dot in the centre. (B) Cartoon of *RBM10* gene structure and the deletion found in patients. The deletion locates at chrX between 46929367 bp and 46930658 bp (hg18), and spans 6 exons ($17^{th}$-$22^{nd}$ exon) of *RBM10*. (C) RT-PCR and (D) western blot performed in patient and healthy control derived lymphoblast cells demonstrated that mRNA (C) and protein (D) of RBM10 MUT from patient derived cells expressed at a similar level as WT in the control, but with a smaller size. In C, both splicing splicing isoforms (see B) can be detected, with large isoform (isoform 1) expressing at higher level. In D, only isoform 1 was investigated using the isoform specific antibody.

## 3.2 Establishment of stable HEK293 cell lines

Although the antibodies against endogenous RBM10 are commercially available, their isoform specificity and sensitivity appeared not to be high enough for the experiments such as immunoprecipitation. To overcome such limitations, we chose to establish the

stably transfected HEK293 cell lines that can express a FALG-HA tagged RBM10 protein in a doxycycline (Dox)-dependent manner. In brief, we first obtained the full length coding sequence (CDS) with stop codon for both RBM10 WT and MUT from HEK293 cells and patient derived lymphoblast cells respectively by RT-PCR (Figure 3.2A and Figure 3.1C), and then cloned them into expression vector, which was transfected into the HEK 293 Flp-In T-REx cell line. After antibiotics selection and expansion, we obtained stable cell lines inducibly expressing of FLAG/HA tagged RBM10 WT and MUT respectively. The expression of RBM10 induced with 1 mg/mL Dox was confirmed by western blot using monoclonal anti-HA. To control and optimize RBM10 overexpression level, we monitored the expression levels of RBM10 WT induced by a serial of Dox concentrations for 16 hours and observed that RBM10 expression level increased with increasing Dox concentrations (Figure 3.2B). We chose 10 ng/mL Dox induction for further experiments, at which exogenous tagged RBM10 was expressed to several fold compared with endogenous level as illustrated in Figure 3.3B using antibody specific to RBM10 large isoform.

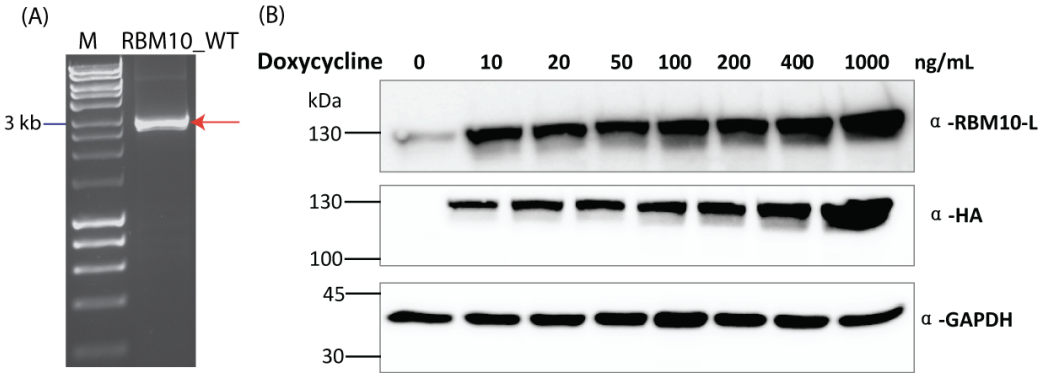


**Figure 3.2 Construction of stable HEK293 cell lines inducibly expressing FLAG/HA tagged RBM10 WT and MUT respectively.** (A) RT-PCR products of full length CDS with stop codon for RBM10 WT from HEK293, as marked with red arrow. (B) RBM10 overexpression level increased with elevated doxycycline (Dox) concentration. RBM10 expression level induced with different concentrations of Dox were detected by antibody specific to RBM10 large isoform (α_RBM10_L) and HA tag (α-HA), respectively. GAPDH was included as a control.

## 3.3 PAR-CLIP reproducibly identifies RBM10 Binding Sites

To precisely identify *in vivo* binding sites of RBM10, we performed PAR-CLIP (Hafner et al. 2010; Lebedeva et al. 2011) (MATERIALS AND METHODS) in HEK293 cells inducibly expressing epitope-tagged RBM10 isoform 1, the major isoform expressed in HEK293. 4-thiouridine (4SU) labeled and crosslinked cells were immunoprecipitated with monoclonal anti-FLAG. The bound RNAs was then partially digested and radioactively labeled. Protein-RNA complexes were resolved on a denaturing gel. The band corresponds to RBM10-RNA complexes were excised (Figure 3.3A). The RNA was recovered, converted in to cDNA and sequenced with Illumina platform. In total, we performed two biological replicates for RBM10 wild type (WT). The sequencing reads were processed and clustered as described in MATERIALS AND METHODS. In all the mappable sequence reads, T to C conversions were significantly enriched compared with all other mutations (Figure 3.3B), manifesting efficient RBM10-RNA crosslinking (Hafner et al. 2010). Most clusters are between 30 nt to 80 nt, with the median size of 37 and 57 nt in two replicates, respectively (Figure 3.3C), demonstrating the high spatial resolution of our PAR-CLIP experiment in determining RNA binding sites. The sequencing and analysis results were summarized in Table 3.1. Requiring at least one T to C conversion in one cluster, we identified 240,172 and 218,281 putative RBM10 binding clusters in the two replicates respectively. Requiring the preferred crosslinking sites, i.e. the position with highest number of T to C conversions within a cluster, to be within the binding regions identified in both replicates, we defined a total of 89,247 highly confident binding clusters (Figure 3.4A). Comparison of the scores of these clusters between the two replicates revealed high correlation (R = 0.797) (Figure 3.4B). Based on these overlapped clusters, we identified 6,396 RBM10 target genes.

| Replicates | # Reads (Non-redundant) | # Mappable Reads | % Mappable Reads | # Uniquely Mappable Reads | # Clusters | # Target Transcripts |
|---|---|---|---|---|---|---|
| Rep 1 | 6,239,308 | 4,313,114 | 69.13% | 2,642,259 | 240,712 | 11,015 |
| Rep 2 | 15,164,275 | 11,077,176 | 73.05% | 6,236,162 | 218,281 | 9,935 |

**Table 3.1 Summary of PAR-CLIP sequencing results, identified clusters and target transcripts for two replicates.**

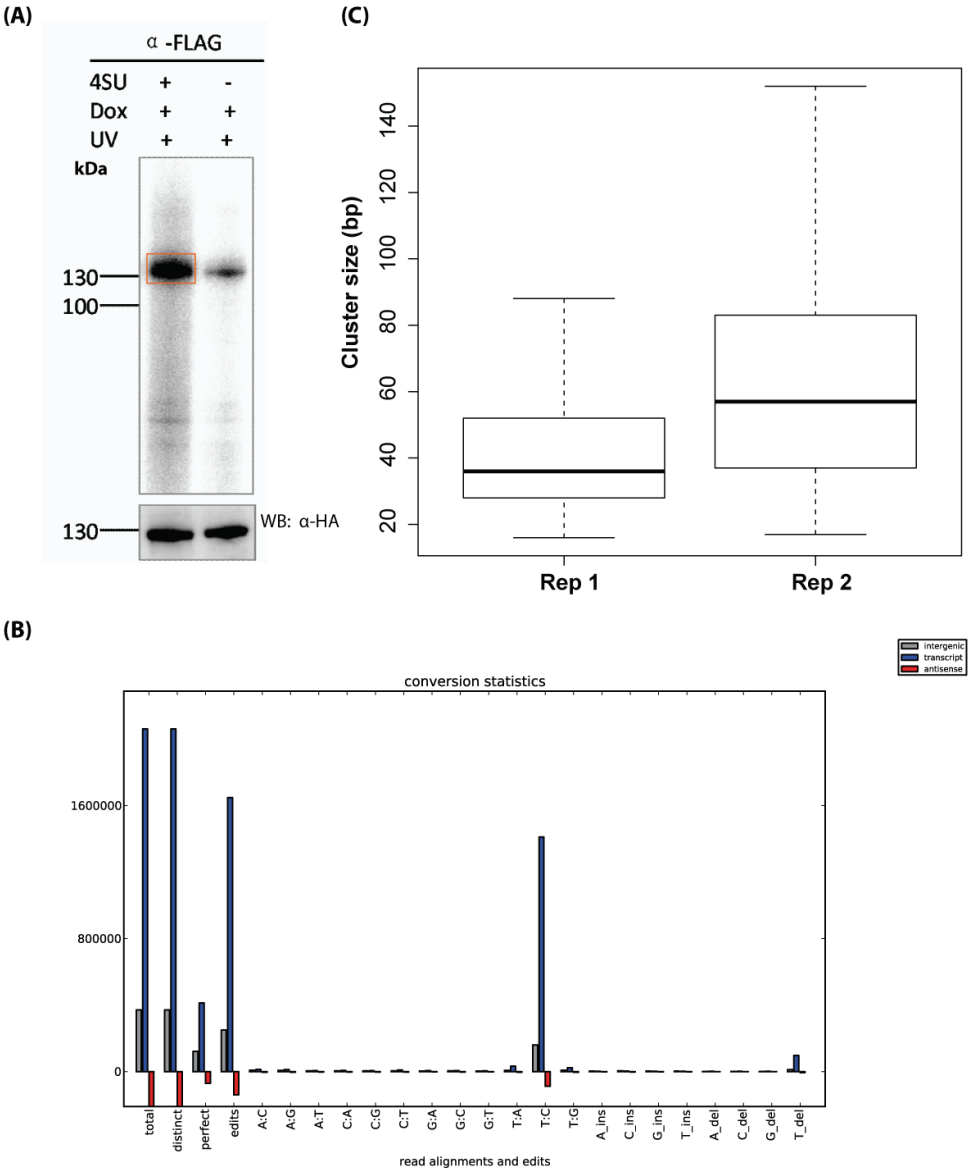


**Figure 3.3 PAR-CLIP experiments.** (A) Autoradiograph of representative PAR-CLIP results. $^{32}$P labeled RBM10-RNA complexes were resolved by SDS-PAGE. RBM10-RNA complexes marked in red box were used for library preparation and sequencing. Cells without 4-thiouridine (4SU) were included as a control. Lower panel showed RBM10 protein expression detected by western blot with HA antibody. Dox: Doxycycline. (B) Distribution of different types of mismatches in aligned reads. T to C conversion and T deletions, the signature for efficient crosslinking, was highly enriched among all types of conversions and deletions respectively in the sequencing reads, especially those aligned on the sense strand of RNA transcripts. Blue: sense;

red: antisense; grey: intergenic. (C) Length distribution of RBM10 binding clusters from two biological replicates.

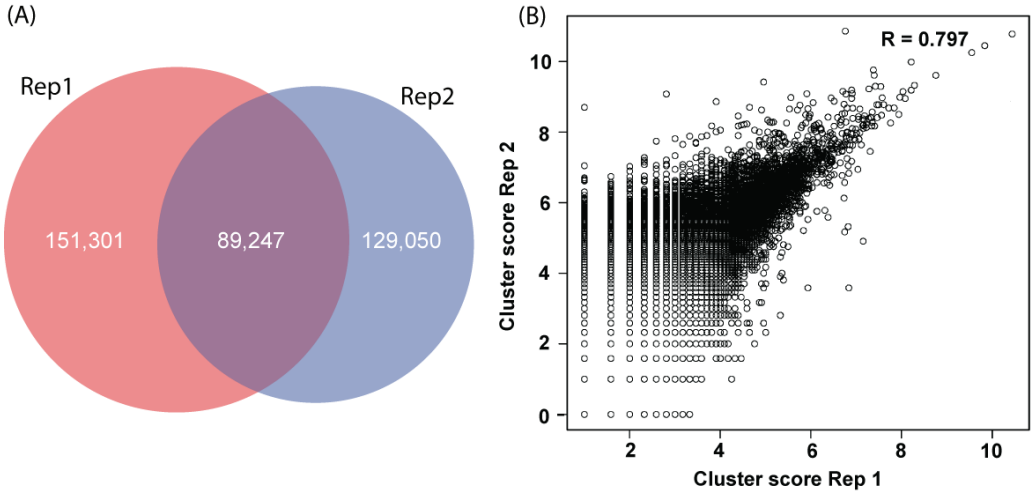


**Figure 3.4 PAR-CLIP reproducibly identifies RBM10 binding sites.** (A) Overlaps of binding clusters between two biological replicates. Clusters were considered overlapped when the preferred crosslinking sites fall in the overlapping regions. (B) Cluster score calculated based on number of T to C conversions ($\log_2$ scale) for the overlapped clusters were significantly correlated between replicates ($R = 0.797$).

## 3.4 RBM10 binds preferentially in the vicinity of splice sites

The majority of the consensus binding clusters are within coding sequence (CDS) and introns (Figure 3.5A). In particular over half the clusters falls in introns, consistent with the predominantly nuclear localization of RBM10 (Inoue et al. 2008) (Figure 3.13A). Given the possible involvement of RBM10 in splicing process, we examined the distribution of PAR-CLIP reads relative to splice sites (MATERIALS AND METHODS). Intriguingly, we found that PAR-CLIP reads were significantly enriched in exons and in the vicinity of both 5'and 3' splice sites of the flanking introns (Figure 3.5B), compared with the randomly selected regions in the same set of protein coding genes. Notably, the PAR-CLIP reads were ~2 fold more enriched at the vicinity of (~ 70 nt upstream) of 3' splice site than that at 5' splice site. Such preferential binding of RBM10 suggests that RBM10 might play crucial roles in splice site recognition, in

particular that of 3'splicing sites, and/or splice site pairing in splicing process. This is consistent with the previous finding that RBM10 is a component of prespliceosomal complex and could interact with several proteins components of U2 snRNP complex (Behzadnia et al. 2007; Hegele et al. 2012).

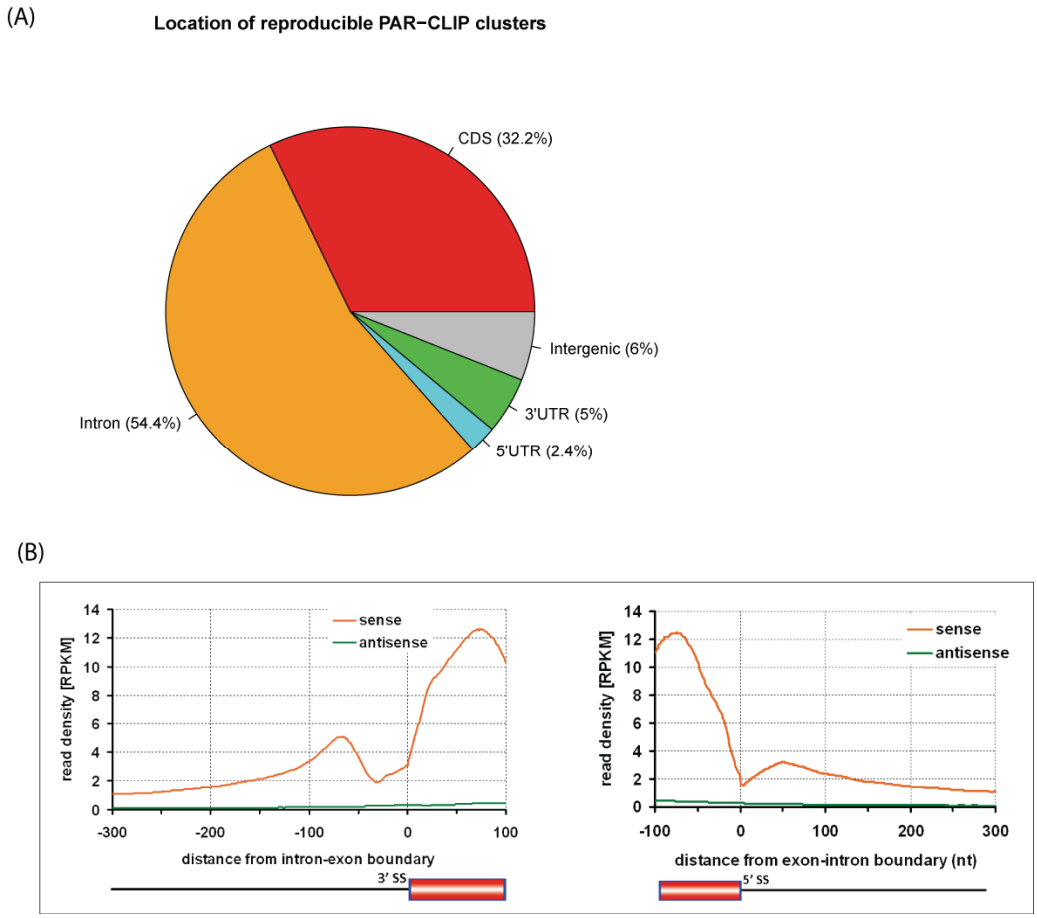


**Figure 3.5 RBM10 binds preferentially in the vicinity of splice sites.** (A) Distribution of overlapped binding clusters in target transcripts based on refseq pre-mRNA annotations. CDS: coding sequence; UTR: untranslated region. (B) Distributions of PAR-CLIP reads along intron-exon and exon-intron boundaries revealed enriched binding to the vicinity of both 3' splice site (3'ss) and 5' ss as well as exonic regions. Reads density was calculated as RPKM unit, i.e. reads per kilobase of nucleotides per million mapped sequence reads; sense and antisense reads density were displayed as red and green respectively; exon and intron were indicated as red box and black line respectively.

## 3.5 RBM10 binds to splicing snRNAs

After identifying the binding sites in the pre-mRNA targets, we carefully checked whether and how RBM10 was associated with splicing snRNAs, considering that splicing regulators might associate with pre-mRNA substrates and spliceosomal snRNPs concomitantly to control the splicing outcomes (Chen and Manley 2009; Will and Lührmann 2010). For this purpose, we mapped PAR-CLIP reads to snRNA gene locus allowing up to 2 mismatches and calculated the reads distribution for both major and minor spliceosomal snRNAs (MATERIALS AND METHODS). As shown in Figure 3.6A, the majority of the reads were located in U2. This distribution is different from another two RBPs: AGO2 and HuR analyzed by PAR-CLIP under the same conditions (Figure 3.6B and C), which implicated the preferential binding of RBM10 on U2 snRNA cannot be due to the cellular abundance of U2 snRNA or experimental artifact. To examine the binding of RBM10 on U2 snRNA in more detail, we calculated the PAR-CLIP reads density, together with the number of T to C conversion events along the U2 consensus sequences. As shown in Figure 3.6D-F, compared with AGO2 and HuR, RBM10 not only exhibited significantly higher number of PAR-CLIP reads mapped on U2 (RPM (Reads per million mappable sequencing reads): 51 vs. 7.8, 3.3) but also considerably higher T to C conversion events at the two crosslinking positions depicted in Figure 3.6G, further demonstrating genuine and specific binding between RBM10 and U2 snRNA. Interestingly, based on proteomic study, RBM10 was found in pre-spliceosomal A complex, where U2 snRNA binds the branch site close to 3’ splicing sites, consistent with the enrichment of RBM10 binding near 3’ splicing sites.

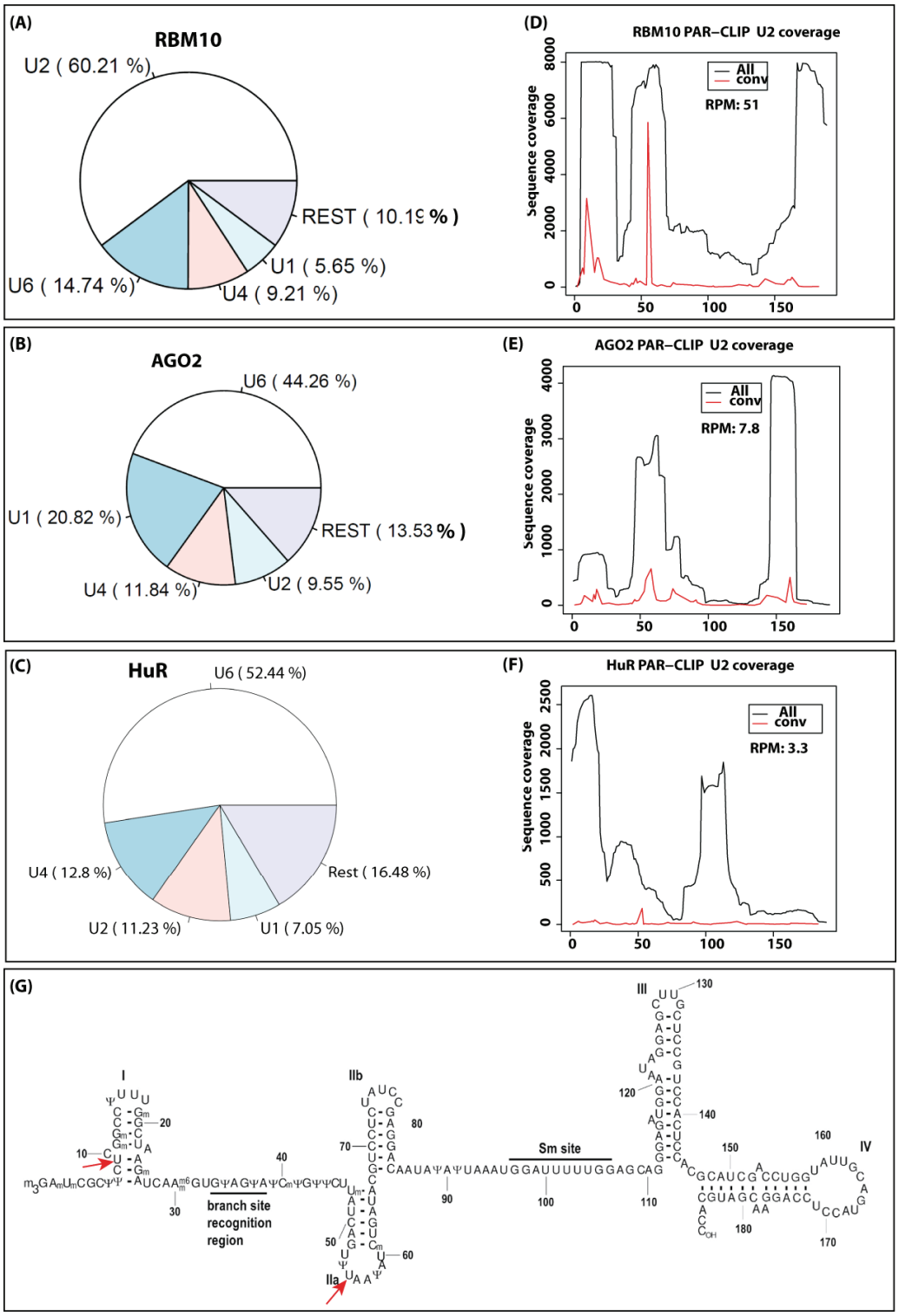


**Figure 3.6 RBM10 associates with splicing snRNAs.** (A-C) Distribution of PAR-CLIP reads mapped to snRNAs for RBM10 (A) was different from previously published AGO2 (B), and HuR (C) PAR-CLIP datasets. (D-F) Distribution of number of PAR-CLIP reads along U2 snRNAs for RBM10 (D), AGO2 (E) and HuR (F) was

depicted in black. Number of T to C conversions were displayed in red. (G) Secondary structure of U2 snRNA, adapted from (Dönmez et al. 2004). (m3G) N2,2,7-trimethylguanosine; (m) 2' O-methyl; (Ψ) pseudouridine; (m6) N6-methyl. Two RBM10 crosslinking sites are indicated by red arrows.

## 3.6 Gene expression changes upon RBM10 depletion or overexpression

To dissect potential transcriptional and post-transcriptional regulation mediated by RBM10, we performed RNA sequencing (RNA-Seq) and quantified gene expression as well as alternative splicing upon RBM10 knockdown (KD) or overexpression (OE) respectively in HEK293 cells (MATERIALS AND METHODS). We assessed the efficiency of KD and OE at mRNA level by qPCR and at protein level by western blot. RBM10 mRNA transcript level was reduced to ~20% after KD for 48, 72 hours. A sufficient reduction at protein level could also be observed (Figure 3.7A). We performed mRNA sequencing for KD and corresponding control samples at three time points (24, 48 and 72 hours, one additional biological replicate at 48 hours). For the OE, RBM10 expression was increased by ~7.5 fold compared to control at mRNA level, and also comparably upregulated at protein level (Figure 3.7A). We sequenced two replicates of the OE and corresponding control samples. Our sequencing results yielded from approximately 45 to 139 millions 100 nt sequencing reads for each sample that can be uniquely mapped to the genome reference (UCSC genome browser hg19) (Table 3.2).

| Samples | RBM10 OE | | | | RBM10 KD | | | | | | | |
|---|---|---|---|---|---|---|---|---|---|---|---|---|
| | Rep1 | Ctrl Rep1 | Rep2 | Ctrl Rep2 | 24 h | Ctrl 24 h | 48 h Rep1 | Ctrl 48 h Rep1 | 48 h Rep2 | Ctrl 48 h Rep2 | 72 h | Ctrl 72 h |
| # of uniquely mappable reads | 50,526,709 | 69,243,971 | 117,767,392 | 123,527,051 | 139,172,185 | 119,276,474 | 47,662,163 | 49,535,341 | 114,986,392 | 132,636,361 | 48,922,747 | 45,231,249 |

**Table 3.2 Summary of RNA-Seq results.**

We estimated the gene expression levels by RPKM (reads per kilobase of exon per million mapped sequence reads, (Mortazavi et al. 2008)) using uniquely mappable reads (MATERIALS AND METHODS). Comparison of expression levels between biological replicates in each condition (Control, OE and KD) revealed high correlation (Figure 3.7B), demonstrating high quality and reproducibility of the RNA-Seq data. Since gene expression of KD samples from three different time points correlated well with each other, we grouped them together for quantifying gene expression and splicing changes. Based on RNA sequencing and RPKM value, *RBM10* mRNA itself was decreased to ~24% upon KD and increased by ~5.5 fold upon OE respectively, consistent with the qPCR measurements. Gene expression changes between OE and control or between KD and control were transformed into Z-value (MATERIALS AND METHODS). At fdr < 0.05, 98 and 100 genes were found to be significantly upregulated and downregulated by at least 1.5 fold upon RBM10 KD (Figure 3.8A, Appendix Table 1), whereas 20 and 42 genes are upregulated and downregulated to the same level (fdr < 0.05, fold change ≥ 1.5) in response to OE of RBM10, respectively (Figure 3.8B, Appendix Table 1). We then compared the expression changes between KD and OE and found that they were not anti-correlated except for a few genes, such as RBM10, SAT1 (Figure 3.8C).

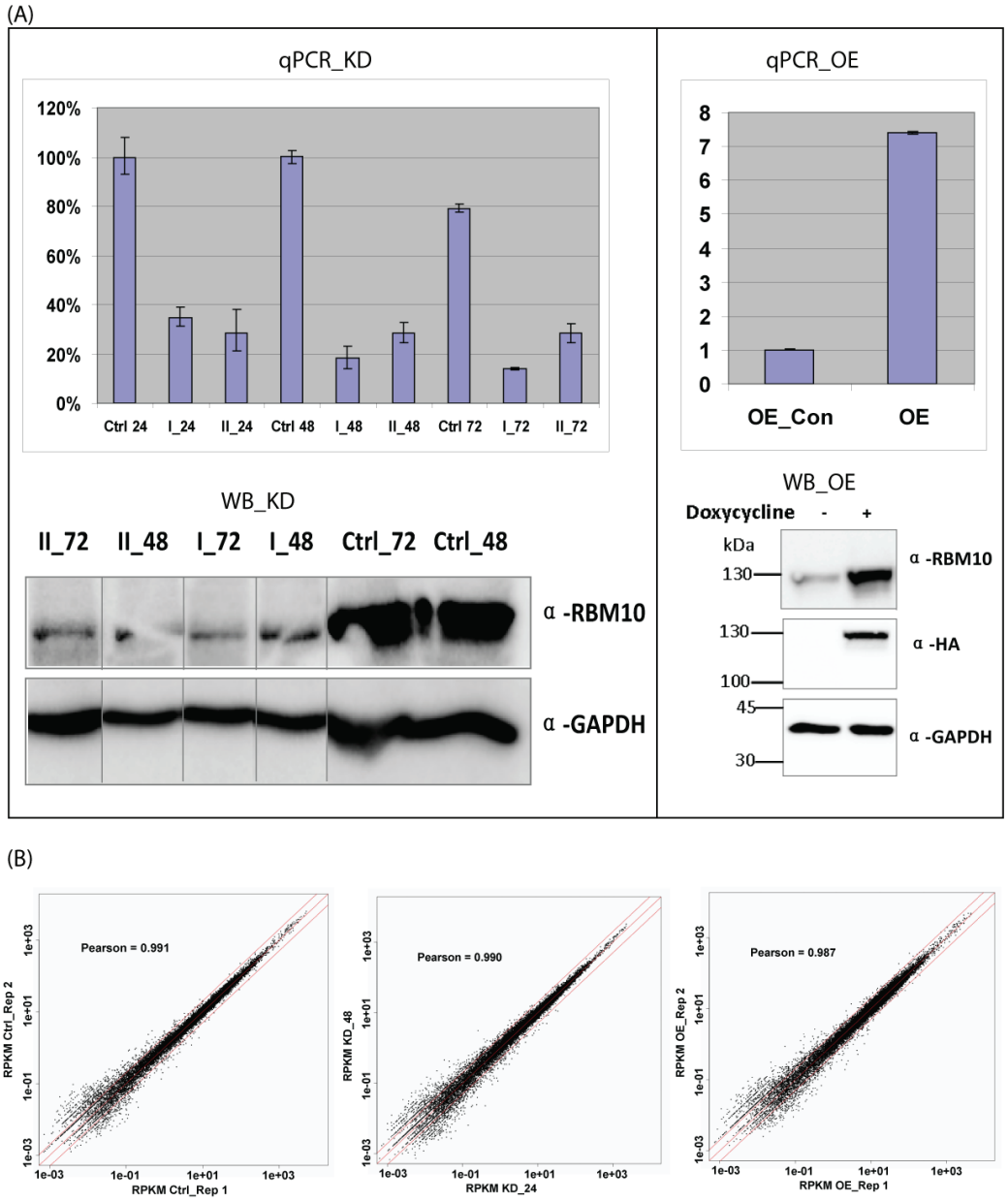


**Figure 3.7 Assessment of RBM10 knockdown (KD) or overexpression (OE) experiments** (A) Efficiency of KD (left) and OE (right) were assessed by qPCR and western blot at mRNA level and protein level respectively. mRNA level was normalized to the level of GAPDH. I: siRNA1, II: siRNA2, WB: western blot. (B) RNA-Seq results are highly reproducible. Gene expression levels estimated by RPKM are well correlated between replicates in each condition: control (left), KD (middle) and OE (right).

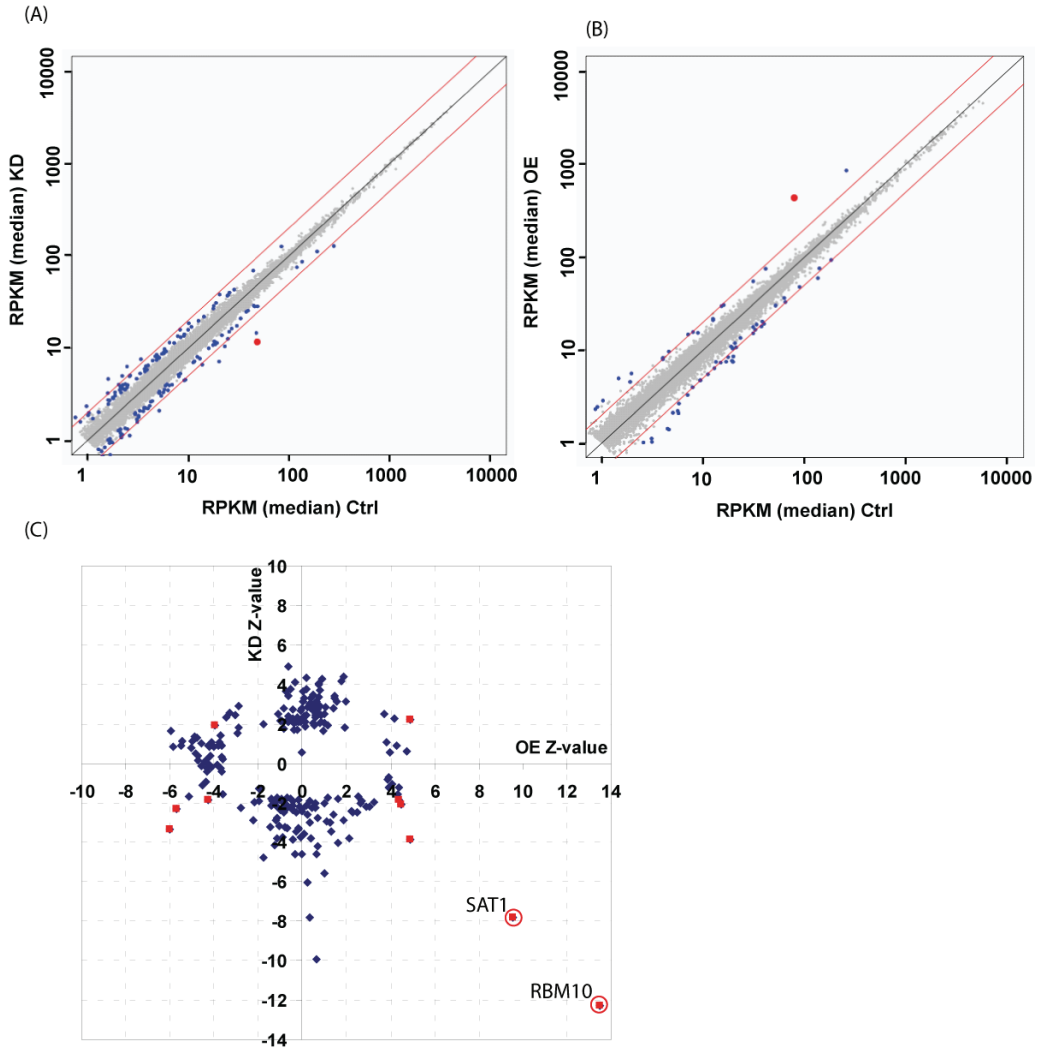


**Figure 3.8 Gene expression changes induced by RBM10 knockdown (KD) or overexpression (OE)** (A, B) Scatter plots showed significantly (fdr < 0.05, fold change ≥ 1.5) up- and down-regulated genes (marked with blue) upon RBM10 KD (A) and OE (B) respectively. Each dot represents one gene. RBM10 was highlighted in red. Red lines demarcate 2-fold change. (C) Gene expression changes upon KD and OE were not anti-correlated except for a few genes such as RBM10, SAT1 highlighted with red cycle. Z-value for each gene was plotted between OE and KD. Blue and red represent genes significantly changed genes in either KD or OE, and in both conditions respectively.

## 3.7 Splicing changes upon RBM10 depletion and overexpression

The specific RNA binding pattern we observed indicated a potential role of RBM10 in splicing regulation. Therefore we sought to further characterize the splicing changes induced by RBM10 OE/KD. Based on RNA sequencing data, we defined the inclusion ratio (PSI: percentage spliced in) of each exon in refseq transcripts as the number of reads exclusively supporting inclusion divided by total number of reads supporting inclusion and skipping for the specific exon (Figure 3.9A) (Polymenidou et al. 2011; Wang et al. 2008). We then compared inclusion ratio between KD and control, OE and control, respectively. The changes were transformed into Z-value (Figure 3.9B) and the results from replicate experiments were combined to evaluate statistical significance using rank product method (MATERIALS AND METHODS). At a stringent cutoff (fdr < 0.05, $|\Delta PSI| \geq 10\%$), we obtained 214 induced inclusion events and 67 skipping events upon RBM10 KD (Appendix Table 2). In comparison, we obtained 91 induced inclusion events and 265 skipping events upon RBM10 OE (Appendix Table 2). We selected 14 candidate splicing changes with different Z-values for validation by qPCR using junction specific primers. The abundance of transcript isoforms including or skipping the alternative spliced exons was normalized to that of constitutive exons (Figure 3.10A). As shown in Figure 3.10B, all the 14 candidate changes were successfully validated and the splicing changes detected by qPCR were quantitatively correlated with that determined by RNA-seq (correlation score R = 0.94) (Figure 3.10C). In contrast to the gene expression changes, the splicing changes induced by RBM10 KD and OE were clearly anti-correlated (Figure 3.11A). The induced splicing changes were grouped into different types of alternative splicing (See Figure1.4) and summarized in Table 3.3. Notably, there are substantially more (214 *vs.* 67) skipping events than inclusion events upon RBM10 OE, while the opposite (91 *vs.* 265) holds true for RBM10 KD (Table 3.3). Moreover, the majority of skipping events induced by RBM10 OE are cassette exons, while only one third of included exons events are cassettes exons (Figure 3.11B). Those results implicated that RBM10 primarily mediated the skipping of cassette exons.

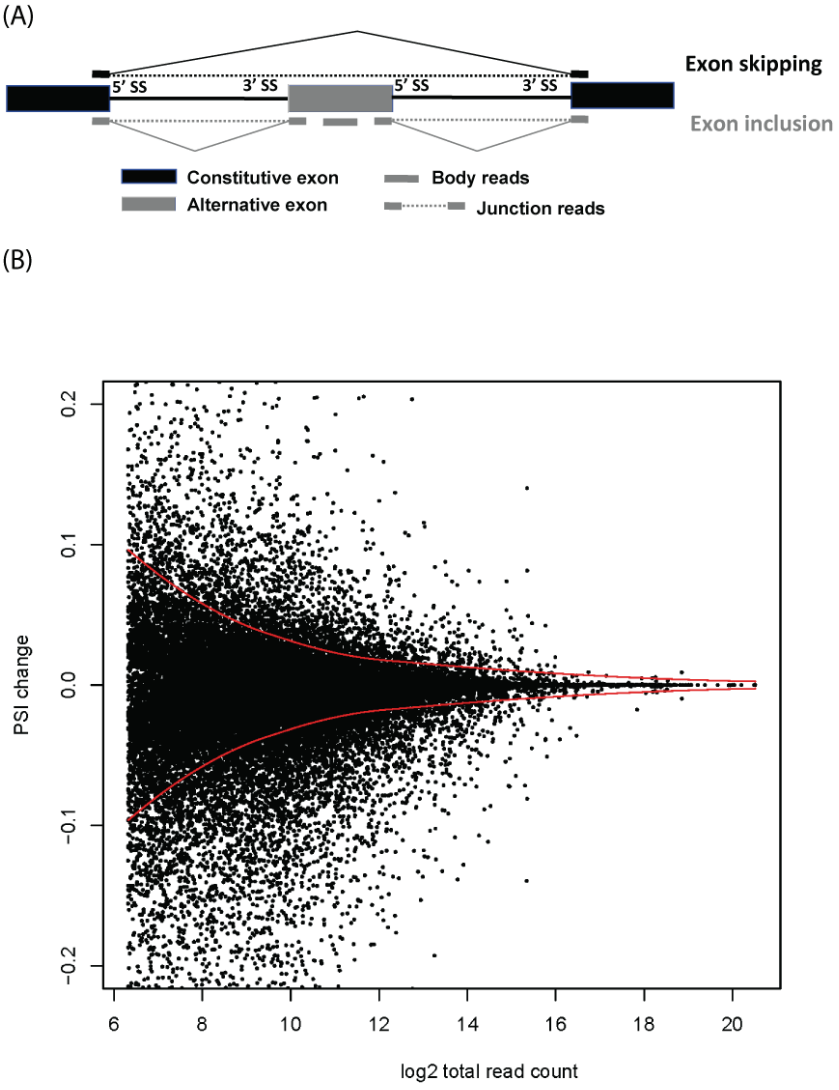


**Figure 3.9 Splicing changes mediated by RBM10 knockdown (KD) or overexpression (OE).** (A) Schematic illustration of the strategy used for quantification of splicing changes. Percentage splicing in (PSI) was calculated for each exon by number of reads exclusively supporting inclusion divided by total number of reads supporting inclusion and skipping. (B) PSI value changes (y axis) between two conditions, represented by the second replicate of OE vs. Ctrl, were normalized by total supporting read count (x axis) and transformed into Z-value, i.e. change divided by the standard derivation in certain defined window with similar read counts. Each dot represents one exon. ±SD (standard deviation) are marked by the red lines. PSI changes detected for exons with less supporting reads tend to be more noisy and therefore statistical significance necessitate higher PSI changes for less abundanct exons.

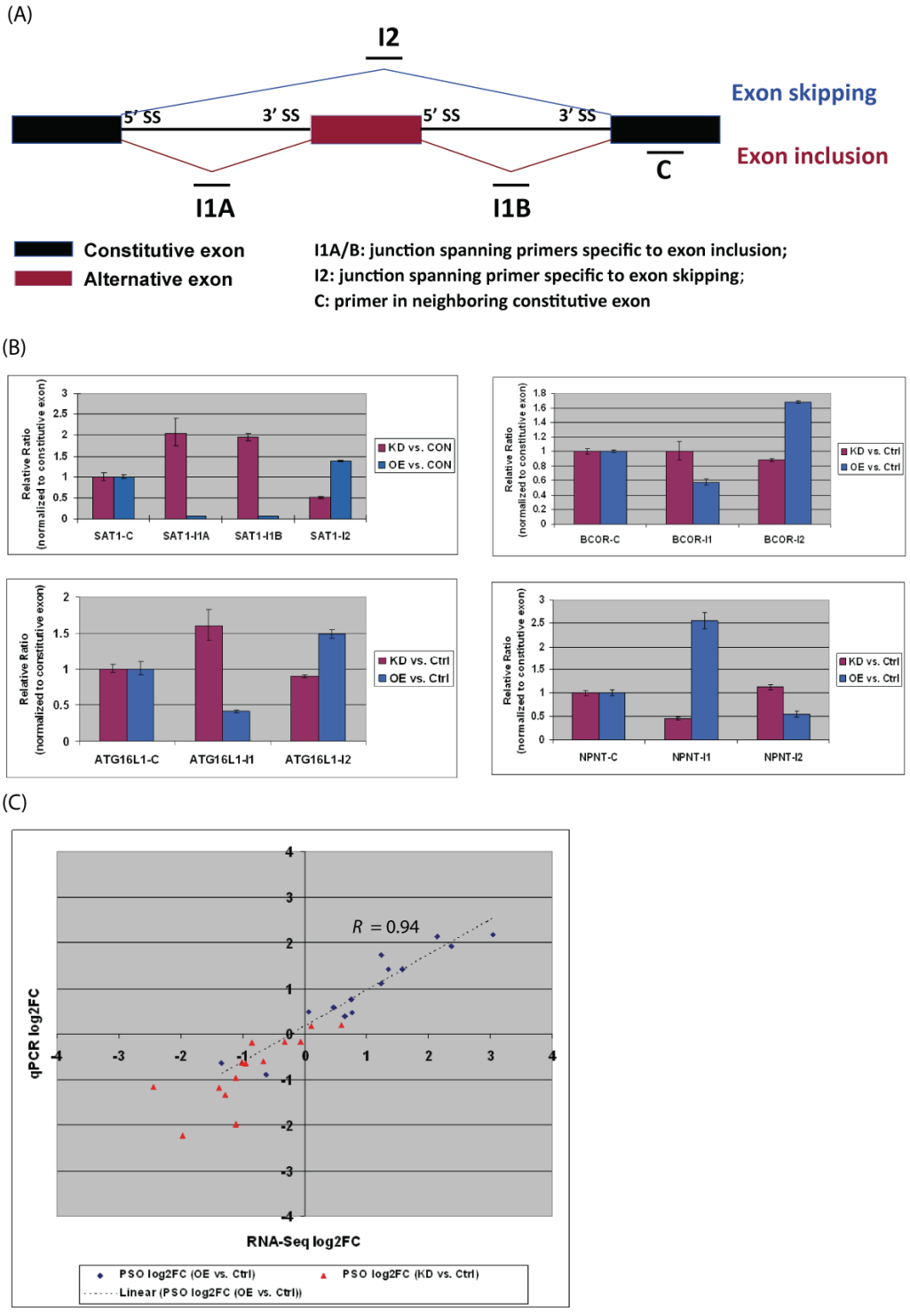


**Figure 3.10 Validation of the splicing changes by qPCR.** (A) Schematic representation of primers designed for the validation. (B) Shown are representative qPCR results for four exons. The abundance of transcript isoforms including or

skipping the alternatively spliced exons was normalized to constitutive exon respectively. The exon inclusion decreased upon RBM10 OE and increased upon RBM10 KD for the first three examples, while the change was opposite for the fourth example. (C) Percentage spicing out (PSO) changes quantified by RNA-seq were nicely correlated with that quantified by qPCR. ($R$ = 0.94, dash line: linear regression).

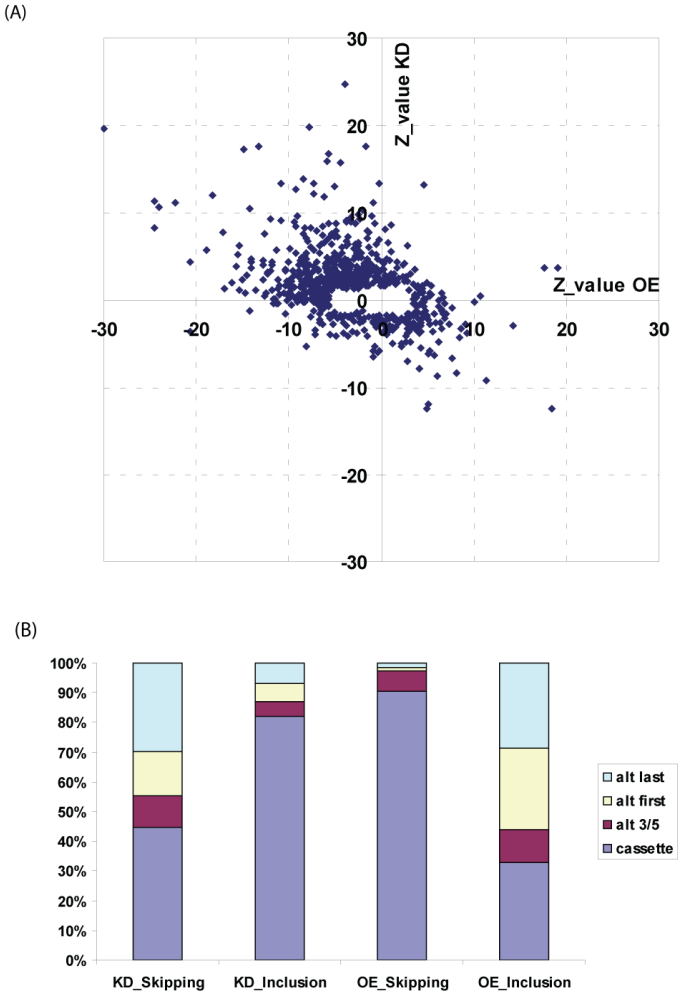


**Figure 3.11 Splicing changes upon RBM10 depletion and overexpression.** (A) Splicing changes induced upon RBM10 KD and OE were clearly anti-correlated. Each dot represents one significantly regulated exon (fdr<0.05, |ΔPSI| ≥ 10%) upon either KD or OE. (B) Proportion of different types of alternatively spliced exons upon RBM10 KD and OE. "alt 3/5" represents exons with alternative 3' and/or 5' splice site.

| | KD_Skipping | KD_Inclusion | OE_Skipping | OE_Inclusion |
|---|---|---|---|---|
| **cassette** | 30 | 176 | 240 | 30 |
| **alt 3/5** | 7 | 10 | 18 | 10 |
| **alt first** | 10 | 13 | 3 | 25 |
| **alt last** | 20 | 15 | 4 | 26 |
| **total** | 67 | 214 | 265 | 91 |

**Table 3.3 Types of alternatively spliced exons upon RBM10 KD and OE.**

## 3.8 RBM10 autoregulation

It is commonly found that RNA binding proteins bound with their own RNAs and thereby control their own expression in an autoregulated manner (Polymenidou et al. 2011; Sun et al. 2010; Wollerton et al. 2004). As shown in Figure 3.12A, we observed that RBM10 bound extensively to its own transcripts. In addition, based on RNA sequencing results, upon RBM10 overexpression (OE), the endogenous mature *RBM10* transcripts was dramatically downregulated. Using qPCR with primers targeting at endogenous mature transcript or primary transcript, we can validate the change in the abundance of mature transcript whereas no significant change was found for primary transcript (Figure 3.12B), indicating the autoregulation occurred posttranscriptionally.

(A)

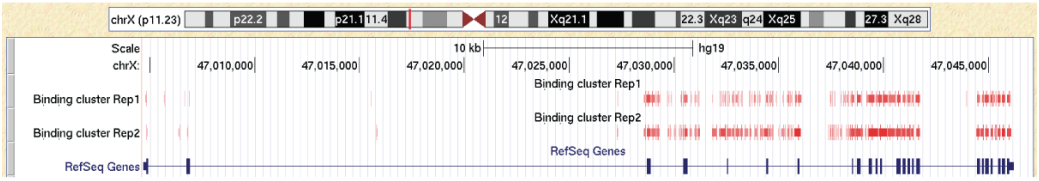


(B)

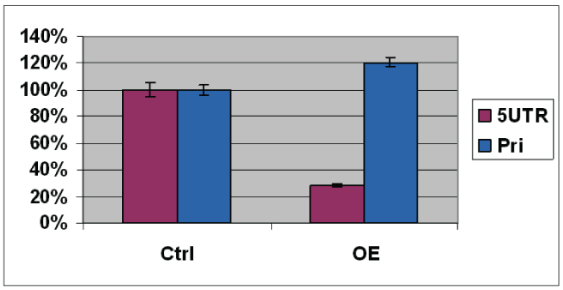


**Figure 3.12 RBM10 autoregulation** (A) RBM10 binds extensively to its own transcript. Binding clusters within *RBM10* were displayed in UCSC genome browser.

(B) Endogenous RBM10 mature transcript but not primary transcript level decreased dramatically upon overexpression (OE) of RBM10 wild type (WT).

## 3.9 RBM10 mutant changes subcellular localization and patient derived lymphoblast cell line showed splicing changes resembling the changes upon RBM10 knockdown

To understand how in-frame deletion in RBM10 could contribute to disease phenotype, we checked in more detail the sequence of deleted fragment and identified a potential nuclear localization signal (NLS) within the deleted sequence (830- 837 aa). To examine whether this finding was relevant to the real impact, we compared the subcelluar localization of wide type RBM10 with that of the mutant. In comparison to the nuclear localization of wild type, RBM10 mutant changed to predominant cytoplasm localization (Figure 3.13A), consistent with the loss of NLS within the deletion (Figure 1.9). This suggests the deletion might lead to loss of nuclear functions of RBM10. To investigate the impact of this deletion on gene expression especially splicing pattern, we performed RNA sequencing on lymphoblast cell lines derived from patient carrying the mutation and those from normal controls respectively. We determined the splicing changes using the same strategy applied on HEK 293 cells, as described above. In total, we identified 84 inclusion and 53 skipping events (fdr $<0.05$, $|\Delta PSI| \geq 10\%$) induced by the mutation. Intriguingly, the splicing changes observed here correlated well with changes induced by RBM10 knockdown in HEK293 (Figure 3.13B). This indicated the loss of function in splicing regulation for the RBM10 mutant, in accordance with the observed subcellular localization change. To further validate the functional impact of the mutant, we overexpressed it in HEK 293 cells. As shown in Figure 3.13C, for the two cassette exons, the overexpression of the mutant could not induce the same splicing changes as that of the wild type.

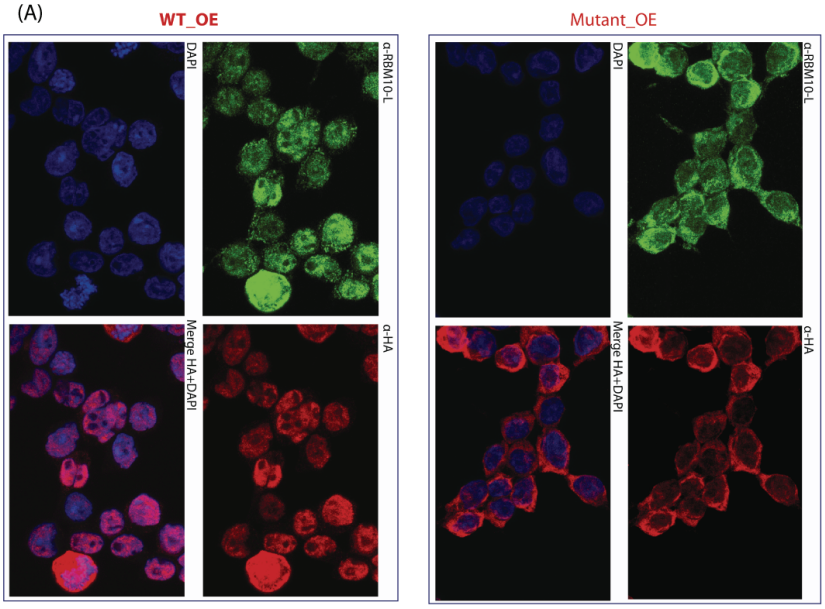
(A)
WT_OE
Mutant_OE
DAPI
α-RBM10-L
Merge HA+DAPI
α-HA

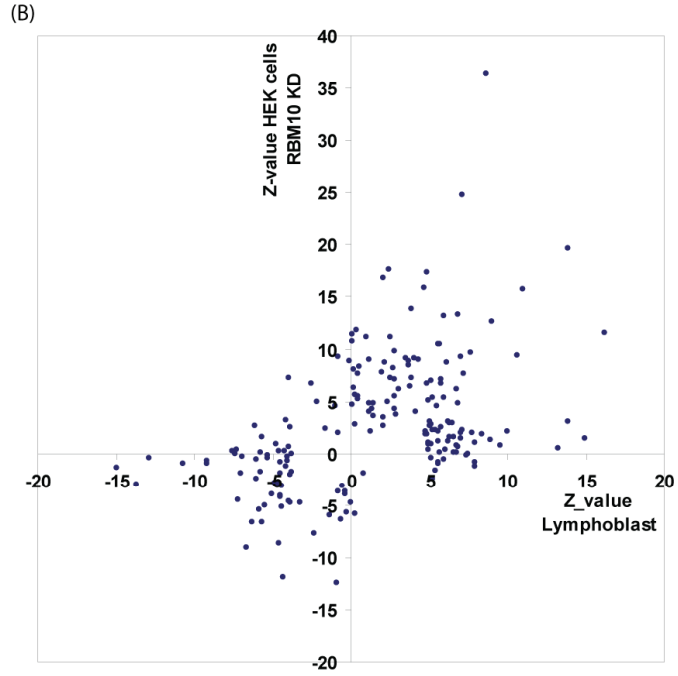
(B)
Z-value HEK cells RBM10 KD
Z_value Lymphoblast
40
35
30
25
20
15
10
5
0
-5
-10
-15
-20
-20
-15
-10
-5
0
5
10
15
20

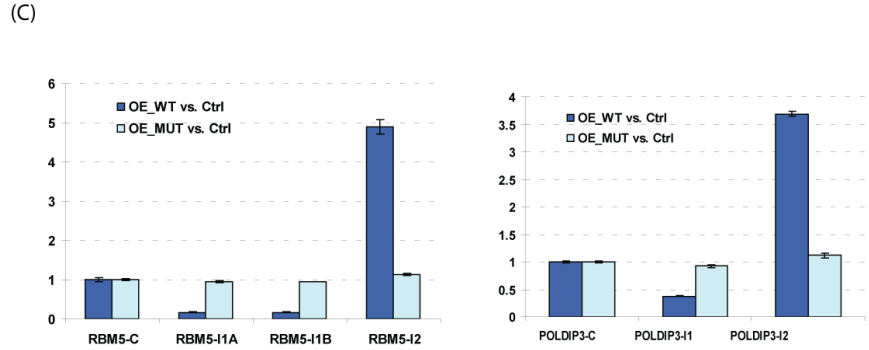
(C)
OE_WT vs. Ctrl
OE_MUT vs. Ctrl
RBM5-C
RBM5-I1A
RBM5-I1B
RBM5-I2
POLDIP3-C
POLDIP3-I1
POLDIP3-I2

**Figure 3.13 RBM10 mutant lost the function on splicing regulation.** (A) Immunostaining showed the subcellular localizations of both RBM10 wild type (WT) and mutant (MUT) in HEK 293. DAPI stains the nucleus; antibody against RBM10 (α-RBM10-L) stains endogenous RBM10 WT, overexpressed RBM10 WT and MUT; antibody against HA (α-HA) stains overexpressed RBM10 WT and MUT. RBM10 WT mostly resided in nucleus, while MUT changed subcellular localization to predominantly cytoplasm. (B) RBM10 MUT induced splicing changes in patient derived lymphoblast cells (Z value in X axis) correlated well with observed changes mediated by RBM10 knockdown (KD) in HEK293 (Z value in Y axis). Each dot represent a significantly regulated exon (fdr < 0.05, $|\Delta PSI| \geq 10\%$) in either HEK293 or lymphoblast cells. Exons significantly regulated in both are marked with red. (C) Overexpression (OE) of RBM10 MUT could not induce the same splicing changes as that of RBM10 WT. Shown are qPCR results of two exon splicing changes upon OE of RBM10 WT and MUT respectively. In contrast to the remarkable changes upon WT OE, MUT OE could not induce significant changes.

# 4 DISCUSSIONS

Nonsense mutations (Johnston et al. 2010) and in-frame deletion (our own observation) in RBM10 have been found to associate with X-linked developmental disorders. To understand possible underlying mechanisms responsible for disease phenotypes, it is essential to decipher the regulatory roles of RBM10. Using PAR-CLIP, we identified 89,247 reproducible binding sites in 6,396 target genes. We further determined RBM10 induced changes in gene expression and particularly alternative splicing by RNA sequencing. In total, we obtained 784 significant splicing changes followed by RBM10 knockdown (KD) or overexpression (OE). Notably, those changes are anti-correlated between KD and OE. Taken together, our results demonstrate that RBM10 functions as a novel splicing regulator via its direct binding to pre-mRNA substrates and potentially coordinates interplays with core splicing machinery and other splicing regulators. Finally, we could demonstrate that in-frame deletion identified in our patient led to the change of its nuclear localization and consequently loss of its function in splicing regulation.

## 4.1 PAR-CLIP recovers transcriptome wide RNA binding sites of RBM10

PAR-CLIP is a robust method for global mapping RNA binding proteins (RBPs)-RNA interactions with several conspicuous features. First, PAR-CLIP is a very sensitive method that could effectively recover binding sites in lowly abundant or unstable transcripts, for example, intronic binding sites in primary transcripts. Second, the specific nucleotide conversion signatures in crosslinking sites (e.g. T to C conversion in 4-thiouridine labeling experiment) allow us to identify binding sites at nucleotide resolution and at the same time to further distinguish true binding signal from background noise. Those advantages render it well applicable in elucidating general regulatory roles of splicing regulating RBPs.

Our PAR-CLIP experiments yielded 89,247 reproducible RBM10 binding clusters in 6,396 target genes. As shown in Figure 3.3A, for these overlapped clusters, two PAR-

CLIP replicate experiments demonstrated good reproducibility. However, a large proportion of clusters (62.8% and 59.1% of all clusters identified in the 1st and 2nd replicates) were detected in only one of the replicates. In principle, the limited overlap could be due to the low quality of our datasets. Alternatively, the non-reproducible clusters might derive from transient and weak binding events. In supporting with this argument, we compared the distribution of score between overlapped and non-overlapped binding clusters identified in only one replicate. As shown in Figure 4.1, the overlapped binding clusters indeed have significantly higher score than those only appear in one replicate ($p < 2e-16$). Therefore, very likely, whereas the overlapped clusters often reflect strong or stable interaction, most of the weak and transient binding might be detected in an irreproducible manner.

A critical parameter of PAR-CLIP experiment that often need to be optimized is the strength of RNase T1 digestion, which can substantially biased the cluster identification (Kishore et al. 2011). Overdigestion leads to small RNA fragments that could not be recovered or uniquely mapped to the genome and thus were discarded. Conversely, insufficient digestion either produces large RNA fragments beyond the size selection range that would be lost during the cloning process or results in larger cluster size, thereby reduces spatial resolution in determining binding sites. In our experiments, we carefully compared and controlled RNase T1 digestion efficiency to eliminate the potential bias. As shown in Figure 4.2, in a third replicate experiment using milder RNase T1 digestion, we obtained significantly larger cluster size (median 75 nt) compared to the two biological replicates with stronger digestions (median 36, 57 nt), as expected. Due to this bias, the third replicate was not used for identifying binding site here.

Notably, more stringent cutoff such as higher number of T to C conversions within clusters (Lebedeva et al. 2011) and/or certain maximum distance or even exact match between preferred crosslinking sites in overlapped binding clusters (Hoell et al. 2011) could be employed to prioritize and define a set of more conservative binding clusters with higher specificity. For example, requiring exact preferred crosslinking sites in overlapped clusters, we could identify 29,330 binding clusters in 4,063 target genes. In this study, in order to characterize as many as possible RBM10 binding sites and at the same time to avoid the artifacts, we require the preferred crosslinking sites, i.e.

the position with highest number of T to C conversions within a cluster, to fall in the binding regions identified in both replicates.

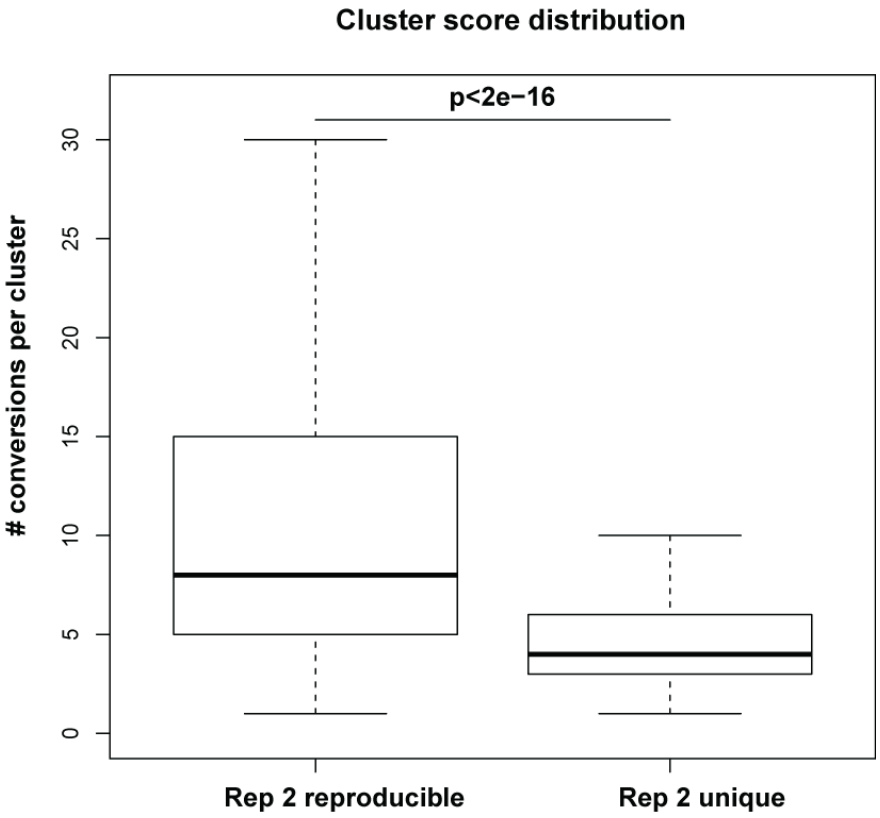


**Figure 4.1 Overlapped clusters show significantly higher scores than non-overlapped binding clusters**. Bar plot demonstrates cluster score distribution represented by number of T to C conversions for overlapped and non-overlapped binding clusters identified from the second PAR-CLIP replicate (Rep 2) experiment. Bold horizontal line in the box depicts the median score.

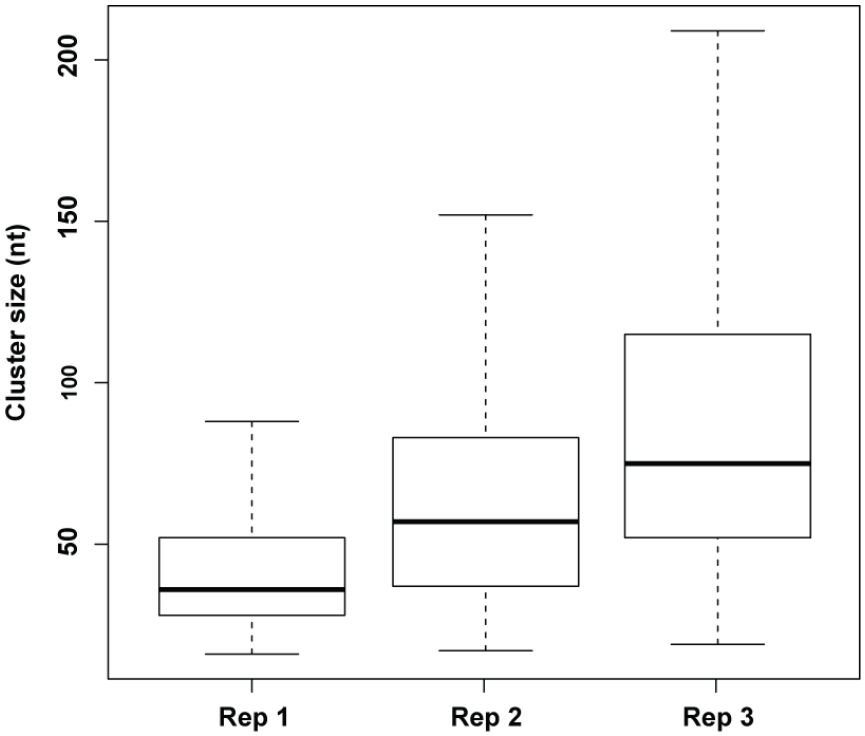


**Figure 4.2 Cluster size distribution with different RNase T1 digestions**. Bar plot demonstrates cluster size distribution of three PAR-CLIP experiments with different T1 digestions. Horizontal line in the box depicts the median length. In a third replicate (Rep 3), milder RNase T1 digestion was used and substantially longer cluster size was obtained in comparison to replicate 1 and 2 (Rep 1 and Rep 2), as expected.

## 4.2 Putative sequence motif of RBM10

To examine the sequence preference of RBM10 binding, we calculated the motifs enriched in the RBM10 exonic and intronic binding clusters separately by comparing with corresponding randomly selected background (Experimental Procedures). Interestingly, we identified a heptamer consensus that was highly enriched in the exonic binding clusters (Figure 4.3 A), and occurred in 19.8 % of all exonic binding clusters compared with 11.8 % in background. The motif occurrence increased to 21.9% in exonic binding clusters and 13.6% background respectively, if calculated with pentamer consensus (Figure 4.3 B). Interestingly, this consensus is a known exon splicing enhancer (ESE) (Fairbrother et al. 2002) and very similar to the identified sequence motif of splicing regulator SR protein: SFSR1 (Sanford et al. 2009). In the intronic binding clusters, we discovered a pyrimidine rich sequence motif (Figure

4.2C). The pyrimidine rich motif is largely degenerate and explains as high as 36.4% of all intronic binding clusters, compared with 25.3% of background sequences,. Given that RBM10 has several domains with RNA binding capacities, it is possible that it recognizes different sequence motifs. However, the direct binding and the affinity of RBM10 with those putative sequence motifs needs to be confirmed by further experiments, such as EMSA, ITC or NMR.

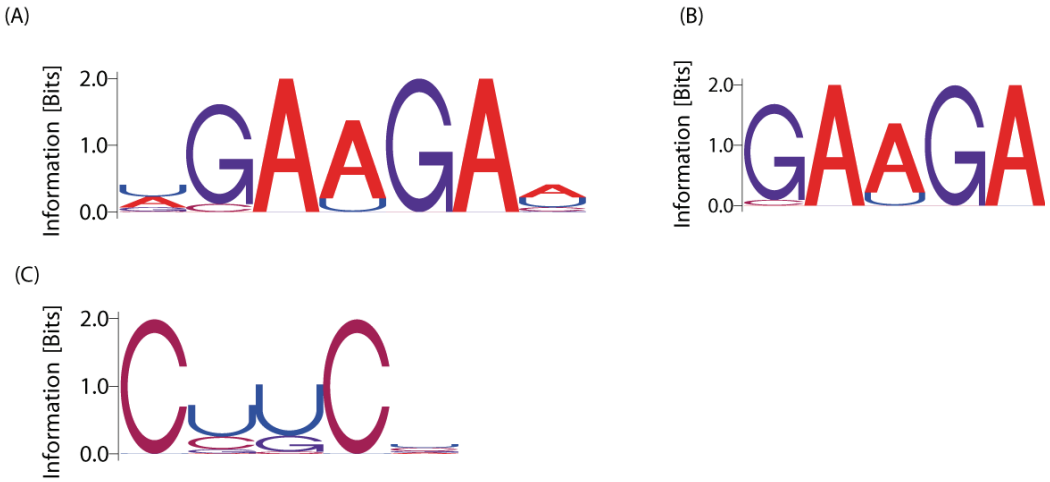


**Figure 4.3 RBM10 sequence motifs.** (A) Heptamer and (B) pentamer sequence motif enriched in RBM10 exonic binding clusters. (C) Pentamer pyrimidine rich sequence motif enriched in RBM10 intronic binding clusters.

## 4.3 RNA-Seq reveals splicing changes induced by RBM10

In total, we detected 198 and 62 gene expression changes upon RBM10 KD and OE respectively. However, only 49 and 34 showed ≥2-fold changes and the changes are not anti-correlated between KD and OE (Figure 3.8C), suggesting that overall gene expression changes were likely to be secondary effect. In sharp contrast, we obtained 784 significant exon splicing changes upon RBM10 overexpression (OE) or knockdown (KD), and these changes are strikingly anti-correlated between KD and OE (Figure 3.11A), implicating that RBM10 functions as a splicing regulator and consistent with the previous finding that RBM10 is a spliceosomal component by proteomics studies. Notably, we found considerably more exon skipping than inclusion events upon RBM10 OE and the opposite holds true for KD, and the disparity is even larger if we restricted to cassette exons (Table 3.3, Figure 3.11B). Of

note, in this study, we might underestimate splicing changes such as (a) exons using alternative 5' or 3' splice site with < 6 nt difference, which our current computational analysis strategy could not confidently detect; (b) splicing changes that trigger nonsense mediated mRNA decay (NMD) pathway, leading to the degradation of whole transcripts; (c) novel splice sites not annotated in the UCSC Genome Browser.

## 4.4 Autoregulation of RBM10

We found RBM10 negatively regulate the abundance of its own transcript, similar to other splicing regulating RBPs, such as PTBP (Wollerton et al. 2004), FOX2 (Damianov and Black 2010) and a number of other SR and hnRNP family members (Lareau et al. 2007). Since the RBM10 primary transcript did not show significant change upon RBM10 overexpression (OE) (Figure 3.12B), we concluded that the regulation is very likely occurring posttranscriptionally. However, whether the regulation is due to splicing changes coupled with nonsense mediated decay (NMD) has not been determined in this study. To address this, NDM pathway will need to be blocked and only then the hypothetic splicing changes in endogenous RBM10 induced by OE will be susceptible to detection.

## 4.5 RBM10 regulates splicing of disease associated genes

Alternative splicing (AS) changes the sequence of the transcripts thereby could alter the functions of proteins they encoded, such as binding properties, subcellular localization etc (Buljan et al. 2012; Ellis et al. 2012; Stamm et al. 2005), or even result in proteins with antagonistic functions (Moore et al. 2010). In addition, AS coupled with nonsense mediated mRNA decay (NMD) could change the abundance of the regulated transcripts. Defects in splicing, either the *trans*-acting factors or *cis*-regulatory elements, are thought to be one of the major causes of disease. In case of *tans* effects, such as RBM10, usually the splicing of multiple downstream targets is affected.

Among the genes of which the abundance and/or splicing are affected upon RBM10 perturbation, many are known to be involved in different diseases. For example, a couple of genes, such as NCOR2 and BCOR etc, have been found to be mutated in

patients carrying autosomal recessive or X-linked cognitive disorders (Najmabadi et al. 2011). BCL6 corepressor (BCOR) functions as a transcriptional corepressor that may specifically inhibit gene expression when recruited to the promoter region by interacting with transcription factor BCL6 (Huynh et al. 2000). The repression may be in part mediated by its interaction with specific class I and II histone deacetylases (HDACs) (Li et al. 2000). Mutations in BCOR have been identified to cause microphthalmia syndromic 2 (MCOPS2, OMIM 300166) (Horn et al. 2005; Ng et al. 2004) and also been implicated in acute myeloid leukemia (AML) (Grossmann et al. 2011; Tiacci et al. 2012). In addition, several genes, such as VCL, have directly been associated with muscular dystrophy. Vinculin (VCL) is a cytoskeletal protein binding to F-actin that is involved in cell-cell and cell-matrix junctions (Bakolitsa et al. 2004; Hu et al. 2007). Defects in VCL are the cause of cardiomyopathy dilated type 1W (OMIM 611407) (Olson et al. 2002) and cardiomyopathy familial hypertrophic 15 (OMIM 613255) (Vasile et al. 2006). VCL knockout mouse displayed heart and brain defects during embryonic development (Xu et al. 1998). Moreover, several other genes, such as CREBBP and LEF1, are found to play important roles in development and mutations of which are associated with leukemia. CREB binding protein (CREBBP) is a ubiquitously expressed coactivator of many different transcription factors which functions by coupling chromatin remodeling to transcription factor recognition (Cho et al. 2004; Kwok et al. 1994; Tsuda et al. 2003). It plays key roles in embryonic development, growth control and homeostasis. Mutations in this gene cause Rubinstein-Taybi syndrome (RSTS1, OMIM 180849) (Murata et al. 2001) and associate with acute myelogenous leukemia (AML, OMIM 601626) (Panagopoulos et al. 2001), spinal and bulbar muscular atrophy (SBMA; OMIM 313200) (Mccampbell et al. 2000), chromosome 16p13.3 duplication syndrome (OMIM 613458) (Thienpont et al. 2010), non-hodgkin lymphoma (OMIM 605027) (Pasqualucci et al. 2011) and acute lymphoblastic leukemia (ALL) (Mullighan et al. 2011). Lymphoid enhancer-binding factor 1 (LEF1) is a transcription factor that regulates T-cell receptor-alpha enhancer function (Reya et al. 2000). It is involved in the Wnt signaling pathway (Boras-Granic et al. 2006) and may participate in hair cell differentiation and follicle morphogenesis (Merrill et al. 2001). Different isoforms exhibit different cellular functions in cancer cells (Jesse et al. 2010). Mutations in this gene have been found in somatic sebaceous tumors (Takeda et al. 2006) and other cancers, including acute

lymphocytic leukemia (Mullighan et al. 2007) and androgen-independent prostate cancer (Li et al. 2009b).

Notably, the frameshift mutations in RBM10 have been manifested to cause more severe disorders than the in-frame mutation (Johnston et al. 2010), suggesting that truncated protein might only partially lose the wild type function. Although the potential target genes under RBM10 regulation have been explored in this study, it is not clear yet how defect in RBM10 can cause the specific phenotypes manifested in the patients. Characterizing the exact mechanisms underlying disease etiology will necessitate further studies on appropriate genetic models.

## 4.6 Conclusion and perspective remarks

In this study, we have (1) characterized the transcriptome wide RNA binding sites and binding pattern of RBM10; (2) determined RBM10 mediated gene expression and splicing changes; (3) identified the functional impact of the in-frame deletion identified in our patient. Taken together, our work demonstrated a scheme for studying the regulatory mechanisms of RNA binding proteins, especially those involved in splicing regulation.

# 5 REFERENCE

Abdel-Wahab O and Levine R. 2011. The Spliceosome as an Indicted Conspirator in Myeloid Malignancies. ***Cancer cell*** 20**:** 420-422.

Adamidi C, Wang Y, Gruen D, Mastrobuoni G, You X, Tolle D, Dodt M, Mackowiak SD, Gogol-Doering A, Oenal P et al. 2011. De novo assembly and validation of planaria transcriptome by massive parallel sequencing and shotgun proteomics. ***Genome Research*** 21**:** 1193-1200.

Agafonov DE, Deckert J, Wolf E, Odenwälder P, Bessonov S, Will CL, Urlaub H, and Lührmann R. 2011. Semiquantitative Proteomic Analysis of the Human Spliceosome via a Novel Two-Dimensional Gel Electrophoresis Method. ***Molecular and Cellular Biology*** 31**:** 2667-2682.

Allo M, Buggiano V, Fededa JP, Petrillo E, Schor I, de la Mata M, Agirre E, Plass M, Eyras E, Elela SA et al. 2009. Control of alternative splicing through siRNA-mediated transcriptional gene silencing. ***Nat Struct Mol Biol*** 16**:** 717-724.

Ayala YM, Pagani F, and Baralle FE. 2006. TDP43 depletion rescues aberrant CFTR exon 9 skipping. ***FEBS letters*** 580**:** 1339-1344.

Baker BS. 1989. Sex in flies: the splice of life. ***Nature*** 340**:** 521-524.

Bakolitsa C, Bobkov AA, Cohen DM, Bankston LA, Cadwell GM, Jennings L, Critchley DR, Craig SW, and Liddington RC. 2004. Structural basis for vinculin activation at sites of cell adhesion. ***Molecular Biology of the Cell*** 15**:** 142a-143a.

Barmada SJ, Skibinski G, Korb E, Rao EJ, Wu JY, and Finkbeiner S. 2010. Cytoplasmic Mislocalization of TDP-43 Is Toxic to Neurons and Enhanced by a Mutation Associated with Familial Amyotrophic Lateral Sclerosis. ***Journal of Neuroscience*** 30**:** 639-649.

Bassell GJ and Kelic S. 2004. Binding proteins for mRNA localization and local translation, and their dysfunction in genetic neurological disease. ***Current Opinion in Neurobiology*** 14**:** 574-581.

Behzadnia N, Golas MM, Hartmuth K, Sander B, Kastner B, Deckert J, Dube P, Will CL, Urlaub H, Stark H et al. 2007. Composition and three-dimensional EM structure of double affinity-purified, human prespliceosomal A complexes. ***EMBO J*** 26**:** 1737-1748.

Berget SM. 1995. Exon Recognition in Vertebrate Splicing. ***Journal of Biological Chemistry*** 270**:** 2411-2414.

Bessonov S, Anokhina M, Will CL, Urlaub H, and Luhrmann R. 2008. Isolation of an active step I spliceosome and composition of its RNP core. ***Nature*** 452**:** 846-850.

Black DL. 2003. MECHANISMS OF ALTERNATIVE PRE-MESSENGER RNA SPLICING. ***Annual Review of Biochemistry*** 72**:** 291-336.

Blencowe BJ. 2000. Exonic splicing enhancers: mechanism of action, diversity and role in human genetic diseases. ***Trends in Biochemical Sciences*** 25**:** 106-110.

Blencowe BJ. 2006. Alternative Splicing: New Insights from Global Analyses. ***Cell*** 126**:** 37-47.

Bonnal S, Martínez C, Förch P, Bachi A, Wilm M, and Valcárcel J. 2008. RBM5/Luca-15/H37 Regulates Fas Alternative Splice Site Pairing after Exon Definition. ***Molecular cell*** 32**:** 81-95.

Boras-Granic K, Chang H, Grosschedl R, and Hamel PA. 2006. Lef1 is required for the transition of Wnt signaling from mesenchymal to epithelial cells in the mouse embryonic mammary gland. ***Developmental Biology*** 295**:** 219-231.

Boutz PL, Stoilov P, Li Q, Lin C-H, Chawla G, Ostrow K, Shiue L, Ares M, and Black DL. 2007. A post-transcriptional regulatory switch in polypyrimidine tract-binding proteins reprograms alternative splicing in developing neurons. ***Genes & Development*** 21**:** 1636-1652.

Breitbart RE, Andreadis A, and Nadal-Ginard B. 1987. Alternative Splicing: A Ubiquitous Mechanism for the Generation of Multiple Protein Isoforms from Single Genes. ***Annual Review of Biochemistry*** 56**:** 467-495.

Buljan M, Chalancon G, Eustermann S, Wagner GP, Fuxreiter M, Bateman A, and Babu MM. 2012. Tissue-Specific Splicing of Disordered Segments that Embed Binding Motifs Rewires Protein Interaction Networks. ***Molecular cell*** 46**:** 871-883.

Buratti E and Baralle FE. 2008. Multiple roles of TDP-43 in gene expression, splicing regulation, and human disease. ***Front Biosci*** 13**:** 867-878.

Buratti E, Brindisi A, Giombi M, Tisminetzky S, Ayala YM, and Baralle FE. 2005. TDP-43 Binds Heterogeneous Nuclear Ribonucleoprotein A/B through Its C-terminal Tail. ***Journal of Biological Chemistry*** 280**:** 37572-37584.

Buratti E, Brindisi A, Pagani F, and Baralle FE. 2004. Nuclear Factor TDP-43 Binds to the Polymorphic TG Repeats in CFTR Intron 8 and Causes Skipping of Exon 9:

A Functional Link with Disease Penetrance. ***The American Journal of Human Genetics*** 74**:** 1322-1325.

Buratti E, Dork T, Zuccato E, Pagani F, Romano M, and Baralle FE. 2001. Nuclear factor TDP-43 and SR proteins promote in vitro and in vivo CFTR exon 9 skipping. ***EMBO J*** 20**:** 1774-1784.

Burge CB, Tuschl T, and Sharp PA. 1999. *Splicing of Precursors to mRNAs by the Spliceosomes*. In *the RNA world* second edition. Cold Spring Harbor Laboratory Press, New York.

Callebaut I and Mornon J-P. 2005. OCRE: a novel domain made of imperfect, aromatic-rich octamer repeats. ***Bioinformatics*** 21**:** 699-702.

Cartegni L, Chew SL, and Krainer AR. 2002. Listening to silence and understanding nonsense: exonic mutations that affect splicing. ***Nat Rev Genet*** 3**:** 285-298.

Cartegni L, Hastings ML, Calarco JA, de Stanchina E, and Krainer AR. 2006. Determinants of Exon 7 Splicing in the Spinal Muscular Atrophy Genes, SMN1 and SMN2. ***The American Journal of Human Genetics*** 78**:** 63-77.

Cartegni L and Krainer AR. 2002. Disruption of an SF2/ASF-dependent exonic splicing enhancer in SMN2 causes spinal muscular atrophy in the absence of SMN1. ***Nat Genet*** 30**:** 377-384.

Chen M and Manley JL. 2009. Mechanisms of alternative splicing regulation: insights from molecular and genomics approaches. ***Nat Rev Mol Cell Biol*** 10**:** 741-754.

Cho KS, Elizondo LI, and Boerkoel CF. 2004. Advances in chromatin remodeling and human disease. ***Current Opinion in Genetics & Development*** 14**:** 308-315.

Cooper TA, Wan L, and Dreyfuss G. 2009. RNA and Disease. ***Cell*** 136**:** 777-793.

Cowper AE, Cáceres JF, Mayeda A, and Screaton GR. 2001. Serine-Arginine (SR) Protein-like Factors That Antagonize Authentic SR Proteins and Regulate Alternative Splicing. ***Journal of Biological Chemistry*** 276**:** 48908-48914.

Damianov A and Black DL. 2010. Autoregulation of Fox protein expression to produce dominant negative splicing factors. ***RNA*** 16**:** 405-416.

Daoud H, Valdmanis PN, Kabashi E, Dion P, DuprÃ© N, Camu W, Meininger V, and Rouleau GA. 2009. Contribution of TARDBP mutations to sporadic amyotrophic lateral sclerosis. ***Journal of Medical Genetics*** 46**:** 112-114.

David CJ and Manley JL. 2010. Alternative pre-mRNA splicing regulation in cancer: pathways and programs unhinged. ***Genes & Development*** 24**:** 2343-2364.

Deckert J, Hartmuth K, Boehringer D, Behzadnia N, Will CL, Kastner B, Stark H, Urlaub H, and Lührmann R. 2006. Protein Composition and Electron Microscopy Structure of Affinity-Purified Human Spliceosomal B Complexes Isolated under Physiological Conditions. ***Molecular and Cellular Biology*** 26**:** 5528-5543.

Disset A, Bourgeois CF, Benmalek N, Claustres M, Stevenin J, and Tuffery-Giraud S. 2006. An exon skipping-associated nonsense mutation in the dystrophin gene uncovers a complex interplay between multiple antagonistic splicing elements. ***Human Molecular Genetics*** 15**:** 999-1013.

DÖNMEZ G, HARTMUTH K, and LÜHRMANN R. 2004. Modified nucleotides at the 5' end of human U2 snRNA are required for spliceosomal E-complex formation. ***RNA*** 10**:** 1925-1933.

Dye MJ, Gromak N, and Proudfoot NJ. 2006. Exon Tethering in Transcription by RNA Polymerase II. ***Molecular cell*** 21**:** 849-859.

Edery P, Marcaillou C, Sahbatou M, Labalme A, Chastang J, Touraine R, Tubacher E, Senni F, Bober MB, Nampoothiri S et al. 2011. Association of TALS Developmental Disorder with Defect in Minor Splicing Component U4atac snRNA. ***Science*** 332**:** 240-243.

Ellis JD, Barrios-Rodiles M, Çolak. R, Irimia M, Kim T, Calarco John A, Wang X, Pan Q, O'Hanlon D, Kim PM et al. 2012. Tissue-Specific Alternative Splicing Remodels Protein-Protein Interaction Networks. ***Molecular cell*** 46**:** 884-892.

Fabrizio P, Dannenberg J, Dube P, Kastner B, Stark H, Urlaub H, and Lührmann R. 2009. The Evolutionarily Conserved Core Design of the Catalytic Activation Step of the Yeast Spliceosome. ***Molecular cell*** 36**:** 593-608.

Fairbrother WG, Yeh R-F, Sharp PA, and Burge CB. 2002. Predictive Identification of Exonic Splicing Enhancers in Human Genes. ***Science*** 297**:** 1007-1013.

Faustino NA and Cooper TA. 2003. Pre-mRNA splicing and human disease. ***Genes & Development*** 17**:** 419-437.

Fox-Walsh KL, Dou Y, Lam BJ, Hung S-p, Baldi PF, and Hertel KJ. 2005. The architecture of pre-mRNAs affects mechanisms of splice-site pairing. ***Proceedings of the National Academy of Sciences of the United States of America*** 102**:** 16176-16181.

Frischmeyer PA and Dietz HC. 1999. Nonsense-Mediated mRNA Decay in Health and Disease. ***Human Molecular Genetics*** 8**:** 1893-1900.

Fujita PA, Rhead B, Zweig AS, Hinrichs AS, Karolchik D, Cline MS, Goldman M, Barber GP, Clawson H, Coelho A et al. 2011. The UCSC Genome Browser database: update 2011. ***Nucleic Acids Research***.

Gabut M, Chaudhry S, and Blencowe BJ. 2008. SnapShot: The Splicing Regulatory Machinery. ***Cell*** 133**:** 192-192.e191.

Garber M, Grabherr MG, Guttman M, and Trapnell C. 2011. Computational methods for transcriptome annotation and quantification using RNA-seq. ***Nat Meth*** 8**:** 469-477.

Garcia-Blanco MA, Baraniak AP, and Lasda EL. 2004. Alternative splicing in disease and therapy. ***Nat Biotech*** 22**:** 535-546.

Gehman LT, Stoilov P, Maguire J, Damianov A, Lin C-H, Shiue L, Ares M, Mody I, and Black DL. 2011. The splicing regulator Rbfox1 (A2BP1) controls neuronal excitation in the mammalian brain. ***Nat Genet*** 43**:** 706-711.

Gerstein MB Lu ZJ Van Nostrand EL Cheng C Arshinoff BI Liu T Yip KY Robilotto R Rechtsteiner A Ikegami K et al. 2010. Integrative Analysis of the Caenorhabditis elegans Genome by the modENCODE Project. ***Science*** 330**:** 1775-1787.

Ghigna C, Giordano S, Shen H, Benvenuto F, Castiglioni F, Comoglio PM, Green MR, Riva S, and Biamonti G. 2005. Cell Motility Is Controlled by SF2/ASF through Alternative Splicing of the Ron Protooncogene. ***Molecular cell*** 20**:** 881-890.

Glisovic T, Bachorik JL, Yong J, and Dreyfuss G. 2008. RNA-binding proteins and post-transcriptional gene regulation. ***FEBS letters*** 582**:** 1977-1986.

Graveley BR, Brooks AN, Carlson JW, Duff MO, Landolin JM, Yang L, Artieri CG, van Baren MJ, Boley N, Booth BW et al. 2011. The developmental transcriptome of Drosophila melanogaster. ***Nature*** 471**:** 473-479.

Green MR. 1986. PRE-mRNA Splicing. ***Annual Review of Genetics*** 20**:** 671-708.

Green MR. 1991. Biochemical Mechanisms of Constitutive and Regulated Pre-mRNA Splicing. ***Annual Review of Cell Biology*** 7**:** 559-599.

Green RE, Lewis BP, Hillman RT, Blanchette M, Lareau LF, Garnett AT, Rio DC, and Brenner SE. 2003. Widespread predicted nonsense-mediated mRNA decay of alternatively-spliced transcripts of human normal and disease genes. ***Bioinformatics*** 19**:** i118-i121.

Griffith M, Griffith OL, Mwenifumbo J, Goya R, Morrissy AS, Morin RD, Corbett R, Tang MJ, Hou Y-C, Pugh TJ et al. 2010. Alternative expression analysis by RNA sequencing. ***Nat Meth*** 7**:** 843-847.

Grossmann V, Tiacci E, Holmes AB, Kohlmann A, Martelli MP, Kern W, Spanhol-Rosseto A, Klein H-U, Dugas M, Schindela S et al. 2011. Whole-exome sequencing identifies somatic mutations of BCOR in acute myeloid leukemia with normal karyotype. ***Blood*** 118**:** 6153-6163.

Guo W, Schafer S, Greaser ML, Radke MH, Liss M, Govindarajan T, Maatz H, Schulz H, Li S, Parrish AM et al. 2012. RBM20, a gene for hereditary cardiomyopathy, regulates titin splicing. ***Nat Med*** 18**:** 766-773.

Hafner M, Landgraf P, Ludwig J, Rice A, Ojo T, Lin C, Holoch D, Lim C, and Tuschl T. 2008. Identification of microRNAs and other small regulatory RNAs using cDNA library sequencing. ***Methods*** 44**:** 3-12.

Hafner M, Landthaler M, Burger L, Khorshid M, Hausser J, Berninger P, Rothballer A, Ascano M, Jungkamp A-C, Munschauer M et al. 2010. Transcriptome-wide Identification of RNA-Binding Protein and MicroRNA Target Sites by PAR-CLIP. ***Cell*** 141**:** 129-141.

Han SP, Tang YH, and Smith R. 2010. Functional diversity of the hnRNPs: past, present and perspectives. ***Biochem J*** 430**:** 379-392.

He H, Liyanarachchi S, Akagi K, Nagy R, Li J, Dietrich RC, Li W, Sebastian N, Wen B, Xin B et al. 2011. Mutations in U4atac snRNA, a Component of the Minor Spliceosome, in the Developmental Disorder MOPD I. ***Science*** 332**:** 238-240.

Hegele A, Kamburov A, Grossmann A, Sourlis C, Wowro S, Weimann M, Will Cindy L, Pena V, Lührmann R, and Stelzl U. 2012. Dynamic Protein-Protein Interaction Wiring of the Human Spliceosome. ***Molecular cell*** 45**:** 567-580.

Hicks MJ, Yang C-R, Kotlajich MV, and Hertel KJ. 2006. Linking Splicing to Pol II Transcription Stabilizes Pre-mRNAs and Influences Splicing Patterns. ***PLoS Biol*** 4**:** e147.

Hoell JI, Larsson E, Runge S, Nusbaum JD, Duggimpudi S, Farazi TA, Hafner M, Borkhardt A, Sander C, and Tuschl T. 2011. RNA targets of wild-type and mutant FET family proteins. ***Nat Struct Mol Biol*** advance online publication.

Hoffman BE and Grabowski PJ. 1992. U1 snRNP targets an essential splicing factor, U2AF65, to the 3' splice site by a network of interactions spanning the exon. ***Genes & Development*** 6**:** 2554-2568.

Hogan DJ, Riordan DP, Gerber AP, Herschlag D, and Brown PO. 2008. Diverse RNA-Binding Proteins Interact with Functionally Related Sets of RNAs, Suggesting an Extensive Regulatory System. ***PLoS Biol*** 6**:** e255.

Hong F, Breitling R, McEntee CW, Wittner BS, Nemhauser JL, and Chory J. 2006. RankProd: a bioconductor package for detecting differentially expressed genes in meta-analysis. ***Bioinformatics*** 22**:** 2825-2827.

Horn D, Chyrek M, Kleier S, Luttgen S, Bolz H, Hinkel G-K, Korenke GC, Ries A, Schell-Apacik C, Tinschert S et al. 2005. Novel mutations in BCOR in three patients with oculo-facio-cardio-dental syndrome, but none in Lenz microphthalmia syndrome. ***Eur J Hum Genet*** 13**:** 563-569.

Hu K, Ji L, Applegate KT, Danuser G, and Waterman-Storer CM. 2007. Differential Transmission of Actin Motion Within Focal Adhesions. ***Science*** 315**:** 111-115.

Huynh KD, Fischle W, Verdin E, and Bardwell VJ. 2000. BCoR, a novel corepressor involved in BCL-6 repression. ***Genes Dev*** 14**:** 1810-1823.

Inoue A, Takahashi KP, Kimura M, Watanabe T, and Morisawa S. 1996. Molecular Cloning of a RNA Binding Protein, S1-1. ***Nucleic Acids Research*** 24**:** 2990-2997.

Inoue A, Tsugawa K, Tokunaga K, Takahashi KP, Uni S, Kimura M, Nishio K, Yamamoto N, Honda K-i, Watanabe T et al. 2008. S1-1 nuclear domains: characterization and dynamics as a function of transcriptional activity. ***Biology of the Cell*** 100**:** 523-535.

Jesse S, Koenig A, Ellenrieder V, and Menke A. 2010. Lef-1 isoforms regulate different target genes and reduce cellular adhesion. ***Int J Cancer*** 126**:** 1109-1120.

Johnson JM, Castle J, Garrett-Engele P, Kan Z, Loerch PM, Armour CD, Santos R, Schadt EE, Stoughton R, and Shoemaker DD. 2003. Genome-Wide Survey of Human Alternative Pre-mRNA Splicing with Exon Junction Microarrays. ***Science*** 302**:** 2141-2144.

Johnston JJ, Teer JK, Cherukuri PF, Hansen NF, Loftus SK, Chong K, Mullikin JC, and Biesecker LG. 2010. Massively Parallel Sequencing of Exons on the X Chromosome Identifies RBM10 as the Gene that Causes a Syndromic Form of Cleft Palate. ***American journal of human genetics*** 86**:** 743-748.

Juneau K, Palm C, Miranda M, and Davis RW. 2007. High-density yeast-tiling array reveals previously undiscovered introns and extensive regulation of meiotic splicing. ***Proceedings of the National Academy of Sciences*** 104**:** 1522-1527.

Jungkamp A-C, Stoeckius M, Mecenas D, Grün D, Mastrobuoni G, Kempa S, and Rajewsky N. 2011. In Vivo and Transcriptome-wide Identification of RNA Binding Protein Target Sites. ***Molecular cell*** 44**:** 828-840.

Kabashi E, Valdmanis PN, Dion P, Spiegelman D, McConkey BJ, Velde CV, Bouchard J-P, Lacomblez L, Pochigaeva K, Salachas F et al. 2008. TARDBP mutations in individuals with sporadic and familial amyotrophic lateral sclerosis. ***Nat Genet*** 40**:** 572-574.

Kapur K, Xing Y, Ouyang Z, and Wong W. 2007. Exon arrays provide accurate assessments of gene expression. ***Genome Biology*** 8**:** R82.

Karni R, de Stanchina E, Lowe SW, Sinha R, Mu D, and Krainer AR. 2007. The gene encoding the splicing factor SF2/ASF is a proto-oncogene. ***Nat Struct Mol Biol*** 14**:** 185-193.

Kashima T and Manley JL. 2003. A negative element in SMN2 exon 7 inhibits splicing in spinal muscular atrophy. ***Nat Genet*** 34**:** 460-463.

Keene JD. 2007. RNA regulons: coordination of post-transcriptional events. ***Nat Rev Genet*** 8**:** 533-543.

Keene JD, Komisarow JM, and Friedersdorf MB. 2006. RIP-Chip: the isolation and identification of mRNAs, microRNAs and protein components of ribonucleoprotein complexes from cell extracts. ***Nat. Protocols*** 1**:** 302-307.

Kishore S, Jaskiewicz L, Burger L, Hausser J, Khorshid M, and Zavolan M. 2011. A quantitative analysis of CLIP methods for identifying binding sites of RNA-binding proteins. ***Nat Meth*** advance online publication.

Kolasinska-Zwierz P, Down T, Latorre I, Liu T, Liu XS, and Ahringer J. 2009. Differential chromatin marking of introns and expressed exons by H3K36me3. ***Nat Genet*** 41**:** 376-381.

Konig J, Zarnack K, Rot G, Curk T, Kayikci M, Zupan B, Turner DJ, Luscombe NM, and Ule J. 2010. iCLIP reveals the function of hnRNP particles in splicing at individual nucleotide resolution. ***Nat Struct Mol Biol*** 17**:** 909-915.

Konig J, Zarnack K, Rot G, Curk T, Kayikci M, Zupan B, Turner DJ, Luscombe NM, and Ule J. 2011. iCLIP - Transcriptome-wide Mapping of Protein-RNA Interactions with Individual Nucleotide Resolution. ***J Vis Exp*****:** e2638.

KORNBLIHTT AR, DE LA MATA M, FEDEDA JP, MUNOZ MJ, and NOGUES G. 2004. Multiple links between transcription and splicing. ***RNA*** 10**:** 1489-1498.

Kwok RPS, Lundblad JR, Chrivia JC, Richards JP, Bachinger HP, Brennan RG, Roberts SGE, Green MR, and Goodman RH. 1994. Nuclear-Protein Cbp Is a Coactivator for the Transcription Factor Creb. ***Nature*** 370**:** 223-226.

Lallena MJ, Chalmers KJ, Llamazares S, Lamond AI, and Valcárcel J. 2002. Splicing Regulation at the Second Catalytic Step by Sex-lethal Involves 3' Splice Site Recognition by SPF45. ***Cell*** 109**:** 285-296.

Lareau LF, Inada M, Green RE, Wengrod JC, and Brenner SE. 2007. Unproductive splicing of SR genes associated with highly conserved and ultraconserved DNA elements. ***Nature*** 446**:** 926-929.

Lebedeva S, Jens M, Theil K, Schwanhäusser B, Selbach M, Landthaler M, and Rajewsky N. 2011. Transcriptome-wide Analysis of Regulatory Interactions of the RNA-Binding Protein HuR. ***Molecular cell*** 43**:** 340-352.

Lefebvre S, Bürglen L, Reboullet S, Clermont O, Burlet P, Viollet L, Benichou B, Cruaud C, Millasseau P, Zeviani M et al. 1995. Identification and characterization of a spinal muscular atrophy-determining gene. ***Cell*** 80**:** 155-165.

Lewis BP, Green RE, and Brenner SE. 2003. Evidence for the widespread coupling of alternative splicing and nonsense-mediated mRNA decay in humans. ***Proceedings of the National Academy of Sciences*** 100**:** 189-192.

Li H and Durbin R. 2009. Fast and accurate short read alignment with Burrows-Wheeler transform. ***Bioinformatics*** 25**:** 1754-1760.

Li H, Handsaker B, Wysoker A, Fennell T, Ruan J, Homer N, Marth G, Abecasis G, Durbin R, and Subgroup GPDP. 2009a. The Sequence Alignment/Map format and SAMtools. ***Bioinformatics*** 25**:** 2078-2079.

Li J, Wang J, Wang J, Nawaz Z, Liu JM, Qin J, and Wong J. 2000. Both corepressor proteins SMRT and N-CoR exist in large protein complexes containing HDAC3. ***EMBO J*** 19**:** 4342-4350.

Li Q, Lee J-A, and Black DL. 2007. Neuronal regulation of alternative pre-mRNA splicing. ***Nat Rev Neurosci*** 8**:** 819-831.

Li Y, Wang L, Zhang M, Melamed J, Liu X, Reiter R, Wei J, Peng Y, Zou X, Pellicer A et al. 2009b. LEF1 in Androgen-Independent Prostate Cancer: Regulation of Androgen Receptor Expression, Prostate Cancer Growth, and Invasion. ***Cancer Research*** 69**:** 3332-3338.

Licatalosi DD, Mele A, Fak JJ, Ule J, Kayikci M, Chi SW, Clark TA, Schweitzer AC, Blume JE, Wang X et al. 2008. HITS-CLIP yields genome-wide insights into brain alternative RNA processing. ***Nature*** 456**:** 464-469.

Listerman I, Sapra AK, and Neugebauer KM. 2006. Cotranscriptional coupling of splicing factor recruitment and precursor messenger RNA splicing in mammalian cells. ***Nat Struct Mol Biol*** 13**:** 815-822.

Liu F and Gong C-X. 2008. Tau exon 10 alternative splicing and tauopathies. ***Molecular Neurodegeneration*** 3**:** 8.

Long JC and Caceres JF. 2009. The SR protein family of splicing factors: master regulators of gene expression. ***Biochem J*** 417**:** 15-27.

Luco RF, Allo M, Schor IE, Kornblihtt AR, and Misteli T. 2011. Epigenetics in Alternative Pre-mRNA Splicing. ***Cell*** 144**:** 16-26.

Lukong KE, Chang K-w, Khandjian EW, and Richard S. 2008. RNA-binding proteins in human genetic disease. ***Trends in Genetics*** 24**:** 416-425.

Lunn MR and Wang CH. 2008. Spinal muscular atrophy. ***The Lancet*** 371**:** 2120-2133.

Makarov EM, Makarova OV, Urlaub H, Gentzel M, Will CL, Wilm M, and Lührmann R. 2002. Small Nuclear Ribonucleoprotein Remodeling During Catalytic Activation of the Spliceosome. ***Science*** 298**:** 2205-2208.

Makarov EM, Owen N, Bottrill A, and Makarova OV. 2011. Functional mammalian spliceosomal complex E contains SMN complex proteins in addition to U1 and U2 snRNPs. ***Nucleic Acids Research*** 40**:** 2639-2652.

Makeyev EV, Zhang J, Carrasco MA, and Maniatis T. 2007. The MicroRNA miR-124 Promotes Neuronal Differentiation by Triggering Brain-Specific Alternative Pre-mRNA Splicing. ***Molecular cell*** 27**:** 435-448.

Makishima H, Visconte V, Sakaguchi H, Jankowska AM, Abu Kar S, Jerez A, Przychodzen B, Bupathi M, Guinta K, Afable MG et al. 2012. Mutations in the spliceosome machinery, a novel and ubiquitous pathway in leukemogenesis. ***Blood*** 119**:** 3203-3210.

Maniatis T and Tasic B. 2002. Alternative pre-mRNA splicing and proteome expansion in metazoans. ***Nature*** 418**:** 236-243.

Martínez-Arribas F, Agudo D, Pollán M, Gómez-Esquer F, Díaz-Gil G, Lucas R, and Schneider J. 2006. Positive correlation between the expression of X-chromosome

RBM genes (RBMX, RBM3, RBM10) and the proapoptotic Bax gene in human breast cancer. ***Journal of Cellular Biochemistry*** 97**:** 1275-1282.

McCampbell A, Taylor JP, Taye AA, Robitschek J, Li M, Walcott J, Merry D, Chai Y, Paulson H, Sobue G et al. 2000. CREB-binding protein sequestration by expanded polyglutamine. ***Hum Mol Genet*** 9**:** 2197-2202.

McManus CJ and Graveley BR. 2011. RNA structure and the mechanisms of alternative splicing. ***Current Opinion in Genetics & Development*** 21**:** 373-379.

Merrill BJ, Gat U, DasGupta R, and Fuchs E. 2001. Tcf3 and Lef1 regulate lineage differentiation of multipotent stem cells in skin. ***Genes Dev*** 15**:** 1688-1705.

Modrek B and Lee C. 2002. A genomic view of alternative splicing. ***Nat Genet*** 30**:** 13-19.

Moore MJ and Silver PA. 2008. Global analysis of mRNA splicing. ***RNA*** 14**:** 197-203.

Moore MJ, Wang Q, Kennedy CJ, and Silver PA. 2010. An Alternative Splicing Network Links Cell-Cycle Control to Apoptosis. ***Cell*** 142**:** 625-636.

Mordes D, Luo X, Kar A, Kuo D, Xu L, Fushimi K, Yu G, Sternberg P, Jr., and Wu JY. 2006. Pre-mRNA splicing and retinitis pigmentosa. ***Mol Vis*** 12**:** 1259-1271.

Mortazavi A, Williams BA, McCue K, Schaeffer L, and Wold B. 2008. Mapping and quantifying mammalian transcriptomes by RNA-Seq. ***Nat Meth*** 5**:** 621-628.

Mullighan CG, Goorha S, Radtke I, Miller CB, Coustan-Smith E, Dalton JD, Girtman K, Mathew S, Ma J, Pounds SB et al. 2007. Genome-wide analysis of genetic alterations in acute lymphoblastic leukaemia. ***Nature*** 446**:** 758-764.

Mullighan CG, Zhang JH, Kasper LH, Lerach S, Payne-Turner D, Phillips LA, Heatley SL, Holmfeldt L, Collins-Underwood JR, Ma J et al. 2011. CREBBP mutations in relapsed acute lymphoblastic leukaemia. ***Nature*** 471**:** 235-U127.

Murata T, Kurokawa R, Krones A, Tatsumi K, Ishii M, Taki T, Masuno M, Ohashi H, Yanagisawa M, Rosenfeld MG et al. 2001. Defect of histone acetyltransferase activity of the nuclear transcriptional coactivator CBP in Rubinsteinâ€“Taybi syndrome. ***Human Molecular Genetics*** 10**:** 1071-1076.

Nagoshi RN and Baker BS. 1990. Regulation of sex-specific RNA splicing at the Drosophila doublesex gene: cis-acting mutations in exon sequences alter sex-specific RNA splicing patterns. ***Genes & Development*** 4**:** 89-97.

Najmabadi H, Hu H, Garshasbi M, Zemojtel T, Abedini SS, Chen W, Hosseini M, Behjati F, Haas S, Jamali P et al. 2011. Deep sequencing reveals 50 novel genes for recessive cognitive disorders. ***Nature*** 478**:** 57-63.

Ng D, Thakker N, Corcoran CM, Donnai D, Perveen R, Schneider A, Hadley DW, Tifft C, Zhang L, Wilkie AO et al. 2004. Oculofaciocardiodental and Lenz microphthalmia syndromes result from distinct classes of mutations in BCOR. ***Nat Genet*** 36**:** 411-416.

Nguyen CD, Mansfield RE, Leung W, Vaz PM, Loughlin FE, Grant RP, and Mackay JP. 2011. Characterization of a Family of RanBP2-Type Zinc Fingers that Can Recognize Single-Stranded RNA. ***Journal of Molecular Biology*** 407**:** 273-283.

Nilsen TW and Graveley BR. 2010. Expansion of the eukaryotic proteome by alternative splicing. ***Nature*** 463**:** 457-463.

Okoniewski MJ and Miller CJ. 2008. Comprehensive Analysis of Affymetrix Exon Arrays Using BioConductor. ***PLoS Comput Biol*** 4**:** e6.

Olson TM, Illenberger S, Kishimoto NY, Huttelmaier S, Keating MT, and Jockusch BM. 2002. Metavinculin mutations alter actin interaction in dilated cardiomyopathy. ***Circulation*** 105**:** 431-437.

Ozsolak F and Milos PM. 2011. RNA sequencing: advances, challenges and opportunities. ***Nat Rev Genet*** 12**:** 87-98.

Pan Q, Shai O, Lee LJ, Frey BJ, and Blencowe BJ. 2008. Deep surveying of alternative splicing complexity in the human transcriptome by high-throughput sequencing. ***Nat Genet*** 40**:** 1413-1415.

Panagopoulos I, Fioretos T, Isaksson M, Samuelsson U, BillstrÃ¶m R, StrÃ¶mbeck B, Mitelman F, and Johansson B. 2001. Fusion of the MORF and CBP genes in acute myeloid leukemia with the t(10;16)(q22;p13). ***Human Molecular Genetics*** 10**:** 395-404.

Papaemmanuil E, Cazzola M, Boultwood J, Malcovati L, Vyas P, Bowen D, Pellagatti A, Wainscoat JS, Hellstrom-Lindberg E, Gambacorti-Passerini C et al. 2011. Somatic SF3B1 Mutation in Myelodysplasia with Ring Sideroblasts. ***New England Journal of Medicine*** 365**:** 1384-1395.

Pasqualucci L, Dominguez-Sola D, Chiarenza A, Fabbri G, Grunn A, Trifonov V, Kasper LH, Lerach S, Tang H, Ma J et al. 2011. Inactivating mutations of acetyltransferase genes in B-cell lymphoma. ***Nature*** 471**:** 189-195.

Patel AA and Steitz JA. 2003. Splicing double: insights from the second spliceosome. ***Nat Rev Mol Cell Biol*** 4**:** 960-970.

Pedrotti S, Busà R, Compagnucci C, and Sette C. 2011. The RNA recognition motif protein RBM11 is a novel tissue-specific splicing regulator. ***Nucleic Acids Research***.

Polymenidou M, Lagier-Tourenne C, Hutt KR, Huelga SC, Moran J, Liang TY, Ling S-C, Sun E, Wancewicz E, Mazur C et al. 2011. Long pre-mRNA depletion and RNA missplicing contribute to neuronal vulnerability from loss of TDP-43. ***Nat Neurosci*** 14**:** 459-468.

Ramani AK, Calarco JA, Pan Q, Mavandadi S, Wang Y, Nelson AC, Lee LJ, Morris Q, Blencowe B, Zhen M et al. 2010. Genome-wide analysis of alternative splicing in Caenorhabditis elegans. ***Genome Research***.

Rappsilber J, Ryder U, Lamond AI, and Mann M. 2002. Large-Scale Proteomic Analysis of the Human Spliceosome. ***Genome Research*** 12**:** 1231-1245.

Reed R. 2000. Mechanisms of fidelity in pre-mRNA splicing. ***Current Opinion in Cell Biology*** 12**:** 340-345.

Reya T, O'Riordan M, Okamura R, Devaney E, Willert K, Nusse R, and Grosschedl R. 2000. Wnt Signaling Regulates B Lymphocyte Proliferation through a LEF-1 Dependent Mechanism. ***Immunity*** 13**:** 15-24.

Rintala-Maki ND, Goard CA, Langdon CE, Wall VE, Traulsen KEA, Morin CD, Bonin M, and Sutherland LC. 2007. Expression of RBM5-related factors in primary breast tissue. ***Journal of Cellular Biochemistry*** 100**:** 1440-1458.

Rutherford NJ, Zhang Y-J, Baker M, Gass JM, Finch NA, Xu Y-F, Stewart H, Kelley BJ, Kuntz K, Crook RJP et al. 2008. Novel Mutations in *TARDBP* (TDP-43) in Patients with Familial Amyotrophic Lateral Sclerosis. ***PLoS Genet*** 4**:** e1000193.

Sanford JR, Wang X, Mort M, VanDuyn N, Cooper DN, Mooney SD, Edenberg HJ, and Liu Y. 2009. Splicing factor SFRS1 recognizes a functionally diverse landscape of RNA transcripts. ***Genome Research*** 19**:** 381-394.

Schwartz S, Meshorer E, and Ast G. 2009. Chromatin organization marks exon-intron structure. ***Nat Struct Mol Biol*** 16**:** 990-995.

Sharma S, Kohlstaedt LA, Damianov A, Rio DC, and Black DL. 2008. Polypyrimidine tract binding protein controls the transition from exon definition to an intron defined spliceosome. ***Nat Struct Mol Biol*** 15**:** 183-191.

Shepard P and Hertel K. 2009. The SR protein family. ***Genome Biology*** 10**:** 242.

Shin C and Manley JL. 2004. Cell signalling and the control of pre-mRNA splicing. ***Nat Rev Mol Cell Biol*** 5**:** 727-738.

Smith CWJ and Valcárcel J. 2000. Alternative pre-mRNA splicing: the logic of combinatorial control. ***Trends in Biochemical Sciences*** 25**:** 381-388.

Sreedharan J, Blair IP, Tripathi VB, Hu X, Vance C, Rogelj B, Ackerley S, Durnall JC, Williams KL, Buratti E et al. 2008. TDP-43 Mutations in Familial and Sporadic Amyotrophic Lateral Sclerosis. ***Science*** 319**:** 1668-1672.

Stamm S, Ben-Ari S, Rafalska I, Tang Y, Zhang Z, Toiber D, Thanaraj TA, and Soreq H. 2005. Function of alternative splicing. ***Gene*** 344**:** 1-20.

Stevens SW, Ryan DE, Ge HY, Moore RE, Young MK, Lee TD, and Abelson J. 2002. Composition and Functional Characterization of the Yeast Spliceosomal Penta-snRNP. ***Molecular cell*** 9**:** 31-44.

Sun S, Zhang Z, Sinha R, Karni R, and Krainer AR. 2010. SF2/ASF autoregulation involves multiple layers of post-transcriptional and translational control. ***Nat Struct Mol Biol*** 17**:** 306-312.

Sutherland LC, Rintala-Maki ND, White RD, and Morin CD. 2005. RNA binding motif (RBM) proteins: A novel family of apoptosis modulators? ***Journal of Cellular Biochemistry*** 94**:** 5-24.

Takeda H, Lyle S, Lazar AJ, Zouboulis CC, Smyth I, and Watt FM. 2006. Human sebaceous tumors harbor inactivating mutations in LEF1. ***Nat Med*** 12**:** 395-397.

Thienpont B, Bena F, Breckpot J, Philip N, Menten B, Van Esch H, Scalais E, Salamone JM, Fong CT, Kussmann JL et al. 2010. Duplications of the critical Rubinstein-Taybi deletion region on chromosome 16p13.3 cause a novel recognisable syndrome. ***J Med Genet*** 47**:** 155-161.

Tiacci E, Grossmann V, Martelli MP, Kohlmann A, Haferlach T, and Falini B. 2012. The corepressors BCOR and BCORL1: two novel players in acute myeloid leukemia. ***Haematologica*** 97**:** 3-5.

Trapnell C, Williams BA, Pertea G, Mortazavi A, Kwan G, van Baren MJ, Salzberg SL, Wold BJ, and Pachter L. 2010. Transcript assembly and quantification by RNA-Seq reveals unannotated transcripts and isoform switching during cell differentiation. ***Nat Biotech*** 28**:** 511-515.

Tsuda M, Takahashi S, Takahashi Y, and Asahara H. 2003. Transcriptional co-activators CREB-binding protein and p300 regulate chondrocyte-specific gene expression via association with Sox9. ***J Biol Chem*** 278**:** 27224-27229.

Ule J. 2008. Ribonucleoprotein complexes in neurologic diseases. ***Current Opinion in Neurobiology*** 18**:** 516-523.

Ule J, Stefani G, Mele A, Ruggiu M, Wang X, Taneri B, Gaasterland T, Blencowe BJ, and Darnell RB. 2006. An RNA map predicting Nova-dependent splicing regulation. ***Nature*** 444**:** 580-586.

Ule J, Ule A, Spencer J, Williams A, Hu J-S, Cline M, Wang H, Clark T, Fraser C, Ruggiu M et al. 2005. Nova regulates brain-specific splicing to shape the synapse. ***Nat Genet*** 37**:** 844-852.

Vargas D, Shah K, Batish M, Levandoski M, Sinha S, Marras Salvatore AE, Schedl P, and Tyagi S. 2011. Single-Molecule Imaging of Transcriptionally Coupled and Uncoupled Splicing. ***Cell*** 147**:** 1054-1065.

Vasile VC, Will ML, Ommen SR, Olson TM, and Ackerman MJ. 2006. Identification of a metavinculin missense mutation, R975W, associated with both hypertrophic and dilated cardiomyopathy. ***Molecular Genetics and Metabolism*** 87**:** 169-174.

Wahl MC, Will CL, and Lührmann R. 2009. The Spliceosome: Design Principles of a Dynamic RNP Machine. ***Cell*** 136**:** 701-718.

Wang ET, Sandberg R, Luo S, Khrebtukova I, Zhang L, Mayr C, Kingsmore SF, Schroth GP, and Burge CB. 2008. Alternative isoform regulation in human tissue transcriptomes. ***Nature*** 456**:** 470-476.

Wang G-S and Cooper TA. 2007. Splicing in disease: disruption of the splicing code and the decoding machinery. ***Nat Rev Genet*** 8**:** 749-761.

Wang L, Lawrence MS, Wan Y, Stojanov P, Sougnez C, Stevenson K, Werner L, Sivachenko A, DeLuca DS, Zhang L et al. 2011. SF3B1 and Other Novel Cancer Genes in Chronic Lymphocytic Leukemia. ***New England Journal of Medicine*** 365**:** 2497-2506.

Wang Z and Burge CB. 2008. Splicing regulation: From a parts list of regulatory elements to an integrated splicing code. ***RNA*** 14**:** 802-813.

Warzecha CC, Sato TK, Nabet B, Hogenesch JB, and Carstens RP. 2009. ESRP1 and ESRP2 Are Epithelial Cell-Type-Specific Regulators of FGFR2 Splicing. ***Molecular cell*** 33**:** 591-601.

Will CL and Lührmann R. 2010. Spliceosome Structure and Function. ***Cold Spring Harbor Perspectives in Biology***.

Winton MJ, Igaz LM, Wong MM, Kwong LK, Trojanowski JQ, and Lee VM-Y. 2008. Disturbance of Nuclear and Cytoplasmic TAR DNA-binding Protein (TDP-

43) Induces Disease-like Redistribution, Sequestration, and Aggregate Formation. ***Journal of Biological Chemistry*** 283**:** 13302-13309.

Witten JT and Ule J. 2011. Understanding splicing regulation through RNA splicing maps. ***Trends in Genetics*** 27**:** 89-97.

Wollerton MC, Gooding C, Wagner EJ, Garcia-Blanco MA, and Smith CWJ. 2004. Autoregulation of Polypyrimidine Tract Binding Protein by Alternative Splicing Leading to Nonsense-Mediated Decay. ***Molecular cell*** 13**:** 91-100.

Xie J and Black DL. 2001. A CaMK IV responsive RNA element mediates depolarization-induced alternative splicing of ion channels. ***Nature*** 410**:** 936-939.

Xu WM, Baribault H, and Adamson ED. 1998. Vinculin knockout results in heart and brain defects during embryonic development. ***Development*** 125**:** 327-337.

Xue Y, Zhou Y, Wu T, Zhu T, Ji X, Kwon Y-S, Zhang C, Yeo G, Black DL, Sun H et al. 2009. Genome-wide Analysis of PTB-RNA Interactions Reveals a Strategy Used by the General Splicing Repressor to Modulate Exon Inclusion or Skipping. ***Molecular cell*** 36**:** 996-1006.

Yang I, Chen E, Hasseman J, Liang W, Frank B, Wang S, Sharov V, Saeed A, White J, Li J et al. 2002. Within the fold: assessing differential expression measures and reproducibility in microarray assays. ***Genome Biology*** 3**:** research0062.0061 - research0062.0012.

Yeo GW, Coufal NG, Liang TY, Peng GE, Fu X-D, and Gage FH. 2009. An RNA code for the FOX2 splicing regulator revealed by mapping RNA-protein interactions in stem cells. ***Nat Struct Mol Biol*** 16**:** 130-137.

Yoshida K, Sanada M, Shiraishi Y, Nowak D, Nagata Y, Yamamoto R, Sato Y, Sato-Otsubo A, Kon A, Nagasaki M et al. 2011. Frequent pathway mutations of splicing machinery in myelodysplasia. ***Nature*** 478**:** 64-69.

Zhang C and Darnell RB. 2011. Mapping in vivo protein-RNA interactions at single-nucleotide resolution from HITS-CLIP data. ***Nat Biotech*** 29**:** 607-614.

Zhang C, Frias MA, Mele A, Ruggiu M, Eom T, Marney CB, Wang H, Licatalosi DD, Fak JJ, and Darnell RB. 2010. Integrative Modeling Defines the Nova Splicing-Regulatory Network and Its Combinatorial Controls. ***Science*** 329**:** 439-443.

Zhang Z, Hesselberth JR, and Fields S. 2007. Genome-wide identification of spliced introns using a tiling microarray. ***Genome Research*** 17**:** 000.

Zhang Z, Lotti F, Dittmar K, Younis I, Wan L, Kasim M, and Dreyfuss G. 2008. SMN Deficiency Causes Tissue-Specific Perturbations in the Repertoire of snRNAs and Widespread Defects in Splicing. ***Cell*** 133**:** 585-600.

# 6 APPENDIX

**Table 1 Differentially expressed genes upon RBM10 knockdown (KD) or overexpression (OE).**

| name | Refseq_ID | chrom | begin | end | Z.OE | fdr.OE | Z.KD | fdr.KD | rpkm.KD | rpkm.OE | log2.fold.KD | log2.fold.OE |
|---|---|---|---|---|---|---|---|---|---|---|---|---|
| MIR3687 | NR_037458 | chr21 | 9826202 | 9826263 | -5.9983 | 0.0000 | -3.3267 | 0.0055 | 29.8993 | 13.4403 | -0.1185 | -1.3967 |
| SFXN2 | NM_178858 | chr10 | 104474297 | 104498946 | -5.9348 | 0.0000 | 1.6544 | 0.0578 | 18.9143 | 13.3661 | 0.2018 | -1.3284 |
| SHMT2 | NM_001166356 | chr12 | 57623355 | 57628718 | -5.8363 | 0.0000 | 0.8424 | 0.4841 | 126.2826 | 96.7719 | 0.0890 | -1.1910 |
| SNORD121B | NR_003690 | chr9 | 33934285 | 33934378 | -5.7016 | 0.0083 | -2.2872 | 0.0098 | 1.6747 | 2.9097 | -0.9387 | -1.6374 |
| GNB1L | NM_053004 | chr22 | 19775933 | 19842462 | -5.5105 | 0.0040 | 0.8809 | 0.4355 | 17.8105 | 14.0710 | 0.1131 | -1.2165 |
| NPEPL1 | NM_001204872 | chr20 | 57264186 | 57290900 | -5.4612 | 0.0050 | 1.1042 | 0.2672 | 4.4363 | 2.9678 | 0.3197 | -1.7151 |
| ACSS1 | NM_032501 | chr20 | 24986872 | 25039616 | -5.1573 | 0.0086 | -1.6987 | 0.0610 | 13.5693 | 12.0884 | -0.3991 | -1.1708 |
| TMEM163 | NM_030923 | chr2 | 135213329 | 135476571 | -5.0513 | 0.0088 | 0.7732 | 0.5728 | 4.6919 | 3.8662 | 0.2195 | -1.4475 |
| TBCD | NM_005993 | chr17 | 80709939 | 80901062 | -5.0078 | 0.0078 | 1.1351 | 0.2699 | 38.3949 | 27.5294 | 0.1739 | -1.0600 |
| RBM5 | NM_005778 | chr3 | 50126351 | 50156392 | -4.8847 | 0.0091 | 1.3584 | 0.1497 | 34.2764 | 29.2425 | 0.1812 | -1.0487 |
| GOLGA8B | NR_027410 | chr15 | 34817483 | 34875771 | -4.8147 | 0.0080 | 0.5011 | 0.8727 | 18.2545 | 12.9371 | 0.1226 | -1.0740 |
| DNAJB6 | NM_005494 | chr7 | 157129709 | 157210133 | -4.8024 | 0.0083 | 1.3077 | 0.1807 | 27.8749 | 24.3954 | 0.2189 | -0.9738 |
| HERC2P2 | NR_002824 | chr15 | 23282264 | 23378259 | -4.7866 | 0.0086 | 1.3219 | 0.1510 | 27.3418 | 22.9534 | 0.2070 | -1.0369 |
| FUS | NM_001170634 | chr16 | 31191430 | 31206192 | -4.7363 | 0.0080 | 0.3507 | 0.9738 | 102.1490 | 137.2725 | -0.0450 | -0.9787 |
| PITHD1 | NM_020362 | chr1 | 24104875 | 24114722 | -4.7192 | 0.0077 | 0.1392 | 1.1106 | 51.0286 | 48.3394 | -0.0037 | -0.9782 |
| SNORD15B | NR_000025 | chr11 | 75115464 | 75115610 | -4.5928 | 0.0345 | -0.1650 | 0.8124 | 2.3320 | 2.0548 | -0.1651 | -1.5983 |
| GSTT2 | NM_000854 | chr22 | 24322313 | 24326106 | -4.5816 | 0.0334 | 0.9823 | 0.0854 | 2.6326 | 3.8740 | 0.8387 | -1.3404 |
| MAD1L1 | NM_003550 | chr7 | 1855427 | 2272583 | -4.5142 | 0.0181 | -1.1139 | 0.3143 | 10.8415 | 11.0266 | -0.2540 | -1.0209 |
| USP19 | NM_001199162 | chr3 | 49145478 | 49158371 | -4.4437 | 0.0176 | 0.0659 | 1.1729 | 16.3826 | 15.7671 | -0.0027 | -0.9789 |
| RTKN | NM_001015056 | chr2 | 74652987 | 74669060 | -4.3878 | 0.0178 | -0.9545 | 0.4346 | 11.1960 | 9.5595 | -0.2497 | -1.0172 |
| CAMK2B | NM_172080 | chr7 | 44256748 | 44365230 | -4.3432 | 0.0184 | -0.4134 | 0.9673 | 4.2765 | 3.5396 | -0.0879 | -1.2480 |
| CPNE1 | NM_001198863 | chr20 | 34213952 | 34252878 | -4.3149 | 0.0175 | -0.2366 | 1.0303 | 71.2400 | 67.9824 | -0.0759 | -0.9046 |
| HDAC4 | NM_006037 | chr2 | 239969863 | 240322643 | -4.2837 | 0.0196 | -0.0469 | 1.1352 | 2.8817 | 2.0873 | -0.1747 | -1.4687 |
| PSMD2 | NM_002808 | chr3 | 184017021 | 184026840 | -4.2803 | 0.0171 | 0.8819 | 0.4401 | 104.6914 | 107.1247 | 0.0265 | -0.8911 |
| APEH | NM_001640 | chr3 | 49711434 | 49720934 | -4.2714 | 0.0198 | -1.8822 | 0.0304 | 32.8240 | 29.0374 | -0.3720 | -0.9087 |
| EML2 | NR_034098 | chr19 | 46112657 | 46148775 | -4.2568 | 0.0173 | 0.2858 | 0.9894 | 10.3049 | 8.2479 | 0.0595 | -1.0220 |
| CLK2P | NR_002711 | chr7 | 23624334 | 23626146 | -4.2429 | 0.0198 | 0.8272 | 0.5152 | 6.9581 | 5.1111 | 0.1506 | -1.0979 |
| ACAA1 | NR_024024 | chr3 | 38164200 | 38178733 | -4.1567 | 0.0281 | 0.3569 | 0.9659 | 13.7738 | 14.8668 | 0.0119 | -0.9108 |
| TPCN1 | NM_017901 | chr12 | 113659259 | 113736389 | -4.1238 | 0.0277 | 1.0643 | 0.3192 | 10.6907 | 6.9730 | 0.2276 | -0.9906 |

| name | Refseq_ID | chrom | begin | end | Z.OE | fdr.OE | Z.KD | fdr.KD | rpkm.KD | rpkm.OE | log2.fold.KD | log2.fold.OE |
|---|---|---|---|---|---|---|---|---|---|---|---|---|
| PSKH1 | NM_006742 | chr16 | 67927174 | 67963581 | -4.1199 | 0.0271 | -0.1721 | 1.0713 | 7.2473 | 7.0107 | -0.0395 | -0.9888 |
| GOLGA8A | NR_027409 | chr15 | 34671269 | 34729667 | -4.0286 | 0.0333 | 0.8145 | 0.5243 | 35.7093 | 26.0366 | 0.1039 | -0.8322 |
| SLC20A2 | NM_006749 | chr8 | 42273992 | 42397068 | -3.9767 | 0.0335 | 1.9004 | 0.0266 | 10.2357 | 5.8711 | 0.4085 | -0.9882 |
| SNORD1C | NR_004397 | chr17 | 74554873 | 74554951 | -3.8408 | 0.0376 | -0.0839 | 0.4073 | 4.0377 | 4.1718 | 0.1139 | -1.1177 |
| LOC440354 | NR_002473 | chr16 | 30278913 | 30317244 | -3.8089 | 0.0379 | 0.9106 | 0.3880 | 2.8758 | 1.7752 | 0.2922 | -1.3392 |
| NDUFAF3 | NM_199074 | chr3 | 49057907 | 49060926 | -3.7603 | 0.0476 | 1.0571 | 0.2743 | 47.4066 | 49.2346 | 0.2291 | -0.7957 |
| MTG1 | NM_138384 | chr10 | 135207620 | 135234174 | -3.7028 | 0.0483 | -0.2714 | 1.0340 | 39.5795 | 42.3392 | -0.0455 | -0.7896 |
| ILK | NM_004517 | chr11 | 6624963 | 6632099 | -3.6886 | 0.0474 | 1.4297 | 0.1150 | 24.9490 | 24.2028 | 0.3008 | -0.8090 |
| COQ6 | NM_182480 | chr14 | 74416642 | 74429813 | -3.6788 | 0.0467 | 0.3008 | 1.0179 | 9.4553 | 10.3392 | 0.0161 | -0.8454 |
| UTP6 | NM_018428 | chr17 | 30190189 | 30228729 | -3.6652 | 0.0488 | 0.9131 | 0.4326 | 48.0587 | 40.6065 | 0.0713 | -0.7790 |
| AP2A2 | NM_012305 | chr11 | 925840 | 1012240 | -3.6456 | 0.0499 | -0.4455 | 0.8954 | 16.9463 | 14.7941 | -0.1086 | -0.7987 |
| RFPL4A | NM_001145014 | chr19 | 56270506 | 56274541 | -3.6286 | 0.0479 | -1.5623 | 0.0635 | 1.4971 | 0.8904 | -0.8542 | -1.7361 |
| GMPPB | NM_013334 | chr3 | 49758931 | 49761384 | -3.6124 | 0.0500 | 0.2078 | 1.0732 | 15.0686 | 16.0562 | -0.0060 | -0.7879 |
| C2orf48 | NM_182626 | chr2 | 10281508 | 10351856 | -3.4352 | 0.0600 | 2.3094 | 0.0058 | 2.8697 | 1.0612 | 0.5592 | -1.5214 |
| RNASET2 | NM_003730 | chr6 | 167343003 | 167370077 | -3.2808 | 0.0876 | 2.5726 | 0.0015 | 17.0048 | 13.6126 | 0.5419 | -0.6968 |
| TRNAU1AP | NM_017846 | chr1 | 28879528 | 28905057 | -3.0411 | 0.1087 | 2.4367 | 0.0040 | 11.5625 | 8.3016 | 0.6281 | -0.7176 |
| SNORD76 | NR_003942 | chr1 | 173835772 | 173835853 | -2.9155 | 0.1219 | 1.4973 | 0.0395 | 31.0678 | 21.9822 | 0.3523 | -0.6141 |
| MPV17 | NM_002437 | chr2 | 27532359 | 27545969 | -2.8755 | 0.1294 | 2.8889 | 0.0007 | 32.6725 | 31.0590 | 0.6404 | -0.6179 |
| GALNS | NM_000512 | chr16 | 88880141 | 88923374 | -2.8631 | 0.1255 | 1.7838 | 0.0386 | 5.2874 | 5.1242 | 0.3871 | -0.7202 |
| MYC | NM_002467 | chr8 | 128748314 | 128753680 | -2.7828 | 0.1477 | -2.2507 | 0.0095 | 49.8787 | 39.0412 | -0.4006 | -0.5957 |
| PORCN | NM_203473 | chrX | 48367370 | 48379202 | -2.2349 | 0.2640 | -2.8988 | 0.0014 | 3.5111 | 4.2794 | -0.7155 | -0.5838 |
| FAM19A5 | NM_001082967 | chr22 | 48885287 | 49147744 | -2.1535 | 0.2965 | -1.9876 | 0.0223 | 2.9249 | 3.3174 | -0.6936 | -0.5823 |
| MIR3911 | NR_037473 | chr9 | 130452965 | 130453074 | -1.9851 | 0.3006 | -1.2840 | 0.0436 | 0.9958 | 1.0139 | -0.5750 | -1.0209 |
| MRC2 | NM_006039 | chr17 | 60704761 | 60770952 | -1.9643 | 0.3399 | -1.8862 | 0.0289 | 2.0036 | 1.3122 | -0.4315 | -0.7485 |
| C3orf42 | NR_026829 | chr3 | 10326102 | 10327430 | -1.7760 | 0.4404 | 1.9632 | 0.0206 | 1.8006 | 0.9929 | 0.4998 | -0.7282 |
| ZNF711 | NM_021998 | chrX | 84498996 | 84528368 | -1.7430 | 0.4519 | -4.7909 | 0.0000 | 150.6704 | 147.3155 | -0.7726 | -0.3813 |
| TMEM150A | NR_033179 | chr2 | 85825669 | 85829822 | -1.4524 | 0.5318 | -3.2222 | 0.0003 | 1.8684 | 2.9188 | -1.2150 | -0.4184 |
| AP3B2 | NM_004644 | chr15 | 83328032 | 83378635 | -1.4143 | 0.5550 | -1.8276 | 0.0381 | 2.4681 | 3.0344 | -0.5939 | -0.3888 |
| SNORD67 | NR_003056 | chr11 | 46783938 | 46784049 | -1.3953 | 0.5554 | -2.1152 | 0.0161 | 0.8741 | 1.2288 | -1.0851 | -0.5307 |
| SNORD18A | NR_002441 | chr15 | 66795582 | 66795652 | -1.3578 | 0.5984 | -1.9062 | 0.0093 | 4.1946 | 3.8023 | -0.8213 | -0.2797 |
| CFD | NM_001928 | chr19 | 859664 | 863610 | -1.2695 | 0.6170 | -1.9992 | 0.0202 | 4.1962 | 5.6424 | -0.6401 | -0.3090 |
| STMN3 | NM_015894 | chr20 | 62271060 | 62284780 | -1.2409 | 0.6600 | -4.1696 | 0.0000 | 26.9196 | 31.5530 | -0.6599 | -0.2786 |
| METRN | NM_024042 | chr16 | 765172 | 767480 | -1.2076 | 0.6684 | -2.8776 | 0.0018 | 14.1462 | 14.3995 | -0.7000 | -0.2674 |
| KCNJ4 | NM_004981 | chr22 | 38822332 | 38851203 | -1.1514 | 0.6909 | -1.7660 | 0.0465 | 2.4360 | 1.6692 | -0.6217 | -0.3906 |

| name | Refseq_ID | chrom | begin | end | Z.OE | fdr.OE | Z.KD | fdr.KD | rpkm.KD | rpkm.OE | log2.fold.KD | log2.fold.OE |
|---|---|---|---|---|---|---|---|---|---|---|---|---|
| VSTM2B | NM_001146339 | chr19 | 30017490 | 30055226 | -1.1471 | 0.6981 | -2.7601 | 0.0024 | 4.6515 | 2.2751 | -0.7020 | -0.3171 |
| POLR2L | NM_021128 | chr11 | 839720 | 842529 | -1.1382 | 0.6970 | -3.7766 | 0.0000 | 97.2496 | 205.4675 | -0.6738 | -0.3051 |
| PCDH19 | NM_001184880 | chrX | 99546641 | 99665271 | -1.1325 | 0.7077 | -2.2026 | 0.0125 | 6.5539 | 4.1298 | -0.6383 | -0.2700 |
| SLC16A9 | NM_194298 | chr10 | 61410521 | 61469649 | -1.0956 | 0.7228 | 2.5021 | 0.0020 | 7.2957 | 5.0657 | 0.6626 | -0.2280 |
| RAB36 | NM_004914 | chr22 | 23487512 | 23506531 | -1.0599 | 0.7227 | -2.3203 | 0.0063 | 5.2025 | 6.4837 | -0.7173 | -0.2429 |
| PTRH1 | NM_001002913 | chr9 | 130476226 | 130477936 | -1.0551 | 0.7374 | -1.8689 | 0.0357 | 3.4129 | 4.2591 | -0.6941 | -0.2536 |
| DPYSL4 | NM_006426 | chr10 | 134000413 | 134019280 | -1.0267 | 0.7533 | -3.1939 | 0.0003 | 6.7612 | 7.1693 | -1.0266 | -0.2258 |
| JPH3 | NM_020655 | chr16 | 87636498 | 87731761 | -0.9925 | 0.7902 | -2.3445 | 0.0066 | 4.1866 | 4.9198 | -0.6509 | -0.2287 |
| GHRLOS | NR_024144 | chr3 | 10327437 | 10335133 | -0.9824 | 0.7857 | 2.1596 | 0.0099 | 1.6440 | 1.1147 | 0.6485 | -0.3387 |
| NTNG2 | NM_032536 | chr9 | 135037333 | 135118220 | -0.9502 | 0.8073 | -1.7992 | 0.0382 | 1.2872 | 1.1078 | -0.8173 | -0.3528 |
| SNORD1B | NR_004396 | chr17 | 74557189 | 74557275 | -0.9214 | 0.7256 | 2.1331 | 0.0394 | 1.2117 | 0.6518 | 0.9129 | -0.5583 |
| ERGIC1 | NM_001031711 | chr5 | 172261222 | 172379688 | -0.8720 | 0.8448 | -3.7351 | 0.0000 | 36.9192 | 43.5215 | -0.6913 | -0.2205 |
| LOC402778 | NM_001170820 | chr11 | 1756029 | 1769349 | -0.8633 | 0.8217 | 1.7753 | 0.0362 | 1.4325 | 0.9847 | 0.8831 | -0.3498 |
| DRD4 | NM_000797 | chr11 | 637304 | 640705 | -0.8531 | 0.8447 | -2.0543 | 0.0182 | 1.6471 | 3.8495 | -0.8798 | -0.2151 |
| PPP2R2C | NM_020416 | chr4 | 6322304 | 6474326 | -0.8493 | 0.8558 | -2.3374 | 0.0065 | 5.0640 | 5.1309 | -0.5948 | -0.1870 |
| TLCD1 | NM_138463 | chr17 | 27051365 | 27053949 | -0.8336 | 0.8559 | 2.7791 | 0.0009 | 18.0294 | 14.2522 | 0.6160 | -0.2011 |
| ADAP1 | NM_006869 | chr7 | 937536 | 994289 | -0.8190 | 0.8656 | -2.4879 | 0.0041 | 4.2644 | 5.5175 | -0.5970 | -0.1791 |
| ID2 | NM_002166 | chr2 | 8822112 | 8824583 | -0.7915 | 0.8780 | -3.2291 | 0.0000 | 21.5626 | 20.1906 | -0.7288 | -0.1735 |
| LOC654342 | NR_027238 | chr2 | 91824708 | 91847975 | -0.7756 | 0.8291 | -2.3204 | 0.0084 | 1.6152 | 2.5936 | -0.9431 | -0.2000 |
| SNORA16A | NR_003035 | chr1 | 28907431 | 28907565 | -0.7425 | 0.8888 | -2.0952 | 0.0161 | 3.2329 | 3.4926 | -0.8068 | -0.1823 |
| CORO1A | NM_007074 | chr16 | 30194730 | 30200396 | -0.7348 | 0.9015 | -2.3401 | 0.0062 | 2.3357 | 2.9610 | -0.9794 | -0.1797 |
| SNORA1 | NR_003026 | chr11 | 93465169 | 93465299 | -0.7155 | 0.9111 | 3.6570 | 0.0000 | 1.6519 | 1.8006 | 1.2624 | -0.1978 |
| SNHG9 | NR_003142 | chr16 | 2014996 | 2015505 | -0.6850 | 0.9135 | -1.7612 | 0.0349 | 31.0450 | 50.5223 | -0.6030 | -0.2065 |
| ERAP2 | NM_022350 | chr5 | 96211643 | 96255406 | -0.6752 | 0.9260 | 2.1403 | 0.0105 | 4.3029 | 2.2553 | 0.6746 | -0.1656 |
| TMEM121 | NM_025268 | chr14 | 105992952 | 105996539 | -0.6676 | 0.9088 | -3.2759 | 0.0000 | 4.8769 | 5.5447 | -0.8477 | -0.1260 |
| LDLR | NM_000527 | chr19 | 11200037 | 11244505 | -0.6594 | 0.9237 | 3.3856 | 0.0000 | 16.1275 | 12.4419 | 0.6466 | -0.1566 |
| CLOCK | NM_004898 | chr4 | 56298659 | 56412997 | -0.6587 | 0.9297 | 2.3655 | 0.0059 | 4.8411 | 2.6791 | 0.5866 | -0.1606 |
| FICD | NM_007076 | chr12 | 108909050 | 108913380 | -0.6390 | 0.9323 | 2.1007 | 0.0137 | 2.9382 | 2.6334 | 0.6485 | -0.1615 |
| NR6A1 | NM_001489 | chr9 | 127284702 | 127533576 | -0.6352 | 0.9268 | 4.8766 | 0.0000 | 5.4562 | 2.5524 | 1.1614 | -0.1336 |
| FAM73A | NM_198549 | chr1 | 78245308 | 78344081 | -0.5570 | 0.9628 | 3.7630 | 0.0000 | 7.7658 | 4.3592 | 0.7588 | -0.0914 |
| GDF7 | NM_182828 | chr2 | 20866423 | 20871250 | -0.5239 | 0.9829 | -1.7863 | 0.0410 | 1.0361 | 1.0472 | -0.6864 | -0.1484 |
| COL27A1 | NM_032888 | chr9 | 116918230 | 117072975 | -0.5104 | 0.9902 | -2.2854 | 0.0084 | 1.6096 | 1.2877 | -1.0017 | -0.1402 |
| F3 | NM_001993 | chr1 | 94994731 | 95007413 | -0.4547 | 1.0108 | 2.7245 | 0.0008 | 2.4135 | 1.7424 | 1.0428 | -0.1360 |
| RLTPR | NM_001013838 | chr16 | 67679029 | 67691472 | -0.4419 | 1.0159 | -2.1714 | 0.0098 | 1.1798 | 1.4957 | -1.2660 | -0.1032 |

| name | Refseq_ID | chrom | begin | end | Z.OE | fdr.OE | Z.KD | fdr.KD | rpkm.KD | rpkm.OE | log2.fold.KD | log2.fold.OE |
|---|---|---|---|---|---|---|---|---|---|---|---|---|
| CTXN1 | NM_206833 | chr19 | 7989380 | 7991051 | -0.4337 | 1.0147 | -3.8889 | 0.0000 | 23.8071 | 26.8287 | -0.8000 | -0.0998 |
| D2HGDH | NM_152783 | chr2 | 242674029 | 242708231 | -0.4292 | 1.0156 | -2.3987 | 0.0065 | 9.0547 | 11.5013 | -0.6798 | -0.0981 |
| C1orf95 | NM_001003665 | chr1 | 226736500 | 226796915 | -0.4175 | 1.0271 | -1.9393 | 0.0249 | 1.0637 | 0.9466 | -0.8582 | -0.1286 |
| CR2 | NM_001877 | chr1 | 207627644 | 207663240 | -0.4085 | 1.0277 | 2.2691 | 0.0077 | 2.9652 | 2.9440 | 0.8424 | -0.1010 |
| ACER2 | NM_001010887 | chr9 | 19408924 | 19452500 | -0.3900 | 1.0244 | 1.7043 | 0.0486 | 1.4189 | 0.7985 | 0.6132 | -0.1337 |
| TMCC1 | NM_001128224 | chr3 | 129366634 | 129612419 | -0.3746 | 1.0472 | 2.0549 | 0.0143 | 2.7126 | 1.8785 | 0.6327 | -0.0804 |
| SRPR | NM_003139 | chr11 | 126132813 | 126138877 | -0.3351 | 1.0509 | 4.1245 | 0.0000 | 56.3896 | 56.3117 | 0.6470 | -0.1281 |
| GLI3 | NM_000168 | chr7 | 42000547 | 42276618 | -0.3264 | 1.0577 | -4.6155 | 0.0000 | 3.6010 | 4.2410 | -1.2915 | -0.0590 |
| CRMP1 | NM_001014809 | chr4 | 5822490 | 5894785 | -0.2963 | 1.0711 | -3.4422 | 0.0000 | 9.2999 | 10.0736 | -0.6817 | -0.0671 |
| RECK | NM_021111 | chr9 | 36036909 | 36124452 | -0.2834 | 1.0710 | 2.1197 | 0.0141 | 3.2264 | 2.3474 | 0.6638 | -0.0425 |
| SYP | NM_003179 | chrX | 49044264 | 49056661 | -0.2684 | 1.0706 | -2.4898 | 0.0047 | 10.1215 | 12.3068 | -0.6123 | -0.0635 |
| INTS10 | NM_018142 | chr8 | 19674917 | 19709586 | -0.2383 | 1.0696 | -3.4058 | 0.0000 | 32.2214 | 42.1358 | -0.6205 | -0.0802 |
| SNORA15 | NR_002957 | chr7 | 56128162 | 56128295 | -0.2365 | 0.9325 | 1.7032 | 0.0083 | 3.2084 | 3.1060 | 0.7870 | 0.0879 |
| ROBO2 | NM_002942 | chr3 | 77089293 | 77699114 | -0.2072 | 1.0799 | 2.3111 | 0.0057 | 2.7907 | 1.3977 | 0.7603 | -0.0020 |
| TBKBP1 | NM_014726 | chr17 | 45772629 | 45789429 | -0.1964 | 1.0818 | -3.2698 | 0.0000 | 10.3153 | 11.4135 | -0.7602 | -0.0518 |
| LOC100288069 | NR_033908 | chr1 | 700244 | 714068 | -0.1837 | 1.0221 | 2.0918 | 0.0124 | 2.0279 | 2.2071 | 0.6227 | 0.0038 |
| GLYCTK | NM_145262 | chr3 | 52321835 | 52329272 | -0.1789 | 1.0876 | -1.8310 | 0.0359 | 1.3488 | 2.1717 | -0.6746 | -0.0085 |
| SNORD97 | NR_004403 | chr11 | 10823013 | 10823155 | -0.1727 | 1.0247 | 2.0936 | 0.0174 | 1.0681 | 0.8079 | 1.2024 | 0.0882 |
| LY6G6D | NM_021246 | chr6 | 31683132 | 31685581 | -0.1530 | 1.0972 | -3.3657 | 0.0000 | 10.1397 | 19.5338 | -1.0560 | -0.0540 |
| CRIP2 | NM_001312 | chr14 | 105941130 | 105946500 | -0.1469 | 1.0969 | -2.1835 | 0.0092 | 1.8464 | 2.2823 | -0.7978 | -0.0004 |
| NCRNA00116 | NR_027063 | chr2 | 110969105 | 110980517 | -0.1314 | 1.0941 | 2.2259 | 0.0097 | 6.3739 | 7.0321 | 0.6494 | -0.0019 |
| DUSP8 | NM_004420 | chr11 | 1575280 | 1593150 | -0.0730 | 1.0939 | 2.2297 | 0.0080 | 4.6337 | 4.1784 | 0.5904 | 0.0341 |
| MIR3936 | NR_037500 | chr5 | 131701181 | 131701291 | -0.0702 | 0.9042 | 2.0969 | 0.0152 | 1.2581 | 1.4937 | 1.2330 | 0.1015 |
| FAM122B | NM_001166599 | chrX | 133903595 | 133931262 | -0.0643 | 1.0872 | -3.7542 | 0.0000 | 20.2056 | 23.8107 | -0.7600 | -0.0409 |
| GREB1L | NM_001142966 | chr18 | 18822202 | 19102791 | -0.0531 | 1.0878 | 2.6869 | 0.0016 | 6.4659 | 4.4337 | 0.6037 | 0.0205 |
| VAMP5 | NM_006634 | chr2 | 85811530 | 85820511 | -0.0423 | 1.0906 | -2.4261 | 0.0052 | 1.0346 | 1.7662 | -1.0492 | 0.0184 |
| DNAJB9 | NM_012328 | chr7 | 108210188 | 108215294 | -0.0294 | 1.0935 | 2.7551 | 0.0009 | 6.6479 | 4.4195 | 0.8150 | 0.0437 |
| SNORD101 | NR_002434 | chr6 | 133136445 | 133136518 | -0.0099 | 0.4435 | 0.5250 | 0.0282 | 2.3136 | 2.2551 | 0.6656 | 0.3079 |
| ADAMTS10 | NM_030957 | chr19 | 8645125 | 8675588 | -0.0085 | 1.0849 | -2.3084 | 0.0079 | 1.3474 | 1.3030 | -0.8959 | 0.0699 |
| ZCCHC12 | NM_173798 | chrX | 117957786 | 117960931 | -0.0065 | 1.0883 | -4.5783 | 0.0000 | 18.6061 | 23.4403 | -0.9721 | -0.0254 |
| CYBRD1 | NM_001127383 | chr2 | 172378865 | 172414643 | 0.0293 | 1.0764 | 3.1376 | 0.0000 | 3.8407 | 2.3847 | 0.9332 | 0.0895 |
| ANKRD52 | NM_173595 | chr12 | 56631590 | 56652143 | 0.0539 | 1.0255 | 3.6541 | 0.0000 | 31.0213 | 31.0559 | 0.5958 | -0.0317 |
| AKR1B1 | NM_001628 | chr7 | 134127106 | 134143888 | 0.0636 | 1.0707 | -3.5492 | 0.0000 | 110.6509 | 152.7199 | -0.6466 | -0.0775 |
| FYCO1 | NM_024513 | chr3 | 45959394 | 46037307 | 0.0684 | 1.0761 | 3.3016 | 0.0003 | 6.5102 | 4.4266 | 0.6999 | 0.0485 |

| name | Refseq_ID | chrom | begin | end | Z.OE | fdr.OE | Z.KD | fdr.KD | rpkm.KD | rpkm.OE | log2.fold.KD | log2.fold.OE |
|---|---|---|---|---|---|---|---|---|---|---|---|---|
| MIR3650 | NR_037423 | chr5 | 38557603 | 38557663 | 0.0962 | 1.0767 | 2.3730 | 0.0323 | 1.0342 | 2.0113 | -1.5657 | 0.1169 |
| ANXA1 | NM_000700 | chr9 | 75766780 | 75785307 | 0.1260 | 1.0574 | 2.1151 | 0.0066 | 5.0567 | 4.1854 | 0.7460 | 0.0966 |
| IGFBP7 | NM_001553 | chr4 | 57897243 | 57976539 | 0.1276 | 1.0232 | 1.8455 | 0.0324 | 3.0966 | 2.5864 | 0.6024 | 0.1688 |
| MGAT4A | NM_012214 | chr2 | 99235568 | 99347589 | 0.1784 | 1.0437 | 2.4126 | 0.0040 | 4.7950 | 3.0253 | 0.6924 | 0.1256 |
| PON2 | NM_001018161 | chr7 | 95034173 | 95064384 | 0.1813 | 1.0556 | 4.3070 | 0.0000 | 29.2053 | 21.5878 | 0.8949 | 0.0229 |
| NR1H2 | NM_007121 | chr19 | 50879684 | 50886267 | 0.1970 | 1.0496 | 3.7318 | 0.0000 | 24.8175 | 21.4769 | 0.7106 | 0.0283 |
| ETV4 | NM_001986 | chr17 | 41605210 | 41623762 | 0.2071 | 1.0413 | -2.1325 | 0.0171 | 5.4429 | 8.1265 | -0.7828 | 0.0669 |
| FLJ23152 | NM_001190766 | chr6 | 17102488 | 17131603 | 0.2272 | 1.0395 | 2.8391 | 0.0006 | 3.7695 | 3.2341 | 0.9203 | 0.0835 |
| WRB | NM_004627 | chr21 | 40752212 | 40769815 | 0.2279 | 1.0399 | -6.0265 | 0.0000 | 16.7143 | 27.8368 | -1.1420 | 0.0373 |
| FAM27A | NR_024060 | chr9 | 45727028 | 45728283 | 0.2553 | 0.6549 | -2.6043 | 0.0026 | 1.6556 | 1.7662 | -0.7940 | 0.1627 |
| FAM129A | NM_052966 | chr1 | 184760165 | 184943682 | 0.3143 | 1.0105 | 3.0061 | 0.0003 | 7.6754 | 4.3662 | 0.7245 | 0.1522 |
| JOSD2 | NM_138334 | chr19 | 51009258 | 51014345 | 0.3325 | 0.9773 | -7.8352 | 0.0000 | 13.6443 | 28.8453 | -1.5039 | 0.0169 |
| CIB2 | NM_006383 | chr15 | 78396990 | 78423878 | 0.3327 | 1.0114 | -1.9127 | 0.0288 | 1.7107 | 1.6937 | -0.6831 | 0.1858 |
| OBSL1 | NM_015311 | chr2 | 220415449 | 220436268 | 0.3389 | 0.9763 | -2.9834 | 0.0012 | 12.9031 | 18.6766 | -0.6736 | 0.0477 |
| GALNT3 | NM_004482 | chr2 | 166604312 | 166650803 | 0.3746 | 0.9862 | 3.0230 | 0.0003 | 9.2849 | 6.9917 | 0.6536 | 0.1528 |
| C6orf72 | NM_138785 | chr6 | 149887527 | 149912067 | 0.4016 | 0.9142 | 3.2709 | 0.0000 | 35.6832 | 27.5264 | 0.5939 | 0.1270 |
| CASP7 | NM_033340 | chr10 | 115438934 | 115490664 | 0.4025 | 0.9683 | -3.7991 | 0.0000 | 15.2999 | 21.4926 | -0.7608 | 0.0459 |
| FNDC3B | NM_022763 | chr3 | 171757417 | 172118492 | 0.4065 | 0.9880 | 2.7800 | 0.0009 | 5.2200 | 3.7370 | 0.7032 | 0.1620 |
| SFRP5 | NM_003015 | chr10 | 99526507 | 99531756 | 0.4356 | 0.9811 | -2.2637 | 0.0080 | 0.9108 | 1.4821 | -1.0539 | 0.2393 |
| MIR1281 | NR_031694 | chr22 | 41488516 | 41488570 | 0.4882 | 0.4509 | 3.4955 | 0.0000 | 4.3668 | 3.4420 | 1.3573 | 0.3628 |
| MPZL3 | NM_198275 | chr11 | 118100335 | 118123011 | 0.4996 | 0.9562 | 2.0478 | 0.0150 | 2.3423 | 1.6973 | 0.7205 | 0.2445 |
| TMEM64 | NM_001008495 | chr8 | 91634222 | 91658133 | 0.5102 | 0.9594 | 2.7146 | 0.0014 | 7.0299 | 5.5645 | 0.6672 | 0.1869 |
| LAMP3 | NM_014398 | chr3 | 182840002 | 182880667 | 0.5206 | 0.9415 | 1.9486 | 0.0219 | 2.4579 | 1.4913 | 0.7109 | 0.2503 |
| KLHL28 | NM_017658 | chr14 | 45393526 | 45431179 | 0.5339 | 0.9528 | 1.9080 | 0.0267 | 2.3116 | 1.6328 | 0.6761 | 0.2914 |
| GPR137B | NM_003272 | chr1 | 236305831 | 236372209 | 0.5832 | 0.9325 | 2.3283 | 0.0065 | 11.2824 | 10.5945 | 0.5887 | 0.1574 |
| SCN1B | NM_199037 | chr19 | 35521591 | 35531353 | 0.5878 | 0.9261 | 2.9166 | 0.0006 | 3.0177 | 2.1134 | 0.9873 | 0.2636 |
| CROT | NM_021151 | chr7 | 86974950 | 87029112 | 0.6082 | 0.9097 | 2.4418 | 0.0038 | 3.8491 | 3.5968 | 0.6036 | 0.2194 |
| RASSF2 | NM_170774 | chr20 | 4760668 | 4804291 | 0.6105 | 0.9182 | -2.0233 | 0.0202 | 2.6845 | 2.8494 | -0.6618 | 0.2557 |
| MMP2 | NM_004530 | chr16 | 55513080 | 55540586 | 0.6153 | 0.9069 | -2.2500 | 0.0085 | 1.0419 | 0.9682 | -1.1280 | 0.3494 |
| HOXA7 | NM_006896 | chr7 | 27193337 | 27196296 | 0.6159 | 0.9137 | 2.5821 | 0.0018 | 7.5945 | 7.1128 | 0.6239 | 0.1831 |
| ATXN1 | NM_000332 | chr6 | 16299342 | 16761721 | 0.6427 | 0.8622 | 3.1023 | 0.0003 | 5.8448 | 3.7808 | 0.7267 | 0.2111 |
| MICA | NR_036523 | chr6 | 31367560 | 31383090 | 0.6454 | 0.8762 | 2.5903 | 0.0016 | 12.8382 | 12.3324 | 0.6663 | 0.1421 |
| HAT1 | NR_027862 | chr2 | 172778934 | 172848600 | 0.6516 | 0.9017 | -9.9248 | 0.0000 | 30.9183 | 53.9913 | -1.7013 | 0.1077 |
| SNORD54 | NR_002437 | chr8 | 56986397 | 56986460 | 0.6559 | 0.6121 | -4.6170 | 0.0025 | 2.5196 | 2.0073 | -0.7923 | 0.5322 |

| name | Refseq_ID | chrom | begin | end | Z.OE | fdr.OE | Z.KD | fdr.KD | rpkm.KD | rpkm.OE | log2.fold.KD | log2.fold.OE |
|---|---|---|---|---|---|---|---|---|---|---|---|---|
| ZDHHC22 | NM_174976 | chr14 | 77597612 | 77608134 | 0.7064 | 0.8592 | -2.7964 | 0.0023 | 2.8088 | 2.9417 | -0.7895 | 0.2591 |
| ZBTB4 | NM_001128833 | chr17 | 7362684 | 7387568 | 0.7081 | 0.8613 | 2.7308 | 0.0008 | 10.7255 | 8.1843 | 0.6425 | 0.1871 |
| UFM1 | NM_016617 | chr13 | 38923941 | 38937143 | 0.7183 | 0.8365 | -4.1876 | 0.0000 | 14.7381 | 16.4956 | -0.7555 | 0.2170 |
| NKIRAS1 | NM_020345 | chr3 | 23933571 | 23958537 | 0.7393 | 0.8597 | 3.3779 | 0.0000 | 10.6349 | 9.1972 | 0.7750 | 0.2206 |
| PGM2L1 | NM_173582 | chr11 | 74041360 | 74109502 | 0.7404 | 0.8613 | 3.9651 | 0.0000 | 3.5841 | 1.9163 | 1.1832 | 0.3404 |
| ENPP5 | NM_021572 | chr6 | 46127761 | 46138717 | 0.7460 | 0.8605 | 4.0396 | 0.0000 | 3.1045 | 1.6536 | 1.5362 | 0.3531 |
| JUN | NM_002228 | chr1 | 59246462 | 59249785 | 0.7759 | 0.8524 | 3.7273 | 0.0000 | 104.9368 | 107.6048 | 0.5866 | 0.1031 |
| TMEM2 | NM_013390 | chr9 | 74298281 | 74383800 | 0.7776 | 0.8510 | 2.8991 | 0.0002 | 6.3844 | 4.6974 | 0.7935 | 0.2461 |
| PBXIP1 | NM_020524 | chr1 | 154916558 | 154928567 | 0.8106 | 0.8304 | 2.0382 | 0.0175 | 7.2595 | 6.5548 | 0.6269 | 0.2244 |
| EYA1 | NM_172060 | chr8 | 72109667 | 72274467 | 0.8484 | 0.8256 | 2.0896 | 0.0142 | 2.1563 | 1.9194 | 0.7782 | 0.3934 |
| TFPI | NM_006287 | chr2 | 188328957 | 188419219 | 0.8599 | 0.8105 | 2.4615 | 0.0022 | 2.5829 | 1.8520 | 0.8304 | 0.4107 |
| ZNF367 | NM_153695 | chr9 | 99148224 | 99180669 | 0.9003 | 0.8006 | 4.2645 | 0.0000 | 12.0221 | 7.3009 | 0.9327 | 0.2686 |
| MIR590 | NR_030321 | chr7 | 73605527 | 73605624 | 0.9450 | 0.6439 | 1.6263 | 0.0154 | 1.5023 | 1.2367 | 0.9480 | 0.3633 |
| RGPD8 | NM_001164463 | chr2 | 113125945 | 113191222 | 0.9794 | 0.6581 | 2.0222 | 0.0140 | 2.1685 | 1.7492 | 0.7220 | 0.4951 |
| RGPD5 | NM_005054 | chr2 | 113125964 | 113191107 | 0.9794 | 0.6581 | 2.0222 | 0.0140 | 2.1685 | 1.7492 | 0.7220 | 0.4951 |
| FAM160B1 | NM_001135051 | chr10 | 116581502 | 116659586 | 0.9890 | 0.7631 | 2.4721 | 0.0031 | 6.1062 | 4.7524 | 0.6216 | 0.3168 |
| ANKRD16 | NM_019046 | chr10 | 5903688 | 5931860 | 1.0127 | 0.7549 | -2.0363 | 0.0182 | 4.9009 | 6.4723 | -0.5967 | 0.2801 |
| TMEM123 | NM_052932 | chr11 | 102267055 | 102323775 | 1.0214 | 0.7227 | -5.5999 | 0.0000 | 38.4978 | 45.7234 | -0.7835 | 0.2203 |
| CHIC1 | NM_001039840 | chrX | 72782983 | 72906937 | 1.0391 | 0.7327 | 2.8143 | 0.0007 | 3.0991 | 1.9422 | 0.8423 | 0.4576 |
| LOC728392 | NM_001162371 | chr17 | 5402746 | 5404319 | 1.1055 | 0.7070 | -2.9588 | 0.0022 | 3.0785 | 4.4350 | -0.8420 | 0.3606 |
| SNCB | NM_001001502 | chr5 | 176047209 | 176057557 | 1.1323 | 0.6816 | -1.7504 | 0.0469 | 1.3256 | 1.4143 | -0.7855 | 0.5769 |
| S1PR1 | NM_001400 | chr1 | 101702304 | 101707076 | 1.1433 | 0.6926 | 1.9009 | 0.0265 | 3.2078 | 2.3237 | 0.6740 | 0.4711 |
| DCAKD | NM_024819 | chr17 | 43100705 | 43138473 | 1.2347 | 0.6551 | -2.9748 | 0.0012 | 17.6212 | 28.2690 | -0.6479 | 0.2018 |
| CCDC23 | NM_199342 | chr1 | 43272722 | 43283059 | 1.3093 | 0.6476 | -3.4818 | 0.0000 | 14.9390 | 19.7242 | -0.6185 | 0.3701 |
| PRTG | NM_173814 | chr15 | 55903738 | 56035177 | 1.3984 | 0.6299 | 2.8075 | 0.0008 | 2.9722 | 1.7177 | 0.8753 | 0.5893 |
| NMB | NM_021077 | chr15 | 85198359 | 85201802 | 1.4084 | 0.6326 | -2.5772 | 0.0028 | 6.7908 | 10.8665 | -0.6570 | 0.3283 |
| C9orf5 | NM_032012 | chr9 | 111777414 | 111882225 | 1.4384 | 0.6132 | 3.3161 | 0.0000 | 13.8161 | 10.5700 | 0.6605 | 0.3499 |
| KIAA0494 | NM_014774 | chr1 | 47140830 | 47184736 | 1.4428 | 0.6206 | 3.4274 | 0.0000 | 22.2743 | 18.1002 | 0.6038 | 0.2941 |
| TGFBR3 | NM_003243 | chr1 | 92145899 | 92371559 | 1.5712 | 0.5342 | 3.1163 | 0.0003 | 8.9695 | 6.9478 | 0.8221 | 0.4129 |
| LOC647310 | NM_001195082 | chr14 | 105864919 | 105880196 | 1.6010 | 0.5008 | -1.8205 | 0.0359 | 0.8329 | 1.0401 | -0.9664 | 0.8043 |
| TCTEX1D2 | NM_152773 | chr3 | 196018089 | 196045165 | 1.6375 | 0.5023 | -4.0252 | 0.0000 | 6.9285 | 13.4652 | -1.0445 | 0.3668 |
| UHMK1 | NM_001184763 | chr1 | 162466963 | 162499419 | 1.7939 | 0.4344 | 4.1322 | 0.0000 | 23.2088 | 14.0277 | 0.6833 | 0.4127 |
| REEP3 | NM_001001330 | chr10 | 65281122 | 65384883 | 1.8616 | 0.4088 | 4.3846 | 0.0000 | 14.2920 | 8.5259 | 0.8778 | 0.5217 |
| SNORD88C | NR_003069 | chr19 | 51305581 | 51305678 | 1.8785 | 0.4208 | -2.8607 | 0.0051 | 6.4898 | 6.4163 | -0.7105 | 0.5051 |

| name | Refseq_ID | chrom | begin | end | Z.OE | fdr.OE | Z.KD | fdr.KD | rpkm.KD | rpkm.OE | log2.fold.KD | log2.fold.OE |
|---|---|---|---|---|---|---|---|---|---|---|---|---|
| LCOR | NM_001170765 | chr10 | 98592016 | 98724198 | 1.9103 | 0.4014 | 1.8147 | 0.0387 | 5.7738 | 4.3297 | 0.3479 | 0.5916 |
| CDKN1B | NM_004064 | chr12 | 12870301 | 12875305 | 1.9588 | 0.3754 | 3.1187 | 0.0003 | 30.6308 | 26.0314 | 0.5956 | 0.4394 |
| ZNF512 | NM_032434 | chr2 | 27805892 | 27845963 | 2.1055 | 0.3553 | -3.7785 | 0.0000 | 15.1057 | 22.2737 | -0.7024 | 0.4183 |
| PAQR6 | NM_024897 | chr1 | 156213206 | 156217843 | 2.2052 | 0.3357 | -2.4571 | 0.0043 | 2.9859 | 6.0800 | -0.7414 | 0.5753 |
| SNORA71B | NR_002910 | chr20 | 37053842 | 37053978 | 2.2686 | 0.3023 | -2.4725 | 0.0080 | 4.4509 | 5.0131 | -0.7661 | 0.6308 |
| MC1R | NM_002386 | chr16 | 89984286 | 89987385 | 2.4950 | 0.2979 | -2.4675 | 0.0041 | 1.8971 | 3.4588 | -0.8984 | 0.7665 |
| MIR614 | NR_030345 | chr12 | 13068762 | 13068852 | 2.5581 | 0.3717 | -1.6883 | 0.0040 | 2.3776 | 2.0576 | -0.8731 | 0.8139 |
| GTF2IP1 | NR_002206 | chr7 | 72569025 | 72621336 | 2.6334 | 0.3406 | -2.0120 | 0.0286 | 1.2977 | 1.1756 | -0.6572 | -0.4655 |
| LHB | NM_000894 | chr19 | 49519236 | 49520347 | 2.7023 | 0.1868 | -1.9273 | 0.0289 | 1.1541 | 2.8912 | -0.8180 | 0.8858 |
| LOC100093631 | NR_003580 | chr7 | 72569011 | 72621336 | 2.8794 | 0.3012 | -2.1972 | 0.0197 | 1.6413 | 1.4867 | -0.6573 | -0.4656 |
| DOK3 | NM_001144876 | chr5 | 176928905 | 176937427 | 3.0670 | 0.1587 | -2.2080 | 0.0096 | 2.4958 | 4.7359 | -0.8515 | 0.8602 |
| CNPY3 | NM_006586 | chr6 | 42896859 | 42907008 | 3.2654 | 0.0843 | -1.9851 | 0.0290 | 25.4571 | 42.9565 | -0.3652 | 0.5928 |
| MIR196A1 | NR_029582 | chr17 | 46709851 | 46709921 | 3.7100 | 0.0745 | 2.5247 | 0.0068 | 2.9555 | 2.5581 | 0.5981 | 1.2431 |
| SPRYD4 | NM_207344 | chr12 | 56862300 | 56864767 | 3.7952 | 0.0375 | 1.0811 | 0.2808 | 12.3761 | 17.0061 | 0.3046 | 0.7995 |
| CEACAM19 | NM_020219 | chr19 | 45174723 | 45187627 | 3.8614 | 0.0333 | -0.8278 | 0.5504 | 3.5955 | 5.9265 | -0.2322 | 0.9927 |
| SLFNL1 | NM_144990 | chr1 | 41481268 | 41487427 | 3.9427 | 0.0329 | -0.7211 | 0.5921 | 1.9188 | 3.1940 | -0.3857 | 1.2569 |
| LOC100506581 | NM_001195125 | chr16 | 87336403 | 87351026 | 3.9440 | 0.0323 | -1.2485 | 0.2300 | 2.8804 | 6.0632 | -0.5330 | 1.0452 |
| SNORD43 | NR_002439 | chr22 | 39715056 | 39715118 | 3.9940 | 0.0329 | 0.5593 | 0.1931 | 2.0529 | 1.9231 | 0.2072 | 1.4752 |
| SNORD36B | NR_000017 | chr9 | 136216948 | 136217019 | 4.0535 | 0.0345 | -1.0649 | 0.2874 | 7.6549 | 11.6958 | -0.1561 | 0.9787 |
| MIR196B | NR_029911 | chr7 | 27209098 | 27209182 | 4.1816 | 0.0841 | 2.2573 | 0.0118 | 2.9308 | 4.9523 | 0.7294 | 1.1001 |
| SNORD58A | NR_002571 | chr18 | 47017652 | 47017717 | 4.3023 | 0.0270 | 0.8969 | 0.4320 | 17.7829 | 22.2703 | 0.1376 | 0.9667 |
| SNORD74 | NR_002579 | chr1 | 173836811 | 173836883 | 4.3480 | 0.0260 | -1.5576 | 0.1074 | 3.9504 | 7.0486 | -0.2721 | 1.0744 |
| PRPF39 | NM_017922 | chr14 | 45553301 | 45584804 | 4.3750 | 0.0280 | -1.2239 | 0.2310 | 15.5173 | 23.0525 | -0.2099 | 0.9387 |
| RHBDD2 | NM_001040457 | chr7 | 75508316 | 75518244 | 4.3993 | 0.0325 | -1.8786 | 0.0327 | 24.5549 | 42.6537 | -0.3121 | 0.8193 |
| NCRNA00120 | NR_002767 | chr6 | 88410019 | 88410933 | 4.4765 | 0.0260 | -2.0841 | 0.0173 | 7.2346 | 10.8287 | -0.5264 | 1.0537 |
| MIR2110 | NR_031747 | chr10 | 115933863 | 115933938 | 4.7275 | 0.0317 | 0.5968 | 0.1176 | 5.0800 | 3.7438 | 0.0963 | 1.5190 |
| NEAT1 | NR_028272 | chr11 | 65190268 | 65194003 | 4.8849 | 0.0250 | -3.8587 | 0.0000 | 36.6498 | 57.6897 | -0.6332 | 0.8619 |
| SNORD59A | NR_002737 | chr12 | 57038810 | 57038885 | 4.8895 | 0.0222 | 2.2041 | 0.0111 | 3.1558 | 3.1833 | 0.3684 | 1.7580 |
| SAT1 | NM_002970 | chrX | 23801274 | 23804327 | 9.5410 | 0.0000 | -7.7977 | 0.0000 | 202.7894 | 552.0175 | -1.1284 | 1.7276 |
| RBM10 | NM_001204466 | chrX | 47004616 | 47046214 | 13.4883 | 0.0000 | -12.2818 | 0.0000 | 29.9654 | 255.1869 | -2.0512 | 2.4600 |

**Table 2 Significantly changed exons (fdr < 0.05, |ΔPSI| ≥ 0.1) on RBM10 knockdown (KD) or overexpression (OE).**

| chrom | begin | end | name | Z.OE | fdr.OE | Z.KD | fdr.KD | ΔPSI_OE | ΔPSI_KD |
|---|---|---|---|---|---|---|---|---|---|
| chr9 | 95874160 | 95874220 | C9orf89 | -12.2441 | 0.0039 | 3.2536 | 0.0016 | -0.7120 | 0.1478 |
| chr6 | 44103064 | 44103103 | TMEM63B | -12.2668 | 0.0037 | 3.0906 | 0.0025 | -0.6761 | 0.1113 |
| chr16 | 3188745 | 3188819 | ZNF213 | -11.1146 | 0.0035 | 2.3130 | 0.0392 | -0.6294 | 0.0887 |
| chr10 | 51886919 | 51886982 | FAM21A | -9.3796 | 0.0078 | 1.6052 | 0.0392 | -0.6283 | 0.0478 |
| chr10 | 51886919 | 51886982 | FAM21B.2 | -9.3796 | 0.0078 | 1.6052 | 0.0392 | -0.6283 | 0.0478 |
| chr13 | 113532530 | 113532617 | ATP11A | -9.6844 | 0.0066 | 2.5530 | 0.0451 | -0.6220 | 0.0773 |
| chr7 | 74299833 | 74299941 | STAG3L2 | -9.1085 | 0.0076 | 2.8296 | 0.0028 | -0.6009 | 0.1316 |
| chr1 | 153945855 | 153945940 | CREB3L4 | -8.4034 | 0.0129 | -0.0479 | 0.9877 | -0.5541 | 0.0000 |
| chr12 | 48360465 | 48360515 | TMEM106C | -24.6010 | 0.0000 | 11.4337 | 0.0000 | -0.5270 | 0.1476 |
| chr12 | 88448116 | 88448190 | CEP290 | -11.1702 | 0.0036 | 1.3391 | 0.1903 | -0.5165 | 0.0230 |
| chr12 | 124428818 | 124428911 | CCDC92 | -8.7596 | 0.0126 | 1.5127 | 0.0556 | -0.5130 | 0.0485 |
| chr12 | 53861588 | 53861627 | PCBP2 | -30.0685 | 0.0033 | 19.6406 | 0.0000 | -0.5093 | 0.1876 |
| chr16 | 3827613 | 3827658 | CREBBP | -9.8762 | 0.0077 | 5.8913 | 0.0000 | -0.4927 | 0.2461 |
| chr12 | 48360990 | 48361044 | TMEM106C | -24.1042 | 0.0000 | 10.6788 | 0.0000 | -0.4869 | 0.1299 |
| chr3 | 50137964 | 50138038 | RBM5 | -11.0342 | 0.0062 | 1.6759 | 0.0390 | -0.4837 | 0.0386 |
| chr22 | 42997975 | 42998062 | POLDIP3 | -20.6083 | 0.0000 | 4.3913 | 0.0004 | -0.4671 | 0.0523 |
| chr1 | 155238498 | 155238583 | CLK2 | -12.6347 | 0.0037 | 7.6091 | 0.0000 | -0.4583 | 0.1331 |
| chr3 | 50141680 | 50141741 | RBM5 | -8.0459 | 0.0148 | 3.0991 | 0.0019 | -0.4569 | 0.1073 |
| chr2 | 131116805 | 131116882 | PTPN18 | -6.1295 | 0.0382 | 2.3197 | 0.0111 | -0.4534 | 0.1150 |
| chrX | 18917290 | 18917344 | PHKA2 | -11.4130 | 0.0054 | 5.8412 | 0.0000 | -0.4484 | 0.2511 |
| chr12 | 48359871 | 48360012 | TMEM106C | -22.3138 | 0.0000 | 11.2014 | 0.0000 | -0.4456 | 0.1095 |
| chr2 | 130918758 | 130918845 | SMPD4 | -10.7853 | 0.0056 | 13.3813 | 0.0000 | -0.4435 | 0.2707 |
| chr3 | 53889320 | 53889368 | IL17RB | -5.7260 | 0.0493 | 2.1205 | 0.0113 | -0.4424 | 0.0987 |
| chr12 | 48359064 | 48359128 | TMEM106C | -24.4865 | 0.0000 | 8.3094 | 0.0000 | -0.4419 | 0.0778 |
| chr12 | 51447560 | 51447643 | LETMD1 | -15.4182 | 0.0019 | 6.3146 | 0.0000 | -0.4383 | 0.1087 |
| chr9 | 80880774 | 80880822 | CEP78 | -8.5303 | 0.0112 | 1.8270 | 0.0215 | -0.4352 | 0.0312 |
| chr8 | 27147672 | 27147695 | TRIM35 | -7.4534 | 0.0237 | 1.5639 | 0.0354 | -0.4349 | 0.0783 |
| chr12 | 54361052 | 54361178 | HOTAIR | -8.6460 | 0.0121 | 4.8909 | 0.0004 | -0.4317 | 0.0930 |
| chr11 | 64799639 | 64799675 | ARL2-SNX15 | -10.0252 | 0.0067 | 0.4770 | 0.6880 | -0.4299 | 0.0180 |
| chr10 | 75551081 | 75551257 | KIAA0913 | -11.8857 | 0.0036 | 1.1136 | 0.1895 | -0.4283 | 0.0268 |
| chr3 | 49054044 | 49054106 | DALRD3 | -9.7915 | 0.0066 | 0.5569 | 0.8907 | -0.4282 | 0.0143 |
| chr11 | 64799639 | 64799675 | SNX15 | -9.9793 | 0.0065 | 0.4333 | 0.7775 | -0.4280 | 0.0150 |
| chr17 | 61803997 | 61804055 | STRADA | -8.1316 | 0.0153 | 3.5931 | 0.0007 | -0.4129 | 0.1337 |
| chr9 | 139291428 | 139291475 | SNAPC4 | -8.2203 | 0.0131 | 0.0693 | 1.0250 | -0.4127 | 0.0012 |
| chr22 | 50895462 | 50895540 | SBF1 | -17.1123 | 0.0025 | 7.8347 | 0.0000 | -0.4117 | 0.0975 |
| chr2 | 131116969 | 131117065 | PTPN18 | -5.2858 | 0.0587 | 2.5524 | 0.0081 | -0.4104 | 0.1218 |
| chrX | 154300601 | 154300618 | BRCC3 | -6.8094 | 0.0254 | 2.2063 | 0.0224 | -0.4056 | 0.0948 |
| chr11 | 47194976 | 47195033 | ARFGAP2 | -7.1903 | 0.0350 | -0.0333 | 1.2079 | -0.4054 | 0.0109 |
| chr1 | 153600596 | 153600715 | S100A13 | -5.7282 | 0.0487 | 1.1423 | 0.1940 | -0.3992 | 0.0617 |
| chr12 | 124858958 | 124859009 | NCOR2 | -8.9487 | 0.0126 | 3.4151 | 0.0025 | -0.3987 | 0.0643 |
| chrX | 23802410 | 23802520 | SAT1 | -29.7193 | 0.0033 | 36.3048 | 0.0000 | -0.3973 | 0.2950 |
| chr12 | 51449926 | 51450028 | LETMD1 | -15.4752 | 0.0024 | 5.1967 | 0.0000 | -0.3961 | 0.0787 |
| chrX | 154012302 | 154012383 | MPP1 | -13.5495 | 0.0022 | 1.1146 | 0.0781 | -0.3931 | 0.0184 |
| chr11 | 47195309 | 47195391 | ARFGAP2 | -8.2913 | 0.0176 | 0.3835 | 1.0906 | -0.3913 | 0.0049 |
| chr7 | 150773999 | 150774114 | FASTK | -16.9666 | 0.0027 | 1.3170 | 0.0801 | -0.3885 | 0.0169 |
| chr16 | 1716073 | 1716178 | CRAMP1L | -7.4923 | 0.0211 | 1.8183 | 0.0414 | -0.3844 | 0.0741 |
| chr20 | 62507168 | 62507228 | TPD52L2 | -14.9205 | 0.0022 | 17.3242 | 0.0000 | -0.3793 | 0.2186 |
| chr11 | 71940706 | 71940796 | INPPL1 | -12.5992 | 0.0035 | 0.5502 | 0.5740 | -0.3777 | 0.0042 |
| chr10 | 104489075 | 104489151 | SFXN2 | -9.6658 | 0.0064 | 2.1273 | 0.0108 | -0.3750 | 0.0457 |
| chr2 | 10917710 | 10917848 | ATP6V1C2 | -3.6216 | 0.3663 | 3.8846 | 0.0048 | -0.3572 | 0.3737 |
| chr11 | 57259063 | 57259099 | SLC43A1 | -6.2616 | 0.0395 | -0.3331 | 0.7211 | -0.3690 | -0.0248 |

| chrom | begin | end | name | Z.OE | fdr.OE | Z.KD | fdr.KD | ΔPSI_OE | ΔPSI_KD |
|---|---|---|---|---|---|---|---|---|---|
| chr21 | 38605662 | 38605743 | DSCR3 | -9.9814 | 0.0062 | 1.6362 | 0.0339 | -0.3679 | 0.0303 |
| chrX | 48838206 | 48838284 | GRIPAP1 | -11.6381 | 0.0035 | 0.0862 | 0.9305 | -0.3665 | 0.0062 |
| chr20 | 31374307 | 31374433 | DNMT3B | -8.9370 | 0.0106 | 2.7351 | 0.0040 | -0.3661 | 0.0510 |
| chr17 | 40965965 | 40966026 | BECN1 | -12.5076 | 0.0035 | 0.8051 | 0.4516 | -0.3655 | 0.0099 |
| chr11 | 63675731 | 63675776 | MARK2 | -7.2859 | 0.0202 | 1.2132 | 0.1037 | -0.3633 | 0.0154 |
| chr6 | 42976430 | 42976484 | PPP2R5D | -15.3708 | 0.0020 | 1.1573 | 0.1861 | -0.3584 | 0.0183 |
| chr15 | 43856300 | 43856363 | PPIP5K1 | -6.9820 | 0.0238 | 7.9571 | 0.0000 | -0.3580 | 0.2616 |
| chr12 | 42625025 | 42629799 | YAF2 | 14.1685 | 0.0000 | -2.9544 | 0.0015 | 0.3560 | -0.0765 |
| chr9 | 72961520 | 72961565 | SMC5 | -7.2890 | 0.0260 | 5.8349 | 0.0000 | -0.3533 | 0.1867 |
| chr11 | 33369711 | 33369774 | HIPK3 | -2.3508 | 0.5546 | 2.7483 | 0.0136 | -0.3532 | 0.1771 |
| chr6 | 145148483 | 145148522 | UTRN | -3.0416 | 0.4344 | 1.9003 | 0.0305 | -0.3526 | 0.0581 |
| chr19 | 18882251 | 18882356 | CRTC1 | -6.6202 | 0.0294 | -2.1572 | 0.0184 | -0.3519 | -0.0561 |
| chr20 | 34246851 | 34246936 | CPNE1 | 19.0642 | 0.0000 | 3.7262 | 0.0014 | 0.3486 | 0.0300 |
| chr6 | 13325325 | 13325406 | TBC1D7 | -11.0013 | 0.0037 | 0.6424 | 0.6059 | -0.3474 | 0.0157 |
| chr17 | 56283825 | 56283908 | MKS1 | -7.5204 | 0.0191 | 2.0354 | 0.0456 | -0.3465 | 0.0499 |
| chr16 | 4927385 | 4927475 | UBN1 | -10.1404 | 0.0061 | 2.1447 | 0.0207 | -0.3461 | 0.0452 |
| chr19 | 39844645 | 39844706 | SAMD4B | -14.0455 | 0.0015 | 4.4023 | 0.0004 | -0.3454 | 0.0732 |
| chr1 | 1244294 | 1244352 | PUSL1 | -10.5059 | 0.0049 | 0.9189 | 0.6331 | -0.3433 | 0.0059 |
| chr12 | 51445874 | 51445990 | LETMD1 | -12.7381 | 0.0036 | 4.0399 | 0.0007 | -0.3430 | 0.0659 |
| chr19 | 46274607 | 46274654 | DMPK | -9.1028 | 0.0140 | -0.2167 | 1.0119 | -0.3424 | -0.0038 |
| chr20 | 24995773 | 24995866 | ACSS1 | -10.3072 | 0.0054 | 1.6360 | 0.0515 | -0.3417 | 0.0211 |
| chr6 | 90327672 | 90327750 | ANKRD6 | -6.1061 | 0.0395 | 2.5791 | 0.0251 | -0.3397 | 0.0594 |
| chr12 | 51449617 | 51449804 | LETMD1 | -14.0924 | 0.0016 | 4.8122 | 0.0001 | -0.3368 | 0.0651 |
| chr2 | 197757069 | 197757125 | PGAP1 | -1.5161 | 0.7645 | 1.8412 | 0.0285 | -0.3337 | 0.0925 |
| chr13 | 114292132 | 114292211 | TFDP1 | -20.7301 | 0.0000 | -3.6305 | 0.0003 | -0.3310 | -0.0283 |
| chr20 | 34243123 | 34243266 | CPNE1 | 17.6743 | 0.0000 | 3.7045 | 0.0038 | 0.3296 | 0.0346 |
| chr17 | 40739851 | 40739882 | FAM134C | -5.7466 | 0.0490 | 2.0358 | 0.0478 | -0.3289 | 0.0689 |
| chr8 | 144889721 | 144889784 | SCRIB | -14.0897 | 0.0019 | 3.7324 | 0.0009 | -0.3265 | 0.0468 |
| chr17 | 35880281 | 35880317 | SYNRG | -5.4029 | 0.0575 | 6.3849 | 0.0000 | -0.3260 | 0.2176 |
| chr17 | 76198783 | 76198832 | AFMID | -9.6373 | 0.0078 | 1.4878 | 0.0782 | -0.3251 | 0.0434 |
| chr2 | 219543890 | 219543984 | STK36 | -5.0458 | 0.0653 | 1.7313 | 0.0368 | -0.3250 | 0.0483 |
| chr2 | 74717151 | 74717254 | TTC31 | -5.9066 | 0.0444 | 0.7328 | 0.7735 | -0.3243 | 0.0168 |
| chr17 | 30688486 | 30688534 | ZNF207 | -12.8458 | 0.0023 | 4.4937 | 0.0020 | -0.3234 | 0.0578 |
| chr2 | 234182366 | 234182423 | ATG16L1 | -6.0292 | 0.0419 | 4.1644 | 0.0004 | -0.3217 | 0.1498 |
| chr1 | 24122998 | 24123076 | GALE | -9.2233 | 0.0083 | 0.1002 | 1.0291 | -0.3213 | 0.0085 |
| chr4 | 106833344 | 106833395 | NPNT | 4.2862 | 0.0191 | -2.5349 | 0.0041 | 0.3209 | -0.0671 |
| chr10 | 127417571 | 127417673 | C10orf137 | -8.8288 | 0.0115 | 4.6260 | 0.0001 | -0.3202 | 0.0854 |
| chrX | 18918787 | 18918817 | PHKA2 | -7.7063 | 0.0195 | 6.0731 | 0.0000 | -0.3189 | 0.3112 |
| chr3 | 184056174 | 184056317 | FAM131A | -4.6417 | 0.0747 | 2.4469 | 0.0075 | -0.3181 | 0.0756 |
| chr4 | 108984778 | 108984819 | LEF1 | -5.9604 | 0.0451 | 1.9961 | 0.0924 | -0.3176 | 0.0642 |
| chr17 | 73887893 | 73887959 | TRIM65 | -9.2691 | 0.0089 | 5.3620 | 0.0000 | -0.3150 | 0.0893 |
| chrX | 39930889 | 39930943 | BCOR | -12.8665 | 0.0024 | 2.4185 | 0.0059 | -0.3133 | 0.0314 |
| chr1 | 53684538 | 53684595 | C1orf123 | -10.4279 | 0.0055 | 3.3661 | 0.0012 | -0.3122 | 0.0578 |
| chr19 | 42396095 | 42396194 | ARHGEF1 | -8.8958 | 0.0107 | 0.6159 | 0.3000 | -0.3122 | 0.0122 |
| chr18 | 34267090 | 34267141 | FHOD3 | -4.1222 | 0.0971 | 3.2425 | 0.0070 | -0.3109 | 0.2219 |
| chr5 | 137495243 | 137495288 | BRD8 | -11.8999 | 0.0036 | 4.0753 | 0.0008 | -0.3098 | 0.0570 |
| chr19 | 41128854 | 41128926 | LTBP4 | -8.4614 | 0.0126 | 7.6271 | 0.0000 | -0.3084 | 0.1738 |
| chr17 | 73284582 | 73284672 | SLC25A19 | -6.7739 | 0.0259 | 3.6192 | 0.0011 | -0.3070 | 0.1144 |
| chr2 | 9531190 | 9531325 | ASAP2 | -2.2455 | 0.5816 | 3.5938 | 0.0010 | -0.3055 | 0.1604 |
| chr12 | 48359620 | 48359780 | TMEM106C | -18.9411 | 0.0022 | 5.8064 | 0.0000 | -0.3039 | 0.0437 |
| chr21 | 40551849 | 40551912 | PSMG1 | -14.5243 | 0.0018 | 2.8109 | 0.0088 | -0.3036 | 0.0250 |
| chrX | 46495023 | 46495083 | SLC9A7 | -4.1560 | 0.0958 | 1.5979 | 0.0374 | -0.3025 | 0.0774 |
| chr8 | 169289 | 169417 | RPL23AP53 | 4.3546 | 0.0217 | 1.0388 | 0.2227 | 0.3019 | 0.0654 |
| chrX | 100276956 | 100277051 | TRMT2B | -5.6218 | 0.0499 | 1.3420 | 0.1240 | -0.3011 | 0.0507 |

| chrom | begin | end | name | Z.OE | fdr.OE | Z.KD | fdr.KD | ΔPSI_OE | ΔPSI_KD |
|---|---|---|---|---|---|---|---|---|---|
| chr18 | 74082482 | 74082550 | ZNF516 | -4.0395 | 0.0990 | 1.8946 | 0.0471 | -0.3006 | 0.1020 |
| chr6 | 144081537 | 144081777 | PHACTR2 | 4.1353 | 0.0220 | -3.7453 | 0.0017 | 0.3000 | -0.1437 |
| chr1 | 47025905 | 47025949 | MKNK1 | -5.5156 | 0.0529 | 2.8401 | 0.0039 | -0.2997 | 0.0585 |
| chr14 | 75349293 | 75349327 | DLST | -6.2876 | 0.0367 | 0.0701 | 1.2352 | -0.2996 | -0.0010 |
| chr22 | 43272893 | 43273016 | PACSIN2 | -14.9895 | 0.0020 | 2.4237 | 0.0070 | -0.2970 | 0.0194 |
| chr10 | 99213555 | 99213603 | ZDHHC16 | -9.2792 | 0.0073 | 8.4098 | 0.0000 | -0.2967 | 0.1594 |
| chr15 | 35812473 | 35814479 | ATPBD4 | 6.4428 | 0.0013 | -1.1169 | 0.1197 | 0.2962 | -0.0355 |
| chr1 | 161197425 | 161197527 | TOMM40L | -8.4558 | 0.0120 | 0.7265 | 0.4202 | -0.2957 | 0.0151 |
| chr21 | 47958395 | 47958515 | DIP2A | -8.2917 | 0.0139 | 0.6394 | 0.4456 | -0.2934 | 0.0172 |
| chr17 | 7530260 | 7530362 | SAT2 | -7.5535 | 0.0187 | 1.2958 | 0.1391 | -0.2933 | 0.0316 |
| chr9 | 86582997 | 86584355 | HNRNPK | -18.2198 | 0.0020 | 12.0619 | 0.0000 | -0.2929 | 0.0736 |
| chr12 | 115117717 | 115117777 | TBX3 | -6.6609 | 0.0290 | 2.4301 | 0.0182 | -0.2928 | 0.0738 |
| chr4 | 20526771 | 20526795 | SLIT2 | -3.3155 | 0.1396 | 8.9429 | 0.0000 | -0.1651 | 0.2920 |
| chr12 | 62959793 | 62959811 | MON2 | -5.2347 | 0.0586 | 3.1620 | 0.0405 | -0.2909 | 0.2687 |
| chr16 | 30770662 | 30770779 | C16orf93 | -7.2968 | 0.0218 | 1.7438 | 0.0772 | -0.2909 | 0.0385 |
| chr9 | 86582997 | 86584295 | HNRNPK | 18.4756 | 0.0000 | -12.4411 | 0.0000 | 0.2908 | -0.0755 |
| chr17 | 76198579 | 76198684 | AFMID | -9.6082 | 0.0075 | 0.4400 | 0.9155 | -0.2906 | -0.0003 |
| chr22 | 37158947 | 37159057 | IFT27 | -11.4646 | 0.0038 | 0.2117 | 1.1687 | -0.2905 | 0.0010 |
| chr10 | 135215032 | 135215094 | MTG1 | -9.8558 | 0.0064 | 1.0403 | 0.2428 | -0.2903 | 0.0100 |
| chr16 | 3073474 | 3073531 | HCFC1R1 | -9.4693 | 0.0065 | 2.9332 | 0.0024 | -0.2896 | 0.0459 |
| chr16 | 16429908 | 16429994 | PKD1P1 | -14.2361 | 0.0017 | -1.2184 | 0.0185 | -0.2891 | -0.0329 |
| chr17 | 73647265 | 73647345 | RECQL5 | -6.5763 | 0.0290 | -1.0021 | 0.2910 | -0.2885 | -0.0204 |
| chr9 | 97693996 | 97695955 | C9orf3 | 3.4688 | 0.0491 | 0.0870 | 1.2361 | 0.2872 | -0.0734 |
| chr17 | 31258344 | 31258420 | TMEM98 | -10.3653 | 0.0058 | 3.5249 | 0.0013 | -0.2861 | 0.0569 |
| chr17 | 73644944 | 73647345 | RECQL5 | 6.4745 | 0.0014 | 0.7855 | 0.4200 | 0.2838 | 0.0115 |
| chr7 | 75040937 | 75041042 | NSUN5P1 | -8.0539 | 0.0171 | 3.4644 | 0.0058 | -0.2807 | 0.0807 |
| chr1 | 16047823 | 16047883 | PLEKHM2 | -9.3129 | 0.0074 | 12.6659 | 0.0000 | -0.2806 | 0.2077 |
| chr16 | 30770498 | 30770568 | C16orf93 | -7.8628 | 0.0174 | 1.0496 | 0.0857 | -0.2805 | 0.0278 |
| chrX | 128691837 | 128691927 | OCRL | -7.5395 | 0.0188 | 1.8887 | 0.0164 | -0.2790 | 0.0296 |
| chr14 | 73745988 | 73746132 | NUMB | -7.8897 | 0.0146 | 2.7581 | 0.0032 | -0.2778 | 0.0423 |
| chr4 | 95508139 | 95509370 | PDLIM5 | 7.0743 | 0.0006 | -1.6086 | 0.0279 | 0.2771 | -0.0515 |
| chr14 | 105915695 | 105915746 | MTA1 | -14.1680 | 0.0017 | 10.4859 | 0.0000 | -0.2756 | 0.0953 |
| chr15 | 63362068 | 63362831 | TPM1 | 10.0171 | 0.0000 | -0.2425 | 0.9017 | 0.2756 | -0.0067 |
| chr19 | 805491 | 805569 | PTBP1 | -16.2115 | 0.0021 | 2.1017 | 0.0198 | -0.2749 | 0.0099 |
| chr6 | 133846291 | 133846392 | EYA4 | 6.5855 | 0.0016 | -3.2998 | 0.0030 | 0.2718 | -0.0979 |
| chr17 | 35567380 | 35567404 | ACACA | -5.2817 | 0.0739 | 2.6920 | 0.0038 | -0.2709 | 0.1181 |
| chr3 | 37402733 | 37402796 | GOLGA4 | -7.2459 | 0.0215 | 1.9752 | 0.0390 | -0.2704 | 0.0386 |
| chr3 | 49879885 | 49879980 | TRAIP | -6.8571 | 0.0301 | 0.0070 | 0.9036 | -0.2691 | 0.0074 |
| chr17 | 7470243 | 7470322 | SENP3 | -11.3279 | 0.0037 | -0.2880 | 0.8148 | -0.2689 | -0.0071 |
| chr2 | 27995540 | 27995559 | MRPL33 | -6.7888 | 0.0269 | 1.3853 | 0.1125 | -0.2688 | 0.0475 |
| chrX | 47509319 | 47509425 | ELK1 | -8.1951 | 0.0150 | 4.2136 | 0.0007 | -0.2682 | 0.0832 |
| chr9 | 96062332 | 96062431 | WNK2 | -3.7885 | 0.1102 | 6.7787 | 0.0000 | -0.2671 | 0.2582 |
| chr18 | 677742 | 677872 | ENOSF1 | -7.9929 | 0.0148 | 1.8003 | 0.0421 | -0.2654 | 0.0534 |
| chr22 | 37457578 | 37457669 | KCTD17 | -6.5168 | 0.0302 | 0.9155 | 0.2667 | -0.2654 | 0.0174 |
| chr14 | 94567084 | 94567117 | IFI27L1 | -4.2764 | 0.0991 | -1.9518 | 0.0266 | -0.2632 | -0.1523 |
| chr17 | 7470243 | 7470322 | SENP3-EIF4A1 | -11.1183 | 0.0038 | -0.2662 | 1.0303 | -0.2631 | -0.0041 |
| chr8 | 48641973 | 48642027 | KIAA0146 | -8.1005 | 0.0147 | 2.5989 | 0.0057 | -0.2628 | 0.0570 |
| chr1 | 153615702 | 153615840 | C1orf77 | -15.7622 | 0.0023 | 3.8540 | 0.0007 | -0.2626 | 0.0312 |
| chr7 | 99688524 | 99688572 | COPS6 | -14.7181 | 0.0021 | 0.8477 | 0.2233 | -0.2613 | 0.0089 |
| chr3 | 49878417 | 49878505 | TRAIP | -6.1851 | 0.0416 | -0.1307 | 1.0928 | -0.2600 | -0.0021 |
| chr17 | 79872479 | 79872578 | SIRT7 | -8.7066 | 0.0128 | 0.5093 | 0.9785 | -0.2586 | -0.0005 |
| chr1 | 26628184 | 26628213 | UBXN11 | -5.9704 | 0.0448 | 3.8600 | 0.0008 | -0.2576 | 0.1393 |
| chr14 | 24572368 | 24572464 | PCK2 | -6.5846 | 0.0301 | 0.5495 | 0.2856 | -0.2573 | 0.0252 |
| chr7 | 97598316 | 97598364 | MGC72080 | -5.9206 | 0.0450 | 4.0068 | 0.0007 | -0.2558 | 0.1273 |

| chrom | begin | end | name | Z.OE | fdr.OE | Z.KD | fdr.KD | ΔPSI_OE | ΔPSI_KD |
|---|---|---|---|---|---|---|---|---|---|
| chr22 | 37162181 | 37162241 | IFT27 | -6.9797 | 0.0238 | 0.6945 | 0.8728 | -0.2554 | 0.0019 |
| chr7 | 75510682 | 75510804 | RHBDD2 | -9.6399 | 0.0076 | 3.4325 | 0.0017 | -0.2551 | 0.0559 |
| chr7 | 128040870 | 128040945 | IMPDH1 | -12.7691 | 0.0038 | 2.3004 | 0.0438 | -0.2545 | 0.0178 |
| chr18 | 677344 | 677444 | ENOSF1 | -7.8199 | 0.0152 | 2.6273 | 0.0042 | -0.2541 | 0.0499 |
| chr9 | 706895 | 707247 | KANK1 | 3.5817 | 0.0415 | 0.5415 | 0.9997 | 0.2536 | 0.0007 |
| chr9 | 131010202 | 131010214 | DNM1 | -4.8031 | 0.0690 | 2.2405 | 0.0155 | -0.2535 | 0.0611 |
| chr3 | 100030676 | 100030721 | TBC1D23 | -5.9490 | 0.0445 | 3.2946 | 0.0032 | -0.2527 | 0.0927 |
| chr1 | 32205710 | 32205779 | BAI2 | -4.1419 | 0.1011 | 1.7445 | 0.0275 | -0.2505 | 0.0532 |
| chr3 | 107770785 | 107770817 | CD47 | -7.0520 | 0.0232 | 4.3480 | 0.0004 | -0.2503 | 0.0913 |
| chr17 | 74087223 | 74087316 | EXOC7 | -9.4020 | 0.0076 | 9.0449 | 0.0000 | -0.2501 | 0.1123 |
| chr17 | 7123782 | 7123848 | ACADVL | -7.6025 | 0.0191 | 2.2981 | 0.0079 | -0.2492 | 0.0369 |
| chr7 | 150774187 | 150774323 | FASTK | -11.5996 | 0.0038 | -0.3968 | 0.8854 | -0.2488 | 0.0011 |
| chr7 | 48142893 | 48143008 | UPP1 | -5.0714 | 0.0659 | 3.7636 | 0.0015 | -0.2479 | 0.1601 |
| chr17 | 38498270 | 38499119 | RARA | 3.6581 | 0.0420 | 0.7075 | 0.2031 | 0.2478 | 0.0544 |
| chr22 | 19462590 | 19462623 | UFD1L | -11.9449 | 0.0033 | 3.4278 | 0.0013 | -0.2476 | 0.0522 |
| chr13 | 37622700 | 37622736 | FAM48A | -5.8036 | 0.0490 | 1.4208 | 0.2957 | -0.2474 | 0.0425 |
| chr17 | 74739479 | 74739538 | MFSD11 | -4.2861 | 0.0875 | 1.6420 | 0.0265 | -0.2469 | 0.0535 |
| chr6 | 43034733 | 43035133 | KLC4 | 4.7572 | 0.0177 | 0.2267 | 1.0521 | 0.2456 | -0.0064 |
| chr5 | 177642276 | 177642431 | AGXT2L2 | -6.6623 | 0.0288 | -1.5669 | 0.0940 | -0.2456 | -0.0561 |
| chr6 | 3015763 | 3015877 | NQO2 | -8.1705 | 0.0142 | 5.3822 | 0.0000 | -0.2455 | 0.1044 |
| chr8 | 62587818 | 62588878 | ASPH | 7.6511 | 0.0007 | -0.7783 | 0.4172 | 0.2444 | -0.0089 |
| chr17 | 8077837 | 8077934 | TMEM107 | -5.2061 | 0.0601 | 2.5246 | 0.0152 | -0.2440 | 0.0898 |
| chr15 | 63358094 | 63358292 | TPM1 | 9.2660 | 0.0000 | -3.6465 | 0.0002 | 0.2434 | -0.0758 |
| chr9 | 95085517 | 95085633 | NOL8 | -3.2368 | 0.1501 | 4.0262 | 0.0008 | -0.2430 | 0.1591 |
| chr19 | 38706992 | 38707043 | DPF1 | -5.1147 | 0.0621 | 2.4854 | 0.0080 | -0.2414 | 0.0753 |
| chr17 | 42809545 | 42809633 | DBF4B | -3.5885 | 0.1224 | 3.4931 | 0.0011 | -0.2406 | 0.1377 |
| chr12 | 30886562 | 30886645 | CAPRIN2 | -2.9578 | 0.1706 | 3.0052 | 0.0086 | -0.2403 | 0.1335 |
| chr3 | 169491818 | 169491885 | MYNN | -3.9920 | 0.1009 | 1.9696 | 0.0487 | -0.2399 | 0.0613 |
| chr17 | 18236479 | 18236602 | SHMT1 | -10.0932 | 0.0063 | 4.3242 | 0.0003 | -0.2396 | 0.0498 |
| chr12 | 88909310 | 88909394 | KITLG | -3.7718 | 0.1186 | 2.3553 | 0.0237 | -0.2394 | 0.0684 |
| chr1 | 26627416 | 26627515 | UBXN11 | -6.8420 | 0.0271 | 3.3379 | 0.0056 | -0.2367 | 0.1248 |
| chr8 | 73942570 | 73942630 | TERF1 | -6.5520 | 0.0301 | 6.4103 | 0.0000 | -0.2363 | 0.1195 |
| chr14 | 104193128 | 104193179 | ZFYVE21 | -6.9892 | 0.0275 | 0.6774 | 0.8918 | -0.2362 | 0.0049 |
| chr3 | 47860725 | 47860754 | DHX30 | -3.9964 | 0.1053 | 2.9535 | 0.0047 | -0.2356 | 0.1220 |
| chr3 | 58127584 | 58127656 | FLNB | -5.9178 | 0.0472 | 3.3612 | 0.0031 | -0.2342 | 0.0593 |
| chr11 | 111753859 | 111753926 | C11orf1 | -7.0047 | 0.0237 | 2.3691 | 0.0251 | -0.2339 | 0.0714 |
| chr19 | 58598272 | 58598375 | ZSCAN18 | -8.4300 | 0.0141 | 0.9299 | 0.2252 | -0.2339 | 0.0110 |
| chr7 | 116774177 | 116774246 | ST7 | -3.7392 | 0.1207 | 9.0284 | 0.0000 | -0.1399 | 0.2323 |
| chr17 | 6353347 | 6353392 | FAM64A | -7.5526 | 0.0184 | 3.2114 | 0.0032 | -0.2315 | 0.0614 |
| chr5 | 102518934 | 102519108 | PPIP5K2 | -5.5375 | 0.0531 | 3.5026 | 0.0008 | -0.2307 | 0.0870 |
| chr19 | 9482285 | 9482428 | ZNF559-ZNF177 | 3.3966 | 0.0517 | 1.9143 | 0.0169 | 0.2304 | 0.0905 |
| chr4 | 110402832 | 110402937 | SEC24B | -5.2173 | 0.0590 | 4.2329 | 0.0013 | -0.2299 | 0.1068 |
| chr16 | 30770974 | 30771045 | C16orf93 | -5.3264 | 0.0655 | 2.0194 | 0.0343 | -0.2299 | 0.0461 |
| chr2 | 202137620 | 202137665 | CASP8 | -3.7177 | 0.1224 | 6.2194 | 0.0000 | -0.2263 | 0.2290 |
| chr20 | 25999467 | 25999548 | LOC100134868 | -0.5273 | 1.0049 | 2.8096 | 0.0032 | -0.2289 | 0.1926 |
| chr16 | 68381533 | 68381581 | PRMT7 | -5.8881 | 0.0443 | 0.9542 | 0.2251 | -0.2280 | 0.0314 |
| chr12 | 49168739 | 49168837 | ADCY6 | -6.3310 | 0.0400 | -0.4888 | 0.5939 | -0.2280 | -0.0112 |
| chr12 | 51451814 | 51451911 | LETMD1 | -10.1874 | 0.0064 | -0.0701 | 1.2191 | -0.2279 | 0.0016 |
| chr5 | 74695134 | 74695212 | COL4A3BP | -3.6072 | 0.1194 | 6.4914 | 0.0000 | -0.1932 | 0.2262 |
| chr8 | 144902835 | 144902886 | PUF60 | -10.8991 | 0.0057 | 9.1342 | 0.0000 | -0.2261 | 0.1020 |
| chr4 | 130017281 | 130017364 | C4orf33 | -3.0266 | 0.1687 | 1.3491 | 0.0440 | -0.2254 | 0.1118 |
| chr12 | 125020110 | 125020157 | NCOR2 | -0.2377 | 0.9919 | 3.1754 | 0.0055 | -0.1133 | 0.2253 |
| chr2 | 74884979 | 74885078 | SEMA4F | -2.7881 | 0.2154 | 2.3661 | 0.0383 | -0.2251 | 0.1864 |
| chr7 | 44687042 | 44687133 | OGDH | -6.4252 | 0.0346 | 8.4951 | 0.0000 | -0.2246 | 0.1555 |

| chrom | begin | end | name | Z.OE | fdr.OE | Z.KD | fdr.KD | ΔPSI_OE | ΔPSI_KD |
|---|---|---|---|---|---|---|---|---|---|
| chr12 | 118455494 | 118455858 | RFC5 | -7.6109 | 0.0191 | 8.2971 | 0.0000 | -0.2244 | 0.1212 |
| chr17 | 75315596 | 75316430 | SEPT9 | 3.8812 | 0.0367 | 1.6916 | 0.0703 | 0.2241 | 0.0782 |
| chr18 | 678695 | 678737 | ENOSF1 | -5.8084 | 0.0492 | 1.8505 | 0.0224 | -0.2235 | 0.0389 |
| chr13 | 52535972 | 52536049 | ATP7B | -4.0737 | 0.0987 | 3.1720 | 0.0021 | -0.2234 | 0.1264 |
| chr16 | 341189 | 341297 | AXIN1 | -8.4919 | 0.0146 | 1.5503 | 0.0542 | -0.2233 | 0.0177 |
| chrX | 152853382 | 152853852 | FAM58A | 8.4950 | 0.0000 | -4.2941 | 0.0001 | 0.2231 | -0.0543 |
| chr15 | 29488633 | 29488768 | FAM189A1 | 3.1714 | 0.0677 | 3.0870 | 0.0143 | 0.2228 | 0.0883 |
| chrX | 152853382 | 152853912 | FAM58A | -8.4975 | 0.0123 | 4.6226 | 0.0002 | -0.2228 | 0.0596 |
| chr4 | 152065371 | 152065440 | SH3D19 | -3.4052 | 0.1372 | 2.3673 | 0.0363 | -0.2227 | 0.0790 |
| chr19 | 1106398 | 1106458 | GPX4 | 4.6789 | 0.0176 | -1.2569 | 0.0889 | 0.2222 | -0.0375 |
| chr17 | 79982153 | 79982215 | LRRC45 | -6.2296 | 0.0370 | 0.6157 | 0.5383 | -0.2219 | 0.0136 |
| chr5 | 177651448 | 177651565 | AGXT2L2 | -4.9170 | 0.0684 | -3.9911 | 0.0002 | -0.2216 | -0.1287 |
| chr4 | 160265187 | 160265211 | RAPGEF2 | -1.3538 | 0.8213 | 1.7544 | 0.0236 | -0.2212 | 0.0958 |
| chr6 | 30887865 | 30887993 | VARS2 | -7.2268 | 0.0250 | 0.0490 | 1.2098 | -0.2208 | -0.0037 |
| chr10 | 99212651 | 99212680 | ZDHHC16 | -5.7117 | 0.0493 | -0.4467 | 0.5693 | -0.2194 | -0.0160 |
| chr17 | 48560003 | 48560067 | RSAD1 | -6.6535 | 0.0271 | -0.2633 | 0.9589 | -0.2193 | -0.0042 |
| chr22 | 31492983 | 31493046 | SMTN | -5.2243 | 0.0586 | 4.8676 | 0.0002 | -0.2190 | 0.1297 |
| chr7 | 86783705 | 86783844 | DMTF1 | -4.8207 | 0.0713 | 3.2567 | 0.0024 | -0.2176 | 0.0721 |
| chr16 | 19088627 | 19088696 | COQ7 | -8.8643 | 0.0098 | 0.3894 | 0.9394 | -0.2175 | 0.0061 |
| chr17 | 71208816 | 71208879 | FAM104A | -4.9156 | 0.0678 | 4.4993 | 0.0003 | -0.2175 | 0.1253 |
| chr7 | 155095534 | 155095605 | INSIG1 | -8.1793 | 0.0147 | 4.7306 | 0.0004 | -0.2173 | 0.0380 |
| chr2 | 236839408 | 236839567 | AGAP1 | -5.1086 | 0.0677 | -1.6406 | 0.0317 | -0.2171 | -0.0275 |
| chr17 | 45012394 | 45012535 | GOSR2 | -12.0517 | 0.0036 | 9.3160 | 0.0000 | -0.2169 | 0.0727 |
| chr9 | 134385129 | 134385195 | POMT1 | -6.5818 | 0.0300 | 0.4236 | 0.9730 | -0.2168 | 0.0035 |
| chr19 | 41289682 | 41289745 | MIA-RAB4B | -6.2473 | 0.0396 | 1.0932 | 0.4750 | -0.2167 | 0.0186 |
| chr17 | 40052872 | 40052902 | ACLY | -9.0708 | 0.0120 | 9.7441 | 0.0000 | -0.2165 | 0.1519 |
| chr3 | 11340835 | 11340890 | ATG7 | -4.2202 | 0.0959 | 1.5917 | 0.0317 | -0.2164 | 0.0328 |
| chr21 | 47845744 | 47845885 | PCNT | -7.9969 | 0.0175 | 3.0320 | 0.0029 | -0.2160 | 0.0327 |
| chr2 | 27535860 | 27535976 | MPV17 | -8.4852 | 0.0137 | 4.0896 | 0.0007 | -0.2156 | 0.0486 |
| chr18 | 32409004 | 32409292 | DTNA | -5.0846 | 0.0649 | 7.2440 | 0.0000 | -0.2152 | 0.1872 |
| chr15 | 40683693 | 40683755 | C15orf23 | -8.5157 | 0.0114 | 0.2452 | 1.0215 | -0.2149 | 0.0013 |
| chr11 | 129993506 | 129993674 | APLP2 | -13.2245 | 0.0025 | 17.6818 | 0.0000 | -0.2148 | 0.1371 |
| chr2 | 173366499 | 173366629 | ITGA6 | -4.5150 | 0.0876 | 5.0076 | 0.0000 | -0.2143 | 0.1338 |
| chr12 | 32890798 | 32890876 | DNM1L | -5.9071 | 0.0464 | 4.8704 | 0.0002 | -0.2143 | 0.0909 |
| chr3 | 140953057 | 140953160 | ACPL2 | 2.7516 | 0.0855 | -2.0374 | 0.0191 | 0.2133 | -0.0960 |
| chr2 | 192265474 | 192265561 | MYO1B | -7.2561 | 0.0215 | 12.1539 | 0.0000 | -0.2130 | 0.1775 |
| chr3 | 50147811 | 50147896 | RBM5 | -7.0951 | 0.0217 | 1.3795 | 0.0857 | -0.2121 | 0.0253 |
| chr5 | 177651642 | 177651730 | AGXT2L2 | -5.0289 | 0.0687 | -1.3209 | 0.0495 | -0.2118 | -0.0602 |
| chr17 | 40963672 | 40963815 | BECN1 | -9.9597 | 0.0075 | 0.4159 | 1.1082 | -0.2117 | 0.0008 |
| chr1 | 97271974 | 97272008 | PTBP2 | 4.5327 | 0.0195 | -0.1534 | 0.6092 | 0.2111 | -0.0202 |
| chr14 | 99876140 | 99876552 | SETD3 | 7.3130 | 0.0007 | -2.6680 | 0.0027 | 0.2107 | -0.0606 |
| chr6 | 111824498 | 111824811 | LOC643749 | 5.6858 | 0.0065 | -1.5793 | 0.0411 | 0.2104 | -0.0337 |
| chr1 | 11888514 | 11888681 | CLCN6 | 3.7545 | 0.0356 | 1.4531 | 0.0932 | 0.2095 | 0.0672 |
| chr19 | 44721943 | 44722005 | ZNF227 | -7.8067 | 0.0165 | 19.8925 | 0.0000 | -0.1833 | 0.2087 |
| chr13 | 95748024 | 95748433 | ABCC4 | -2.7722 | 0.1918 | 4.9557 | 0.0002 | -0.1932 | 0.2082 |
| chr9 | 130660234 | 130660289 | ST6GALNAC6 | -3.1247 | 0.1656 | 1.9241 | 0.0194 | -0.2081 | 0.0905 |
| chr13 | 115004464 | 115004503 | CDC16 | -6.6546 | 0.0289 | 1.2790 | 0.0705 | -0.2077 | 0.0208 |
| chr18 | 55218546 | 55218606 | FECH | -7.3999 | 0.0210 | 0.6947 | 0.2497 | -0.2074 | 0.0111 |
| chr7 | 64377407 | 64377496 | ZNF273 | -2.3805 | 0.2536 | 5.4664 | 0.0000 | -0.1328 | 0.2072 |
| chr16 | 89805885 | 89805961 | FANCA | -7.3225 | 0.0244 | 0.1936 | 1.0242 | -0.2072 | 0.0029 |
| chr22 | 37456862 | 37456962 | KCTD17 | -5.8313 | 0.0492 | 0.0999 | 0.5257 | -0.2072 | 0.0188 |
| chr11 | 71712450 | 71713965 | IL18BP | 4.1626 | 0.0240 | 0.8890 | 0.3893 | 0.2069 | 0.0374 |
| chr20 | 43251647 | 43251719 | ADA | -4.3042 | 0.0925 | 1.9100 | 0.0472 | -0.2065 | 0.0693 |
| chr7 | 72422690 | 72422834 | NSUN5P2 | -6.2271 | 0.0372 | 1.5853 | 0.2141 | -0.2062 | 0.0338 |

| chrom | begin | end | name | Z.OE | fdr.OE | Z.KD | fdr.KD | ΔPSI_OE | ΔPSI_KD |
|---|---|---|---|---|---|---|---|---|---|
| chr17 | 45012394 | 45014205 | GOSR2 | 11.4062 | 0.0000 | -9.1435 | 0.0000 | 0.2057 | -0.0703 |
| chr9 | 96069058 | 96069103 | WNK2 | -2.5688 | 0.2119 | 3.1052 | 0.0021 | -0.2053 | 0.1625 |
| chr17 | 79246315 | 79246427 | SLC38A10 | -6.7673 | 0.0300 | 0.5018 | 0.6631 | -0.2052 | 0.0081 |
| chr1 | 117149113 | 117149173 | IGSF3 | -2.5124 | 0.2161 | 6.2061 | 0.0000 | -0.1859 | 0.2051 |
| chr2 | 191213613 | 191213757 | INPP1 | 3.5707 | 0.0471 | -2.6985 | 0.0032 | 0.2049 | -0.1120 |
| chr17 | 48561066 | 48561121 | RSAD1 | -6.8377 | 0.0247 | 0.4318 | 0.7723 | -0.2044 | 0.0082 |
| chr22 | 29946716 | 29946832 | THOC5 | -5.9619 | 0.0425 | -0.7248 | 0.2408 | -0.2042 | -0.0072 |
| chr6 | 99851704 | 99851758 | SFRS18 | -7.3586 | 0.0203 | 3.3240 | 0.0021 | -0.2042 | 0.0442 |
| chr17 | 6553301 | 6553398 | MED31 | -7.7239 | 0.0183 | 4.1032 | 0.0006 | -0.2040 | 0.0489 |
| chr16 | 2127598 | 2127727 | TSC2 | -6.3947 | 0.0371 | 7.4824 | 0.0000 | -0.2032 | 0.1279 |
| chr15 | 80390757 | 80390920 | ZFAND6 | 9.0206 | 0.0000 | -2.6992 | 0.0018 | 0.2027 | -0.0490 |
| chr1 | 92732256 | 92732298 | GLMN | -3.7806 | 0.1177 | 1.6394 | 0.0295 | -0.2027 | 0.0657 |
| chr3 | 12571260 | 12571372 | TSEN2 | 6.8199 | 0.0012 | -2.0487 | 0.4482 | 0.2018 | 0.0012 |
| chr16 | 4871547 | 4871598 | GLYR1 | -5.3350 | 0.0739 | -1.8305 | 0.0462 | -0.2001 | -0.0261 |
| chr17 | 643744 | 643840 | FAM57A | -8.5165 | 0.0111 | 1.3252 | 0.0591 | -0.1999 | 0.0144 |
| chr1 | 71531360 | 71531435 | ZRANB2 | -8.4242 | 0.0114 | 13.9095 | 0.0000 | -0.1999 | 0.1577 |
| chr14 | 89656727 | 89656793 | FOXN3 | 0.3946 | 0.9934 | 2.9534 | 0.0118 | 0.1243 | 0.1991 |
| chr16 | 705028 | 705147 | WDR90 | -4.5322 | 0.0954 | 2.3851 | 0.0072 | -0.1991 | 0.0496 |
| chr13 | 52534283 | 52534458 | ATP7B | -4.0435 | 0.1051 | 2.5239 | 0.0166 | -0.1990 | 0.0985 |
| chr2 | 114379302 | 114379593 | RPL23AP7 | 4.8423 | 0.0146 | -1.6873 | 0.0440 | 0.1981 | -0.0575 |
| chr3 | 10106039 | 10106113 | FANCD2 | -5.4390 | 0.0572 | 3.4432 | 0.0012 | -0.1976 | 0.0408 |
| chr8 | 22396981 | 22397011 | PPP3CC | -3.9623 | 0.1090 | 2.6117 | 0.0202 | -0.1971 | 0.1207 |
| chr2 | 202028557 | 202037411 | CFLAR | 2.6189 | 0.0934 | -4.1040 | 0.0001 | 0.1963 | -0.1673 |
| chr5 | 177649852 | 177649935 | AGXT2L2 | -4.1112 | 0.0986 | -3.6949 | 0.0011 | -0.1959 | -0.1330 |
| chr14 | 53518561 | 53518645 | DDHD1 | -4.3112 | 0.1053 | 5.4348 | 0.0001 | -0.1957 | 0.1443 |
| chr13 | 37584688 | 37584792 | FAM48A | -8.1650 | 0.0148 | 7.0943 | 0.0000 | -0.1953 | 0.0919 |
| chr17 | 76167590 | 76167730 | SYNGR2 | -11.7692 | 0.0036 | 4.4629 | 0.0004 | -0.1951 | 0.0312 |
| chr8 | 82597997 | 82598198 | IMPA1 | 3.8159 | 0.0412 | -0.7546 | 0.1371 | 0.1945 | -0.0315 |
| chr5 | 94988820 | 94988918 | RFESD | -4.1223 | 0.0998 | 3.7231 | 0.0007 | -0.1937 | 0.1215 |
| chr7 | 107866088 | 107866145 | NRCAM | -2.5821 | 0.2131 | 5.4801 | 0.0000 | -0.1935 | 0.1850 |
| chr22 | 46704046 | 46704104 | GTSE1 | -7.0204 | 0.0240 | 1.4410 | 0.0553 | -0.1933 | 0.0374 |
| chr2 | 202027718 | 202037411 | CFLAR | -2.6346 | 0.2161 | 3.9590 | 0.0008 | -0.1932 | 0.1621 |
| chr6 | 122749047 | 122749101 | HSF2 | -5.3301 | 0.0584 | 7.7065 | 0.0000 | -0.1925 | 0.1392 |
| chr16 | 88037900 | 88038017 | BANP | -4.8102 | 0.0711 | -2.0296 | 0.0333 | -0.1922 | -0.0452 |
| chr22 | 39150646 | 39150711 | SUN2 | -3.2422 | 0.1705 | 3.8734 | 0.0007 | -0.1921 | 0.1136 |
| chr6 | 30709568 | 30709644 | FLOT1 | -6.5613 | 0.0290 | 0.0357 | 0.5339 | -0.1919 | -0.0061 |
| chr20 | 25187157 | 25187226 | ENTPD6 | -5.9618 | 0.0488 | 3.8089 | 0.0008 | -0.1910 | 0.0611 |
| chr3 | 9739394 | 9739550 | MTMR14 | 6.2085 | 0.0038 | -0.0214 | 0.5567 | 0.1907 | -0.0078 |
| chr10 | 76995373 | 76995501 | COMTD1 | -6.0710 | 0.0396 | -0.6033 | 0.2947 | -0.1906 | -0.0129 |
| chr10 | 21158668 | 21158770 | NEBL | -2.5454 | 0.2206 | 1.9089 | 0.0204 | -0.1903 | 0.0817 |
| chr10 | 97445312 | 97445393 | TCTN3 | -5.0861 | 0.0639 | 2.0295 | 0.0123 | -0.1902 | 0.0419 |
| chr7 | 5232748 | 5232802 | WIPI2 | -4.2002 | 0.0923 | 1.7008 | 0.0391 | -0.1902 | 0.0598 |
| chr7 | 101843350 | 101843452 | CUX1 | 4.4706 | 0.0209 | 1.6947 | 0.2090 | 0.1895 | 0.0330 |
| chr12 | 22797144 | 22797349 | ETNK1 | 4.1415 | 0.0209 | -0.5019 | 0.5336 | 0.1891 | -0.0054 |
| chr2 | 128520635 | 128520733 | WDR33 | -5.9348 | 0.0527 | 15.9032 | 0.0000 | -0.1131 | 0.1886 |
| chr15 | 101886946 | 101887982 | PCSK6 | 8.5853 | 0.0000 | -3.2105 | 0.0236 | 0.1870 | -0.0333 |
| chr7 | 75042066 | 75042210 | NSUN5P1 | -6.6440 | 0.0290 | 2.4907 | 0.0116 | -0.1867 | 0.0489 |
| chr21 | 46221198 | 46221313 | UBE2G2 | 5.8902 | 0.0071 | -2.5387 | 0.0036 | 0.1858 | -0.0587 |
| chr11 | 126139039 | 126139310 | FOXRED1 | 4.9673 | 0.0146 | -1.8876 | 0.0422 | 0.1852 | -0.0494 |
| chr2 | 69372457 | 69373496 | ANTXR1 | 5.2796 | 0.0080 | -2.7474 | 0.0026 | 0.1848 | -0.0673 |
| chrX | 128718320 | 128718344 | OCRL | -3.4145 | 0.1347 | 3.1331 | 0.0025 | -0.1843 | 0.0738 |
| chr6 | 116895220 | 116895334 | RWDD1 | -8.4227 | 0.0114 | -0.1579 | 0.8866 | -0.1839 | 0.0050 |
| chr7 | 5780603 | 5781446 | RNF216 | -5.1167 | 0.0624 | 1.6818 | 0.0273 | -0.1839 | 0.0315 |
| chr9 | 131355261 | 131355321 | SPTAN1 | -5.7736 | 0.0474 | 7.1952 | 0.0000 | -0.1833 | 0.1006 |
| chr12 | 53565109 | 53565225 | CSAD | -2.1891 | 0.2574 | 2.6072 | 0.0177 | -0.1832 | 0.1441 |

| chrom | begin | end | name | Z.OE | fdr.OE | Z.KD | fdr.KD | ΔPSI_OE | ΔPSI_KD |
|---|---|---|---|---|---|---|---|---|---|
| chr6 | 133846152 | 133846253 | EYA4 | -4.7351 | 0.0738 | 2.1604 | 0.0151 | -0.1831 | 0.0413 |
| chr16 | 20835760 | 20835849 | LOC81691 | -3.6357 | 0.1207 | 4.5136 | 0.0002 | -0.1826 | 0.1534 |
| chr4 | 79366675 | 79366866 | FRAS1 | -2.9734 | 0.1698 | 1.7436 | 0.0300 | -0.1819 | 0.0563 |
| chr7 | 134620438 | 134620516 | CALD1 | 5.3125 | 0.0083 | 0.6723 | 0.1382 | 0.1814 | 0.0176 |
| chr16 | 20855255 | 20855348 | LOC81691 | -4.1835 | 0.0926 | 2.6463 | 0.0057 | -0.1812 | 0.0798 |
| chr19 | 1358586 | 1358699 | MUM1 | -3.6387 | 0.1206 | -3.9868 | 0.0002 | -0.1811 | -0.1031 |
| chr17 | 8132459 | 8132524 | CTC1 | 1.5918 | 0.2617 | -3.0922 | 0.0044 | 0.1070 | -0.1803 |
| chr11 | 3382972 | 3383119 | ZNF195 | -4.4499 | 0.0844 | 2.7402 | 0.0251 | -0.1802 | 0.0341 |
| chr3 | 48752747 | 48752960 | IP6K2 | 6.7518 | 0.0016 | -1.4648 | 0.0414 | 0.1797 | -0.0469 |
| chrX | 41414852 | 41414888 | CASK | -4.4865 | 0.0786 | 4.1305 | 0.0007 | -0.1797 | 0.1066 |
| chr3 | 184033276 | 184033333 | EIF4G1 | -8.8823 | 0.0113 | 4.0130 | 0.0025 | -0.1795 | 0.0407 |
| chr16 | 68381113 | 68381197 | PRMT7 | -5.8496 | 0.0492 | 1.4297 | 0.1244 | -0.1794 | 0.0170 |
| chr19 | 57953252 | 57953379 | ZNF749 | -1.1662 | 0.8830 | 4.0168 | 0.0007 | -0.1386 | 0.1791 |
| chr17 | 76202026 | 76202131 | AFMID | -6.8942 | 0.0252 | 0.6326 | 0.3297 | -0.1789 | 0.0154 |
| chr7 | 108161919 | 108161965 | PNPLA8 | -1.6667 | 0.3502 | 3.4392 | 0.0014 | -0.1043 | 0.1789 |
| chr6 | 135818325 | 135818387 | AHI1 | 1.7446 | 0.2153 | 3.7132 | 0.0014 | 0.1148 | 0.1789 |
| chr19 | 39838927 | 39839029 | SAMD4B | -5.3480 | 0.0572 | 1.1335 | 0.0476 | -0.1787 | 0.0600 |
| chr16 | 3335680 | 3335754 | ZNF263 | -4.8256 | 0.0736 | 7.3062 | 0.0000 | -0.1784 | 0.1654 |
| chr19 | 11456802 | 11456981 | TMEM205 | -5.7656 | 0.0530 | 16.8246 | 0.0000 | -0.1097 | 0.1781 |
| chr1 | 85724617 | 85724744 | C1orf52 | -7.2267 | 0.0211 | -3.9287 | 0.0002 | -0.1779 | -0.0629 |
| chr7 | 48141420 | 48141579 | UPP1 | -3.8602 | 0.1062 | 3.9344 | 0.0010 | -0.1779 | 0.1304 |
| chr11 | 59423428 | 59423518 | PATL1 | -5.4489 | 0.0599 | 2.1838 | 0.0113 | -0.1778 | 0.0337 |
| chr4 | 79366675 | 79367787 | FRAS1 | 2.9239 | 0.0795 | -1.9163 | 0.0159 | 0.1778 | -0.0638 |
| chr7 | 5780603 | 5781275 | RNF216 | 4.7371 | 0.0171 | -1.9189 | 0.0220 | 0.1777 | -0.0315 |
| chr1 | 26623409 | 26623486 | UBXN11 | -4.2418 | 0.0950 | 2.2220 | 0.0120 | -0.1771 | 0.0332 |
| chr16 | 703745 | 703803 | WDR90 | -3.1926 | 0.1540 | 2.4285 | 0.0076 | -0.1771 | 0.0587 |
| chr3 | 52185031 | 52185187 | POC1A | -1.9331 | 0.3497 | 2.9842 | 0.0024 | -0.1770 | 0.1261 |
| chrX | 47847923 | 47848017 | ZNF182 | -0.4238 | 1.0011 | 2.5631 | 0.0181 | -0.1624 | 0.1765 |
| chr17 | 42228328 | 42228412 | C17orf53 | -3.6919 | 0.1204 | 1.9829 | 0.0169 | -0.1761 | 0.0705 |
| chr19 | 47910608 | 47910823 | MEIS3 | 3.4356 | 0.0494 | -2.4937 | 0.0050 | 0.1758 | -0.1119 |
| chr7 | 148456395 | 148456446 | CUL1 | -7.0547 | 0.0271 | 0.7846 | 0.3202 | -0.1757 | 0.0134 |
| chr22 | 24042912 | 24043032 | LOC91316 | -2.5997 | 0.2087 | 2.4979 | 0.0118 | -0.1756 | 0.1075 |
| chr7 | 100033253 | 100033390 | C7orf47 | -8.2782 | 0.0136 | -0.1128 | 0.5641 | -0.1754 | -0.0015 |
| chr9 | 134385289 | 134385383 | POMT1 | -8.2884 | 0.0149 | 1.0566 | 0.3064 | -0.1749 | 0.0064 |
| chr6 | 33271731 | 33271766 | TAPBP | -3.2775 | 0.1479 | 2.2325 | 0.0097 | -0.1746 | 0.0604 |
| chr2 | 74601449 | 74601862 | DCTN1 | 3.6896 | 0.0569 | -2.9249 | 0.0017 | 0.1744 | -0.1341 |
| chr20 | 60704840 | 60705008 | LSM14B | -7.4420 | 0.0191 | 1.8372 | 0.0203 | -0.1741 | 0.0184 |
| chr4 | 1805418 | 1805563 | FGFR3 | 4.2907 | 0.0187 | -2.8434 | 0.0015 | 0.1734 | -0.0605 |
| chr14 | 56130672 | 56130759 | KTN1 | -6.7228 | 0.0270 | 5.4186 | 0.0000 | -0.1732 | 0.0627 |
| chr11 | 63991571 | 63991682 | TRPT1 | -5.9978 | 0.0414 | 0.6864 | 0.4037 | -0.1730 | 0.0147 |
| chr9 | 128283748 | 128284044 | MAPKAP1 | 6.6110 | 0.0017 | 0.2585 | 0.8374 | 0.1730 | 0.0000 |
| chr14 | 24911383 | 24911466 | SDR39U1 | -7.1359 | 0.0236 | 0.5130 | 0.1811 | -0.1730 | 0.0198 |
| chr7 | 97499089 | 97499125 | ASNS | -6.2886 | 0.0395 | 0.0022 | 0.9153 | -0.1721 | 0.0063 |
| chr2 | 136374237 | 136374327 | R3HDM1 | -1.7843 | 0.6463 | 3.1988 | 0.0028 | -0.1718 | 0.1114 |
| chr10 | 75294357 | 75294528 | USP54 | -2.6944 | 0.2048 | 1.8549 | 0.0284 | -0.1717 | 0.1299 |
| chrX | 102612010 | 102612089 | WBP5 | -6.6807 | 0.0274 | 0.4317 | 0.2129 | -0.1717 | 0.0103 |
| chr13 | 42795399 | 42795530 | DGKH | 2.9155 | 0.0823 | -3.5655 | 0.0002 | 0.1715 | -0.1450 |
| chr21 | 34954470 | 34954552 | DONSON | -7.9264 | 0.0184 | 3.1049 | 0.0017 | -0.1710 | 0.0323 |
| chr19 | 39880899 | 39880929 | PAF1 | -7.0711 | 0.0239 | 0.7237 | 0.4772 | -0.1705 | 0.0094 |
| chr9 | 123222849 | 123222945 | CDK5RAP2 | -4.9615 | 0.0725 | 1.8681 | 0.0217 | -0.1695 | 0.0435 |
| chrX | 100306805 | 100307105 | TRMT2B | -2.4053 | 0.2421 | -2.5451 | 0.0036 | -0.1695 | -0.1094 |
| chr11 | 6630301 | 6630387 | ILK | -5.6962 | 0.0489 | 0.4523 | 0.7650 | -0.1690 | 0.0061 |
| chr1 | 242012413 | 242012518 | EXO1 | -5.0809 | 0.0640 | 5.5081 | 0.0001 | -0.1678 | 0.0785 |
| chr3 | 12571260 | 12572512 | TSEN2 | -5.6461 | 0.0495 | 2.4568 | 0.1000 | -0.1673 | 0.0086 |
| chr9 | 129157853 | 129159912 | FAM125B | 4.5784 | 0.0168 | -0.6610 | 0.7625 | 0.1670 | -0.0045 |

| chrom | begin | end | name | Z.OE | fdr.OE | Z.KD | fdr.KD | ΔPSI_OE | ΔPSI_KD |
|---|---|---|---|---|---|---|---|---|---|
| chr2 | 32422412 | 32422461 | SLC30A6 | -2.4856 | 0.2180 | -1.5030 | 0.0404 | -0.1664 | -0.1064 |
| chr22 | 50687531 | 50687597 | HDAC10 | -3.2291 | 0.1492 | -1.7782 | 0.0203 | -0.1663 | -0.0913 |
| chr2 | 36787927 | 36788008 | FEZ2 | -2.9503 | 0.2158 | 2.2298 | 0.0224 | -0.1663 | 0.0720 |
| chr11 | 47521004 | 47521156 | CELF1 | 4.8377 | 0.0167 | 2.0698 | 0.0117 | 0.1661 | 0.0447 |
| chr17 | 7469033 | 7469081 | SENP3 | -6.8420 | 0.0270 | -0.4352 | 0.7868 | -0.1657 | -0.0061 |
| chr1 | 207941123 | 207941168 | CD46 | 4.1308 | 0.0220 | -7.7870 | 0.0000 | 0.1441 | -0.1651 |
| chr12 | 132466033 | 132466141 | EP400 | -3.3826 | 0.1404 | 3.1836 | 0.0021 | -0.1648 | 0.0798 |
| chr12 | 8852380 | 8853210 | RIMKLB | -2.8373 | 0.1854 | 6.4885 | 0.0000 | -0.1647 | 0.1317 |
| chr5 | 68590619 | 68590727 | CCDC125 | -3.3308 | 0.1444 | 1.9840 | 0.0178 | -0.1646 | 0.0607 |
| chrX | 100306772 | 100307105 | TRMT2B | 2.3589 | 0.1207 | 2.7449 | 0.0039 | 0.1645 | 0.1165 |
| chr8 | 143605598 | 143605665 | BAI1 | -2.4631 | 0.2219 | 1.3707 | 0.0483 | -0.1643 | 0.0470 |
| chr20 | 35401796 | 35402154 | DSN1 | 4.4532 | 0.0190 | -1.5393 | 0.0887 | 0.1635 | -0.0364 |
| chr1 | 114940561 | 114940612 | TRIM33 | -4.3542 | 0.0850 | 4.6099 | 0.0004 | -0.1628 | 0.1183 |
| chr5 | 179674438 | 179674510 | MAPK9 | -8.2584 | 0.0146 | 8.3890 | 0.0000 | -0.1616 | 0.0777 |
| chr2 | 220422064 | 220422340 | OBSL1 | -2.1961 | 0.2636 | 1.9677 | 0.0190 | -0.1612 | 0.0921 |
| chr10 | 51338276 | 51338363 | LOC728407 | -2.0551 | 0.2819 | 1.9466 | 0.0445 | -0.1611 | 0.0944 |
| chr7 | 48139266 | 48139384 | UPP1 | -1.6466 | 0.7180 | 3.4340 | 0.0053 | -0.1175 | 0.1608 |
| chr19 | 46119718 | 46119816 | EML2 | -3.8092 | 0.1116 | 2.1258 | 0.0159 | -0.1607 | 0.0338 |
| chr3 | 52232687 | 52232864 | ALAS1 | -4.2212 | 0.1080 | 6.0948 | 0.0000 | -0.1603 | 0.1301 |
| chr1 | 207963597 | 207963690 | CD46 | -4.4323 | 0.0828 | 15.7557 | 0.0000 | -0.1012 | 0.1601 |
| chr17 | 7469033 | 7469081 | SENP3-EIF4A1 | -6.6223 | 0.0301 | -0.4064 | 0.7181 | -0.1600 | -0.0060 |
| chr5 | 179673027 | 179674510 | MAPK9 | 8.1978 | 0.0000 | -8.3640 | 0.0000 | 0.1599 | -0.0775 |
| chrX | 117162386 | 117162460 | KLHL13 | 2.8578 | 0.1099 | 2.1429 | 0.0137 | 0.1598 | 0.1086 |
| chr2 | 27997290 | 27997397 | MRPL33 | -6.1755 | 0.0379 | 2.0285 | 0.0379 | -0.1594 | 0.0335 |
| chr17 | 17083920 | 17083983 | MPRIP | -6.2333 | 0.0382 | 11.7847 | 0.0000 | -0.1594 | 0.1470 |
| chr3 | 15046063 | 15046120 | NR2C2 | -2.4380 | 0.2311 | 1.9573 | 0.0275 | -0.1593 | 0.1084 |
| chr3 | 49759663 | 49759791 | GMPPB | -5.2092 | 0.0684 | 1.6795 | 0.0406 | -0.1590 | 0.0200 |
| chr22 | 17630431 | 17630635 | CECR5 | -8.0579 | 0.0174 | 2.3675 | 0.0070 | -0.1586 | 0.0200 |
| chr5 | 68667280 | 68667384 | RAD17 | -2.0566 | 0.3948 | 2.5635 | 0.0063 | -0.1586 | 0.1455 |
| chr12 | 4716492 | 4716553 | DYRK4 | -4.0373 | 0.0989 | 4.1275 | 0.0005 | -0.1583 | 0.0887 |
| chr1 | 228328824 | 228328989 | GUK1 | -8.1703 | 0.0154 | -5.1819 | 0.0000 | -0.1577 | -0.0632 |
| chr20 | 61557790 | 61557903 | DIDO1 | 3.4766 | 0.0494 | -0.3847 | 0.6453 | 0.1573 | -0.0037 |
| chr7 | 99159510 | 99159596 | ZNF655 | -2.5683 | 0.2156 | 4.9771 | 0.0001 | -0.1120 | 0.1571 |
| chr19 | 35996840 | 35996888 | DMKN | -4.7327 | 0.0724 | 1.6385 | 0.0384 | -0.1568 | 0.0267 |
| chr14 | 64682003 | 64682072 | SYNE2 | -2.6195 | 0.2054 | 5.6444 | 0.0000 | -0.1328 | 0.1564 |
| chr3 | 78696778 | 78696805 | ROBO1 | -1.3183 | 0.8314 | -1.8262 | 0.0218 | -0.1563 | -0.0757 |
| chr3 | 12944272 | 12944322 | IQSEC1 | -2.8655 | 0.1825 | 2.0574 | 0.0301 | -0.1556 | 0.0342 |
| chr20 | 8782702 | 8782820 | PLCB1 | -2.2210 | 0.2880 | -2.2500 | 0.0060 | -0.1556 | -0.0903 |
| chr6 | 33271409 | 33271766 | TAPBP | 2.8616 | 0.0826 | -3.2520 | 0.0009 | 0.1545 | -0.0830 |
| chr7 | 122076413 | 122076434 | CADPS2 | -1.7952 | 0.3193 | 3.1400 | 0.0025 | -0.1229 | 0.1544 |
| chr9 | 112918598 | 112918777 | PALM2-AKAP2 | 3.4626 | 0.0487 | -2.8873 | 0.0075 | 0.1544 | -0.0678 |
| chr5 | 176520138 | 176520332 | FGFR4 | -3.2214 | 0.1607 | -2.0249 | 0.0163 | -0.1540 | -0.0681 |
| chr2 | 178128130 | 178128617 | NFE2L2 | 3.7325 | 0.0365 | 0.2861 | 1.0299 | 0.1539 | -0.0079 |
| chr11 | 47586981 | 47587348 | PTPMT1 | -6.6763 | 0.0290 | 1.1187 | 0.1300 | -0.1539 | 0.0140 |
| chr16 | 77769724 | 77769883 | NUDT7 | -2.6672 | 0.5894 | -1.5325 | 0.0499 | -0.1534 | -0.0865 |
| chr2 | 74759745 | 74759841 | HTRA2 | -5.9850 | 0.0420 | 0.4563 | 0.9519 | -0.1534 | 0.0003 |
| chr9 | 112918598 | 112918777 | AKAP2 | 3.4378 | 0.0496 | -2.8923 | 0.0075 | 0.1533 | -0.0692 |
| chr14 | 31398406 | 31398517 | STRN3 | 3.9470 | 0.0262 | -1.4147 | 0.0677 | 0.1533 | -0.0236 |
| chr15 | 43857064 | 43857190 | PPIP5K1 | -4.2310 | 0.0970 | 2.8071 | 0.0032 | -0.1526 | 0.0527 |
| chr12 | 57682791 | 57682823 | R3HDM2 | -2.4817 | 0.2257 | 2.7394 | 0.0101 | -0.1520 | 0.0952 |
| chr12 | 2974520 | 2974565 | FOXM1 | -4.8956 | 0.0681 | 8.7410 | 0.0000 | -0.1468 | 0.1518 |
| chr15 | 42550135 | 42551188 | TMEM87A | 3.6449 | 0.0402 | -2.8281 | 0.0034 | 0.1514 | -0.0805 |
| chr3 | 9874787 | 9874929 | TTLL3 | 4.1146 | 0.0216 | 0.7862 | 0.3512 | 0.1509 | 0.0240 |
| chr2 | 55252221 | 55254621 | RTN4 | 6.5111 | 0.0019 | -1.0871 | 0.0537 | 0.1509 | -0.0247 |

| chrom | begin | end | name | Z.OE | fdr.OE | Z.KD | fdr.KD | ΔPSI_OE | ΔPSI_KD |
|---|---|---|---|---|---|---|---|---|---|
| chr1 | 154186368 | 154186422 | C1orf43 | -8.6265 | 0.0108 | 2.1928 | 0.0362 | -0.1508 | 0.0196 |
| chr19 | 35988548 | 35988583 | DMKN | -5.3006 | 0.0583 | -2.6815 | 0.0079 | -0.1502 | -0.0704 |
| chr20 | 35402064 | 35402230 | DSN1 | -4.9255 | 0.0677 | 3.4017 | 0.0013 | -0.1499 | 0.0547 |
| chr14 | 105707601 | 105707751 | BRF1 | -3.8370 | 0.1129 | 1.4303 | 0.0440 | -0.1495 | 0.0183 |
| chr1 | 935071 | 935167 | HES4 | -9.6842 | 0.0064 | -0.4475 | 0.3963 | -0.1494 | -0.0037 |
| chr12 | 121840544 | 121840610 | RNF34 | -6.0884 | 0.0418 | 6.7912 | 0.0000 | -0.1488 | 0.0976 |
| chr9 | 130494842 | 130494970 | TOR2A | -5.5734 | 0.0531 | -3.8499 | 0.0007 | -0.1484 | -0.0729 |
| chr3 | 128598332 | 128598684 | ACAD9 | 3.6805 | 0.0398 | -0.2839 | 0.2692 | 0.1475 | -0.0253 |
| chr22 | 19462992 | 19463125 | UFD1L | -8.5930 | 0.0127 | 3.1010 | 0.0019 | -0.1473 | 0.0341 |
| chr4 | 185621973 | 185622035 | MLF1IP | -3.9458 | 0.1109 | 2.5545 | 0.0052 | -0.1471 | 0.0370 |
| chr19 | 55967002 | 55967212 | ISOC2 | -7.6161 | 0.0212 | -1.7923 | 0.0314 | -0.1470 | -0.0172 |
| chr19 | 47910608 | 47910685 | MEIS3 | -2.8410 | 0.1966 | 2.3008 | 0.0267 | -0.1468 | 0.0893 |
| chr17 | 60601596 | 60601692 | TLK2 | -2.7535 | 0.1918 | 5.1636 | 0.0000 | -0.1235 | 0.1466 |
| chr12 | 50481145 | 50481268 | SMARCD1 | -6.5842 | 0.0347 | 2.7234 | 0.0148 | -0.1464 | 0.0367 |
| chr8 | 93933730 | 93933888 | C8orf83 | 1.5758 | 0.2339 | -2.0364 | 0.0294 | 0.1464 | -0.1118 |
| chr1 | 29386933 | 29386996 | EPB41 | -4.7742 | 0.0726 | 2.2379 | 0.0319 | -0.1462 | 0.0292 |
| chr5 | 137292165 | 137292231 | FAM13B | -2.6301 | 0.2158 | 2.8984 | 0.0090 | -0.1461 | 0.0720 |
| chr2 | 128492953 | 128495628 | WDR33 | 4.9544 | 0.0106 | -12.4253 | 0.0000 | 0.1111 | -0.1460 |
| chr5 | 96064856 | 96064913 | CAST | -3.9861 | 0.1107 | 4.7348 | 0.0002 | -0.1457 | 0.0871 |
| chr14 | 31388171 | 31388312 | STRN3 | 3.8526 | 0.0363 | -1.8173 | 0.0457 | 0.1457 | -0.0443 |
| chr12 | 133438918 | 133439011 | CHFR | -2.5395 | 0.2143 | 2.1991 | 0.0096 | -0.1455 | 0.0616 |
| chr3 | 105270987 | 105271026 | ALCAM | -2.8217 | 0.1866 | 2.0082 | 0.0137 | -0.1450 | 0.0671 |
| chr9 | 4726082 | 4726227 | AK3 | -4.5682 | 0.0939 | -1.8238 | 0.0228 | -0.1449 | -0.0515 |
| chr12 | 44165022 | 44165168 | IRAK4 | -2.1972 | 0.2965 | 3.4633 | 0.0049 | -0.1199 | 0.1447 |
| chr2 | 228217229 | 228217289 | MFF | -7.1310 | 0.0215 | -3.4630 | 0.0003 | -0.1444 | -0.0533 |
| chr5 | 180660412 | 180660435 | TRIM41 | -1.5408 | 0.3739 | 3.1227 | 0.0114 | -0.1005 | 0.1442 |
| chr15 | 48444430 | 48444481 | MYEF2 | -3.6435 | 0.1181 | 2.9178 | 0.0056 | -0.1434 | 0.0729 |
| chr12 | 56822332 | 56822436 | TIMELESS | -6.2841 | 0.0352 | 0.2266 | 0.9711 | -0.1432 | 0.0021 |
| chr6 | 30709390 | 30709481 | FLOT1 | -5.6896 | 0.0490 | -1.6914 | 0.0239 | -0.1432 | -0.0356 |
| chr1 | 40029507 | 40029594 | PABPC4 | -8.3496 | 0.0141 | 1.7519 | 0.1140 | -0.1430 | 0.0043 |
| chr10 | 27044583 | 27044670 | ABI1 | -5.6327 | 0.0501 | 2.9140 | 0.0049 | -0.1428 | 0.0468 |
| chr9 | 134385289 | 134385449 | POMT1 | 6.9043 | 0.0014 | -0.3388 | 0.6271 | 0.1428 | -0.0020 |
| chrX | 17762190 | 17762339 | SCML1 | -7.3775 | 0.0238 | 13.4252 | 0.0000 | -0.1427 | 0.1340 |
| chr22 | 50688855 | 50688952 | HDAC10 | -3.7029 | 0.1447 | -2.8011 | 0.0069 | -0.1426 | -0.0861 |
| chr10 | 89267589 | 89267995 | MINPP1 | 2.8867 | 0.0809 | -1.9214 | 0.0345 | 0.1425 | -0.0519 |
| chrX | 13781863 | 13781974 | OFD1 | -3.5227 | 0.1354 | 3.4964 | 0.0038 | -0.1424 | 0.0610 |
| chr1 | 155224190 | 155224247 | FAM189B | -6.3791 | 0.0382 | -1.0902 | 0.0919 | -0.1416 | -0.0028 |
| chr1 | 76194085 | 76194173 | ACADM | -5.5549 | 0.0529 | 2.1105 | 0.0115 | -0.1415 | 0.0326 |
| chr3 | 52185031 | 52185116 | POC1A | 1.2655 | 0.3652 | -3.0911 | 0.0008 | 0.1159 | -0.1413 |
| chr12 | 32891197 | 32891230 | DNM1L | -2.9876 | 0.1702 | 6.0078 | 0.0000 | -0.1165 | 0.1410 |
| chr12 | 50419180 | 50419307 | RACGAP1 | 5.1733 | 0.0093 | 0.4467 | 0.6134 | 0.1408 | -0.0099 |
| chr5 | 172659106 | 172660212 | NKX2-5 | 4.0320 | 0.0231 | -2.1547 | 0.0313 | 0.1407 | -0.0480 |
| chr7 | 65226632 | 65226735 | CCT6P1 | -2.9468 | 0.1752 | 2.3253 | 0.0084 | -0.1398 | 0.0662 |
| chr9 | 134369791 | 134369873 | PRRC2B | -6.7511 | 0.0273 | 6.2828 | 0.0000 | -0.1397 | 0.0517 |
| chr15 | 102191898 | 102191976 | TM2D3 | -6.3417 | 0.0383 | 1.2571 | 0.0638 | -0.1394 | 0.0191 |
| chrX | 123155216 | 123155281 | STAG2 | -3.8823 | 0.1058 | 4.1799 | 0.0004 | -0.1387 | 0.0837 |
| chr3 | 121438492 | 121438600 | GOLGB1 | -1.7048 | 0.7183 | 3.1190 | 0.0017 | -0.1386 | 0.1341 |
| chr19 | 5218797 | 5218809 | PTPRS | -3.3524 | 0.1627 | 4.0815 | 0.0007 | -0.1385 | 0.1329 |
| chr16 | 15141853 | 15141956 | NTAN1 | -4.1715 | 0.1049 | 2.2882 | 0.0121 | -0.1382 | 0.0518 |
| chr11 | 3068982 | 3069231 | CARS | 4.4945 | 0.0221 | -2.0184 | 0.0285 | 0.1379 | -0.0595 |
| chr11 | 47586981 | 47587538 | PTPMT1 | 6.1186 | 0.0036 | -0.7343 | 0.1778 | 0.1378 | -0.0099 |
| chrX | 23752457 | 23752484 | ACOT9 | -2.2955 | 0.2468 | 1.6895 | 0.0343 | -0.1378 | 0.1219 |
| chr11 | 47587457 | 47587538 | PTPMT1 | -6.0618 | 0.0395 | 0.5090 | 0.4892 | -0.1375 | 0.0066 |
| chr8 | 130916744 | 130916831 | FAM49B | -2.5927 | 0.2114 | -1.4343 | 0.0433 | -0.1367 | -0.0404 |
| chr1 | 28887624 | 28887772 | TRNAU1AP | 2.8885 | 0.0816 | -3.7672 | 0.0019 | 0.1361 | -0.0961 |

| chrom | begin | end | name | Z.OE | fdr.OE | Z.KD | fdr.KD | ΔPSI_OE | ΔPSI_KD |
|---|---|---|---|---|---|---|---|---|---|
| chr1 | 148574736 | 148574987 | NBPF15 | -3.0513 | 0.1642 | -2.3143 | 0.0092 | -0.1360 | -0.0420 |
| chr1 | 228296655 | 228296722 | MRPL55 | -5.7446 | 0.0490 | -0.6823 | 0.3131 | -0.1352 | -0.0082 |
| chr18 | 34238037 | 34238151 | FHOD3 | -2.6343 | 0.2315 | 2.8178 | 0.0051 | -0.1351 | 0.0690 |
| chr19 | 54964724 | 54964835 | LENG8 | -6.6662 | 0.0272 | 2.0401 | 0.0142 | -0.1349 | 0.0173 |
| chr12 | 39711874 | 39712003 | KIF21A | -2.5696 | 0.2155 | 2.8832 | 0.0051 | -0.1348 | 0.0539 |
| chr11 | 124496368 | 124496505 | TBRG1 | -2.5595 | 0.2210 | 2.7761 | 0.0106 | -0.1348 | 0.0741 |
| chr22 | 31644347 | 31644755 | LIMK2 | 2.9810 | 0.0767 | -2.5479 | 0.0166 | 0.1347 | -0.0681 |
| chr22 | 28250841 | 28250927 | PITPNB | -7.3787 | 0.0203 | 3.9369 | 0.0008 | -0.1346 | 0.0390 |
| chr19 | 50315507 | 50315592 | FUZ | -5.1135 | 0.0625 | 3.0676 | 0.0021 | -0.1341 | 0.0460 |
| chr3 | 56667071 | 56667871 | C3orf63 | 4.5710 | 0.0198 | -0.7428 | 0.4155 | 0.1338 | -0.0071 |
| chr1 | 155223874 | 155223985 | FAM189B | -6.7053 | 0.0341 | -2.5315 | 0.0063 | -0.1335 | -0.0287 |
| chr17 | 1012173 | 1012324 | ABR | 3.0319 | 0.0751 | 1.1195 | 0.0446 | 0.1332 | 0.0468 |
| chr1 | 935245 | 935552 | HES4 | -7.4239 | 0.0203 | 0.1332 | 0.7622 | -0.1332 | 0.0017 |
| chr21 | 47711247 | 47711376 | YBEY | -6.3618 | 0.0349 | 0.6397 | 0.4254 | -0.1326 | 0.0084 |
| chr6 | 90321990 | 90322089 | ANKRD6 | -2.8526 | 0.1843 | 2.2862 | 0.0139 | -0.1326 | 0.0908 |
| chr12 | 44132112 | 44132194 | PUS7L | -2.9562 | 0.1969 | 1.4750 | 0.0399 | -0.1322 | 0.0325 |
| chr3 | 134277991 | 134278271 | CEP63 | -1.9690 | 0.3195 | 2.5881 | 0.0096 | -0.1321 | 0.1017 |
| chr10 | 3147306 | 3147351 | PFKP | -6.3437 | 0.0381 | 0.7801 | 0.3140 | -0.1320 | 0.0071 |
| chr11 | 34119244 | 34119308 | CAPRIN1 | -7.9312 | 0.0154 | 6.6960 | 0.0000 | -0.1317 | 0.0440 |
| chr21 | 47965793 | 47965874 | DIP2A | -3.7374 | 0.1159 | 1.4508 | 0.0413 | -0.1317 | 0.0470 |
| chr22 | 51208332 | 51208444 | RABL2B | -3.9132 | 0.1194 | 2.1128 | 0.0128 | -0.1316 | 0.0410 |
| chr3 | 14489089 | 14489324 | SLC6A6 | -4.1266 | 0.0955 | 2.6774 | 0.0040 | -0.1315 | 0.0345 |
| chr17 | 40717000 | 40717065 | COASY | -5.9855 | 0.0488 | 0.0445 | 1.2414 | -0.1302 | -0.0007 |
| chr14 | 102384167 | 102384284 | PPP2R5C | -3.8901 | 0.1068 | -1.6904 | 0.0222 | -0.1301 | -0.0317 |
| chr14 | 52493918 | 52494062 | NID2 | -3.5898 | 0.1207 | 2.4477 | 0.0071 | -0.1295 | 0.0584 |
| chrX | 44921891 | 44921993 | KDM6A | -3.0044 | 0.2055 | 4.7734 | 0.0001 | -0.1293 | 0.1259 |
| chr20 | 62152636 | 62152716 | PPDPF | -7.3452 | 0.0212 | -0.1995 | 0.9851 | -0.1290 | 0.0022 |
| chr15 | 84872928 | 84873083 | LOC388152 | -5.5811 | 0.0525 | -1.9932 | 0.0157 | -0.1289 | -0.0213 |
| chr19 | 39998891 | 39999121 | DLL3 | -6.0124 | 0.0412 | 3.6832 | 0.0012 | -0.1286 | 0.0527 |
| chr3 | 112736294 | 112736449 | C3orf17 | -3.8000 | 0.1116 | 1.6210 | 0.0289 | -0.1284 | 0.0283 |
| chr21 | 47965793 | 47966219 | DIP2A | 3.6536 | 0.0418 | -1.4173 | 0.0283 | 0.1281 | -0.0409 |
| chr12 | 2970464 | 2970578 | FOXM1 | -3.7386 | 0.1156 | 4.4991 | 0.0005 | -0.1280 | 0.0758 |
| chr22 | 42564614 | 42564742 | TCF20 | -3.0989 | 0.1702 | 2.5845 | 0.0047 | -0.1279 | 0.0805 |
| chr15 | 93426814 | 93427008 | LOC100507217 | -4.0366 | 0.1056 | -2.5073 | 0.0033 | -0.1276 | -0.0467 |
| chr8 | 103862226 | 103862372 | AZIN1 | 4.9880 | 0.0102 | -6.0522 | 0.0000 | 0.1275 | -0.0697 |
| chr20 | 32661624 | 32661672 | RALY | -6.1625 | 0.0394 | 1.9795 | 0.0324 | -0.1274 | 0.0332 |
| chr12 | 44152088 | 44152561 | PUS7L | 1.8548 | 0.1973 | -2.6122 | 0.0097 | 0.1272 | -0.1177 |
| chr8 | 62575376 | 62578165 | ASPH | 3.8679 | 0.0323 | -3.0853 | 0.0147 | 0.1271 | -0.0292 |
| chr16 | 3336022 | 3336149 | ZNF263 | -3.7687 | 0.1117 | 9.0981 | 0.0000 | -0.1122 | 0.1270 |
| chr12 | 988738 | 989197 | WNK1 | 4.6475 | 0.0165 | 13.2922 | 0.0000 | 0.1077 | 0.1267 |
| chr1 | 206905919 | 206907626 | MAPKAPK2 | 4.4951 | 0.0164 | 1.3118 | 0.0760 | 0.1266 | 0.0144 |
| chr5 | 92877577 | 92879730 | FLJ42709 | 2.7028 | 0.0936 | 2.6714 | 0.0113 | 0.1266 | 0.0840 |
| chr3 | 44379943 | 44380326 | C3orf23 | 1.8096 | 0.4332 | 2.6001 | 0.0057 | 0.1265 | 0.1101 |
| chr19 | 35998359 | 35998413 | DMKN | -3.9384 | 0.1060 | 2.9457 | 0.0091 | -0.1264 | 0.0703 |
| chr11 | 34119244 | 34120607 | CAPRIN1 | 7.5685 | 0.0008 | -6.6937 | 0.0000 | 0.1259 | -0.0436 |
| chr17 | 34842778 | 34842810 | ZNHIT3 | -5.2442 | 0.0585 | 2.5155 | 0.0128 | -0.1259 | 0.0319 |
| chr1 | 110167924 | 110168055 | AMPD2 | -3.8718 | 0.1119 | 1.8676 | 0.0191 | -0.1257 | 0.0311 |
| chr19 | 41942296 | 41942377 | ATP5SL | -5.4764 | 0.0554 | 4.6442 | 0.0003 | -0.1256 | 0.0593 |
| chr1 | 32794668 | 32794761 | HDAC1 | -7.3410 | 0.0211 | 1.9455 | 0.0152 | -0.1251 | 0.0141 |
| chr9 | 112184997 | 112185132 | PTPN3 | -2.6179 | 0.2110 | 1.6350 | 0.0391 | -0.1249 | 0.0493 |
| chr2 | 209169569 | 209170271 | PIKFYVE | 3.0321 | 0.0746 | -2.0304 | 0.0318 | 0.1247 | -0.0536 |
| chr17 | 55709151 | 55710544 | MSI2 | 5.6502 | 0.0069 | -6.2648 | 0.0000 | 0.1246 | -0.0745 |
| chr9 | 79999500 | 80000106 | VPS13A | 4.2464 | 0.0195 | -3.4967 | 0.0016 | 0.1246 | -0.0618 |
| chr15 | 80199970 | 80200048 | ST20 | -2.3026 | 0.2411 | 1.5573 | 0.0393 | -0.1242 | 0.0645 |

| chrom | begin | end | name | Z.OE | fdr.OE | Z.KD | fdr.KD | ΔPSI_OE | ΔPSI_KD |
|---|---|---|---|---|---|---|---|---|---|
| chr11 | 47591251 | 47591443 | PTPMT1 | -6.7977 | 0.0294 | 1.8724 | 0.1757 | -0.1241 | 0.0100 |
| chr17 | 17046869 | 17046983 | MPRIP | -4.8571 | 0.0771 | 2.8987 | 0.0032 | -0.1238 | 0.0312 |
| chr21 | 34614190 | 34614282 | IFNAR2 | -1.8806 | 0.3072 | 2.4770 | 0.0082 | -0.1237 | 0.0810 |
| chr11 | 43913590 | 43913679 | ALKBH3 | -3.9172 | 0.1050 | 2.3192 | 0.0352 | -0.1236 | 0.0560 |
| chr22 | 30812222 | 30812964 | SEC14L2 | 2.8106 | 0.0829 | -2.2164 | 0.0084 | 0.1230 | -0.0625 |
| chr19 | 39998469 | 39998554 | DLL3 | -5.7849 | 0.0473 | 3.4393 | 0.0060 | -0.1227 | 0.0549 |
| chr3 | 14489089 | 14489693 | SLC6A6 | 3.8207 | 0.0334 | -2.9856 | 0.0014 | 0.1221 | -0.0330 |
| chrX | 47039278 | 47039439 | RBM10 | 10.7150 | 0.0000 | 0.5083 | 0.5480 | 0.1220 | 0.0031 |
| chr13 | 103422361 | 103422436 | C13orf27 | -4.2678 | 0.0884 | 2.1597 | 0.0129 | -0.1218 | 0.0431 |
| chr19 | 8548041 | 8548095 | HNRNPM | -8.3027 | 0.0147 | 5.0191 | 0.0001 | -0.1213 | 0.0418 |
| chr1 | 155223649 | 155223769 | FAM189B | -6.3922 | 0.0382 | -2.6283 | 0.0039 | -0.1212 | -0.0145 |
| chr2 | 272191 | 272305 | ACP1 | 6.1510 | 0.0037 | -4.7187 | 0.0000 | 0.1209 | -0.0627 |
| chr11 | 47657096 | 47657123 | MTCH2 | -3.6830 | 0.1203 | 1.7104 | 0.0266 | -0.1208 | 0.0409 |
| chr3 | 58117653 | 58117746 | FLNB | -2.8633 | 0.1919 | 2.4979 | 0.0095 | -0.1208 | 0.0538 |
| chr1 | 38262415 | 38262492 | MANEAL | -4.7794 | 0.0785 | 2.4709 | 0.0344 | -0.1207 | 0.0229 |
| chr12 | 56536618 | 56536717 | ESYT1 | -5.7821 | 0.0472 | 0.1655 | 1.0102 | -0.1206 | 0.0020 |
| chr14 | 59006788 | 59006854 | KIAA0586 | -1.8111 | 0.3195 | 2.1637 | 0.0113 | -0.1204 | 0.1133 |
| chr7 | 150945570 | 150945749 | SMARCD3 | -1.8444 | 0.3544 | -2.0904 | 0.0096 | -0.1202 | -0.0882 |
| chr14 | 23374814 | 23374868 | RBM23 | -5.5669 | 0.0584 | 2.5097 | 0.0051 | -0.1202 | 0.0316 |
| chr1 | 24125376 | 24125502 | GALE | -3.2981 | 0.1628 | -1.8625 | 0.0475 | -0.1201 | -0.0364 |
| chr12 | 44152503 | 44152562 | PUS7L | -1.3416 | 0.5482 | 2.8202 | 0.0026 | -0.1065 | 0.1191 |
| chr22 | 38155423 | 38155963 | TRIOBP | 4.2595 | 0.0216 | -5.4494 | 0.0000 | 0.1191 | -0.0639 |
| chrX | 148623563 | 148623611 | CXorf40A | 2.1967 | 0.1378 | -1.9886 | 0.0163 | 0.1190 | -0.1153 |
| chrX | 148623563 | 148623630 | CXorf40A | -2.1967 | 0.2639 | 1.9199 | 0.0264 | -0.1190 | 0.1153 |
| chr19 | 39998469 | 39999121 | DLL3 | 5.6231 | 0.0061 | -3.6309 | 0.0013 | 0.1188 | -0.0558 |
| chr9 | 134378288 | 134378700 | POMT1 | 3.3287 | 0.0542 | -2.9685 | 0.0023 | 0.1187 | -0.0586 |
| chrX | 128627016 | 128627052 | SMARCA1 | 2.3932 | 0.1236 | 3.9969 | 0.0008 | 0.1055 | 0.1186 |
| chr7 | 102389398 | 102390105 | FAM185A | 2.9542 | 0.0775 | -1.5136 | 0.0333 | 0.1185 | -0.0309 |
| chr2 | 112186885 | 112187197 | LOC541471 | 4.3459 | 0.0241 | -0.1539 | 1.0954 | 0.1183 | 0.0086 |
| chr1 | 113247721 | 113247790 | RHOC | -3.5719 | 0.1202 | 4.1213 | 0.0007 | -0.1182 | 0.0767 |
| chrX | 47039278 | 47039436 | RBM10 | -10.4015 | 0.0072 | -1.4730 | 0.1016 | -0.1181 | -0.0190 |
| chr22 | 51221466 | 51221714 | RABL2B | -3.6854 | 0.1310 | -1.8211 | 0.0231 | -0.1179 | -0.0319 |
| chr14 | 31050281 | 31050322 | G2E3 | 2.4958 | 0.1072 | -2.3792 | 0.0169 | 0.1178 | -0.0809 |
| chrX | 19372608 | 19372701 | PDHA1 | -7.3411 | 0.0217 | 0.4597 | 0.7798 | -0.1174 | 0.0025 |
| chr6 | 86248555 | 86248582 | SNX14 | -2.3132 | 0.3277 | 2.0075 | 0.0219 | -0.1172 | 0.0840 |
| chr22 | 19958738 | 19958858 | ARVCF | -1.8282 | 0.3161 | -1.9940 | 0.0125 | -0.1171 | -0.0696 |
| chr2 | 74900803 | 74900955 | SEMA4F | -1.7436 | 0.3297 | 1.7926 | 0.0420 | -0.1169 | 0.0622 |
| chr16 | 3335058 | 3335239 | ZNF263 | -3.6162 | 0.1189 | 7.2545 | 0.0000 | -0.1166 | 0.1151 |
| chr10 | 1089938 | 1090111 | IDI1 | -5.3256 | 0.0584 | 3.6177 | 0.0015 | -0.1165 | 0.0348 |
| chr3 | 47323629 | 47323875 | KIF9 | 2.8264 | 0.0842 | -1.4915 | 0.0425 | 0.1163 | -0.0470 |
| chr22 | 31492718 | 31492883 | SMTN | -3.6286 | 0.1196 | 3.9662 | 0.0007 | -0.1162 | 0.0737 |
| chr1 | 26623917 | 26623972 | UBXN11 | -2.8551 | 0.1874 | 2.1863 | 0.0137 | -0.1160 | 0.0380 |
| chr7 | 56141866 | 56141911 | SUMF2 | -3.9614 | 0.1092 | 2.0621 | 0.0382 | -0.1160 | 0.0259 |
| chr11 | 88053980 | 88059611 | CTSC | 4.4923 | 0.0177 | 0.8625 | 0.1660 | 0.1159 | 0.0183 |
| chr5 | 92880500 | 92880621 | FLJ42709 | 1.5743 | 0.2719 | 2.2684 | 0.0362 | 0.1020 | 0.1157 |
| chr18 | 77227449 | 77227582 | NFATC1 | -3.6826 | 0.1160 | 2.3553 | 0.0077 | -0.1157 | 0.0432 |
| chr6 | 111805946 | 111806064 | LOC643749 | 2.2364 | 0.1339 | -1.9525 | 0.0421 | 0.1153 | -0.0747 |
| chr12 | 3938075 | 3938196 | PARP11 | 1.1966 | 0.3263 | 2.5571 | 0.0129 | 0.1152 | 0.1152 |
| chr15 | 75198618 | 75198706 | C15orf17 | -4.1732 | 0.0947 | 2.0790 | 0.0164 | -0.1150 | 0.0262 |
| chr16 | 11794307 | 11794420 | TXNDC11 | -2.3991 | 0.2435 | -2.0548 | 0.0108 | -0.1146 | -0.0565 |
| chr16 | 586028 | 586142 | SOLH | -2.4571 | 0.2221 | 2.2265 | 0.0158 | -0.1137 | 0.0716 |
| chr1 | 24304400 | 24304763 | SRSF10 | 6.3204 | 0.0015 | -2.5388 | 0.0032 | 0.1137 | -0.0183 |
| chr14 | 60752341 | 60752459 | PPM1A | -5.6070 | 0.0530 | -1.7408 | 0.0148 | -0.1130 | -0.0298 |
| chr14 | 105181620 | 105181677 | INF2 | -2.5006 | 0.2201 | 2.1069 | 0.0282 | -0.1128 | 0.0403 |
| chr3 | 184033919 | 184034006 | EIF4G1 | -6.3954 | 0.0421 | -0.0249 | 0.5269 | -0.1123 | -0.0054 |

| chrom | begin | end | name | Z.OE | fdr.OE | Z.KD | fdr.KD | ΔPSI_OE | ΔPSI_KD |
|---|---|---|---|---|---|---|---|---|---|
| chr22 | 30812222 | 30812392 | SEC14L2 | -2.5845 | 0.2144 | 2.4075 | 0.0106 | -0.1123 | 0.0669 |
| chr11 | 85342188 | 85342360 | TMEM126B | 5.1975 | 0.0096 | -5.7825 | 0.0000 | 0.1121 | -0.0608 |
| chr6 | 131201283 | 131201346 | EPB41L2 | 4.5626 | 0.0168 | 0.1647 | 0.4728 | 0.1119 | 0.0092 |
| chr21 | 34955793 | 34955972 | DONSON | -5.8093 | 0.0491 | 2.6559 | 0.0049 | -0.1118 | 0.0211 |
| chr6 | 13604707 | 13605970 | SIRT5 | 3.0656 | 0.0731 | -4.8077 | 0.0000 | 0.1050 | -0.1115 |
| chr4 | 6988888 | 6989076 | TBC1D14 | 2.4947 | 0.1073 | -2.2226 | 0.0252 | 0.1115 | -0.0585 |
| chr16 | 3338453 | 3338570 | ZNF263 | -3.7849 | 0.1162 | 3.3946 | 0.0015 | -0.1111 | 0.0530 |
| chr10 | 46048559 | 46048652 | MARCH8 | -1.8944 | 0.3039 | 3.0348 | 0.0021 | -0.1107 | 0.0909 |
| chr8 | 48641494 | 48641609 | KIAA0146 | -4.2030 | 0.0928 | 1.6415 | 0.0319 | -0.1107 | 0.0245 |
| chr6 | 127607194 | 127607322 | RNF146 | -2.1554 | 0.2630 | 2.3981 | 0.0060 | -0.1105 | 0.0697 |
| chr1 | 21616856 | 21616982 | ECE1 | 2.5148 | 0.1027 | 2.1557 | 0.0098 | 0.1099 | 0.0530 |
| chr21 | 27369674 | 27369731 | APP | -6.2319 | 0.0380 | 6.6696 | 0.0000 | -0.1097 | 0.0608 |
| chrX | 48833332 | 48834847 | GRIPAP1 | 5.3045 | 0.0074 | 0.7881 | 0.2372 | 0.1097 | 0.0095 |
| chr5 | 79281393 | 79281482 | MTX3 | -1.9069 | 0.3264 | 4.1087 | 0.0047 | -0.1095 | 0.1043 |
| chr1 | 46871709 | 46871750 | FAAH | -1.6647 | 0.3760 | 1.7706 | 0.0446 | -0.1091 | 0.0858 |
| chr7 | 102389398 | 102389864 | FAM185A | -2.5333 | 0.2161 | 1.4339 | 0.0406 | -0.1086 | 0.0380 |
| chr18 | 77227449 | 77228177 | NFATC1 | 3.4213 | 0.0506 | -1.6732 | 0.0260 | 0.1086 | -0.0361 |
| chr12 | 6781515 | 6781698 | ZNF384 | -4.3212 | 0.0972 | 2.3387 | 0.0295 | -0.1085 | 0.0325 |
| chr4 | 54245239 | 54245284 | FIP1L1 | -1.7225 | 0.3393 | 1.9132 | 0.0391 | -0.1085 | 0.0723 |
| chr14 | 60752341 | 60755272 | PPM1A | 5.3966 | 0.0068 | 1.7329 | 0.0192 | 0.1084 | 0.0296 |
| chr16 | 16412407 | 16412591 | PKD1P1 | -3.1640 | 0.1526 | -3.6248 | 0.0002 | -0.1082 | -0.0459 |
| chr1 | 243305587 | 243305765 | CEP170 | 2.7431 | 0.0878 | -2.4589 | 0.0093 | 0.1076 | -0.0577 |
| chr7 | 135071821 | 135073646 | CNOT4 | 3.8171 | 0.0554 | -3.3732 | 0.0011 | 0.1075 | -0.0599 |
| chr7 | 39828080 | 39828203 | NCRNA00265 | -2.5187 | 0.2259 | 2.3510 | 0.0111 | -0.1073 | 0.1031 |
| chr20 | 47897439 | 47897501 | NCRNA00275 | -5.6880 | 0.0500 | 8.7690 | 0.0000 | -0.1067 | 0.0739 |
| chr1 | 160209486 | 160210160 | DCAF8 | -5.3414 | 0.0558 | 2.1319 | 0.0339 | -0.1067 | 0.0227 |
| chr8 | 54723723 | 54723777 | ATP6V1H | -3.1137 | 0.1685 | 2.2008 | 0.0089 | -0.1065 | 0.0672 |
| chr1 | 144951760 | 144952376 | PDE4DIP | -2.0062 | 0.3075 | -1.2205 | 0.0274 | -0.1064 | -0.0606 |
| chr19 | 35760705 | 35760906 | USF2 | -7.3880 | 0.0216 | -1.1546 | 0.1212 | -0.1063 | -0.0097 |
| chr22 | 40666125 | 40666284 | TNRC6B | -1.5242 | 0.3790 | 1.7241 | 0.0390 | -0.1061 | 0.0900 |
| chr19 | 9434901 | 9435080 | ZNF559 | 1.1313 | 0.4406 | -1.7721 | 0.0279 | 0.1058 | -0.0748 |
| chr12 | 57487189 | 57487381 | NAB2 | -1.9589 | 0.3069 | -2.3024 | 0.0225 | -0.1058 | -0.0970 |
| chr17 | 41247862 | 41247939 | BRCA1 | -2.4325 | 0.2365 | 1.6607 | 0.0288 | -0.1055 | 0.0405 |
| chr11 | 59564755 | 59564869 | STX3 | -2.6060 | 0.2242 | 1.6154 | 0.0383 | -0.1053 | 0.0300 |
| chr10 | 34661425 | 34661464 | PARD3 | -3.4639 | 0.1918 | 3.7843 | 0.0032 | -0.1052 | 0.1009 |
| chr9 | 139728171 | 139728794 | C9orf86 | 6.1000 | 0.0052 | -8.6469 | 0.0000 | 0.1050 | -0.0947 |
| chr7 | 23016311 | 23016427 | FAM126A | -2.9929 | 0.1779 | 1.6927 | 0.0242 | -0.1050 | 0.0280 |
| chr7 | 30540151 | 30540297 | GGCT | -5.2725 | 0.0583 | 2.3149 | 0.0182 | -0.1046 | 0.0294 |
| chr1 | 153631613 | 153631660 | SNAPIN | -4.1176 | 0.0971 | 2.5768 | 0.0063 | -0.1042 | 0.0290 |
| chr22 | 40797596 | 40797679 | SGSM3 | -3.6922 | 0.1333 | 2.3403 | 0.0070 | -0.1040 | 0.0394 |
| chr2 | 62065672 | 62065840 | FAM161A | -1.7493 | 0.3771 | 2.2846 | 0.0374 | -0.1039 | 0.0788 |
| chrX | 137792978 | 137793827 | FGF13 | 2.8699 | 0.0826 | -2.6443 | 0.0030 | 0.1037 | -0.0598 |
| chr7 | 151892991 | 151893096 | MLL3 | 1.4953 | 0.6420 | 1.8867 | 0.0266 | 0.1029 | 0.0483 |
| chr6 | 112020717 | 112020873 | FYN | -4.4230 | 0.0880 | -1.7471 | 0.0318 | -0.1027 | -0.0205 |
| chr17 | 52981068 | 52981153 | TOM1L1 | -3.5901 | 0.1271 | 2.9811 | 0.0034 | -0.1026 | 0.0380 |
| chr19 | 59056791 | 59056904 | TRIM28 | -7.5614 | 0.0215 | 0.1080 | 1.0248 | -0.1025 | 0.0007 |
| chr11 | 8933999 | 8934080 | C11orf17 | -2.8572 | 0.1866 | 2.2886 | 0.0147 | -0.1025 | 0.0541 |
| chr11 | 88061279 | 88061364 | CTSC | 4.1132 | 0.0220 | 1.2579 | 0.0690 | 0.1024 | 0.0227 |
| chr10 | 99502850 | 99502921 | ZFYVE27 | 2.7739 | 0.0844 | -1.8295 | 0.0427 | 0.1021 | -0.0554 |
| chr16 | 167299 | 167374 | NPRL3 | -3.6308 | 0.1190 | 1.9454 | 0.0325 | -0.1019 | 0.0180 |
| chr19 | 19144939 | 19145047 | ARMC6 | -2.8145 | 0.1863 | -1.4425 | 0.0405 | -0.1018 | -0.0348 |
| chr1 | 160209011 | 160210160 | DCAF8 | 5.0939 | 0.0091 | -2.1844 | 0.0287 | 0.1017 | -0.0234 |
| chrX | 17763575 | 17763659 | SCML1 | -4.8307 | 0.0686 | 7.9367 | 0.0000 | -0.1016 | 0.0879 |
| chr10 | 103874162 | 103874723 | LDB1 | 3.5755 | 0.0422 | 3.4937 | 0.0038 | 0.1016 | 0.0644 |

| chrom | begin | end | name | Z.OE | fdr.OE | Z.KD | fdr.KD | ΔPSI_OE | ΔPSI_KD |
|---|---|---|---|---|---|---|---|---|---|
| chr1 | 78187515 | 78187610 | USP33 | -2.6573 | 0.2111 | 3.5888 | 0.0009 | -0.1015 | 0.0646 |
| chr12 | 6660563 | 6660669 | IFFO1 | -2.5076 | 0.2161 | 3.7829 | 0.0011 | -0.1012 | 0.0859 |
| chr19 | 37826070 | 37826159 | HKR1 | 1.6863 | 0.2123 | 2.0595 | 0.0147 | 0.1012 | 0.0874 |
| chr11 | 118127952 | 118128028 | MPZL2 | -1.7197 | 0.3348 | 2.3595 | 0.0113 | -0.1010 | 0.0750 |
| chr1 | 24137225 | 24137289 | HMGCL | -2.2877 | 0.2418 | 2.1014 | 0.0336 | -0.1008 | 0.0727 |
| chr2 | 209169569 | 209169737 | PIKFYVE | -2.5643 | 0.2329 | 3.1303 | 0.0017 | -0.1008 | 0.0663 |
| chr12 | 58113881 | 58114046 | OS9 | -5.0767 | 0.0638 | 4.0785 | 0.0008 | -0.1006 | 0.0372 |
| chr7 | 101842081 | 101842147 | CUX1 | -1.9634 | 0.2917 | 3.2021 | 0.0121 | -0.1003 | 0.0725 |
| chr11 | 85340175 | 85340306 | TMEM126B | -1.7239 | 0.3542 | 17.5847 | 0.0000 | -0.0411 | 0.2853 |
| chr13 | 114103313 | 114103457 | ADPRHL1 | 0.5053 | 1.0317 | -3.9708 | 0.0007 | 0.0518 | -0.2527 |
| chr19 | 40871459 | 40871492 | PLD3 | -0.2323 | 1.0767 | 13.4431 | 0.0000 | -0.0074 | 0.2519 |
| chr3 | 171404474 | 171404588 | PLD1 | 0.1888 | 0.9918 | 3.6065 | 0.0099 | 0.0494 | 0.2391 |
| chr7 | 73604576 | 73604636 | EIF4H | -3.9281 | 0.1111 | 24.7426 | 0.0000 | -0.0694 | 0.2214 |
| chr5 | 135271311 | 135271413 | FBXL21 | 0.1907 | 0.9917 | 4.1669 | 0.0025 | 0.0554 | 0.2011 |
| chr3 | 145795648 | 145795711 | PLOD2 | 1.0265 | 0.5852 | 8.6605 | 0.0000 | 0.0439 | 0.1925 |
| chr15 | 86201767 | 86201821 | AKAP13 | -0.6997 | 0.9782 | 3.3070 | 0.0058 | -0.0494 | 0.1898 |
| chr12 | 123687796 | 123687922 | MPHOSPH9 | -2.4663 | 0.2630 | 9.8696 | 0.0000 | -0.0883 | 0.1840 |
| chr11 | 47310518 | 47310578 | MADD | -1.1064 | 0.5602 | 5.4861 | 0.0000 | -0.0515 | 0.1825 |
| chr12 | 133770013 | 133770119 | ZNF268 | -1.4623 | 0.7526 | 4.7925 | 0.0004 | -0.0517 | 0.1817 |
| chr1 | 10386168 | 10386417 | KIF1B | -0.6025 | 1.1034 | 6.4515 | 0.0000 | -0.0160 | 0.1792 |
| chr6 | 107351228 | 107351311 | C6orf203 | 0.7966 | 0.9281 | 2.7393 | 0.0084 | 0.0479 | 0.1760 |
| chr21 | 38792600 | 38792686 | DYRK1A | -1.3265 | 0.8306 | 3.9236 | 0.0007 | -0.0613 | 0.1751 |
| chr22 | 18310409 | 18310547 | MICAL3 | -0.7616 | 0.9110 | 3.5580 | 0.0009 | -0.0698 | 0.1700 |
| chr2 | 85582198 | 85582293 | ELMOD3 | -0.5383 | 1.0671 | -2.7293 | 0.0024 | -0.0237 | -0.1681 |
| chr16 | 24804793 | 24804970 | TNRC6A | -0.8662 | 0.9806 | 11.1789 | 0.0000 | -0.0141 | 0.1665 |
| chr14 | 51193950 | 51194469 | NIN | -0.4320 | 1.0298 | 4.8136 | 0.0002 | -0.0083 | 0.1654 |
| chr12 | 56606779 | 56606922 | RNF41 | -2.8410 | 0.1849 | 8.8061 | 0.0000 | -0.0911 | 0.1603 |
| chr2 | 228194321 | 228194499 | MFF | -3.2737 | 0.1540 | 9.4094 | 0.0000 | -0.0779 | 0.1579 |
| chr8 | 67478298 | 67478478 | MYBL1 | -0.5918 | 0.8949 | 3.6712 | 0.0011 | -0.0321 | 0.1565 |
| chr8 | 59571753 | 59571966 | NSMAF | 0.4961 | 0.5508 | -1.6322 | 0.0269 | 0.0928 | -0.1542 |
| chr8 | 145024351 | 145025044 | PLEC | 0.7098 | 0.9306 | 2.0590 | 0.0413 | -0.0452 | 0.1529 |
| chr16 | 67289655 | 67289833 | SLC9A5 | -0.6260 | 1.0076 | -1.9143 | 0.0370 | 0.0775 | -0.1524 |
| chr2 | 179188903 | 179188996 | OSBPL6 | -1.3592 | 0.4383 | 4.3916 | 0.0003 | -0.0990 | 0.1521 |
| chr9 | 98269218 | 98269481 | PTCH1 | 0.1635 | 0.9925 | -2.6284 | 0.0137 | 0.0815 | -0.1496 |
| chr10 | 77163513 | 77163815 | NCRNA00245 | -0.6228 | 1.0532 | -2.3607 | 0.0227 | -0.0364 | -0.1471 |
| chr3 | 129210983 | 129211037 | IFT122 | -0.1952 | 0.9534 | 3.1484 | 0.0017 | -0.0087 | 0.1465 |
| chr10 | 101510125 | 101510153 | CUTC | -1.4986 | 0.4278 | 7.0413 | 0.0000 | -0.0500 | 0.1462 |
| chr8 | 99963828 | 99964326 | OSR2 | 0.7877 | 0.8193 | 2.4247 | 0.0200 | 0.0321 | 0.1459 |
| chr10 | 111985761 | 111986041 | MXI1 | 0.6600 | 0.9850 | 6.6524 | 0.0000 | 0.0281 | 0.1457 |
| chr19 | 42862938 | 42863106 | MEGF8 | 2.8886 | 0.0814 | -6.8913 | 0.0000 | 0.0995 | -0.1448 |
| chr7 | 86988521 | 86988646 | CROT | 1.0619 | 0.3898 | 5.6490 | 0.0000 | 0.0468 | 0.1439 |
| chr5 | 179234002 | 179234123 | SQSTM1 | 0.3565 | 1.1058 | 1.7501 | 0.0229 | 0.0078 | 0.1438 |
| chr2 | 136399105 | 136399360 | R3HDM1 | -0.8744 | 0.7425 | -6.3792 | 0.0000 | -0.0335 | -0.1434 |
| chr10 | 70136949 | 70138427 | RUFY2 | 1.2324 | 0.3140 | -4.9056 | 0.0000 | 0.0757 | -0.1420 |
| chr10 | 104687101 | 104687375 | CNNM2 | 1.4292 | 0.6020 | 3.1139 | 0.0026 | 0.0865 | 0.1420 |
| chr10 | 32561941 | 32562010 | EPC1 | -0.1416 | 1.0571 | 1.7580 | 0.0383 | -0.0050 | 0.1418 |
| chr2 | 102477286 | 102477448 | MAP4K4 | 2.8466 | 0.0812 | 6.3175 | 0.0000 | 0.0987 | 0.1414 |
| chr18 | 44398313 | 44398410 | PIAS2 | -0.5241 | 0.9138 | -2.0429 | 0.0096 | -0.0378 | -0.1401 |
| chr10 | 124187791 | 124187936 | PLEKHA1 | -0.3126 | 1.0318 | 6.8644 | 0.0000 | -0.0096 | 0.1396 |
| chr1 | 212939530 | 212939615 | NSL1 | -1.7921 | 0.3200 | 2.7607 | 0.0125 | -0.0826 | 0.1377 |
| chr1 | 249152710 | 249153125 | ZNF692 | 1.2388 | 0.7581 | -3.4223 | 0.0003 | 0.0479 | -0.1371 |
| chr6 | 38580609 | 38580809 | BTBD9 | 2.2175 | 0.3998 | -2.0151 | 0.0244 | 0.0955 | -0.1362 |
| chr14 | 56139889 | 56139973 | KTN1 | -2.3864 | 0.2322 | 9.2674 | 0.0000 | -0.0618 | 0.1359 |
| chr1 | 249153116 | 249153315 | ZNF692 | -1.0374 | 0.9550 | 3.4572 | 0.0010 | -0.0397 | 0.1359 |

| chrom | begin | end | name | Z.OE | fdr.OE | Z.KD | fdr.KD | ΔPSI_OE | ΔPSI_KD |
|---|---|---|---|---|---|---|---|---|---|
| chr8 | 99963746 | 99964326 | OSR2 | -0.9309 | 0.9667 | -2.3594 | 0.0179 | -0.0400 | -0.1357 |
| chr13 | 77807290 | 77807398 | MYCBP2 | 0.5490 | 0.8757 | 4.8169 | 0.0001 | 0.0629 | 0.1324 |
| chr10 | 29821457 | 29822387 | SVIL | 0.3656 | 1.0175 | -3.3251 | 0.0007 | 0.0236 | -0.1305 |
| chr22 | 31927043 | 31927115 | SFI1 | 1.1042 | 0.6800 | 3.0635 | 0.0026 | 0.0871 | 0.1302 |
| chr10 | 35484054 | 35484142 | CREM | 2.5325 | 0.1090 | 4.2331 | 0.0004 | 0.0948 | 0.1298 |
| chr20 | 13795063 | 13795161 | C20orf7 | 1.2950 | 0.5260 | 2.5453 | 0.0151 | 0.0572 | 0.1295 |
| chr21 | 34113649 | 34113933 | GCFC1 | -1.3010 | 0.8271 | 6.1006 | 0.0000 | -0.0580 | 0.1277 |
| chr7 | 86988521 | 86989425 | CROT | -0.8021 | 0.6522 | -5.1978 | 0.0000 | -0.0359 | -0.1275 |
| chr16 | 19537040 | 19537183 | CP110 | -2.3694 | 0.2304 | 5.6748 | 0.0000 | -0.0887 | 0.1274 |
| chr16 | 90061100 | 90063028 | AFG3L1P | -0.4915 | 0.9140 | -3.1255 | 0.0013 | -0.0241 | -0.1258 |
| chr21 | 38791206 | 38792686 | DYRK1A | 0.8289 | 0.8632 | -2.8027 | 0.0037 | -0.0043 | -0.1246 |
| chr4 | 144378832 | 144378922 | GAB1 | 0.1738 | 0.9921 | 2.3622 | 0.0265 | 0.0085 | 0.1240 |
| chr16 | 90061166 | 90063028 | AFG3L1P | 0.1506 | 1.0432 | 3.5016 | 0.0016 | 0.0105 | 0.1235 |
| chr9 | 94841345 | 94841848 | SPTLC1 | 2.2485 | 0.1315 | -5.2223 | 0.0000 | 0.0844 | -0.1230 |
| chr4 | 153273621 | 153274110 | FBXW7 | -0.7749 | 1.0098 | 2.1684 | 0.0257 | -0.0673 | 0.1219 |
| chr20 | 31393143 | 31393213 | DNMT3B | -1.0416 | 0.6066 | 4.0468 | 0.0012 | -0.0500 | 0.1214 |
| chr2 | 190647739 | 190647849 | ORMDL1 | -2.2094 | 0.2740 | 4.9317 | 0.0001 | -0.0782 | 0.1214 |
| chr9 | 116172896 | 116173029 | POLE3 | 1.3492 | 0.6216 | -2.2813 | 0.0152 | 0.0401 | -0.1212 |
| chr10 | 75871666 | 75871870 | VCL | -0.6914 | 0.9159 | 8.8046 | 0.0000 | -0.0201 | 0.1206 |
| chr20 | 31394014 | 31394133 | DNMT3B | -1.1819 | 0.9624 | 4.1897 | 0.0010 | -0.0481 | 0.1206 |
| chr19 | 52374550 | 52376959 | ZNF577 | -0.0376 | 1.1261 | 2.2260 | 0.0306 | -0.0104 | 0.1202 |
| chr2 | 201445257 | 201445391 | SGOL2 | 0.0681 | 1.1309 | 3.4833 | 0.0011 | 0.0056 | 0.1198 |
| chr2 | 100627958 | 100628033 | AFF3 | -0.9008 | 0.9696 | 2.0754 | 0.0113 | -0.0997 | 0.1193 |
| chr15 | 66801178 | 66801230 | ZWILCH | -0.8179 | 1.0247 | -2.5748 | 0.0057 | -0.0445 | -0.1192 |
| chr19 | 56909645 | 56909752 | LOC386758 | -1.5051 | 0.4094 | -3.9978 | 0.0002 | -0.0671 | -0.1186 |
| chr19 | 13002300 | 13002336 | GCDH | -0.2970 | 1.0326 | -2.6338 | 0.0028 | -0.0226 | -0.1171 |
| chr13 | 52733332 | 52733670 | NEK3 | 0.9027 | 0.4520 | -2.0329 | 0.0253 | 0.0662 | -0.1167 |
| chr7 | 11101417 | 11101468 | PHF14 | 0.3673 | 0.9965 | -3.6255 | 0.0004 | 0.0162 | -0.1165 |
| chr12 | 4654947 | 4654998 | RAD51AP1 | 0.1281 | 1.1278 | 4.4870 | 0.0014 | 0.0045 | 0.1161 |
| chr19 | 10398211 | 10399198 | ICAM4 | 0.2076 | 1.1050 | 1.7616 | 0.0221 | 0.0081 | 0.1160 |
| chr16 | 24816025 | 24816172 | TNRC6A | -2.5390 | 0.2149 | 6.6695 | 0.0000 | -0.0870 | 0.1160 |
| chr7 | 48002884 | 48004229 | HUS1 | -0.4974 | 0.8855 | 5.3067 | 0.0000 | -0.0169 | 0.1159 |
| chr3 | 170857258 | 170857345 | TNIK | -0.7253 | 0.8572 | 2.6664 | 0.0042 | -0.0334 | 0.1153 |
| chr16 | 67290371 | 67290592 | SLC9A5 | -0.4128 | 1.0659 | -2.4429 | 0.0036 | -0.0204 | -0.1150 |
| chr2 | 128520059 | 128522553 | WDR33 | 5.0406 | 0.0133 | -11.8566 | 0.0000 | 0.0889 | -0.1148 |
| chr9 | 130496577 | 130496843 | TOR2A | -2.7005 | 0.2155 | -3.7193 | 0.0002 | -0.0898 | -0.1143 |
| chr11 | 46387793 | 46388534 | DGKZ | 0.1786 | 0.9292 | -3.6389 | 0.0007 | -0.0090 | -0.1142 |
| chr2 | 25642383 | 25642404 | DTNB | -0.2720 | 1.0077 | 2.1920 | 0.0096 | -0.0218 | 0.1139 |
| chrX | 102939608 | 102939657 | MORF4L2 | -5.1404 | 0.0620 | 13.1314 | 0.0000 | -0.0945 | 0.1136 |
| chr17 | 74086409 | 74086478 | EXOC7 | -1.3996 | 0.9142 | 7.7302 | 0.0000 | -0.0332 | 0.1131 |
| chr16 | 81056201 | 81056303 | CENPN | 0.4087 | 1.0535 | 8.2100 | 0.0000 | 0.0114 | 0.1125 |
| chr1 | 15834367 | 15834402 | CASP9 | 0.2629 | 1.0874 | 1.8414 | 0.0391 | 0.0102 | 0.1120 |
| chr22 | 25849282 | 25849401 | CRYBB2P1 | -2.2468 | 0.2466 | 5.4247 | 0.0000 | -0.0800 | 0.1118 |
| chr12 | 113758135 | 113758303 | SLC24A6 | -0.8517 | 0.9879 | -1.8142 | 0.0202 | -0.0374 | -0.1114 |
| chr1 | 19638739 | 19638852 | PQLC2 | 0.8264 | 0.5022 | -3.4012 | 0.0004 | 0.0370 | -0.1107 |
| chr7 | 12727790 | 12730556 | ARL4A | 0.3768 | 0.8916 | 1.6919 | 0.0478 | 0.0270 | 0.1107 |
| chr17 | 25928385 | 25928427 | KSR1 | -0.2057 | 0.9908 | -2.5258 | 0.0036 | -0.0446 | -0.1104 |
| chr1 | 47069856 | 47069966 | MKNK1 | -0.0181 | 1.0954 | 2.1776 | 0.0103 | 0.0036 | 0.1104 |
| chr1 | 47069898 | 47069966 | MKNK1 | 0.0181 | 1.0961 | -2.1776 | 0.0079 | -0.0036 | -0.1104 |
| chr22 | 38453261 | 38453496 | PICK1 | 0.7415 | 0.9599 | -1.9729 | 0.0255 | 0.0609 | -0.1099 |
| chr7 | 99117791 | 99117927 | ZKSCAN5 | 0.5638 | 0.9494 | 2.2944 | 0.0312 | 0.0318 | 0.1098 |
| chr15 | 37391101 | 37391597 | MEIS2 | -0.2889 | 0.9696 | -1.6330 | 0.0362 | -0.0445 | -0.1086 |
| chr16 | 4715102 | 4715152 | MGRN1 | 0.2270 | 1.1072 | -2.3366 | 0.0060 | 0.0091 | -0.1079 |
| chr18 | 28648264 | 28648310 | DSC2 | -0.0486 | 1.1083 | -2.0256 | 0.0133 | -0.0065 | -0.1075 |
| chr19 | 56910262 | 56910539 | LOC386758 | -1.8810 | 0.3072 | -3.3868 | 0.0004 | -0.0921 | -0.1073 |

| chrom | begin | end | name | Z.OE | fdr.OE | Z.KD | fdr.KD | ΔPSI_OE | ΔPSI_KD |
|---|---|---|---|---|---|---|---|---|---|
| chr16 | 67290813 | 67291016 | SLC9A5 | -0.1373 | 1.1350 | -2.0362 | 0.0098 | -0.0045 | -0.1069 |
| chr17 | 65871671 | 65871860 | BPTF | -0.2310 | 1.1211 | -5.7948 | 0.0000 | -0.0188 | -0.1067 |
| chr2 | 30371110 | 30371407 | YPEL5 | 0.9298 | 0.5016 | 4.5972 | 0.0007 | 0.0428 | 0.1066 |
| chr19 | 44464338 | 44464508 | ZNF221 | -0.4012 | 0.9998 | -1.8054 | 0.0314 | 0.0889 | -0.1062 |
| chr16 | 81056359 | 81056487 | CENPN | -0.8083 | 0.9622 | -5.7494 | 0.0000 | -0.0220 | -0.1060 |
| chr14 | 23445853 | 23445921 | JUB | -0.2833 | 1.1288 | 2.5820 | 0.0251 | -0.0417 | 0.1054 |
| chr12 | 48739127 | 48739257 | ZNF641 | 0.2129 | 1.0535 | 1.9478 | 0.0145 | 0.0264 | 0.1052 |
| chr16 | 4715099 | 4715152 | MGRN1 | -0.2270 | 1.0727 | 2.2144 | 0.0097 | -0.0091 | 0.1049 |
| chr8 | 74621266 | 74621397 | STAU2 | -1.2909 | 0.9401 | 4.2933 | 0.0004 | -0.0561 | 0.1046 |
| chr2 | 24285933 | 24286550 | FKBP1B | 1.4841 | 0.3733 | -2.2118 | 0.0075 | 0.0907 | -0.1046 |
| chr18 | 59829485 | 59829562 | PIGN | 0.8162 | 0.4953 | 2.0888 | 0.0262 | 0.0487 | 0.1041 |
| chrX | 48752634 | 48752784 | TIMM17B | -2.0138 | 0.2828 | 10.4218 | 0.0000 | -0.0365 | 0.1039 |
| chr19 | 3366572 | 3366664 | NFIC | 0.5896 | 0.9144 | 2.7720 | 0.0108 | 0.0523 | 0.1033 |
| chr1 | 54354916 | 54355136 | YIPF1 | 2.7081 | 0.0921 | -4.7581 | 0.0000 | 0.0922 | -0.1033 |
| chr7 | 73151550 | 73151721 | ABHD11 | -0.4634 | 1.0099 | -6.0050 | 0.0000 | -0.0137 | -0.1028 |
| chr1 | 9797555 | 9797612 | CLSTN1 | -1.5777 | 0.8502 | 7.9817 | 0.0000 | -0.0332 | 0.1028 |
| chr15 | 30011980 | 30012220 | TJP1 | -1.8177 | 0.3160 | 3.3129 | 0.0051 | -0.0834 | 0.1026 |
| chr12 | 27829996 | 27830029 | PPFIBP1 | -0.1366 | 1.0689 | 2.4097 | 0.0392 | -0.0165 | 0.1024 |
| chr2 | 55495952 | 55496315 | MTIF2 | 2.0935 | 0.1509 | -4.9570 | 0.0000 | 0.0707 | -0.1022 |
| chr20 | 508576 | 508693 | CSNK2A1 | -0.9769 | 0.9631 | 9.7155 | 0.0000 | -0.0137 | 0.1021 |
| chr15 | 66801083 | 66801230 | ZWILCH | 1.6988 | 0.2162 | 4.4298 | 0.0005 | 0.0808 | 0.1016 |
| chr3 | 184055098 | 184055159 | FAM131A | 0.2257 | 1.0178 | 2.0042 | 0.0164 | 0.0148 | 0.1008 |
| chr5 | 171341346 | 171341409 | FBXW11 | -1.8403 | 0.3125 | 4.1535 | 0.0008 | -0.0887 | 0.1007 |
| chr17 | 15580489 | 15580594 | TRIM16 | -1.6735 | 0.3452 | 2.1038 | 0.0385 | -0.0994 | 0.1004 |
| chr2 | 202098165 | 202098345 | CASP8 | 0.5861 | 1.0169 | -2.2554 | 0.0079 | 0.0493 | -0.1002 |
| chr17 | 78395627 | 78395762 | FLJ35220 | -0.5210 | 0.9381 | -2.3096 | 0.0051 | -0.0494 | -0.1002 |

**Table 3 Significantly changed exons (fdr < 0.05, $|\Delta PSI| \geq 0.1$) in patient derived lymphoblast cells.**

| chrom | start | end | gene | Z.Lympho | Z.KD.Hek | ΔPSI Lympho |
|---|---|---|---|---|---|---|
| chr1 | 109778598 | 109778728 | SARS | 7.9653 | 1.0094 | -0.1395 |
| chr1 | 109779012 | 109779170 | SARS | 9.5807 | 0.7685 | -0.1676 |
| chr1 | 154235578 | 154235980 | UBAP2L | -6.1140 | 2.6276 | 0.1302 |
| chr1 | 154832170 | 154832338 | KCNN3 | -5.4774 | | 0.2188 |
| chr1 | 154942507 | 154943223 | SHC1 | -3.8040 | -0.0127 | 0.1485 |
| chr1 | 155279579 | 155279756 | FDPS | 7.0368 | 2.0174 | -0.1146 |
| chr1 | 156107444 | 156107657 | LMNA | -5.7495 | -1.7399 | 0.1218 |
| chr1 | 16047823 | 16047883 | PLEKHM2 | 9.0081 | 12.6659 | -0.3448 |
| chr1 | 207963597 | 207963690 | CD46 | 11.0202 | 15.7557 | -0.3647 |
| chr1 | 221910184 | 221910802 | DUSP10 | -7.5814 | 0.2497 | 0.3038 |
| chr1 | 46018107 | 46018235 | AKR1A1 | 5.5844 | -0.8014 | -0.1112 |
| chr1 | 8021713 | 8021795 | PARK7 | -4.1225 | 3.1336 | 0.1035 |
| chr1 | 8930510 | 8930569 | ENO1 | 13.8453 | 3.0928 | -0.1377 |
| chr1 | 8930510 | 8931635 | ENO1 | -13.6773 | -2.9837 | 0.1358 |
| chr10 | 121341970 | 121342069 | TIAL1 | -5.5396 | -5.0989 | 0.1302 |
| chr10 | 121341970 | 121342120 | TIAL1 | 4.9514 | 5.1364 | -0.1166 |
| chr10 | 135168794 | 135168940 | C10orf125 | -4.0894 | -0.7561 | 0.1881 |
| chr10 | 81940696 | 81940892 | ANXA11 | 5.1503 | 2.8315 | -0.1966 |
| chr10 | 97975076 | 97975145 | BLNK | 5.7380 | | -0.1592 |
| chr11 | 34119244 | 34119308 | CAPRIN1 | 5.7916 | 6.6960 | -0.1474 |
| chr11 | 34119244 | 34120607 | CAPRIN1 | -5.7109 | -6.6937 | 0.1450 |

| chrom | start | end | gene | Z.Lympho | Z.KD.Hek | ΔPSI Lympho |
|---|---|---|---|---|---|---|
| chr11 | 35229651 | 35229753 | CD44 | 4.9596 | 0.3062 | -0.1525 |
| chr11 | 47317046 | 47317118 | MADD | -4.0711 | -0.3533 | 0.2619 |
| chr11 | 72403797 | 72403830 | ARAP1 | 4.9005 | 1.8507 | -0.2476 |
| chr11 | 73429657 | 73429763 | RAB6A | -7.1730 | -4.5101 | 0.2788 |
| chr11 | 73429829 | 73429935 | RAB6A | 4.7645 | 1.7813 | -0.2054 |
| chr11 | 85988959 | 85989780 | EED | -4.5067 | -1.9487 | 0.2140 |
| chr12 | 108957835 | 108957931 | ISCU | -6.9969 | -1.9369 | 0.1868 |
| chr12 | 113355351 | 113355505 | OAS1 | 22.6033 | | -0.2807 |
| chr12 | 113355351 | 113355831 | OAS1 | -21.7527 | | 0.2716 |
| chr12 | 42745686 | 42745851 | PPHLN1 | -3.9988 | -4.5669 | 0.1342 |
| chr12 | 53861588 | 53861627 | PCBP2 | 13.8917 | 19.6406 | -0.2677 |
| chr12 | 988738 | 989197 | WNK1 | 6.8850 | 13.2922 | -0.2392 |
| chr12 | 989886 | 990165 | WNK1 | 6.2739 | 1.6255 | -0.1981 |
| chr13 | 37584688 | 37584792 | FAM48A | 5.7561 | 7.0943 | -0.2277 |
| chr14 | 104151322 | 104151373 | KLC1 | 7.9172 | -1.2307 | -0.3651 |
| chr14 | 105915695 | 105915746 | MTA1 | 5.5954 | 10.4859 | -0.2215 |
| chr14 | 20813090 | 20813246 | PARP2 | -9.1954 | -0.7860 | 0.3905 |
| chr14 | 20813090 | 20813285 | PARP2 | 8.9202 | 1.2477 | -0.3778 |
| chr14 | 51193950 | 51194469 | NIN | 6.8128 | 4.8136 | -0.2478 |
| chr14 | 52344334 | 52344375 | GNG2 | 5.4643 | | -0.2887 |
| chr14 | 70233828 | 70234097 | SRSF5 | -4.4310 | -5.1412 | 0.1112 |
| chr14 | 91636346 | 91636530 | C14orf159 | -6.0781 | -0.5960 | 0.2520 |
| chr14 | 91636346 | 91636545 | C14orf159 | 6.5401 | 0.0390 | -0.2690 |
| chr15 | 100161077 | 100161285 | MEF2A | 7.1330 | 2.1878 | -0.3839 |
| chr15 | 23027800 | 23027922 | NIPA2 | -4.3728 | -3.0924 | 0.1766 |
| chr15 | 72495362 | 72495529 | PKM2 | 16.2219 | 11.6108 | -0.1425 |
| chr15 | 93426814 | 93427008 | LOC100507217 | -6.0401 | -2.5073 | 0.3658 |
| chr16 | 167299 | 167374 | NPRL3 | 7.7339 | 1.9454 | -0.3367 |
| chr16 | 2169114 | 2169186 | PKD1 | -4.2215 | 0.1575 | 0.2656 |
| chr16 | 89603172 | 89604129 | SPG7 | 5.9375 | 5.2830 | -0.2351 |
| chr17 | 25928385 | 25928427 | KSR1 | 5.2602 | -2.5258 | -0.2503 |
| chr17 | 26873724 | 26874427 | UNC119 | 5.6176 | 2.0587 | -0.1166 |
| chr17 | 3594249 | 3594321 | P2RX5 | 5.5694 | 1.2018 | -0.2862 |
| chr17 | 3594249 | 3594321 | P2RX5-TAX1BP3 | 5.5694 | 1.2018 | -0.2862 |
| chr17 | 45012394 | 45012535 | GOSR2 | 6.9832 | 9.3160 | -0.1776 |
| chr17 | 45012394 | 45014205 | GOSR2 | -6.6864 | -9.1435 | 0.1709 |
| chr17 | 46134393 | 46134483 | NFE2L1 | 5.2169 | 5.2927 | -0.1427 |
| chr17 | 75446612 | 75446868 | SEPT9 | -4.6316 | 0.1618 | 0.1629 |
| chr17 | 78292989 | 78293112 | RNF213 | 5.0561 | 3.0262 | -0.1306 |
| chr17 | 78292989 | 78295262 | RNF213 | -4.8253 | -2.9073 | 0.1253 |
| chr18 | 9944920 | 9945055 | VAPA | 5.3809 | -1.6893 | -0.1745 |
| chr19 | 1244735 | 1244824 | ATP5D | 6.3100 | 2.8774 | -0.1282 |
| chr19 | 18682613 | 18682697 | UBA52 | -14.9212 | -1.4511 | 0.1478 |
| chr19 | 18682613 | 18682719 | UBA52 | 14.9212 | 1.4511 | -0.1478 |
| chr19 | 41128854 | 41128926 | LTBP4 | 7.1670 | 7.6271 | -0.3478 |
| chr19 | 59066231 | 59066355 | CHMP2A | -3.9953 | 0.6344 | 0.1232 |
| chr2 | 127815048 | 127815177 | BIN1 | 5.3744 | 2.1987 | -0.2104 |
| chr2 | 201724402 | 201724469 | CLK1 | -5.0628 | -3.8985 | 0.1009 |
| chr2 | 201724847 | 201724938 | CLK1 | -6.2674 | -6.6080 | 0.1195 |
| chr2 | 202028557 | 202037411 | CFLAR | -4.5208 | -4.1040 | 0.1140 |
| chr2 | 220110191 | 220110244 | STK16 | 4.9936 | 0.8638 | -0.3205 |

| chrom | start | end | gene | Z.Lympho | Z.KD.Hek | ΔPSI Lympho |
|---|---|---|---|---|---|---|
| chr2 | 220110200 | 220110518 | STK16 | -5.2847 | -0.4396 | 0.2772 |
| chr2 | 228194321 | 228194499 | MFF | 10.6066 | 9.4094 | -0.4048 |
| chr2 | 231193471 | 231193546 | SP140L | 5.4916 | | -0.2992 |
| chr2 | 272191 | 272305 | ACP1 | -3.9071 | -4.7187 | 0.1333 |
| chr2 | 30371110 | 30371407 | YPEL5 | 5.5361 | 4.5972 | -0.2415 |
| chr20 | 17949017 | 17949154 | SNX5 | 4.9976 | 1.0283 | -0.1960 |
| chr20 | 37050733 | 37050888 | LOC388796 | -10.7259 | -0.9850 | 0.4558 |
| chr20 | 37050738 | 37050888 | LOC388796 | -9.2258 | -0.9684 | 0.3928 |
| chr20 | 37063669 | 37064018 | LOC388796 | -7.2761 | 0.3756 | 0.2900 |
| chr20 | 37063839 | 37063962 | LOC388796 | 7.9510 | -0.8030 | -0.3369 |
| chr20 | 44441254 | 44441435 | UBE2C | 5.2666 | 2.3098 | -0.2268 |
| chr20 | 44441254 | 44442103 | UBE2C | -3.7912 | -1.8232 | 0.1570 |
| chr20 | 47897439 | 47897501 | NCRNA00275 | 6.0930 | 8.7690 | -0.1579 |
| chr20 | 508576 | 508693 | CSNK2A1 | 7.6843 | 9.7155 | -0.3237 |
| chr20 | 62507168 | 62507228 | TPD52L2 | 4.8351 | 17.3242 | -0.2568 |
| chr21 | 27369674 | 27369731 | APP | 4.8503 | 6.6696 | -0.2796 |
| chr22 | 38155423 | 38155963 | TRIOBP | -5.8195 | -5.4494 | 0.3506 |
| chr22 | 50315944 | 50316091 | CRELD2 | 5.9713 | -0.6129 | -0.2177 |
| chr3 | 120321054 | 120321258 | NDUFB4 | 6.8777 | 0.5873 | -0.1705 |
| chr3 | 124807153 | 124807214 | SLC12A8 | 5.8939 | | -0.2137 |
| chr3 | 180693100 | 180693192 | FXR1 | 6.7863 | 6.1524 | -0.2021 |
| chr3 | 39449110 | 39449277 | RPSA | -12.8957 | -0.5022 | 0.1237 |
| chr3 | 39449111 | 39449277 | RPSA | 13.2069 | 0.4317 | -0.1272 |
| chr3 | 47033964 | 47034045 | NBEAL2 | 5.1392 | 0.8693 | -0.1971 |
| chr3 | 50141680 | 50141741 | RBM5 | 6.2380 | 3.0991 | -0.3244 |
| chr4 | 83346715 | 83346820 | HNRPDL | -5.6735 | 1.5518 | 0.1081 |
| chr5 | 133481431 | 133483920 | TCF7 | 5.1407 | -0.4479 | -0.2041 |
| chr5 | 133481914 | 133483920 | TCF7 | -4.7698 | 0.9613 | 0.1869 |
| chr5 | 149782683 | 149782875 | CD74 | 12.0132 | | -0.1231 |
| chr5 | 150521093 | 150521216 | ANXA6 | 6.7823 | 0.0520 | -0.1370 |
| chr5 | 175786483 | 175786570 | KIAA1191 | 5.1202 | 6.9852 | -0.2197 |
| chr6 | 101304178 | 101307078 | ASCC3 | -4.5748 | -8.6206 | 0.2117 |
| chr6 | 158093755 | 158094977 | ZDHHC14 | -7.4312 | -0.0220 | 0.3243 |
| chr6 | 158093800 | 158094977 | ZDHHC14 | 7.4883 | 0.0160 | -0.3280 |
| chr6 | 167347578 | 167347624 | RNASET2 | 7.3501 | -0.1473 | -0.1398 |
| chr6 | 167360169 | 167360227 | RNASET2 | 7.0573 | 1.4809 | -0.1837 |
| chr6 | 167362057 | 167362113 | RNASET2 | 8.3619 | 1.8175 | -0.2921 |
| chr6 | 167365975 | 167366036 | RNASET2 | 6.7271 | 0.7610 | -0.1466 |
| chr6 | 30610544 | 30610788 | ATAT1 | 4.7459 | 2.1417 | -0.3008 |
| chr6 | 30610544 | 30612448 | ATAT1 | -4.6407 | -2.9555 | 0.2947 |
| chr6 | 31549590 | 31549636 | LTB | 7.5652 | | -0.2538 |
| chr6 | 31620023 | 31620170 | BAG6 | -3.8849 | 2.5411 | 0.1149 |
| chr6 | 3264442 | 3264559 | PSMG4 | -4.5044 | -0.8769 | 0.2368 |
| chr7 | 138745083 | 138745884 | ZC3HAV1 | -3.8697 | -2.0063 | 0.1379 |
| chr7 | 142962353 | 142962389 | GSTK1 | -4.4677 | -4.1795 | 0.1660 |
| chr7 | 143530339 | 143530976 | LOC154761 | 10.2223 | | -0.4519 |
| chr7 | 150779850 | 150780413 | TMUB1 | 5.7914 | 2.4585 | -0.1891 |
| chr7 | 73604576 | 73604636 | EIF4H | 7.0827 | 24.7426 | -0.1614 |
| chr7 | 97501030 | 97501308 | ASNS | -5.3316 | -0.1398 | 0.2820 |
| chr8 | 128996149 | 128996450 | PVT1 | 6.0618 | 0.3776 | -0.2913 |
| chr8 | 42396764 | 42397516 | C8orf40 | -4.1461 | -1.2337 | 0.1692 |
| chr8 | 74917030 | 74917120 | LY96 | -4.2055 | | 0.2190 |

| chrom | start | end | gene | Z.Lympho | Z.KD.Hek | ΔPSI Lympho |
|---|---|---|---|---|---|---|
| chr8 | 90775056 | 90775210 | RIPK2 | 6.1905 | 1.1637 | -0.2537 |
| chr9 | 116344351 | 116344522 | RGS3 | 5.6921 | 0.1022 | -0.3079 |
| chr9 | 132686122 | 132686305 | FNBP1 | 9.9842 | 2.1599 | -0.2851 |
| chr9 | 139620762 | 139620868 | SNHG7 | -5.7401 | 0.1427 | 0.1042 |
| chr9 | 139744957 | 139745012 | PHPT1 | 5.6282 | -0.9416 | -0.1190 |
| chr9 | 95055892 | 95056038 | IARS | -3.9876 | 7.1854 | 0.1703 |
| chrX | 102939608 | 102939657 | MORF4L2 | 5.9473 | 13.1314 | -0.2269 |
| chrX | 153585618 | 153585642 | FLNA | -6.9149 | -0.3667 | 0.1498 |
| chrX | 23802410 | 23802520 | SAT1 | 8.6398 | 36.3048 | -0.2078 |
| chrX | 46495023 | 46495083 | SLC9A7 | 6.6207 | 1.5979 | -0.3299 |
| chrX | 48752634 | 48752784 | TIMM17B | 5.7149 | 10.4218 | -0.1922 |
| chrX | 48755194 | 48755365 | PQBP1 | 6.5022 | 2.8872 | -0.2103 |
| chrX | 78207689 | 78207832 | P2RY10 | 6.0091 | | -0.1778 |

# 7 ZUSAMMENFASSUNG

Defekte in *RBM10* sind die Ursache für das TARP-Syndrom und für weitere, weniger schwere Entwicklungsstörungen. Man hat herausgefunden, dass das durch RBM10 kodierte RNA-Bindeprotein Teil des Splicosoms ist, doch ist ansonsten nur wenig bekannt über seine Zielgene oder darüber, welche molekularen Mechanismen der Regulation durch RBM10 zugrunde liegen. In dieser Arbeit konnten wir durch photoactivatable-ribonucleoside-enhanced Crosslinking und Immunoprezipitation 89.247 Bindestellen von RBM10 in 6.396 Zielgenen bestimmen. Diese Bindestellen finden sich vermehrt in der Nähe von 5' und 3' Splice-Sites in Introns und in Exons, was vermuten lässt, dass RBM10 eine Rolle bei der Splicing-Regulation spielen könnte. Dazu passend konnten wir auch feststellen, dass RBM10 speziell an U2 snRNA bindet. Durch RNA-Sequenzierung konnten wir 281 Änderungen des Splicings nach Abreicherung und 356 nach Anreicherung von RBM10 bestimmen. Dabei sind die Änderung des Splicings durch An- und Abreicherung von RBM10 größtenteils anti-korreliert. Folglich hängt alternatives Splicing von der zellularen RBM10-Konzentration ab und wird vermutlich direkt von dieser reguliert. Schließlich konnten wir zeigen, dass die bei einem Patienten vorliegende in-frame Deletion von RBM10 dessen normale Lokalisierung im Zellkern verändert und auf diese Weise seine Funktion bei der Splicing-Regulation stört. Insgesamt zeigen unsere umfangreichen, Genom-weiten Daten, dass RBM10 ein neuer Splicing-Regulator ist, der durch direktes Binden an pre-mRNA-Materiel wirkt und möglicherweise das Zusammenspiel zwischen dem zentralen Splicingmechanismus und anderen Splicing-Regulatoren koordiniert.

# 8 PUBILCATIONS

1. Adamidi C*, **Wang Y***, Gruen D*, Mastrobuoni G*, You X*, Tolle D, Dodt M, Mackowiak SD, Gogol-Doering A, Oenal P et al. 2011. *De novo* assembly and validation of planaria transcriptome by massive parallel sequencing and shotgun proteomics**. Genome Research** 21: 1193-1200. (* equal contribution)

2. Onal P, Grun D, Adamidi C, Rybak A, Solana J, Mastrobuoni G, **Wang Y**, Rahn H-P, Chen W, Kempa S et al. 2012. Gene expression of pluripotency determinants is conserved between mammalian and planarian stem cells. EMBO J 31: 2755-2769.

# DECLARATION

The project was conceived and performed in the group of "Novel Sequencing Technology, Medical and Functional Genomics" in Berlin Institute for Medical Systems Biology at Max-Delbrück-Center for Molecular Medicine under the supervision of Dr. Wei Chen. I hereby declare that this thesis is the results of my own original research work. Contributions from others involved are clearly and specifically indicated in the acknowledgement. The thesis is submitted to Department of Biology, Chemistry and Pharmacy of Freie Universität Berlin to obtain the academic degree of Doctor rerum naturalium (Dr. rer. nat.) and has not been submitted to anywhere else for any degree.

August 2012
Berlin
Yongbo Wang

# Curriculum Vitae

For reasons of data protection,
the curriculum vitae is not included in the online version